15/12

Rapport
Report

Congestion Management in the Nordic Power Market – Nodal Pricing versus Zonal Pricing

Endre Bjørndal
Mette Bjørndal
Victoria Gribkovskaia

SNF
Et selskap i NHH-miljøet

SAMFUNNS- OG NÆRINGSLIVSFORSKNING AS

Institute for Research in Economics and Business Administration

SNF
Samfunns- og næringslivsforskning AS

- er et selskap i NHH-miljøet med oppgave å initiere, organisere og utføre eksternfinansiert forskning. Norges Handelshøyskole og Stiftelsen SNF er aksjonærer. Virksomheten drives med basis i egen stab og fagmiljøene ved NHH.

SNF er ett av Norges ledende forskningsmiljø innen anvendt økonomisk-administrativ forskning, og har gode samarbeidsrelasjoner til andre forskningsmiljøer i Norge og utlandet. SNF utfører forskning og forskningsbaserte utredninger for sentrale beslutningstakere i privat og offentlig sektor.

Forskningen organiseres i programmer og prosjekter av langsiktig og mer kortsiktig karakter. Alle publikasjoner er offentlig tilgjengelig.

SNF
Institute for Research in Economics and Business Administration

- is a company within the NHH group. Its objective is to initiate, organize and conduct externally financed research. The company shareholders are the Norwegian School of Economics (NHH) and the SNF Foundation. Research is carried out by SNF´s own staff as well as faculty members at NHH.

SNF is one of Norway´s leading research environment within applied economic administrative research. It has excellent working relations with other research environments in Norway as well as abroad. SNF conducts research and prepares research-based reports for major decision-makers both in the private and the public sector.

Research is organized in programmes and projects on a long-term as well as a short-term basis. All our publications are publicly available.

SNF Report No 15/12

Congestion Management in the Nordic Power Market – Nodal Pricing versus Zonal Pricing

Endre Bjørndal

Mette Bjørndal

Victoria Gribkovskaia

SNF Project No 3146:

Virkninger av alternativ organisering av det nordiske kraftmarkedet

The project is financed by Norwegian Water Resources and Energy Directorate

INSTITUTE FOR RESEARCH IN ECONOMICS AND BUSINESS ADMINISTRATION
BERGEN, MAY 2013

ISBN 978-82-491-0815-2 Printed version
ISBN 978-82-491-0816-9 Electronic version
ISSN 0803-4036

Preface

The project has been carried out by Samfunns- og næringslivsforskning AS (SNF) by the following persons:

- Associate Professor Endre Bjørndal, NHH (project manager)
- Professor Mette Bjørndal, NHH
- PhD Scholar Victoria Gribkovskaia, NHH/SNF

We thank NVE for providing us with data for the network model and for the bid curves, and for discussions during the project. We especially thank Finn Ljåstad Pettersen. We also thank Statnett for comments in the early phase of the project.

Contents

1. Introduction

The Nord Pool area covers presently Norway, Sweden, Denmark, Finland and Estonia. Previously, prices were calculated also for a German price area (Kontek), however, since November 2009, this price area has been replaced by market coupling with the central western European area. At Nord Pool Spot area prices are calculated for the day-ahead market. Since the market is settled many hours before real time, imbalances occur, and they are settled by intraday trading in Elbas and in the close to real time regulation markets. Nord Pool Spot is a voluntary pool. However, trades between Elspot areas are mandatory. Nord Pool Spot covers about 70 % of the physical power in the Nordic region (except Iceland), and the pool is used not only for mandatory trades but also to increase legitimacy of prices and as a counterpart.

There are three types of bids at Nord Pool Spot. These are hourly bids for individual hours, block bids that create dependency between hours, since a block bid is accepted only for a whole block of hours, and finally, flexible hourly bids, which are sell bids for hours with highest prices. In the analysis we don't have information on block bids and flexible hourly bids, so we will treat all bids as hourly bids. Accepted block bids will sometimes be part of the bid curves, however, as price independent buy or sell bids.

Considering congestion, the day-ahead market takes grid constraints partly into account by calculating different prices for relatively few price areas. For most of the cases considered in this report there are 10 price areas in the Nord Pool area, and transfer capacities are given by the system operators between these areas before the market agents submit bids, and Nord Pool calculates area prices. This means that zonal pricing or market splitting is used in the day-ahead market for the presumably largest and long-lasting congestions within Norway and for congestions on the borders of the control areas, including two price areas in Denmark. Moreover, from November 2011, due to European regulation, Sweden is split into 4 price areas. For constraints internal to the price areas, they are resolved by counter trading or re-dispatching in the regulation market. The system operators in the Nord Pool area are transmission system operators, owning and controlling the national grids. They are incentive regulated and the net effects of the incomes from zonal pricing and the expenses from re-dispatching are passed on to domestic customers. This may also give incentives to relieve internal constraints by reducing transfer capacity between the Nord Pool bidding areas.

Congestion management affects the efficiency of the Nordic electricity market and the prices quoted in the day-ahead market of Nord Pool Spot. NVE describe in the tender documents that they particularly want to consider how more pricing areas and the implementation of a more detailed network model in the calculation of the spot prices can contribute to more efficient price signals to producers and consumers, depending on where they are located. For analysis of congestion management within an exchange area, with a market infrastructure that allows for a certain number of geographic prices on an hourly basis, the optimal (economic) power flow model is often used as the reference point. This is normally a single period model that maximizes social surplus, given the supply and demand curves that exist for each connection point in the network, as well as the limitations imposed by thermal and other capacity constraints in the transmission grid. The optimal power flow is a snapshot, and the dynamic adjustment over time is left to the players, which means that supply curves for a period include opportunity costs such as water values, etc. The question then is whether the procedures for market clearance can achieve a solution that is close to the optimal power flow with optimal prices for each generation and load point (optimal nodal prices).

Our analysis of congestion management methods for the Nordic electricity market takes as a starting point the optimal power flow for a single hour. The efficiency of a specific market mechanism can then be evaluated based on the degree to which one can realize the optimal power flow. In the Nordic power market this is dependent on the formulation of practical rules for area price determination at Nord Pool Spot. These rules imply a number of simplifications and approximations compared to the optimal power flow benchmark. For a start, prices are not noted for each connection point in the system, instead area prices are computed, that are uniform within larger areas of the network. The number of price areas and how the boundaries of these are exactly determined, therefore, affects economic efficiency. Another simplification is that market participants bid within each zone and not at each generation or load point. This results in uncertainty regarding the effects of a bid on the system, and consequently a possibility that the capacity control is imprecise. Likewise, the transmission capacities are often associated with transfer interfaces that include several transmission lines. This also results in a rougher capacity control compared to if line capacities were used individually. In the whole Nordic system there is a practice of "moving" a transmission constraint within a price area to an area boundary, by reducing capacity between price areas. Previous work has shown that this is a practice that can be costly and greatly affects the level of the area prices in different regions.

A common Nordic power exchange gives the opportunity to determine locational prices in a way similar to the optimal power flow, where the congestion costs are determined at market clearing. By including a detailed network model in the price calculation, the system operator's definition of trade capacities becomes redundant. Prices and power flows can be calculated simultaneously for each hour based on an optimization procedure in which the social welfare based on the players' bids to the power exchange in the various areas is maximized. However, this requires more and smaller areas than today's 10 price areas at Nord Pool Spot. More and smaller areas are necessary to determine the exact location of production and consumption in the network.

The aim of the project has been to investigate the effects of a market system, which takes advantage of more information about the physical system in terms of capacities and flows, and the location of supply and demand bids. We have used the OptFlow model, with a more detailed representation of the Nordic electricity market and a possibility to solve different power flow models, including a DC approximation of the full AC power flows. Different market scenarios have been developed and the model is used to investigate questions like:

- How are the nodal prices compared to area prices or zonal prices for different scenarios?
- How do production and consumption patterns change under different pricing mechanisms?
- Which constraints are binding in the different scenarios?
- How does the determination of transfer capacities between bidding areas affect the utilization of the transmission network?
- How do transfer capacities affect prices?
- How does the implementation of security requirements affect prices?
- How detailed should your model be to have an efficient market solution?

2. Locational price models

The objective of a deregulated power market is efficiency in the short and long run, through at competitive short term power market with efficient utilization of existing resources, as well as an optimal long term development of the power system. The efficient short run utilization of limited generation and transmission capacity can in principle be found by solving an optimal economic dispatch problem, where the difference between consumer benefits and production cost is maximized, subject to generation and transmission constraints. The latter include thermal and security constraints. If we solve this optimal economic dispatch problem, we get a value of power for each location in the transmission system, and this is a benchmark for the value of power at different locations that can be used for assessing congestion management methods. In this chapter we shortly describe the three locational price models that we analyze in this report. The nodal prices are the based on the value of power obtained from an optimal economic dispatch problem. Simplified zonal prices and optimal zonal prices represent two different simplifications or approximations of the nodal prices. A more formal description of the different locational price models can be found in Appendix 2.

2.1 Nodal pricing

Schweppe et al. (1988) described nodal prices as the locational prices consistent with the principle of prices equal to marginal cost in a power market. Nodal prices maximize net social welfare given the physical constraints of the transmission network and transmission losses (if included in the model). Hogan (1992) introduced the concept of contract networks, providing financial capacity rights, and Harvey et al. (1996) describe the inclusion of contingency heuristics.

Due to the fact that power flows in an electricity network obey certain physical laws and the nature of electricity flow is such that it cannot be routed and will take all available paths between origin and destination, nodal prices or locational marginal prices as they are frequently called possess some specific properties. A single limitation can induce price differences throughout the network, there may be flow from a high price node to a low price node, and a new line may result in lower social surplus (see for instance Wu et al., 1996).

If the network on the left hand side of Figure 2-1 represents all injection and withdrawal points in a network, and all links between the nodes, the nodal pricing mechanism will result in a price for each connection point in the system.

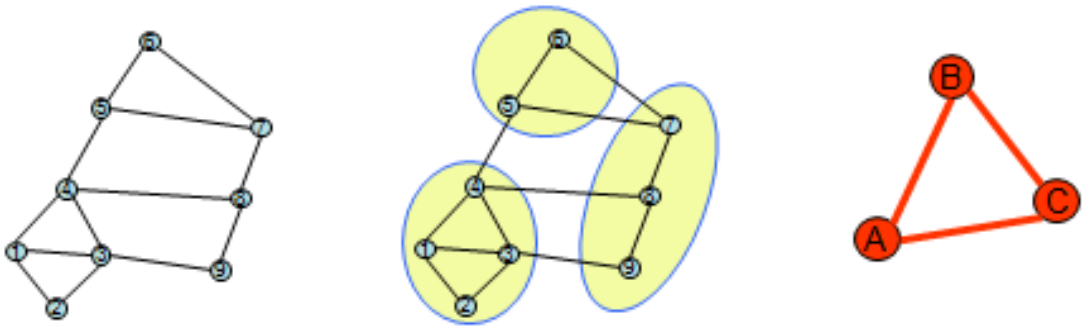

Figure 2-1 Locational prices

2.2 Zonal prices

Zonal prices is a "simplification" of nodal prices, implying fewer prices than there are connection points, and some sort of aggregation. How this aggregation is specifically done, is however not well defined. What is to be aggregated? It can be prices only or the physical network model itself. This is illustrated by the middle and right hand side of Figure 2-1.

2.2.1 Optimal zonal prices

Aggregating prices only, i.e. economic aggregation, the topology of the network is represented in full while the prices within (pre)defined zones are required to be uniform. This is illustrated by the middle part of Figure 2-1, where the 9 nodes have been divided into three groups, but the original network is still visible. In this case, bids are given for nodes and the capacities are set for individual lines, but prices are determined for zones. We will call these prices optimal zonal prices, since they are found by solving an optimal economic power flow problem, with the extra requirements that prices of nodes belonging to the same zone are to be equal.

Optimal zonal prices have been studied by Bjørndal and Jörnsten (2001). They are second best compared to optimal nodal prices. Different divisions are preferred by different agents (producers and consumers in a node have opposite interests for instance) and grid revenues may be negative under optimal zonal prices. There may be many variants of "adverse flows", i.e. power flowing from high prices to low prices, and it is very difficult to find an optimal zone division. This depends on market characteristics and hourly costs, topology of the network etc., which makes it difficult to decide upon a division if it is to be fixed for a longer period. If there are too few zones, it may be impossible to find prices that are uniform within predefined areas and in addition clear the market subject to all relevant constraints.

2.2.2 Simplified zonal prices

The area prices or zonal prices used in the Nordic power market are better represented by the right hand part of Figure 2-1. In this pricing approach, which we call simplified zonal prices, the original detailed network and the three defined zones have been replaced by three aggregated nodes and some aggregated connections between these. We can say that the network has been physically aggregated, and the network has been highly simplified, thus neglecting the physical characteristics of the power flows. This is not straightforward for electricity networks. Injections and withdrawals in different nodes within a zone can in general have very different effects on the power system. It is also an open question how to determine characteristics of aggregated lines, i.e. admittance and capacity. Contrary to ordinary transportation networks where flows can be routed, an aggregated line consisting of two individual links may have flows in opposite directions. In such a case, both individual lines may be overloaded even if the sum of the flows is zero.

In the simplified zonal price model, detailed information on nodal bids is lost, and constraints within a zone are not represented. Setting capacities on aggregated lines is difficult, if they are too restrictive, the power system may not be fully utilized, if they are too encouraging, the market outcomes may result in infeasible flows.

3. Case study – calibration of model and data

We analyze the effect of different congestion management methods on hourly prices/quantities for different supply/demand scenarios. Our simulation cases differ only with respect to the supply and demand bid curves, while the topology and capacities of the network are kept constant.

3.1 Topology and capacities

3.1.1 Topology

The network topology is illustrated by Figure 3-1. The Norwegian part of the network model has 178 nodes and 242 lines, and it corresponds roughly to the Norwegian central grid. The network model for Sweden is simpler, with roughly 27 nodes and 42 lines, and is based on the Samlast model (SINTEF, 2012). The other Nord Pool Spot price areas DK1, DK2 and Finland are represented with a single node each. The same is true for Kontek and Estonia, for the cases where these price areas existed.

3.1.2 Line parameters

The admittance value for each line is based on reactance, resistance and line voltage numbers. The thermal capacity for each line is based on line voltage and maximal line current. The specific formulas for admittance and thermal capacities are given in Appendix A.2. Line parameters for Norwegian nodes are given in Statnett (2010) or supplied by our contact persons in NVE. Parameters for the Swedish network are taken from the Samlast model (SINTEF, 2012) provided to us by NVE. Capacities for lines between countries, except between Sweden and Norway, have been set to Net Transfer Capacity values (see Nord Pool Spot, 2012).

3.1.3 Security constraints

We have included security constraints for the Norwegian part of the network. Each security constraint models the potential outage of a network component. The outage of a component will typically lead to a redirection of the power flow. The effect of outage on power flow could be determined endogenously as part of the optimization procedure, or it could be specified in advance. An example of the former type of approach is found in Peperman & Willems (2003), and Statnett's procedure is an example of the latter type. The restrictions implied by Statnett's approach can be modeled as "cut constraints". An example of a cut constraint described in Statnett (2010) is the constraint related to the Vemork-Flesaker line. If it should fall out, 35 % of the power currently flowing over this line is assumed to be redirected to the Tokke-Flesaker line, which has a thermal capacity of 710 MW at a temperature of 10ºC. Hence, the flow over Tokke-Flesaker plus 35 % of the flow over Vemork-Flesaker should not exceed 710 MW. Our model includes 38 such constraints, and they are explained in more detail in Appendices A2 and A3.

Figure 3-1 Network topology

3.2 Bid curves

Our model has piece-wise linear bid curves for supply and demand (see also appendix A4). We consider supply and demand for a single hour, hence features involving multiple hours, such as block bids and ramping restrictions, are not included. Since we apply different bottleneck handling methods while keeping the bid curve scenarios constant, we implicitly assume that the choice of method does not affect the bid curves. In practice this might not be true, since the chosen bottleneck method will affect prices, and hence the expected water values that are embedded in the bid curves.

We have constructed 8 bid curve scenarios, based on data for 8 hours in 2009/2010, as shown in Table 3-1 below. The cases were chosen to reflect different conditions with respect to load and import in Norway, as shown in the last two columns of the table. Since bids to Nord Pool Spot are only related to price areas, we do not have any data for supply and demand curves for smaller areas, matching the more disaggregated topology of our network model. Thus, for Norway and Sweden we have constructed nodal bid curves, to be described in more detail below. For the remaining Elspot bidding areas we have used the actual bid curves from Nord Pool. Table 3-2 gives an overview of the Elspot areas for the different cases. In the following chapters we will look into the details of the results for some of the cases.

Table 3-1 Overview of selected cases

Load	Import	Date	Hour	Load (GWh)	Net import (GWh)
Medium	High	5/5-2010	21	13,87	4,6
Medium	Medium	30/3-2009	6	14,38	-0,1
Medium	Low	7/10-2010	11	14,22	-4,3
Low	High	1/8-2010	6	8,48	3,6
Low	Low	1/9-2009	1	9,04	-3
High	Low	15/12-2010	19	20,95	-3,2
High	High	10/1-2010	15	20,89	2,3
Record		6/1-2010	10	23,99	0,7

Table 3-2 NordPool bidding areas

Date	No. of bidding areas in Norway	SE, DK1, DK2, FI	Estonia	Kontek
5/5-2010	5	x	x	
30/3-2009	2	x		x
7/10-2010	5	x	x	
1/8-2010	5	x	x	
1/9-2009	3	x		x
15/12-2010	5	x	x	
10/1-2010	3	x		
6/1-2010	3	x		

3.2.1 Data issues

For each of the case hours, Statnett has given us nodal data on generation and exchange in the Norwegian central grid. Load for each node is calculated as the difference between generation and exchange. Some issues related to data quality had to be addressed in this phase of the project. For many nodes/hours the computed load numbers were negative, and there were also many instances with higher reported generation than installed effect. According to Statnett these problems are mainly caused by inaccurate reporting, where generation/load has not been assigned to the correct nodes. We have handled these data problems by reallocating generation/load among nodes. Nodes with unreasonably high generation numbers and/or negative load have been grouped together with neighboring nodes. A total of 128 of the 177 nodes have been assigned to 24 groups. For each of the 24 groups, the total generation and load was reallocated among the member nodes according to a fixed set of weights, while keeping the sum constant for the group. We used maximum generation and load as allocation weights for generation and load, respectively, and the weights can be found in Tables 8.2 in Statnett (2010).

3.2.2 Generation bid curves for Norway and Sweden

The bid curves that we have used have from one to six linear segments, as illustrated in Figure 3-2, 3-3 and 3-4 below. The total capacity for each of the Norwegian nodes is set equal to available winter effect as given in Table 8-1 in Statnett (2010). For the Swedish nodes we have made a rough estimation of nodal capacities based on data for actual generation for SE1-SE4 obtained from Svenska Kraftnät (see svk.se), and we have also taken into account the capacity data given in Nord Pool Spot (2011).

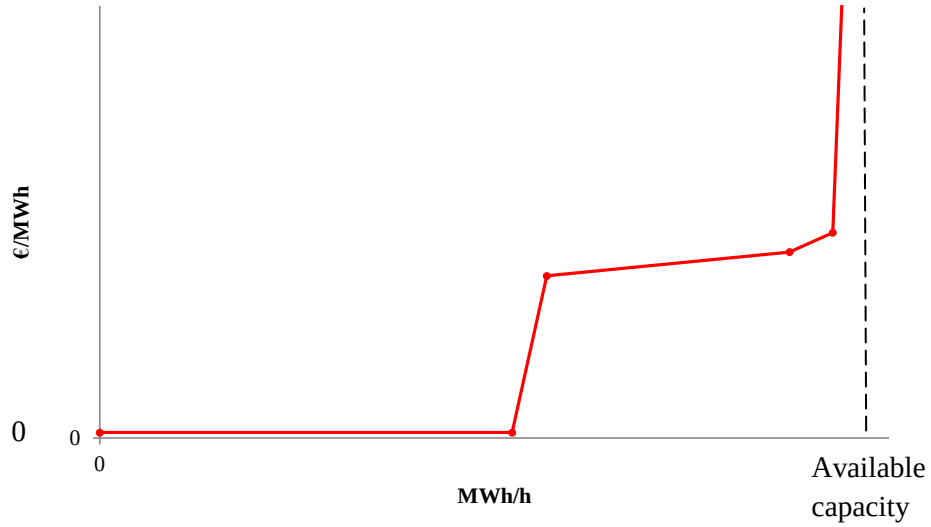

Figure 3-2 Bid curve – hydro/wind power

For most of the Norwegian nodes as well as nodes in northern Sweden (SE1 and SE2), with mostly hydro power, we have used bid curves similar to the one shown in Figure 3-2. The first bid curve segment have a constant marginal cost of 2,5 Euros/MWh, and may represent intermittent power

generation, e.g., river hydro power plants and/or wind. The size of the first segment, i.e., the amount of capacity in the first segment, has been set by taking into account the location of wind and river plants, as given in the data set for Samkjøringsmodellen. In addition to the actual "intermittent" capacities we have added capacity to the "intermittent" bid curve segment in order to calibrate our bid curves to the observed Nord Pool Spot bid curves. The extra capacity added in this manner is allocated among the nodes in proportion to the total available nodal capacities.

The shapes of the hydro/wind bid curves differ depending on the location of the node/case in question, and this will be discussed further in the section on calibration below.

We have assumed most of the capacity in SE3, except for the Ringhals and Forsmark nodes, to be thermal, and for these nodes have used bid curves equal to the one shown in Figure 3-3, with a constant marginal cost equal to 60 Euros/MWh. Bid curves for the Mongstad and Kårstø generation plants in Norway have been set in the same way. For the three nuclear plants in Sweden we have used a constant marginal cost of 4 Euros/MWh, as illustrated in Figure 3-4.

Figure 3-3 Bid curve – thermal power

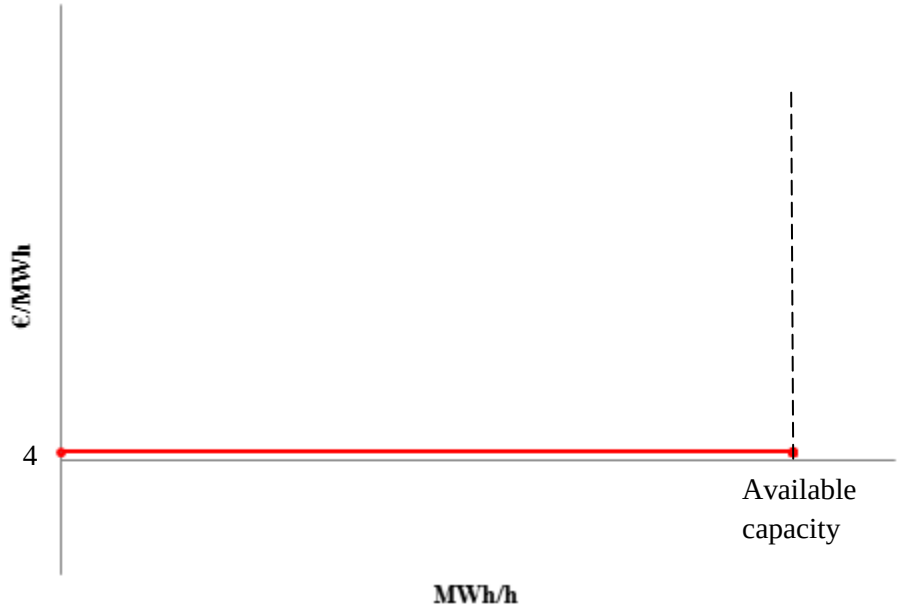

Figure 3-4 Bid curve – nuclear power

3.2.3 Load bid curves for Norway and Sweden

For load we have determined the bid curves for the respective cases based on observed load, as reported by Statnett / Svenska Kraftnät. The general shape of the demand curves is as shown in Figure 3-5. The bid curve for each node has an inelastic part given by the vertical segment. We also allow for elastic demand if the price offered at the node drops below a certain level. The elastic part of the bid curve may consist of up to two linear segments, as shown in the figure.

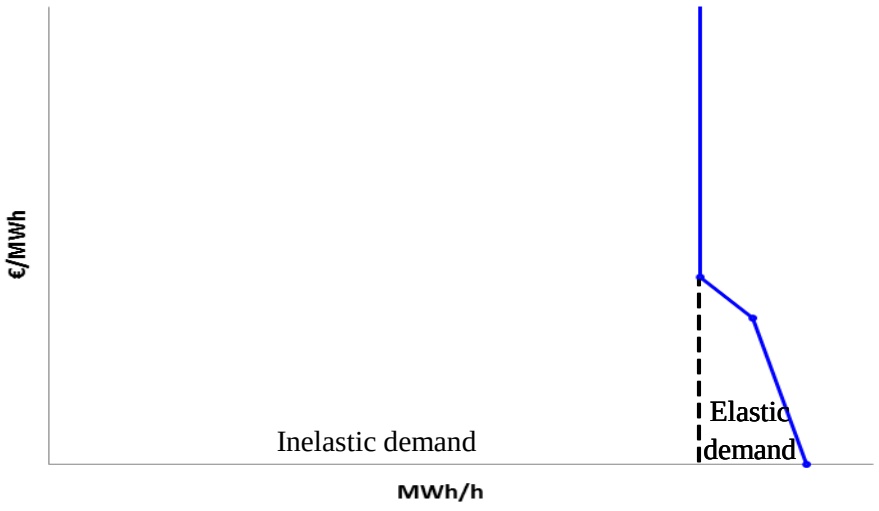

Figure 3-5 Load bid curve

3.2.4 Calibration of demand bid curves for Norway and Sweden

In this section we explain how the bid curves have been calibrated, and we use the case corresponding to hour 19 on the date 15/12-2010, as an illustrative example.

For each Nord Pool Spot bid area NO1-NO5 and SE we perform the following steps in order to calibrate the load bid curves:

1) The inelastic (nodal) load quantity is set equal to total load minus load for industrial consumers in the node[1].

2) The elastic segment is determined by setting the two break point prices, as well as the relative sizes of the two elastic segments, in order to make the shape of the aggregate OptFlow demand bid curves match the shape of the corresponding Nord Pool curves. If necessary, we also scale the total elastic demand (observed load for industrial consumers in the top load hour).

Figure 3-6 shows the demand bid curve for the node Halden, and Figure 3-7 shows the aggregate demand curve for NO1, i.e., the bidding zone that Halden belonged to on December 15, 2010. The inelastic demand for Halden is 149 MWh/h, while the inelastic demand for NO1 is 6754 MWh/h. The most elastic demand curve segment is defined for prices between 82 Euros/MWh and 60 Euros per MWh, while demand elasticity is lower for prices below 60[2]. Note that the aggregate OptFlow demand curve gives higher demand for any price level than the corresponding Nord Pool Spot demand curve. This is as expected, since the OptFlow curve is based on total load, including load that is not channeled through Nord Pool Spot.

[1] The only information we have on load for industrial consumers is for Norway (KII), and it is the consumption during the top load hour for each year. We have used the average consumption during the top load hour for 2009 and 2010. We do not have information on industrial consumption in Sweden. In our base case we model (almost) all load in Sweden as inelastic.

[2] The following table shows the implied demand elasticities, measured at the mid-point of each of the elastic curve segments:

	NO1	NO2	NO3	NO4	NO5	SE
Segment 1	-6,45	-32,00	-8,11	-1,36	-7,95	-1,35
Segment 2	-0,14	-0,21	-0,33	-0,82	-0,05	-0,33

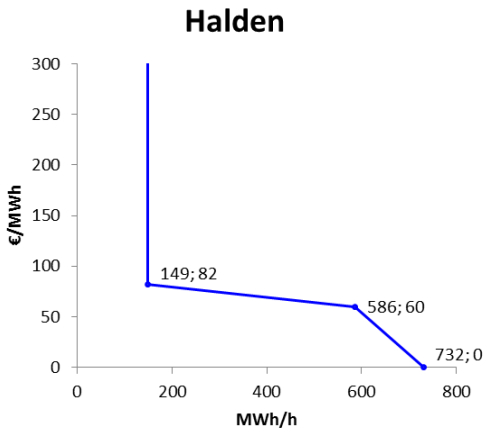

Figure 3-6 OptFlow demand bid curve for Halden, 15/12-2010, hour 19

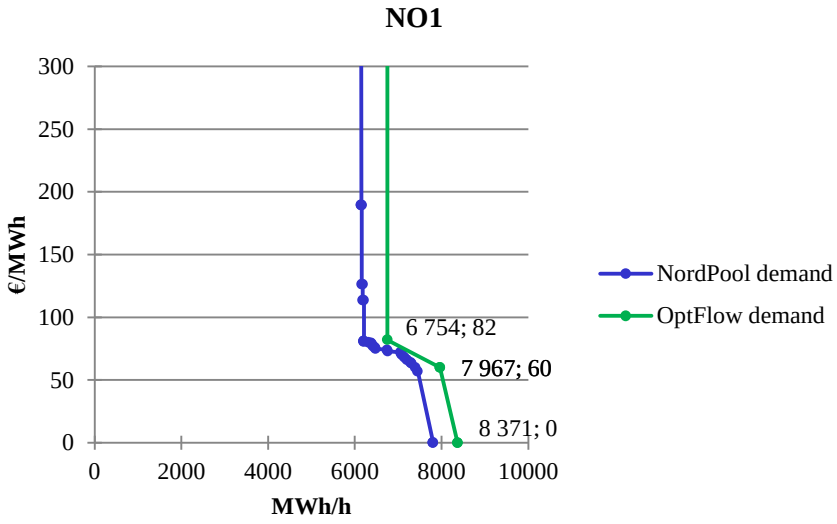

Figure 3-7 Aggregated demand bid curves for NO1, 15/12-2010, hour 19

3.2.5 Calibration of supply bid curves for Norway and Sweden

Similarly to the procedure described in the previous section, the generation bid curves for each of the bid areas NO1-NO5 and SE have been calibrated using the following procedure:

1) Determine break point prices as well as relative segment sizes for hydro/intermittent nodes in order to make the aggregate OptFlow supply bid curves match the corresponding NordPool curves.

2) Shift all generation bid curves in order to make the horizontal distance between the aggregate OptFlow curve and the Nord Pool curve approximately equal to the distance between the corresponding aggregate load curves. The increased generation is allocated among nodes in proportion to available capacities in the respective nodes.

For the case in question, step 1 resulted in supply bid curves like the example shown for Sima (NO1) in Figure 3-8. The maximal winter effect for Sima is 878 MWh/h. In order to satisfy the distance requirement in Step 2 we added 9,6 % to the initial capacities of all the nodes in NO1, hence the model "capacity" for Sima is 962 MWh/h. The fact that the distance between this "capacity" and the bid curve is considerable is due to the fact that the price at the end point of the bid curve is set to a very high number (10000) in order to make the slopes of the aggregate OptFlow and Nord Pool Spot curves approximately equal. The resulting aggregate supply bid curve for NO1 is shown in Figure 3-9.

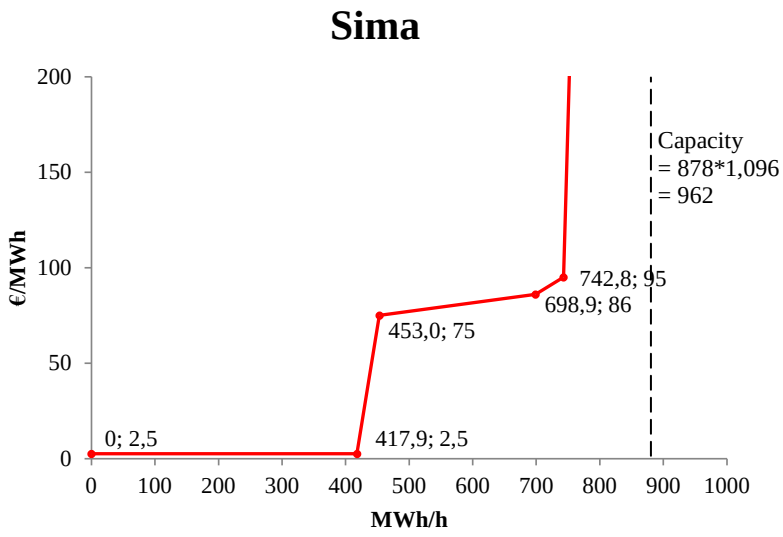

Figure 3-8 OptFlow supply bid curve for Sima, 15/12-2010, hour 19

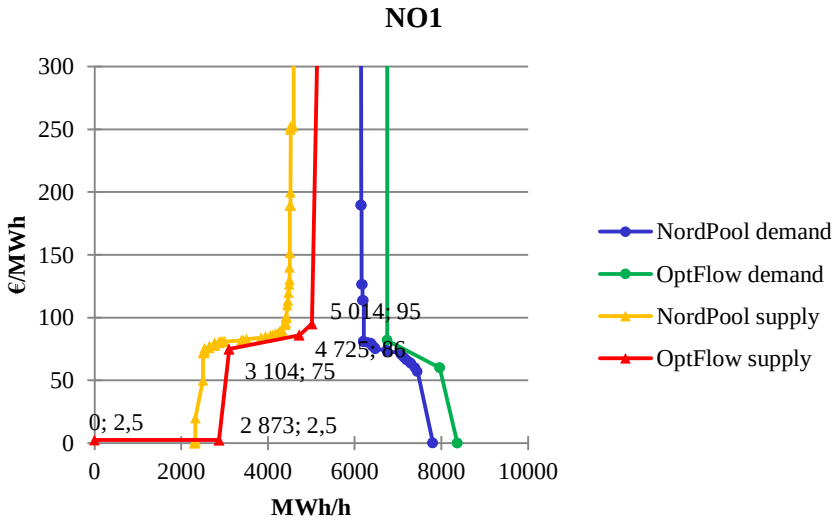

Figure 3-9 Nord Pool Spot and calibrated aggregate OptFlow bid curves for NO1, 15/12-2010, hour 19

4. Results for 15-12-2010 hour 19

4.1 Calibration of bid curves

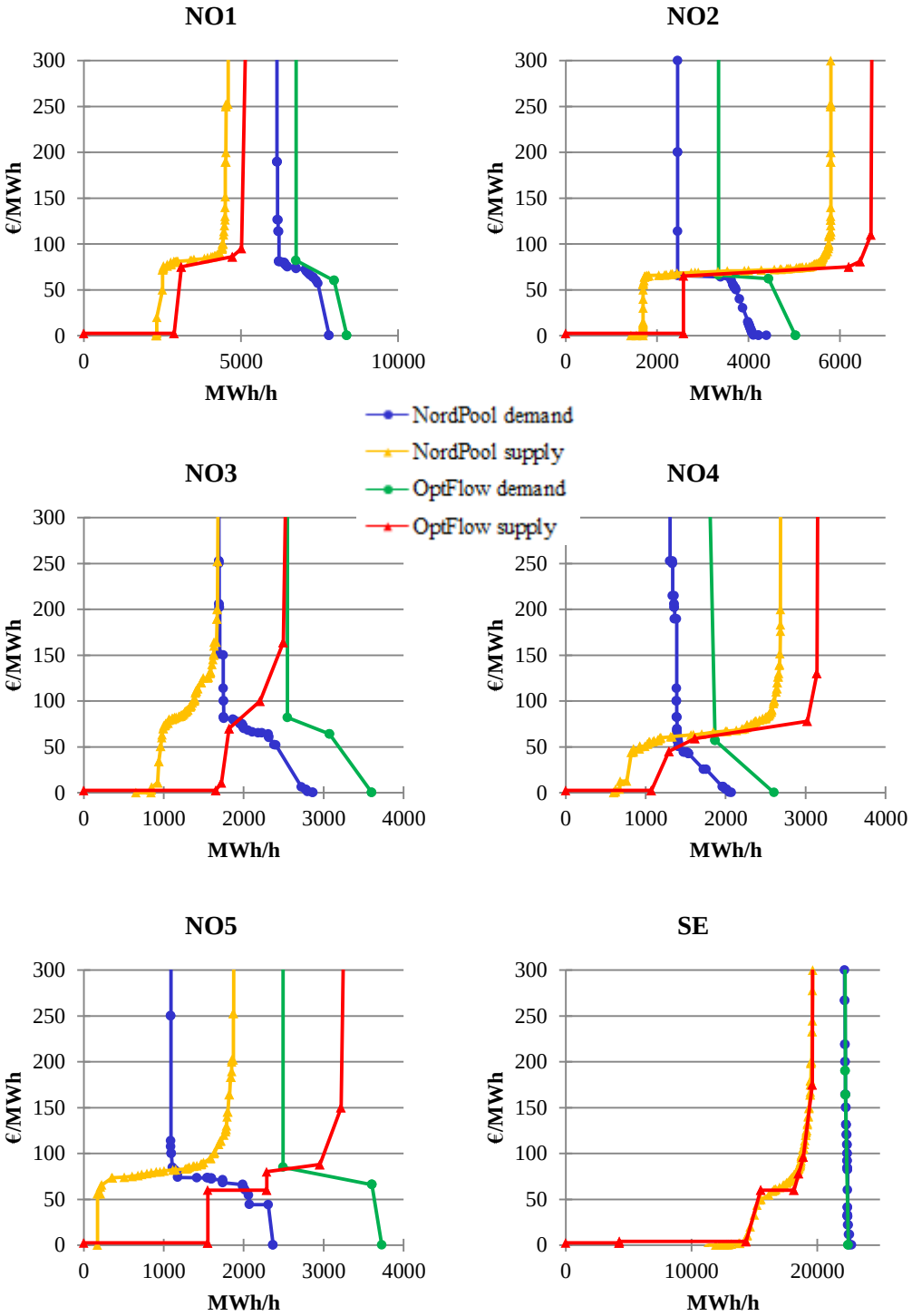

Figure 4-1 Nord Pool Spot bid curves and aggregate OptFlow bid curves for Norway and Sweden, 15/12-2010, hour 19

Figure 4-1 compares the constructed disaggregated bid curves to the actual Nord Pool bid curves, by aggregating the disaggregated curves of the OptFlow model for the different price areas. Figure 4-1 shows the aggregate OptFlow bid curves for all 5 Norwegian areas and the Swedish price area that applied to the specific date in December 2010[3]. We see that the shapes of the (aggregated) constructed OptFlow curves reflect the actual Nord Pool bid curves quite closely, however, the volumes are different. This is so because the Nord Pool bid curves only cover parts of the actual load / production (on average 70-80 %). In order to evaluate the effect on the power system in more detail, i.e. similar to the production and exchange data received from Statnett, we need to model the total load, covering (at least close to) 100 % of the supply and demand for the Norwegian areas[4].

The remaining Elspot price areas are modeled as single nodes in the disaggregated OptFlow model, and we have used the actual Nord Pool bid curves for hour 19 on 15/12-2010. These bid curves are shown in Figure 4-2.

[3] The Nord Pool Spot bid curves include accepted block bids. We have also adjusted the NO2 and NO4 bid curves for export to the Netherlands and import from Russia, respectively, in order to distinguish clearly between domestic and foreign demand/supply.

[4] We have used data from Svenska Kraftnät to calibrate the Swedish bid curves. As can be seen from Figure 4-1, the calibrated curves are almost identical to the Nord Pool Spot bid curves. We expected higher volumes also for the Swedish curves, and the data allow for different interpretations. We have tested the effects of increasing the supply and demand volumes by approximately 10 %, the effects are small, and we have kept the curves in Figure 4-1 for the analyses that follows.

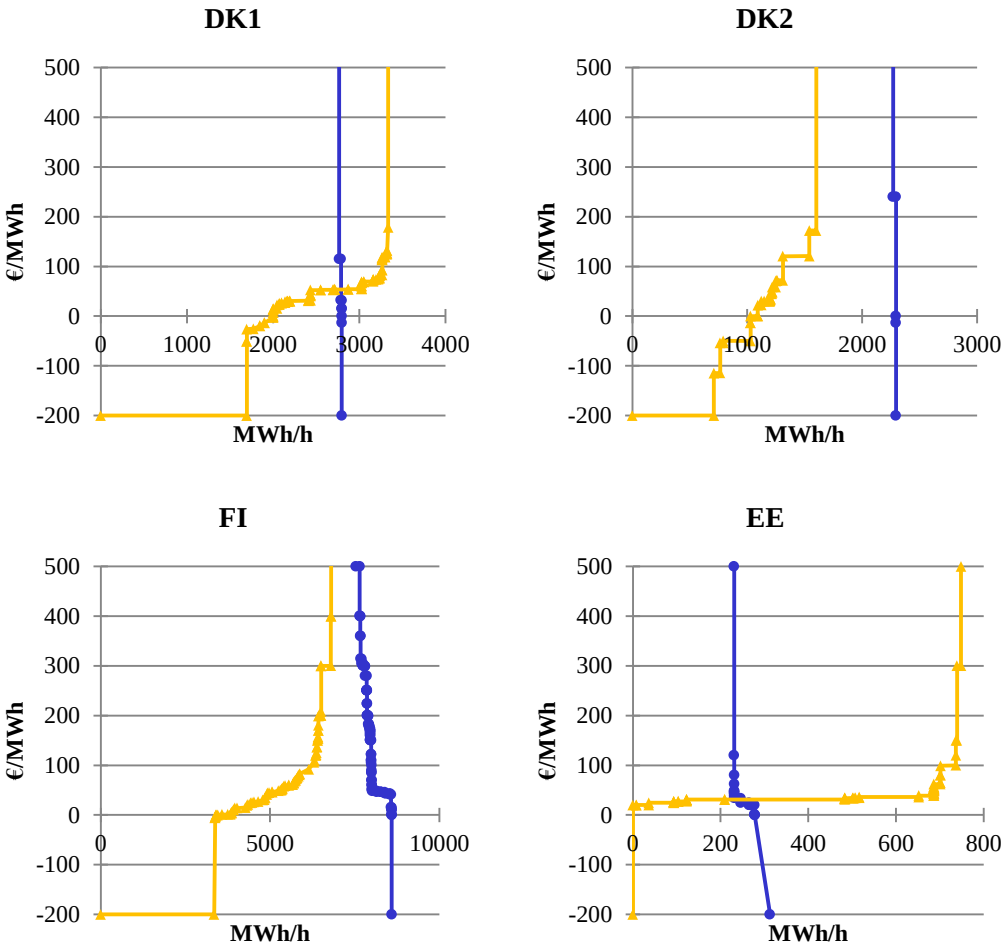

Figure 4-2 OptFlow bid curves = Nord Pool Spot for other Elspot areas, 15/12-2010, hour 19

In Table 4-1 – Table 4-4 we compare the actual Nord Pool Spot prices and quantities of hour 19 15/12-2010 to prices and quantities obtained from the OptFlow model. Columns (I) show the actual values from the Elspot market clearing. The corresponding OptFlow values shown in columns (II) and (III) are computed using two different bid curve scenarios: For the values in columns (II), the actual bid curves submitted to Nord Pool Spot for this hour are used, whereas the numbers in columns (III) result from computing the "Nord Pool Spot market clearing" using our calibrated bid curves. For the OptFlow computations we have used the actual Nord Pool capacities for (aggregate) interzonal connections. Intrazonal capacity constraints, constraints related to Kirchhoff's second law, as well as security constraints, have all been relaxed. Hence, the OptFlow model used closely resembles the model used for the computation of the Elspot prices.

If we consider the three price vectors in Table 4-1, we see that the Elspot prices (I) and the area prices calculated by the OptFlow model with Nord Pool Spot bid curves (II) match exactly[5]. This shows that the OptFlow model is capable of reproducing the Nord Pool Spot results when using the same bid

[5] We do not reproduce the actual Elspot system price in the Optflow model, however, this may be due to differences in accepted block bids between the system price and the actual area prices.

curves. Moreover, the differences between the actual Elspot prices (I) and the OptFlow area prices calculated on the basis of the disaggregated OptFlow bid curves (III) are quite small. Contrary to (I) and (II), the disaggregated bid curves cover 100 % of production and consumption, thus it is difficult to calibrate the bid curves so as to match the prices of the aggregated curves exactly. However, the relatively small differences between (I) and (III) show that the disaggregation we have developed works reasonably well in aggregate, although it still leaves a great deal of uncertainty with respect to how accurate the distribution of production and consumption on the nodes within the bidding areas is. This is however, as close as we can come with the data provided.

Table 4-2 – Table 4-4 show production, load and exchange for the Nord Pool Spot areas for the three model variants. The differences between the Elspot quantities (I) and OptFlow quantities with Elspot bids (II) are due to imports from and exports to the power markets adjacent to the Nord Pool area, i.e., Russia, Latvia, Poland, Germany, and the Netherlands[6]. The OptFlow quantities with Elspot bids (II) differ somewhat from the OptFlow quantities with calibrated bid curves (III), especially for Norway, but the exchange quantities match quite well. This is expected, since at Nord Pool Spot, trades across price areas must be bid into Elspot, while trades within the price areas need not to do so. The generation and load volumes of solution (III) is thus expected to be higher than the Elspot volumes in (I) and (II) for the Norwegian areas, while the exchange values of the various solutions in Table 4-4 should be (at least approximately) equal. Refer also the above comments to Figure 4-1.

Based on the limited data available on disaggregated bid curves, we conclude that the disaggregation in (III) is a reasonable starting point for analyzing different congestion management methods for hour 19, 15/12-2010. In order to evaluate the effects on the disaggregated power system, we need all production and consumption represented. Thus, the prices and quantities of column (III) is the starting point of our comparisons, i.e. column (III) will represent the "Nord Pool Spot" area price solution.

Table 4-1 Comparison of prices for three model variants, 15/12-2010, hour 19

Bidding area	(I) NPS actual area prices	(II) OptFlow prices with NPS bid curves	(III) OptFlow prices with calibrated bid curves
NO1	104,56	104,56	105,63
NO2	104,56	104,56	105,63
NO3	130,50	130,51	130,70
NO4	130,50	130,51	130,70
NO5	104,56	104,56	105,63
DK1	130,50	130,51	130,70
DK2	130,50	130,51	130,70
SE	130,50	130,51	130,70
FI	130,50	130,51	130,70
EE	38,95	38,95	38,95

[6] In order to reproduce the Elspot prices we have accounted for exports and imports by including price independent bids in the adjacent areas. The flows between Norway and the Netherlands, and between Russia and Finland/Norway, are included in the Elspot bid curves for NO2, NO4, and Finland, respectively. We have adjusted the respective bid curves for NO2, NO4, and Finland so that solution (II) only represent domestic generation and load. The quantities used for imports and exports are based on the exchange data published at Nord Pool Spot's web page.

Table 4-2 Comparison of production quantities for three model variants, 15/12-2010, hour 19

Bidding area	(I) NPS production	(II) OptFlow production with NPS bid curves	(III) OptFlow production with calibrated bid curves
NO1	4435	4435	5021
NO2	5762	5762	6645
NO3	1580	1580	2344
NO4	2693	2666	3142
NO5	1656	1656	3028
DK1	3323	3323	3323
DK2	1994	1541	1541
SE	19619	19219	19201
FI	7765	6378	6378
EE	723	668	668

Table 4-3 Comparison of load quantities for three model variants, 15/12-2010, hour 19

Bidding area	(I) NPS load	(II) OptFlow load with NPS bid curves	(III) OptFlow load with calibrated bid curves
NO1	6210	6210	6754
NO2	3152	2451	3344
NO3	1746	1746	2548
NO4	1388	1388	1850
NO5	1092	1091	2494
DK1	2993	2767	2767
DK2	2294	2294	2294
SE	22334	22334	22293
FI	7984	7984	7984
EE	358	231	231

Table 4-4 Comparison of exchange quantities for three model variants, 15/12-2010, hour 19

Bidding area	(I) NPS net exchange	(II) OptFlow net exchange with NPS bid curves	(III) OptFlow net exchange with calibrated bid curves
NO1	-1775	-1775	-1734
NO2	2610	3311	3300
NO3	-166	-166	-204
NO4	1305	1278	1292
NO5	565	565	534
DK1	330	556	556
DK2	-300	-753	-753
SE	-2715	-3115	-3091
FI	-219	-1606	-1606
EE	365	437	437

In the following, we compare prices and quantities for different congestion management methods, including nodal pricing, optimal zonal pricing (taking into account all constraints) and simplified zonal pricing (area prices like Nord Pool Spot, disregarding loop flow and intrazonal constraints).

4.2 Prices

Table 4-5 compares four sets of prices for hour 19 on 15/12-2010. Actual Nord Pool Spot prices are given in the first price column (corresponding to (I) / (II) in Table 4-1), while the second and third columns show, respectively, the simplified and optimal zonal prices calculated by the OptFlow model. The simplified zonal prices correspond to (III) in Table 4-1, while optimal zonal prices take into account the specific location of all bids on the nodes and all constraints of the disaggregated power system. The three rightmost columns show descriptive statistics for the optimal nodal prices within each price zone. We see that when moving from simplified zonal prices (= area prices) to optimal zonal or nodal prices, prices increase in NO1, NO2, NO5, while prices decrease in NO4. The prices in the other areas remain almost the same or vary around the corresponding simplified zonal prices. Note however, that the price vectors are not directly comparable, since actual and simplified area prices do not take into account all constraints in the system. We will come back to this point later.

Table 4-5 OptFlow prices versus actual Nord Pool Spot prices, 15/12-2010, hour 19

Bidding	Actual	Zonal prices		Optimal nodal prices		
area	NPS	Simplified	Optimal	Average	Min	Max
NO1	104,56	105,63	137,08	131,15	131,12	131,28
NO2	104,56	105,63	110,00	131,13	131,13	131,14
NO3	130,50	130,70	137,57	131,44	131,33	131,72
NO4	130,50	130,70	87,53	80,09	74,89	120,09
NO5	104,56	105,63	1999,87	774,29	125,22	2000,00
DK1	130,50	130,70	114,43	131,13	131,13	131,13
DK2	130,50	130,70	172,00	131,13	131,13	131,13
SE	130,50	130,70	137,24	130,54	93,65	132,52
FI	130,50	130,70	134,86	129,27	129,27	129,27
EE	38,95	38,95	36,10	38,95	38,95	38,95

From Table 4-5, we notice that NO5 experiences a tremendous price increase compared to the simplified zonal prices, and that the maximum nodal price in NO5 is equal to the price cap of Nord Pool Spot of 2000 Euros/MWh (the optimal zonal price in area NO5 is also close to the price cap). In Figure 4-3 we have sorted the optimal nodal prices from the lowest to the highest. The colors show which bidding area the nodal prices belong to. On the first axis the price columns are weighted by the consumption in the nodes. The figure shows that only a few prices are close to the maximum price, whereas the other prices take on values mostly below 132 Euros/MWh. The figure shows that most of the price variation is linked to a small share of the total consumption.

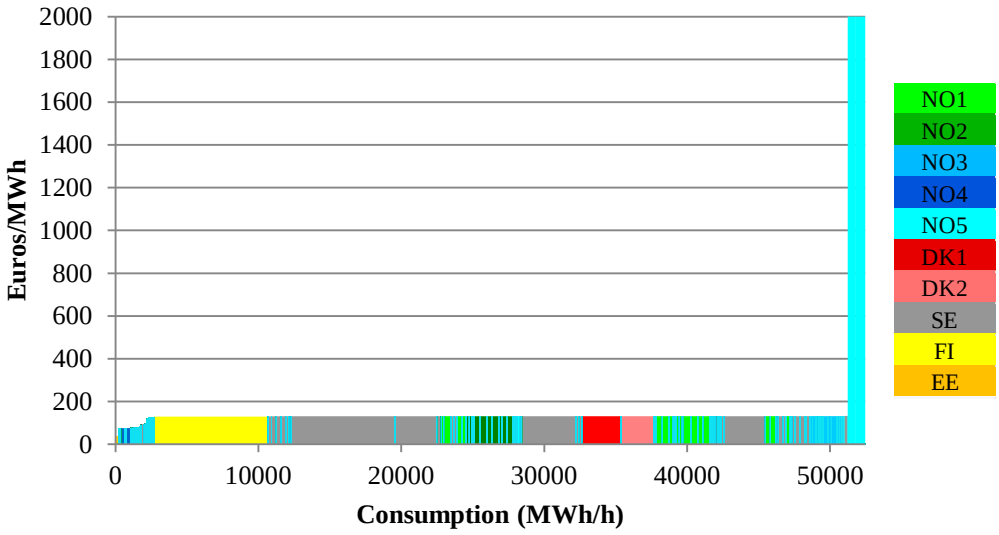

Figure 4-3 Variation in nodal prices, 15/12-2010, hour 19

Looking more closely at the price data, we see that the nodes with prices equal to the price cap are Arna, Fana, and Mongstad. In Figure 4-4 we show the market clearing prices and quantities for these nodes together with the bid curves in the nodes. Considering the Arna node, the red colored upward sloping curve is the supply curve, and the dotted vertical line close to its steepest part represents the quantity supplied at the market clearing price of 2000 Euros/MWh. The demand curve in Arna is represented by the vertical blue line, showing an inelastic demand of 677 MWh/h. The Nord Pool Spot price cap of 2000 Euros/MWh is implemented in the OptFlow model, and can be illustrated in the Arna node by the horizontal blue colored segment of the demand curve[7].

[7] Likewise, a horizontal segment at price equal to 2000 Euros/MWh could represent the price cap in the supply curves. This is however not implemented in the OptFlow model.

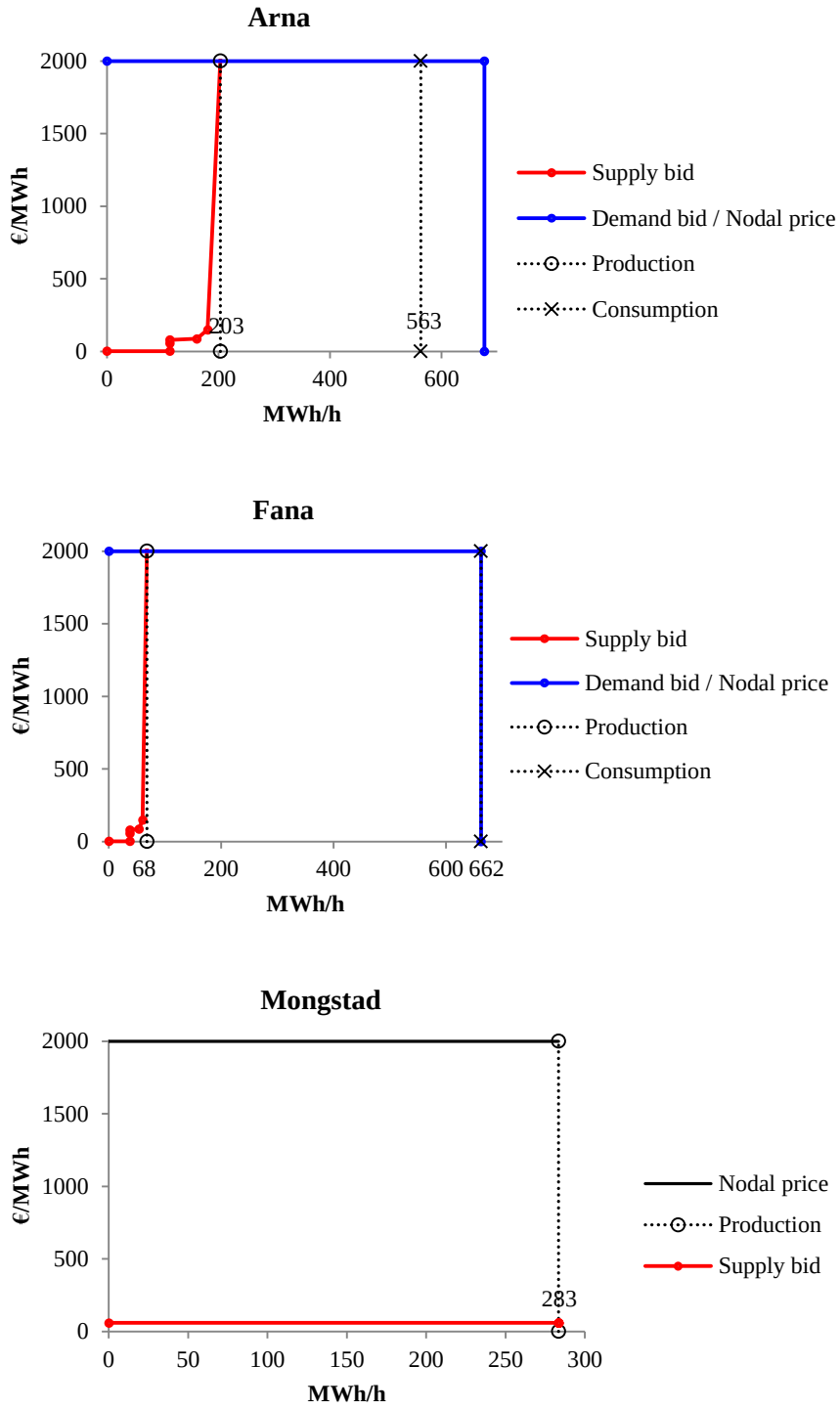

Figure 4-4 Bid curves and market clearing prices and quantities for Arna, Fana, and Mongstad, 15/12-2010, hour 19

From Figure 4-4 we see that at the market clearing consumption quantity in the Arna node is on the horizontal extension of the demand curve, at 563 MWh/h. This is the optimal solution returned when allowing for nodal pricing and taking into account all constraints of the problem, i.e. both the thermal capacity constraints and the cut constraints imposed for security reasons. The solution is technically

feasible in the OptFlow model, however, in economic terms, we are dealing with an infeasibility. The difference between the inelastic demand and the "market clearing" demand can be interpreted as the necessary curtailment of consumption in the Arna node in order to obtain a feasible flow. The difficult constraints in the present case are the cut constraints Bergen 1 and Bergen 2, which impose the following requirements:

Bergen 1: Flow (Fana-Samnanger) + Flow (Evanger-Dale) $\leq$ 670 MW

Bergen 2: Flow (Fana-Samnanger) + Flow (Dale-Arna) $\leq$ 670 MW

In the present case, these two cut constraints are not possible to comply with unless the price is at the price cap and the quantity is lower than 677 MWh/h[8].

This corresponds to the situation referred to by Bye et al. (2010) and described by various other reports like Baldursson et al. (2011); that is to say, for long periods the Norwegian power system has been operated at below agreed upon security standards, due to high loads and/or lack of transmission capacity. In a nodal pricing system, this becomes very visible, as do the representations of the security constraints imposed. In the following analyses of the 15/12-2010, hour 19 case, we relax the infeasible cut constraints. I.e. the Bergen 1 and Bergen 2 cut constraints are removed from the disaggregated optimization problems of the OptFlow model. The relaxation will change the optimal nodal and zonal prices, while the simplified zonal prices will be unaffected, since the cut constraints are not directly included in this price calculation anyway[9].

Summary data for the new prices is given in Table 4-6 and shows that all prices are now below 141 Euros/MWh. Moving from simplified zonal prices to optimal zonal or nodal prices results in price increases in NO1, NO2, NO3, NO5, and FI. Prices decrease in NO4, while for the rest of the areas optimal prices vary around the simplified area prices or are fairly unaffected by the change (EE). Again, the price vectors are not directly comparable, since actual and simplified area prices do not take into account all constraints in the system, thus at these prices, the resulting flows will not comply with the system constraints.

[8] In the present case, there are alternative optimal solutions, curtailing demand in Arna or Fana, or a combination of the two. In principle, we could also have solutions producing at levels above the capacity limits in the Arna, Fana or Mongstad nodes. However, in our implementation, infeasibilities will always be handled by curtailing demand.

[9] In practice, the cut constraints may affect the import and export capacities that the system operators set between the bidding areas, and that are given to the Elspot market clearing.

Table 4-6 Prices with relaxed Bergen security constraints, 15/12-2010, hour 19

Bidding area	Actual NPS	Zonal prices		Optimal nodal prices		
		Simplified	Optimal	Average	Min	Max
NO1	104,56	105,63	140,51	139,25	139,21	139,40
NO2	104,56	105,63	110,00	139,23	139,23	139,24
NO3	130,50	130,70	141,04	139,59	139,45	139,91
NO4	130,50	130,70	88,19	80,74	74,77	126,58
NO5	104,56	105,63	140,35	135,65	125,22	139,24
DK1	130,50	130,70	124,77	139,23	139,23	139,23
DK2	130,50	130,70	120,61	139,23	139,23	139,23
SE	130,50	130,70	140,69	138,51	93,65	140,83
FI	130,50	130,70	138,17	137,09	137,09	137,09
EE	38,95	38,95	36,10	38,95	38,95	38,95

Figure 4-5 and Figure 4-6 show the optimal nodal prices for consumption and production respectively, where prices are sorted from lowest to highest, and column widths represent volumes. For a quick visual comparison of aggregate price differences, the simplified zonal prices are shown in a similar way. Since the simplified zonal prices are also sorted from lowest to highest, the curves cannot be compared directly for each MW, in the sense that a specific point on the first axis may represent different locations in the two curves. For instance, the maximum priced node belonging to NO5 is located in the right hand part of the optimal nodal price curve, whereas it is located in the price segment at 105,63 Euros/MWh in the left hand part of the simplified zonal price curve. Thus the nodes / areas may have different sequencing in the two figures and in the two curves shown.

Comparing the total volume weighted prices (i.e. the areas under the curves) we notice that for this hourly case, the nodal prices are on average higher than the simplified zonal prices. The reason for this is that the nodal prices include shadow prices for all transmission constraints (except cut constraints Bergen 1 and Bergen 2), whereas the simplified zonal prices do not, thus implying a solution that results in infeasible flows (see also next section). We also notice that the nodes in a specific bidding area like NO1 and NO5 are placed at several different locations along the first axis, i.e. some nodes should be in the lower end of the price distribution, whereas others should be in the high price end, although for NO1 especially and NO5, the nodal price differences within the zones are not very large.

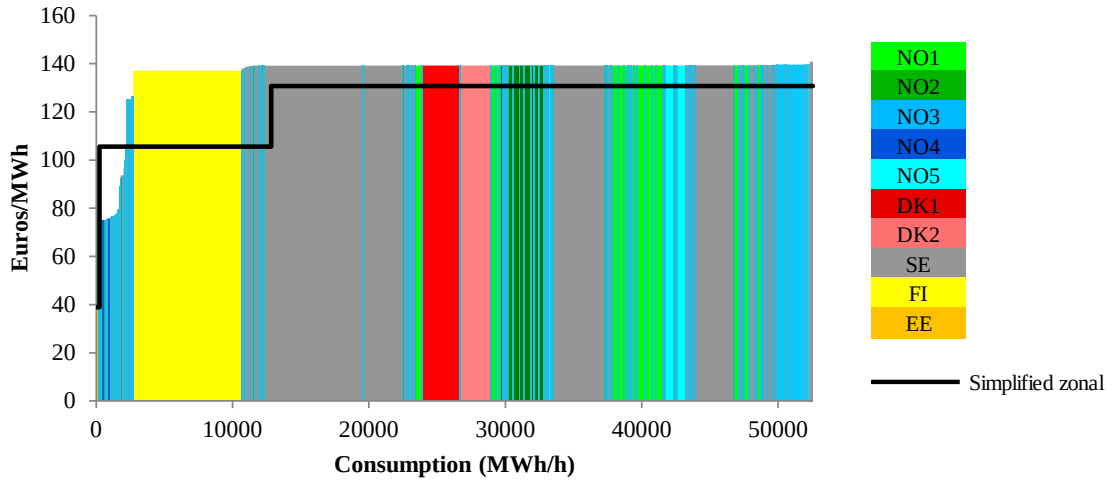

Figure 4-5 Nodal prices and load quantities, 15/12-2010, hour 19

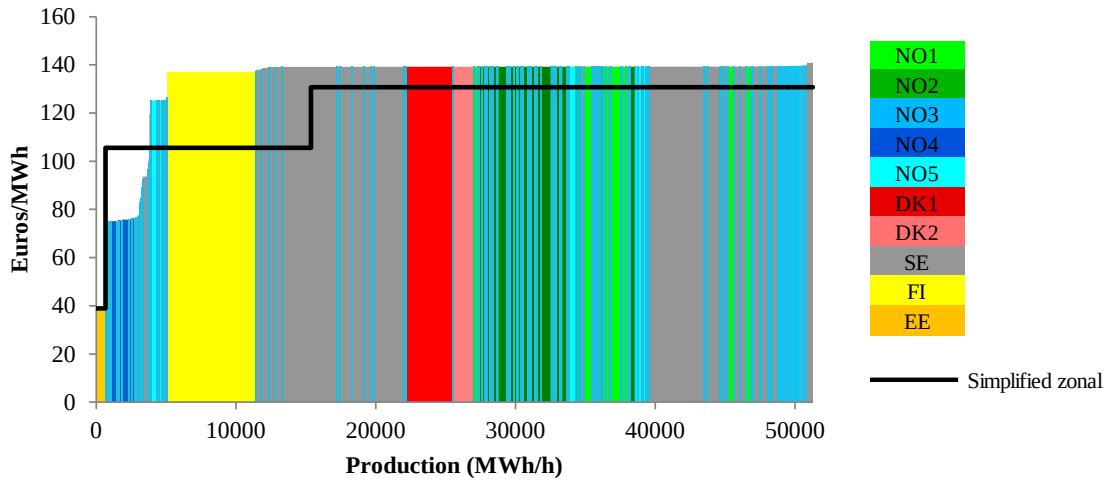

Figure 4-6 Nodal prices and production quantities, 15/12-2010, hour 19

Figure 4-7 and Figure 4-8 further illustrate the geographical variation in the optimal nodal prices. The color scale show different price intervals and the nodes are weighted by load and generation volumes. The node sizes show the concentration of load and production, although this also depends on the level of detail available on the power system in different parts of the Nordic power system (DK1, DK2, FI and EE being represented by single nodes). The figures also show that for the present hour there are exports from the Nord Pool area to Lithuania, the Netherlands and Germany (Figure 4-7) and imports to the Nord Pool area from Russia and Germany (Figure 4-8).

It is interesting to note from Table 4-6 and Figure 4-5 – Figure 4-8 that even if Sweden now has 27 different prices instead of one the prices are very similar, except for the Tornehamn node, with relatively low quantities.

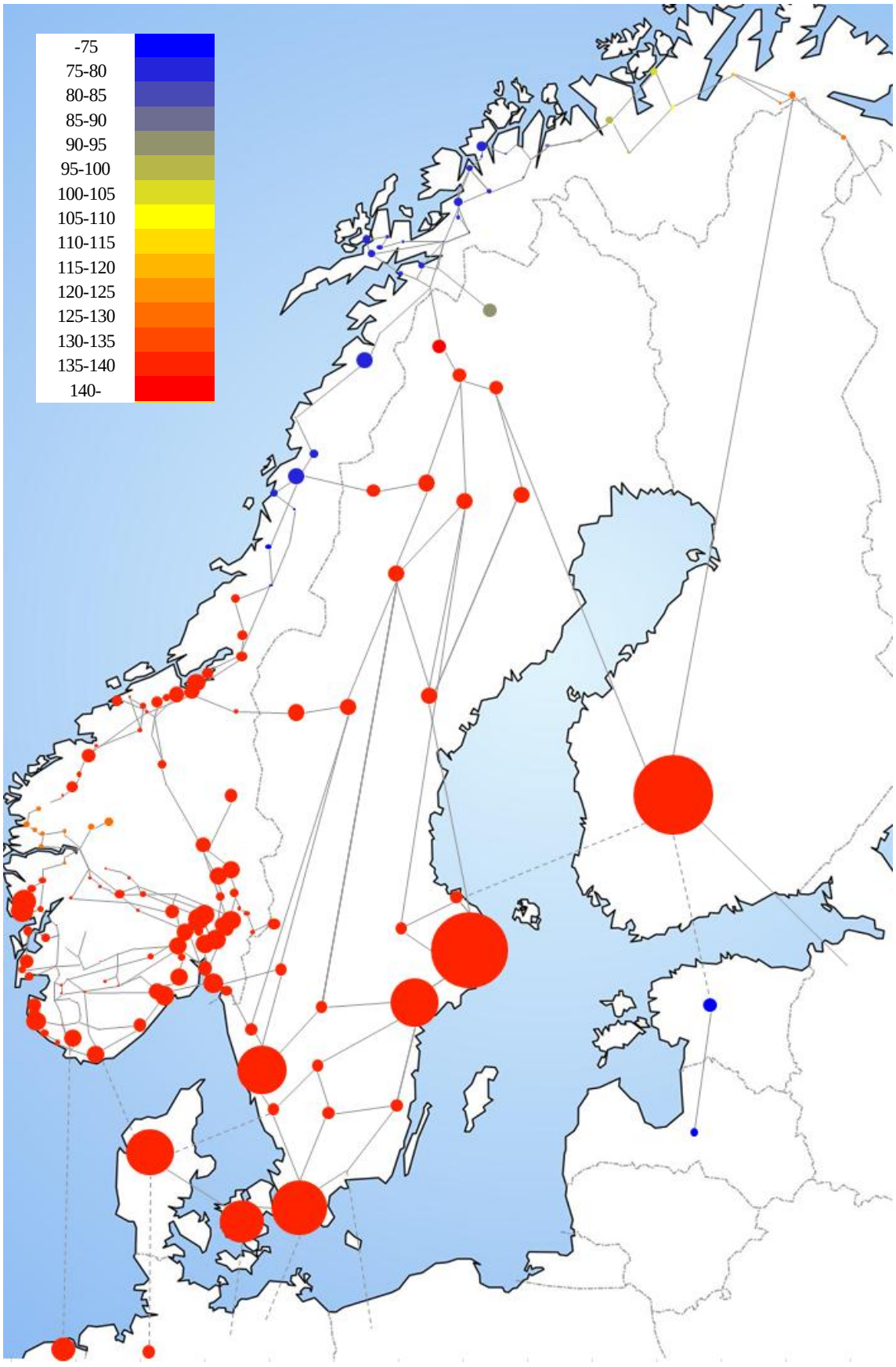

Figure 4-7 Nodal prices weighted by consumption, 15/12-2010, hour 19

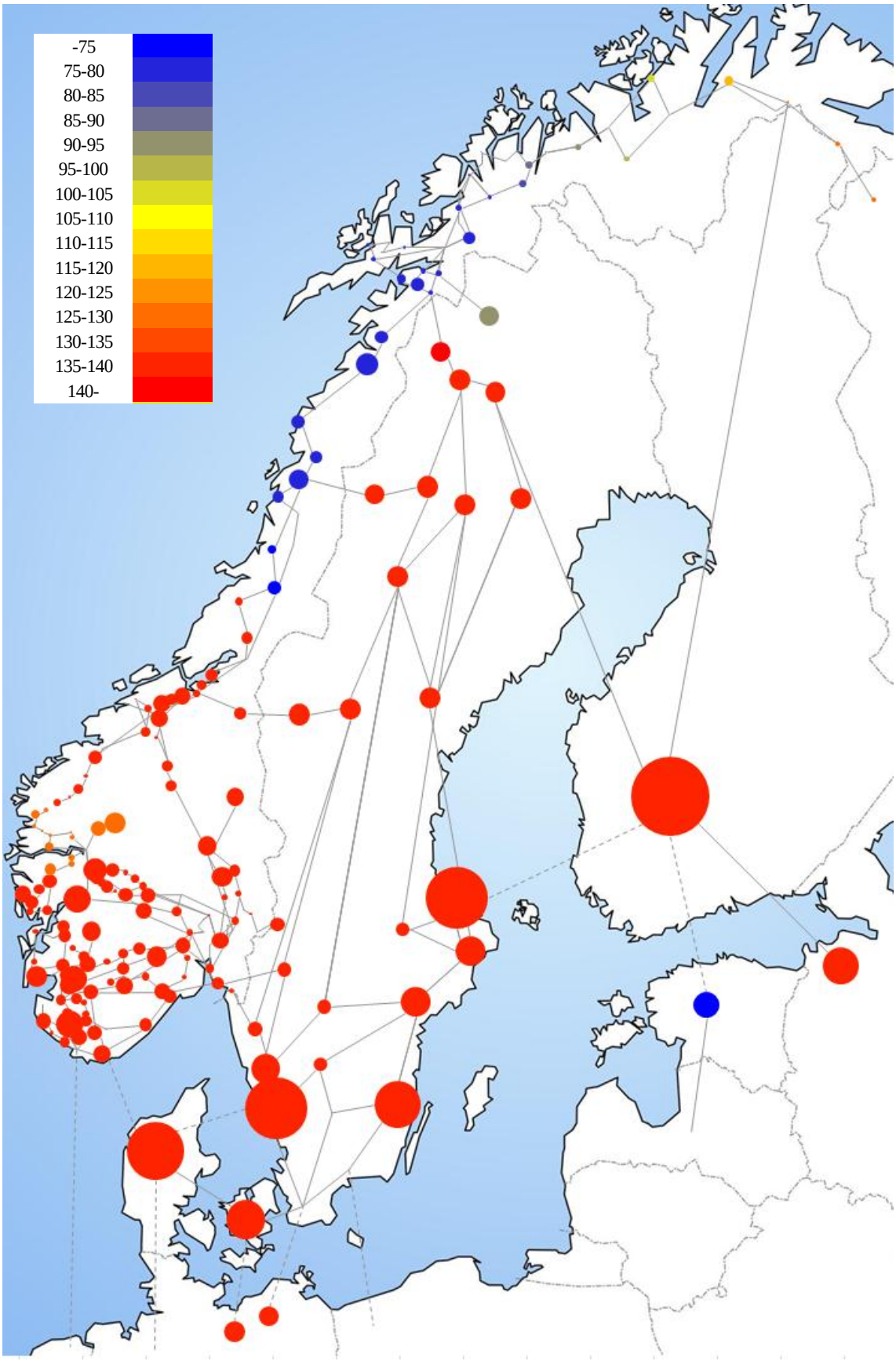

Figure 4-8 Nodal prices weighted by production, 15/12-2010, hour 19

In Figure 4-9 and Figure 4-10 we compare simplified and optimal zonal prices. The figures are similar to Figure 4-5 and Figure 4-6 for optimal nodal prices, except that we have sorted simplified zonal prices from lowest to highest, and shown the corresponding optimal zonal price in the same sequence. Thus it is easier to compare the changes that result in the zonal prices from taking into account all constraints and the specific location of bids to nodes (optimal zonal prices) instead of only a subset of the constraints or some indirect representation of the constraints (simplified zonal prices). Figure 4-9 and Figure 4-10 elaborates on what is already shown in Table 4-6, that some zonal prices increase while others decrease. Moreover, as a weighted average, prices increase when all constraints are taken care of in the optimal zonal prices. The simplified zonal prices are lower on average (volume weighted), but on the other hand, as we will look more closely into in the next section, they result in infeasible power flows.

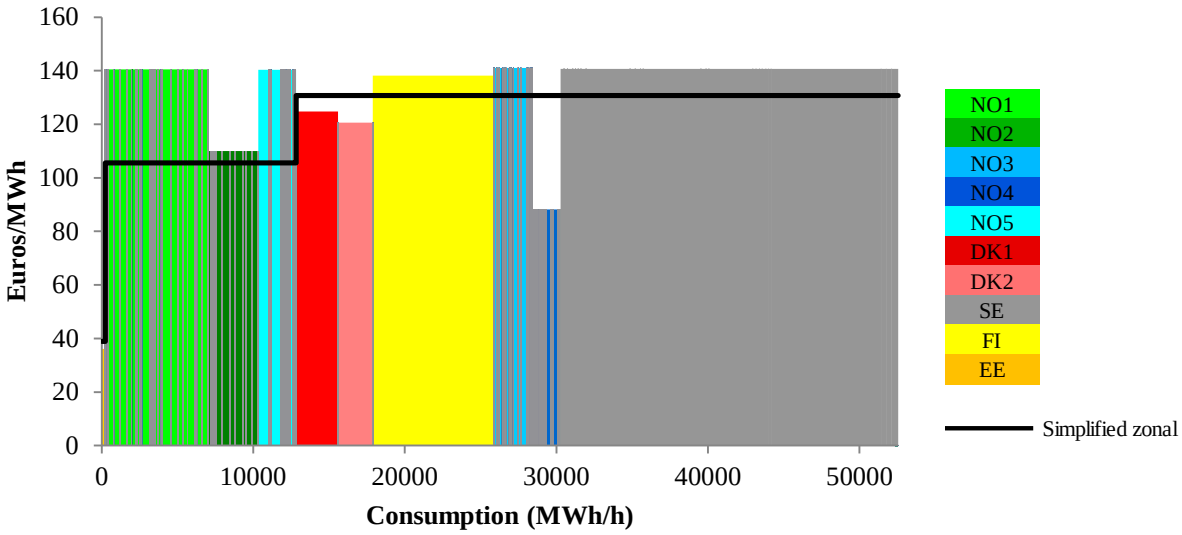

Figure 4-9 Optimal zonal prices and load quantities, 15/12-2010, hour 19

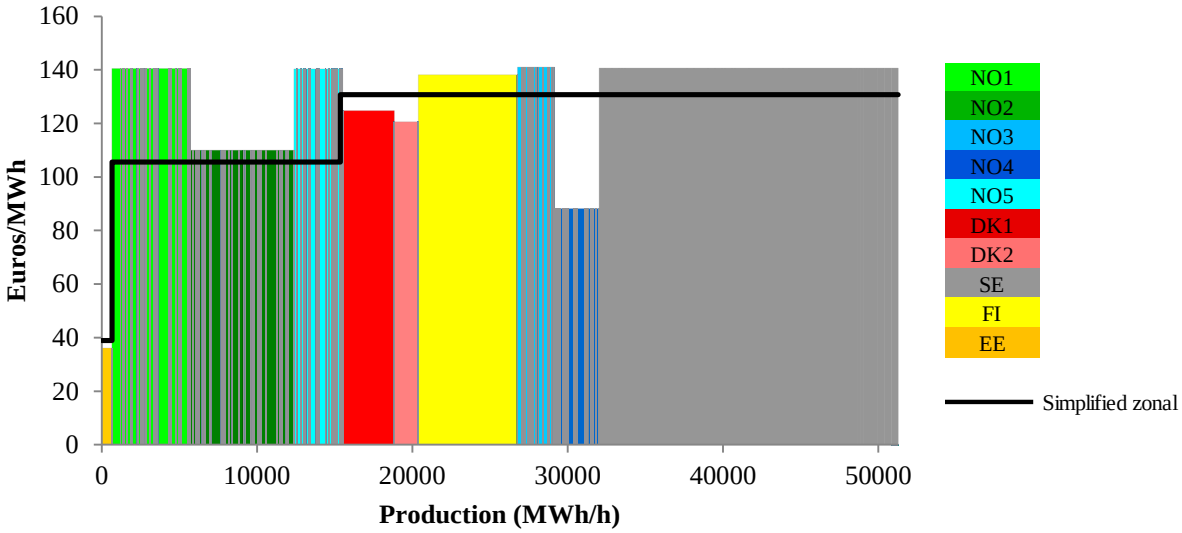

Figure 4-10 Optimal zonal prices and production quantities, 15/12-2010, hour 19

4.3 Power flows and bottlenecks

Since we do not consider power losses, price differences are related to bottlenecks in the power system. In this section we show a summary of the capacity utilization of the grid for the present case, and we investigate the status of the capacity constraints under the various pricing methodologies.

The power flows of the simplified zonal solution have been calculated using a two-stage approach. In the first stage, we compute the nodal supply and demand quantities from the simplified zonal prices (where line capacity constraints have been replaced by aggregate inter-zonal capacity constraints[10], and where loop flow is not considered). This can be done since we have constructed the disaggregated supply and demand curves, thus we allocate the zonal supply and demand to the nodes belonging to each zone. Based on the nodal load and generation quantities from the first stage, we compute the final line flows, using a detailed network model that also takes loop flow into consideration, but without considering any network capacity constraints, except some restrictions with respect to flows over HVDC lines[11]. Thus we obtain the power flows that will result from injections and withdrawals in the nodes that are consistent with the simplified zonal prices (refer also chapter 2). In case of ties, we choose a solution that maximizes social surplus. A similar procedure is used to find the flows in the unconstrained solutions[12].

Figure 4-11 shows the power flow of the nodal price solution. The links are weighted by the flow sizes, HVDC links are shown by dotted lines, and the binding thermal capacity constraints are shown in red colors. We notice that there are four links that are operated on their thermal capacity limits, and their capacities and the shadow prices on the constraints are shown in Table 4-7. The shadow prices show the value of increasing the corresponding thermal capacity limits, i.e. the increase in social surplus. For the present case, being able to increase the flow from EE to FI and from Tornehamn to Sildvik has the highest values.

Table 4-7 Shadow prices for binding capacity constraints with nodal pricing, 15/12-2010, hour 19

From	To	Max	Shadow price
EE	FI	365	98,15
Tornehamn	Sildvik	166	48,26
FI	Forsmark	550	2,07
DK1	Ringhals	740	0,02

[10] We have also included the cut constraints for Sweden (cut 2) and DK1 (cut B) that was used by Nord Pool Spot for this hour.

[11] Letting the flow over HVDC lines vary freely introduces too much freedom, and the solutions that we obtained with unrestricted HVDC flows were in many cases unreasonable. Since the flow over an HVDC line can be controlled in practice we think it is reasonable to restrict the flow over HVDC lines in the second stage. For the NO2-DK1 and DK2-SE lines we fix the flow in the second stage based on the first stage results. For the FI-SE line (Fenno-Skan) the situation is more complicated, since there is also an AC connection between Finland and Sweden, and the FI-SE flow from the first stage could represent either of the two connections between the two price areas. Instead of fixing the flow over the FI-SE HVDC line we have chosen to impose the capacity constraint for this line in the second stage. The flow in the second stage is chosen such that the sum of thermal losses is minimized.

[12] For the unconstrained solution, we impose the capacity constraints on the HVDC lines mentioned in footnote 11.

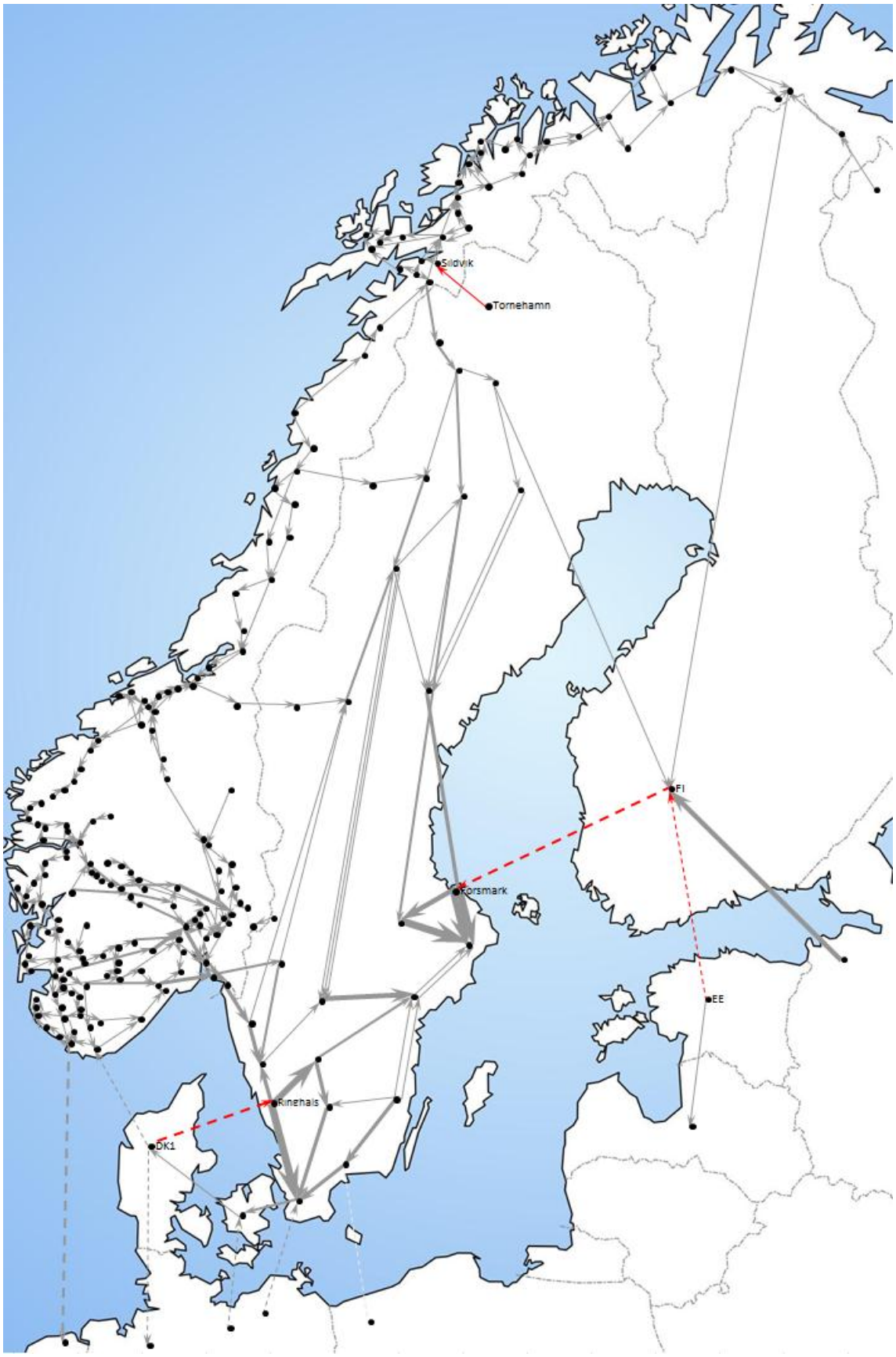

Figure 4-11 Line flows and thermal bottlenecks for optimal nodal price solution, 15/12-2010, hour 19

The histograms in Figure 4-12 – Figure 4-14 describe the utilization of the lines' thermal capacity limits under the three pricing methodologies that we consider. For nodal pricing, optimal, and simplified zonal pricing, respectively, the figures show the number of lines operating within different intervals of capacity utilization. We distinguish between inter-zonal lines (red color) and intra-zonal lines (blue color). For instance, in Figure 4-12 we can see that in the nodal price solution 7 lines (4 inter-zonal and 3 intra-zonal) are operated at between 90 and 100 % of their capacity. For the present case, we notice that, regardless of congestion management method, most of the lines are operated well below their thermal capacity limits. We can also see from Figure 4-14 that the simplified zonal approach results in infeasible power flows over some lines, i.e. power flows that exceed the line capacities. The figure shows that this occurred for 2 out of 301 lines, and one of these lines is inter-zonal.

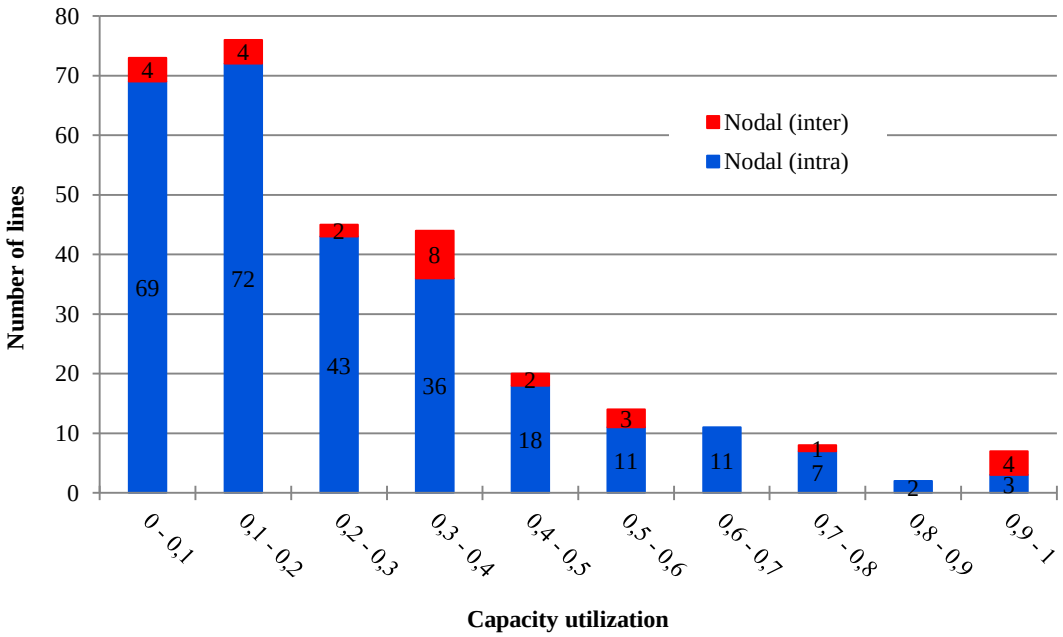

Figure 4-12 Line capacity utilization with nodal pricing, 15/12-2010, hour 19

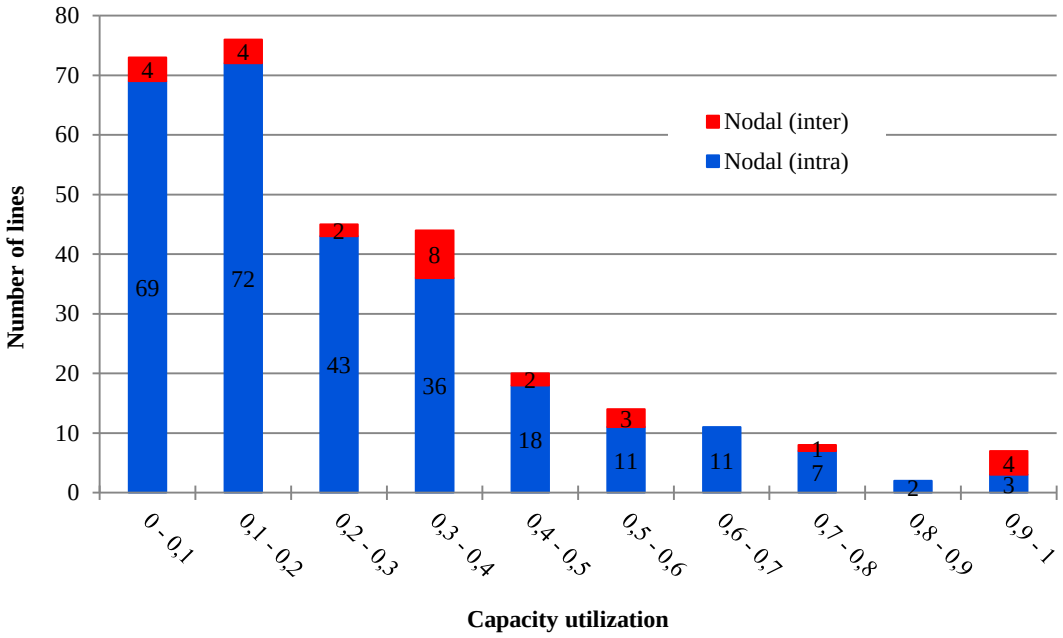

Figure 4-13 Line capacity utilization with optimal zonal pricing, 15/12-2010, hour 19

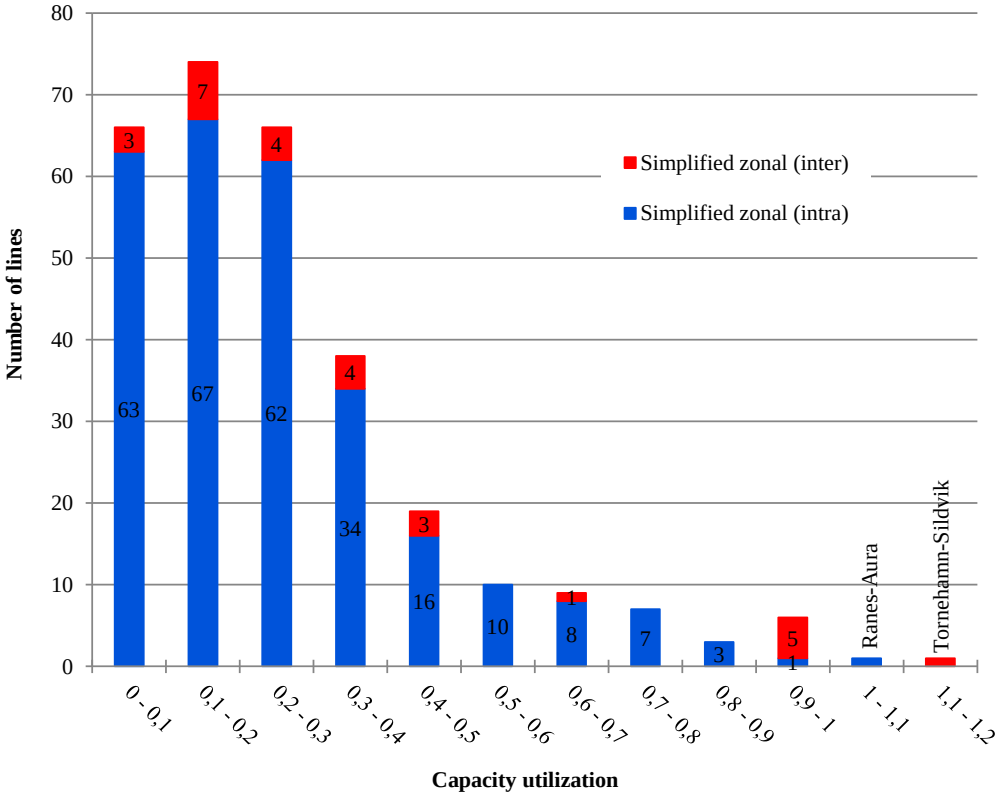

Figure 4-14 Line capacity utilization with simplified zonal pricing, 15/12-2010, hour 19

As discussed in section 4.2, the present case represents an instance in which it is necessary to relax some of the cut constraints: Bergen 1 and Bergen 2. In the nodal price solution, we have the following:

Bergen 1: Flow (Fana-Samnanger) + Flow (Evanger-Dale) ≤ 670 MW

475 + 266 = 744 > 670

Bergen 2: Flow (Fana-Samnanger) + Flow (Dale-Arna) ≤ 670 MW

475 + 293 = 768 > 670

This means that the relaxed cut constraints are overloaded by approximately 11 % and 15 % in the nodal price solution.

Figure 4-15 – Figure 4-17 show the utilization of the cut constraints for the different pricing methods, including the relaxed Bergen cuts. The figures show that Bergen 1 and Bergen 2 are infeasible in all the three solutions. Looking more closely at the nodal price solution, there are three cut constraints that are operated on their capacity limit[13]. The shadow prices for these three, Hasle eksport, Nordland, and Fardal overskudd 1, are given in Table 4-8.

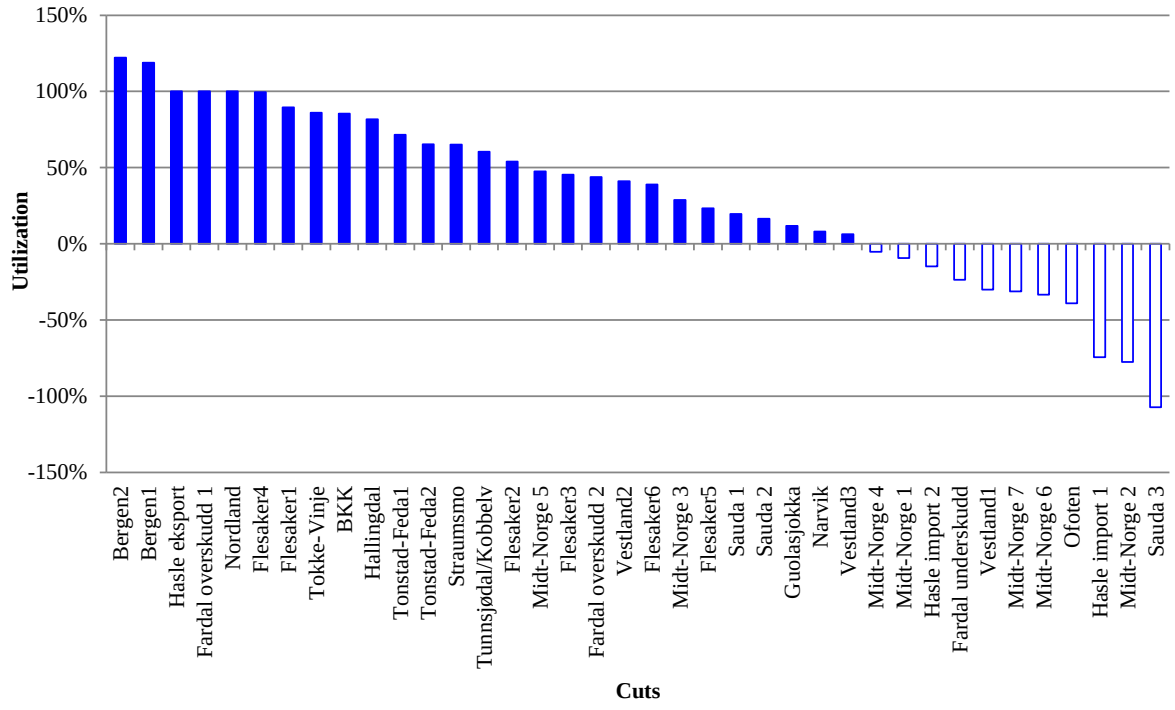

Figure 4-15 Cut capacity utilization with nodal pricing, 15/12-2010, hour 19

[13] In Figure 4-15, it seems like Flesaker 4 = 0.45 · Flow (Rjukan-Sylling) + Flow (Rød-Hasle) ≤ 1170 is also on its capacity limit. However, the capacity utilization is 99.5 % and the shadow price of the cut constraint is 0. Note also that since the cut constraints are direction dependent, capacity utilization below – 100 % does not constitute a problem.

Table 4-8 Shadow prices for cut capacity constraints with nodal pricing, 15/12-2010, hour 19

Cut name	Capacity	From	To	Share of flow included	Shadow price
Hasle eksport	1600	Hasle	Borgvik	1	*0,08*
		Halden	Skogssäter	1	
Nordland	1000	Ofoten	Ritsem	1	*65,26*
		Nedre Røssåga	Ajaure	1	
		Tunnsjødal	Verdal	1	
		Tunnsjødal	Namsos	1	
		Sildvik	Tornehamn	1	
Fardal overskudd 1	750	Modalen	Evanger	1	*14,02*
		Fardal	Aurland1	1	

While all the cut constraints, except the ones that are relaxed, are fulfilled in the optimal nodal and optimal zonal price solutions, we can see from Figure 4-17 that the Nordland cut is not satisfied in the simplified zonal solution. I.e. in addition to 2 of the thermal constraints, also one of the cut constraints is violated in the simplified zonal solution.

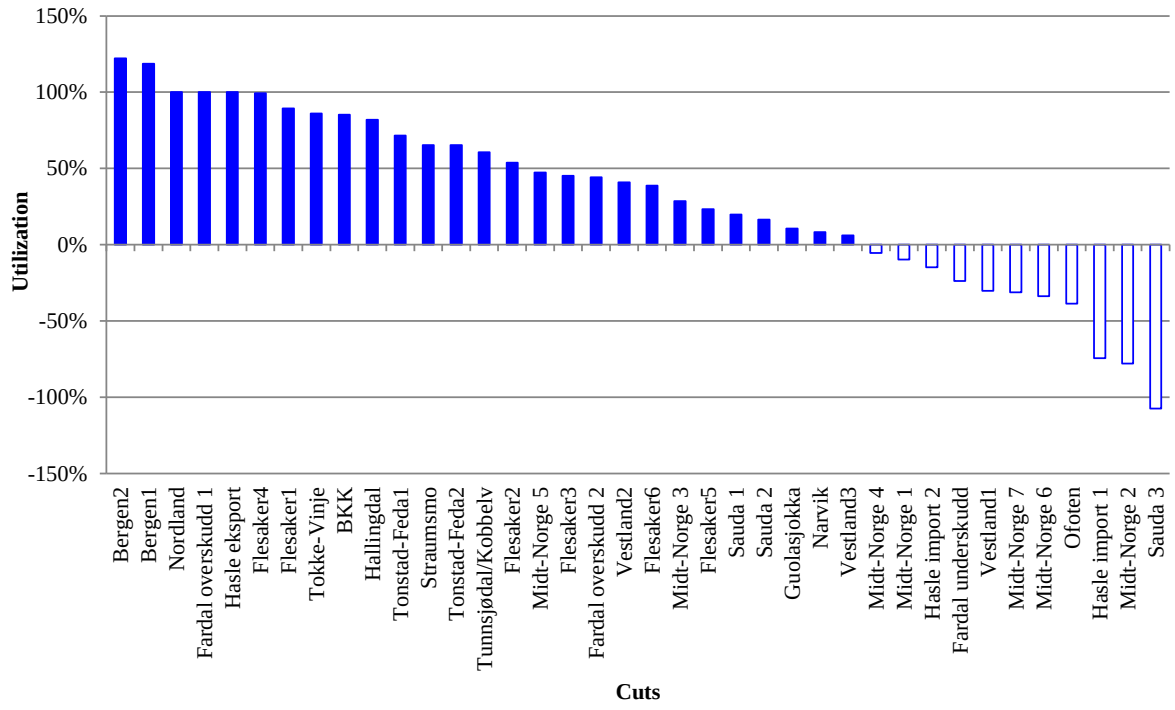

Figure 4-16 Cut capacity utilization with optimal zonal pricing, 15/12-2010, hour 19

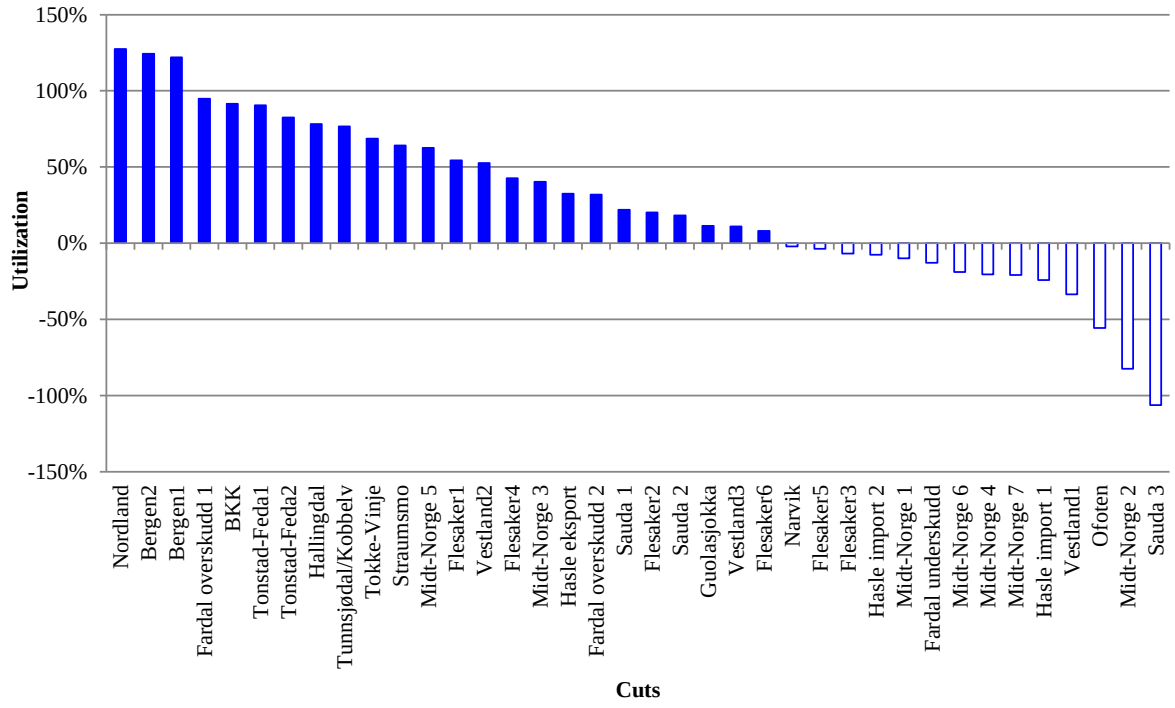

Figure 4-17 Cut capacity utilization with simplified zonal pricing, 15/12-2010, hour 19

4.4 Load and generation quantities

In this section we compare the load and generation quantities produced by the different pricing methods. In Figure 4-18 we show the differences in load for each node, i.e. the difference between the quantities consumed in the simplified zonal solution and the quantities consumed in the optimal nodal and the optimal zonal solutions. We notice that the differences are quite small. The consumed quantities at optimal nodal and zonal prices are almost identical, and the differences between these two solutions and the simplified zonal solution are quite small. This is due to the relatively inelastic demand in the present case. With rather high prices, the market outcomes are on the inelastic parts of the demand curves, even in nodes where there is some elastic demand (like energy-intensive industry).

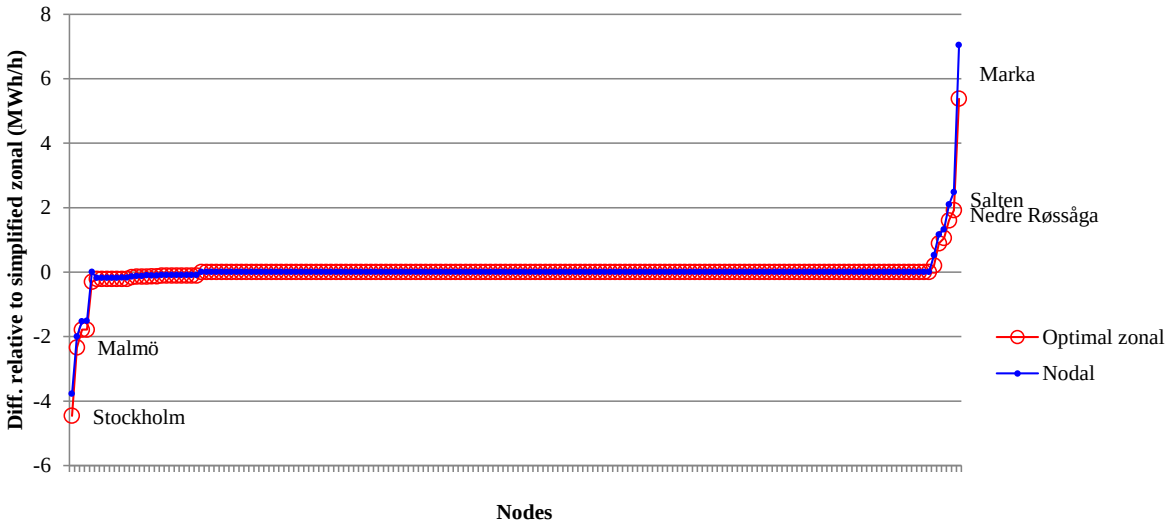

Figure 4-18 Differences in load between simplified zonal and the other two pricing approaches, 15/12-2010, hour 19

Figure 4-19 shows the same differences for generation quantities. We observe that in general, the quantity differences are larger for generation than for consumption, especially between the simplified zonal solution and the other two solutions. Optimal nodal and optimal zonal quantities are quite similar, except for EE. The latter can be illustrated by Figure 4-20, which shows the stepwise generation bid curve for Estonia. At the optimal nodal price / simplified zonal price (these are equal according to Table 4-6) the price curve hits the supply curve at an almost horizontal part. Even a very small price reduction would change the quantity quite much when the supply curve takes this form.

In Figure 4-21 we show the bid curves for Nedre Røssåga, the node where the optimal nodal / optimal zonal generation differs most from the generation at the simplified zonal price. From the upper part of the figure we see that the change in nodal price is quite large, and this leads to a significant reduction in quantity produced. For the optimal zonal price in the lower part of the figure, we see that the price reduction is smaller. However, the quantity reduction is of similar size. This is one of the instances where the optimal zonal price solution has a price strictly higher than the marginal cost (see also Appendix 5 for a description of this phenomenon).

The production of Nedre Røssåga is strongly affected by the limitations of the Nordland cut. This is also the case for the other nodes in Figure 4-21 that have large reductions in generation when moving from the simplified zonal solution to the optimal nodal/zonal price. Similarly, the largest positive quantity differences are linked to nodes that are located close to the Fardal cut (refer Table 4-8 which shows the cut constraints with positive shadow prices). These two cuts will be discussed further in Section 4.6.2, where we discuss the number of price areas.

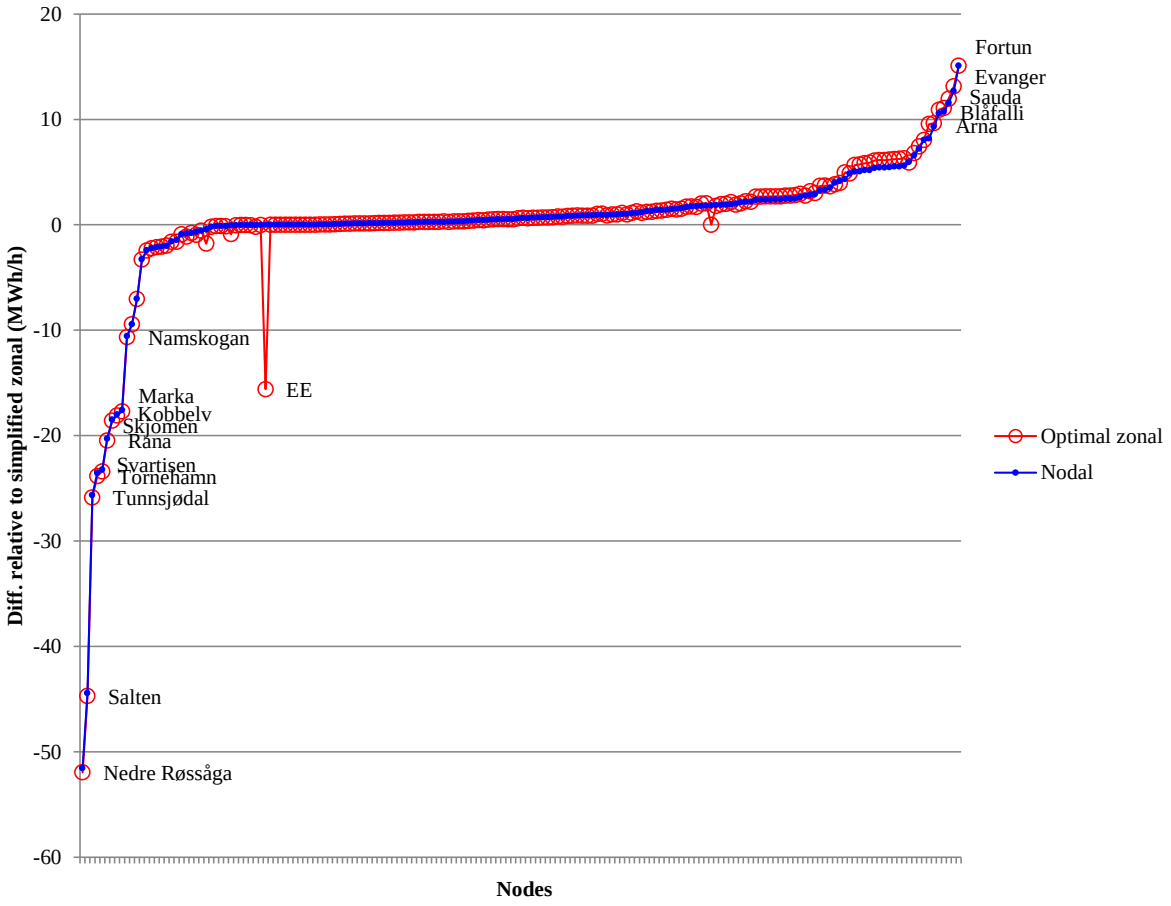

Figure 4-19 Differences in generation between simplified zonal and the other two pricing approaches

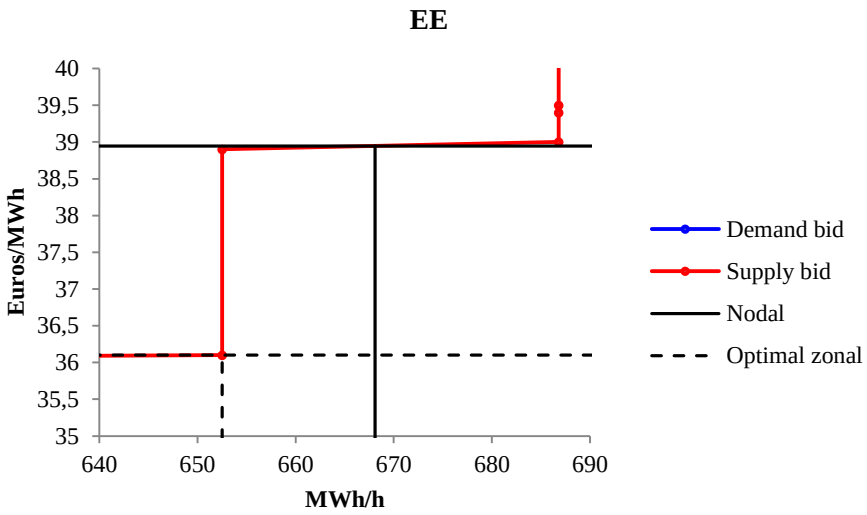

Figure 4-20 Differences in generation, Estonia

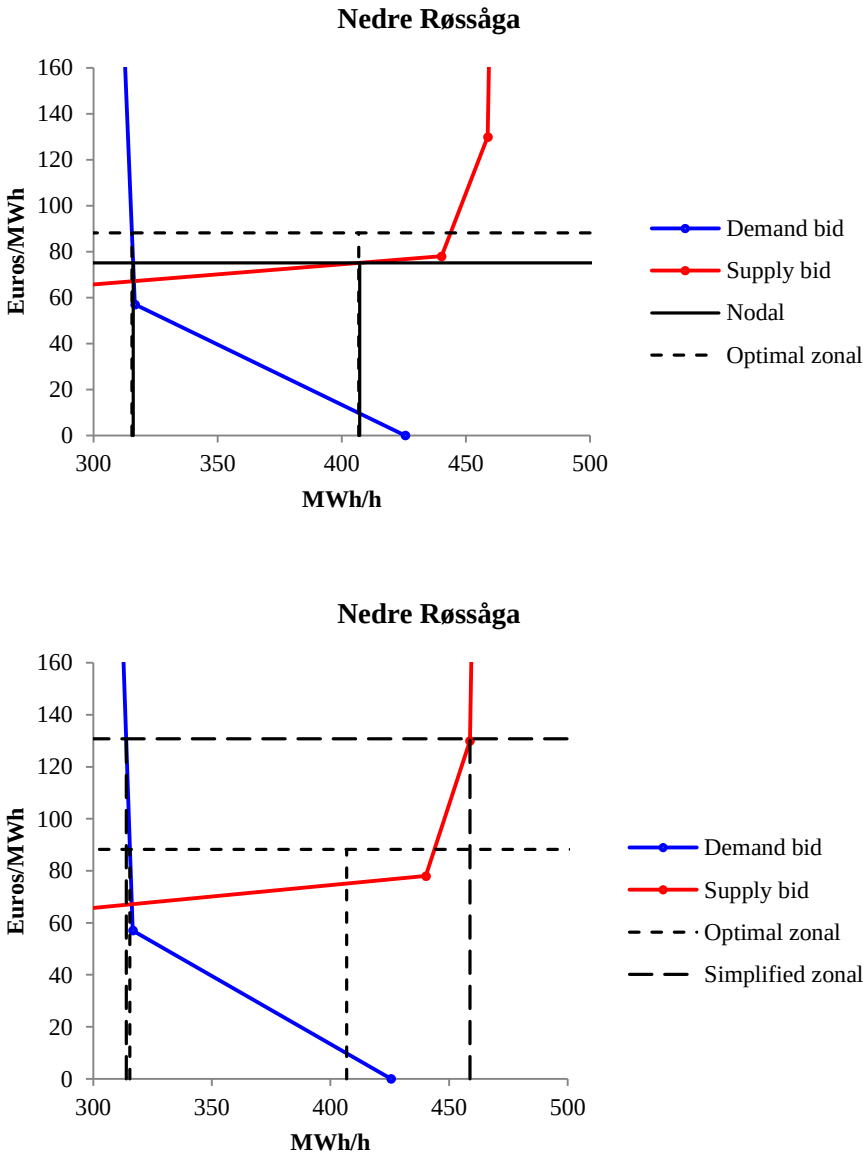

Figure 4-21 Differences in generation, Nedre Røssåga

4.5 Surpluses

In Table 4-9 we show the changes in surplus compared to the unconstrained market solution. The absolute values of the consumer surpluses are not very meaningful, since demand is very inelastic, at least for high prices, and we have capped the consumer surplus at the price cap of 2000 Euros / MWh. This way, the consumer surplus and the total social surplus are very much affected by the price cap. Moreover, since the surpluses of the simplified zonal solution are not comparable to the optimal nodal and zonal prices that take into account all constraints, we have shown the number of overloaded thermal and security constraints in the last row of the table. Alternatively, we should model counter trading, and take into account any efficiency effect from those. This is however, not straightforward. In order to obtain reasonable solutions in such a model, we need to make assumptions on the degree of

flexibility in real time for the different producers and consumers (demand response). If we assume the same bid curves both for the day-ahead and the balancing / regulation market, an optimal re-dispatch takes us to the optimal nodal price solution. This is if we do not take into account any start up restrictions or other kinds of inflexibility neither in the day-had market nor the real time market.

For the present case, we see that moving from simplified zonal prices to optimal zonal or nodal prices leads to a reduction in consumer surplus, and an increase in producer surplus and grid revenue. The grid revenue increases most with optimal zonal prices, and the producer surplus increases most with nodal pricing. Since we disregard some constraints in the simplified zonal solution, the total surplus seems to go down a bit, however this must be balanced by the infeasibilities that are left in the simplified zonal solution and which are dealt with in the optimal zonal and optimal nodal solutions. In the end, the infeasibilities must be taken care of in the simplified zonal solution too, this may be costly for society, and this cost is not reflected in Table 4-9.

Table 4-9 Unconstrained surplus and surplus differences (1000 Euros), 15/12-2010, hour 19

	Un-constrained	Simplified zonal	Optimal zonal	Nodal
Producers	6799,5	38,0	451,8	624,8
Consumers	99249,1	-111,7	-639,5	-761,4
Grid	0,0	68,6	170,4	120,9
Total	106048,7	-5,1	-17,3	-15,6
Infeasibilities	2 lines 1 cut	2 lines 1 cut	None	None

(Bergen 1 and Bergen 2 are overloaded in all solutions.)

We see that the difference between total surplus in the unconstrained solution and the optimal nodal price solution is 15600 Euros. This corresponds to the minimum congestion cost possible for this hour. The optimal zonal price solution would lead to a small increase in the congestion cost, to 15700 Euros.

4.6 Sensitivity analyses

In this section we present different sensitivity analyses. We have focused on the effects of

- The transfer limits set between zones
- The number of price areas
- The implementation of security constraints
- Increasing the demand elasticity

4.6.1 Effects of capacities in aggregated network

In this section we show how the capacities set on the aggregated zonal interfaces affect the area prices of the simplified zonal model and the utilization of individual link capacities and cut constraints. We focus on the links and cuts that at some point are violated or close to being so.

As an example, consider the capacity between NO1 and SE, often referred to as the Hasle interface[14]. Figure 4-22 shows the effects of changing the aggregate capacity of NO1-SE on some of the individual line flows that are at the capacity limit (green lines) or above (red and blue lines). The nominal capacity of the NO1-SE connection is 2145 MW (dotted vertical line on the right hand side), while the capacity given to the market for the specific hour is 600 MW (dotted vertical line on the left hand side of the figure). We notice that when reducing the capacity of NO1-SE the utilization of Tornehamn-Sildvik and Ranes-Aura increases, but most of the increase takes place below the Nord Pool Spot capacity of 600 MW. The lines marked in green color are unaffected by the NO1-SE capacities. However, some of these flows are restricted to be on or below the capacity limits[15].

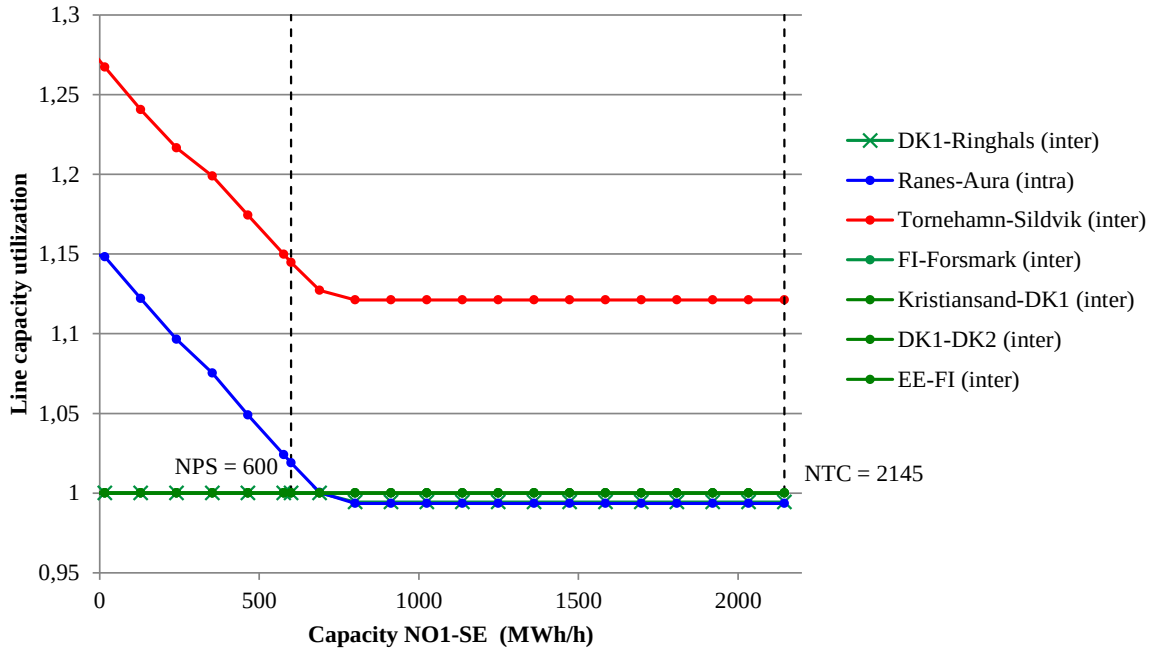

Figure 4-22 Line capacity utilization versus capacity NO1-SE

Figure 4-23 shows similar effects for the cut constraints. Again we focus on the constraints that are close to or above the capacity limit. We see that the Nordland cut and the infeasible Bergen cuts become more overloaded when decreasing the capacity of NO1-SE. Again most of the effect takes place at capacities lower than the Nord Pool Spot transfer capacity.

[14] The capacity between NO1 and Sweden has often been reduced in the Nord Pool Spot market clearing due to constraints internal to Southern Norway and / or Sweden. "Hasletrappen" for instance indicates a heuristic for how the Norwegian system operator sets capacity at NO1-SE based on the expected load in the Oslo-region. The higher the load in Oslo, the lower the export capacity to Sweden, and this is due to the capacity of the Hallingdal and Flesaker interfaces within Southern Norway.

[15] This is in order to obtain reasonable flows when transferring the net injections of the simplified aggregated market clearing model into the disaggregated network model.

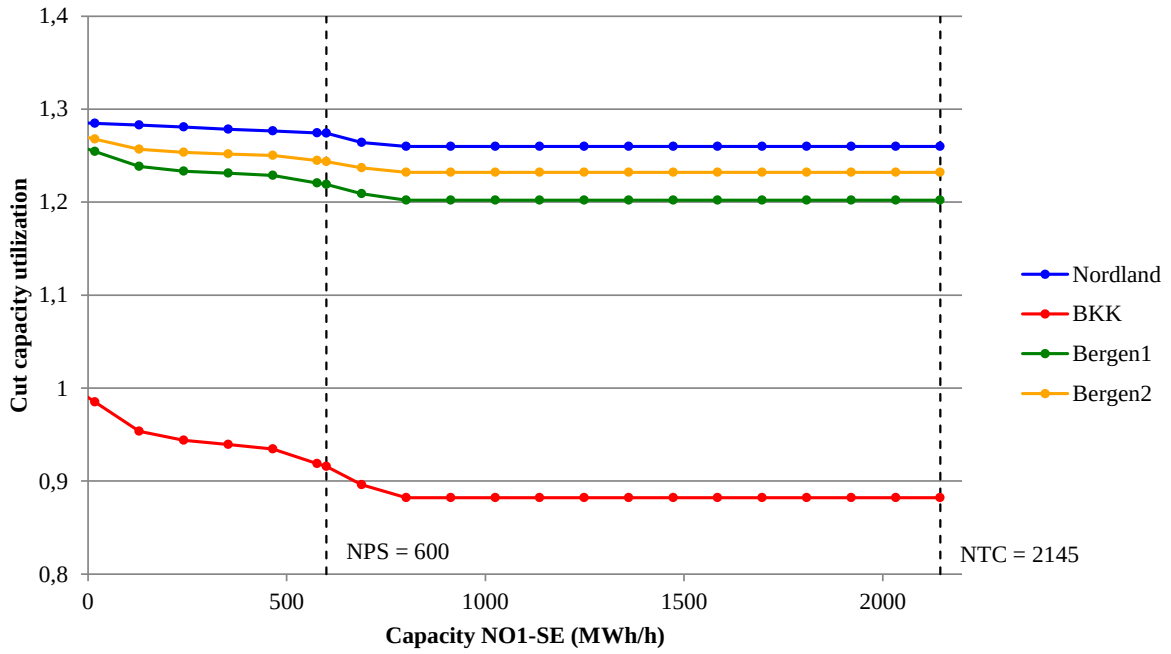

Figure 4-23 Cut capacity utilization versus capacity NO1-SE

Figure 4-24 shows the different area prices, and their dependence on the capacities set in the simplified zonal solution. We see that the capacity of NO1-SE can potentially have a large effect on the area prices. In this case, all prices except EE are equal at the NTC capacity, at the Nord Pool Spot capacity of 600 MW, some of the prices differ, and at even lower capacities the price differences can be considerable.

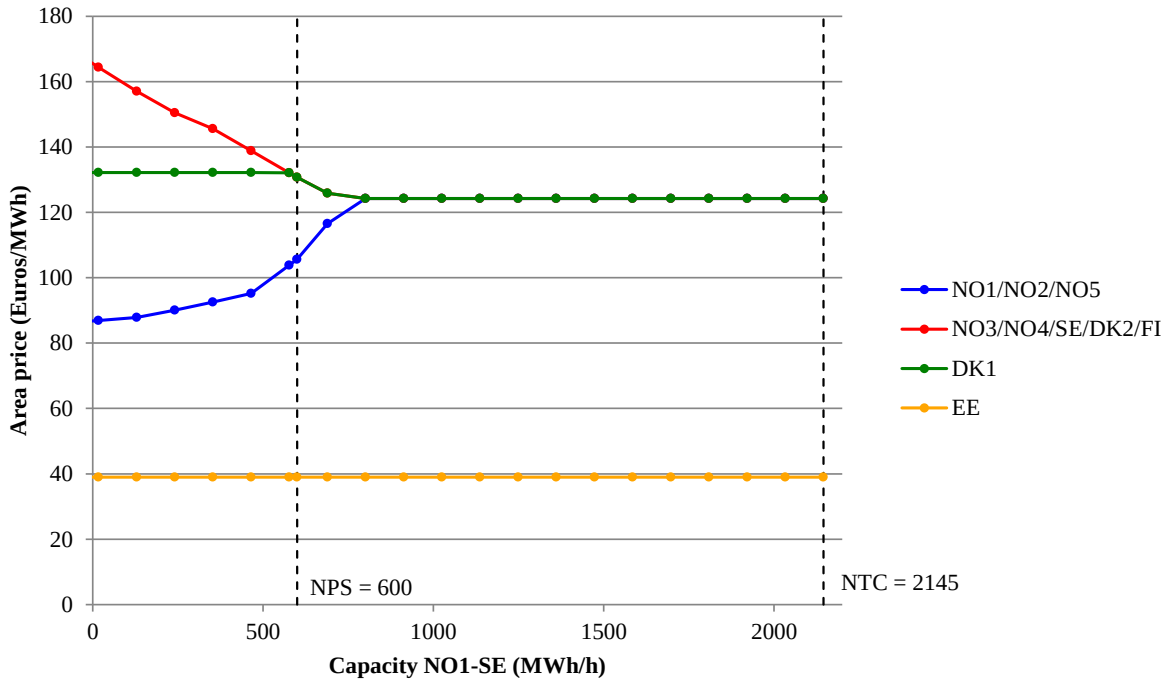

Figure 4-24 Area prices versus capacity NO1-SE

Figure 4-25 – Figure 4-27 show similar sensitivity analyses for the NO4-SE interface. Decreasing the capacity set on the NO4-SE interface in the simplified zonal model mostly increases the flows on the individual links that are close to or above capacity limit. The picture is different for the cut constraints, and Figure 4-26 shows that a reduction in the capacity NO4-SE to about half its NTC capacity will decrease the utilization of the Nordland cut. This will also affect prices considerably, as shown in Figure 4-27.

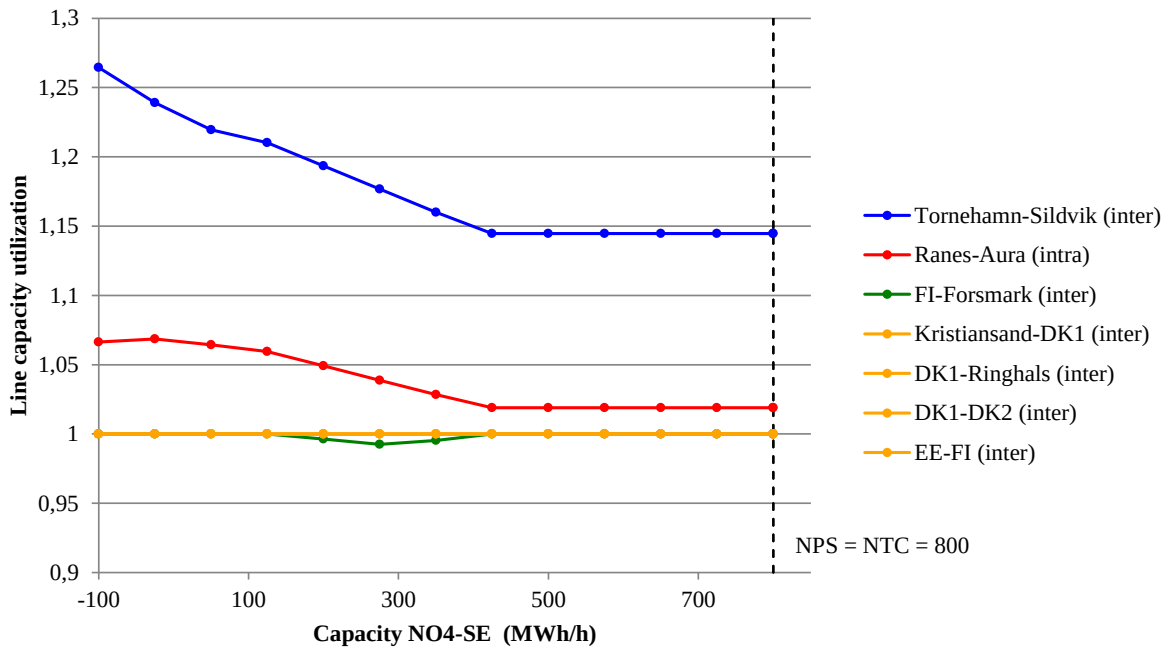

Figure 4-25 Line capacity utilization versus capacity NO4-SE

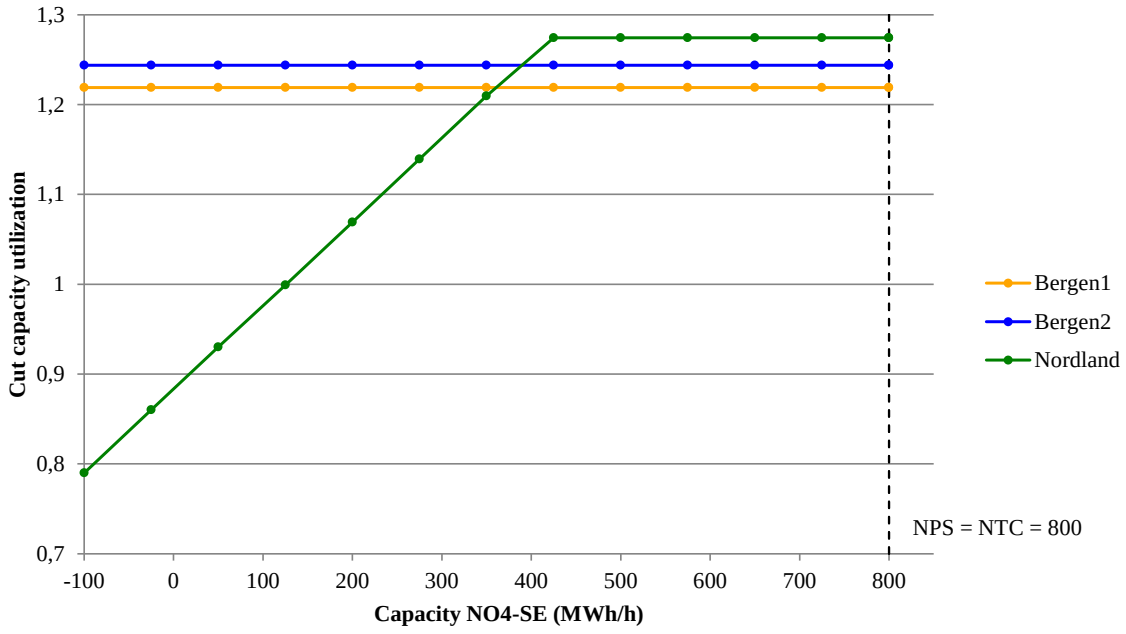

Figure 4-26 Cut capacity utilization versus capacity NO4-SE

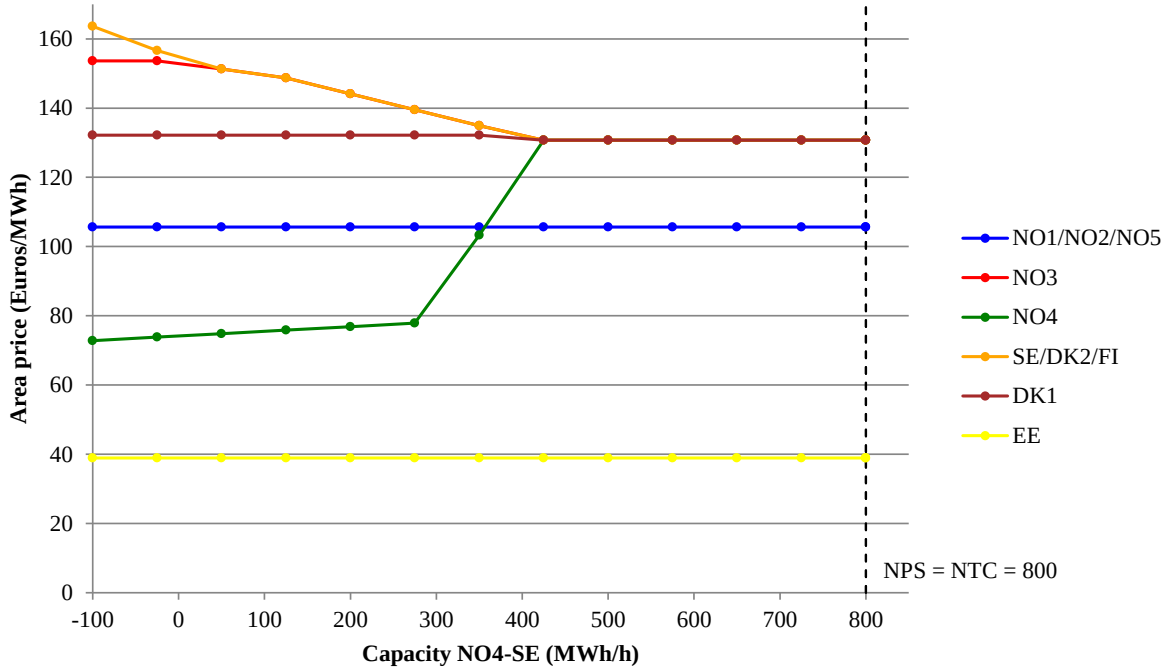

Figure 4-27 Area prices versus capacity NO4-SE

Finally, Figure 4-28 – Figure 4-30 show the effects of reducing the capacity between DK1 and SE. We notice from Figure 4-28 that some lines will have increased flow while others will decrease when capacity is reduced. The cut constraints shown in Figure 4-29 are not so sensitive towards this capacity, although at very low capacities, the BKK cut becomes active. Prices shown in Figure 4-30 are however sensitive already from the first MW of reduced capacity. A reduction in capacity of about 100 MW would effectively split the Nord Pool market into two price areas in addition to Estonia.

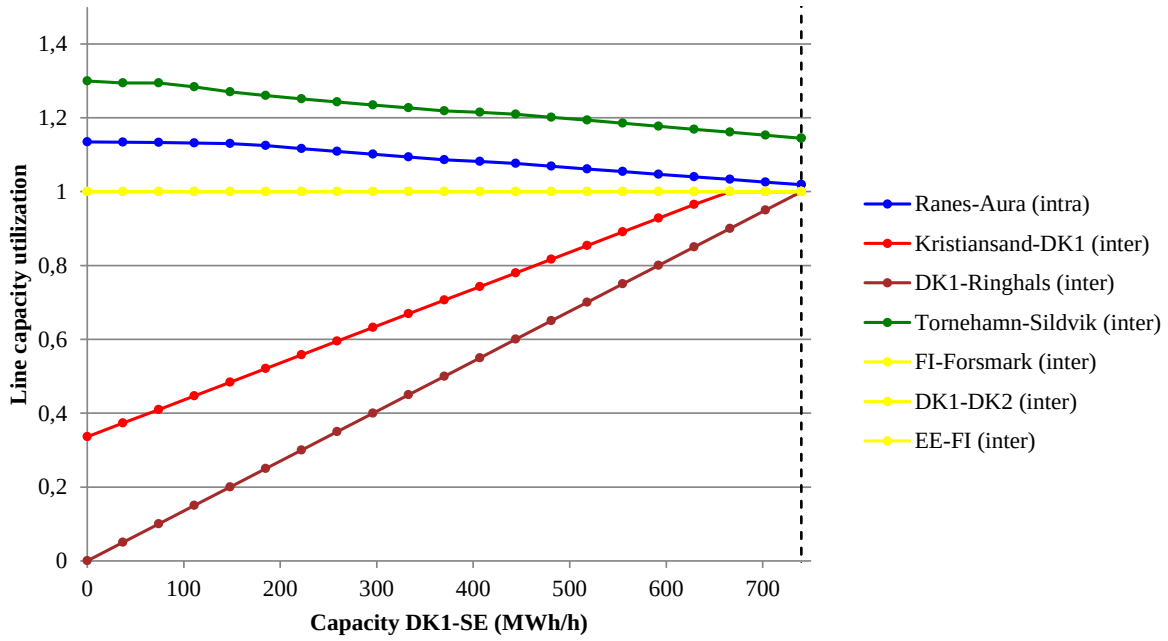

Figure 4-28 Line capacity utilization versus capacity DK1-SE

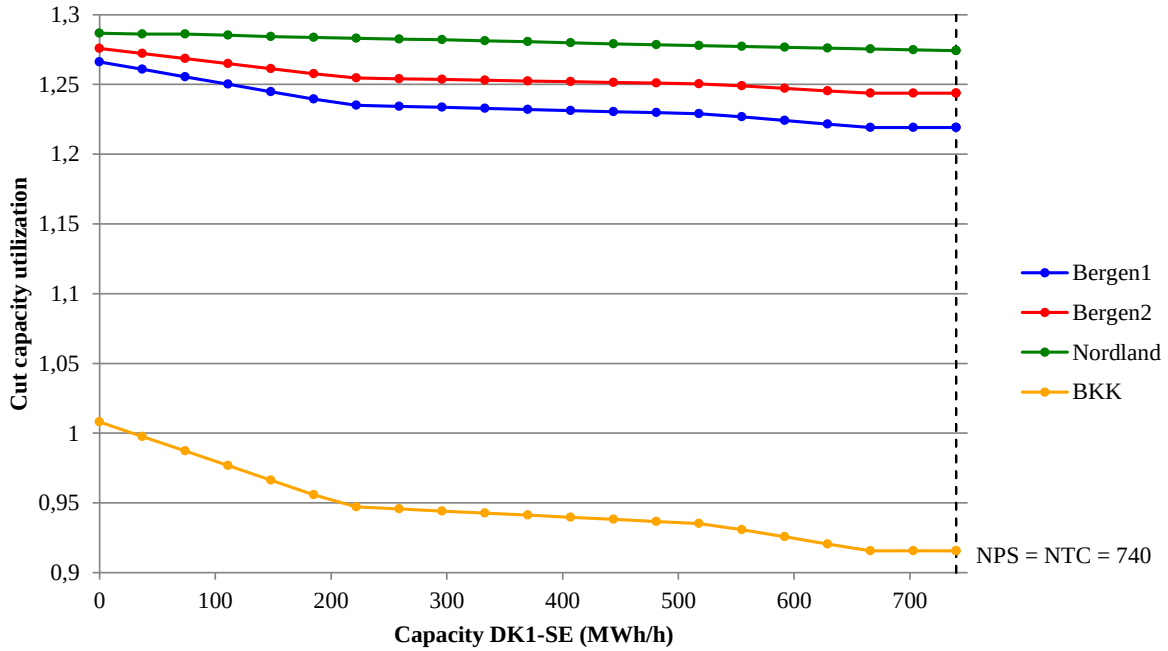

Figure 4-29 Cut capacity utilization versus capacity DK1-SE

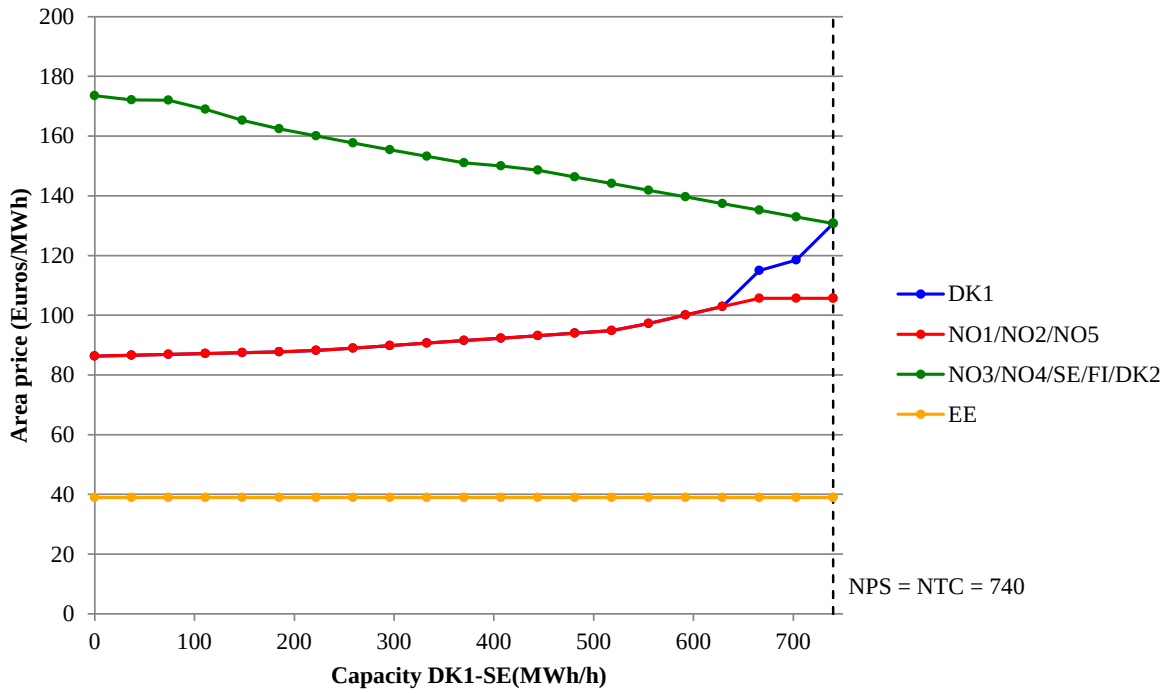

Figure 4-30 Area prices versus capacity DK1-SE

In practice there are many ways of combining the capacities over all the interfaces. To conclude this section we show the effect of setting zonal interface capacities in two different ways, i.e. we compare the prices and infeasibilities at the actual Nord Pool capacities to the prices and infeasibilities that would result when using the flows of the optimal nodal price solution and the optimal zonal price solution instead. Table 4-10 shows the NPS capacities between zones, as well as the flow-based capacities that we have used. Since we have used the actual flows of the nodal and optimal zonal solutions, the corresponding capacities are shown here as single-sided.

Table 4-10 Capacities for links between zones in the simplified zonal model

Links between zones		NPS capacity		Cap. from nodal model		Cap. from opt. zonal model	
		Forward	Backward	Forward	Backward	Forward	Backward
DK1	DK2	590	600	0	435	0	433
DK1	NO2	950	1000	27	0	23	0
DK1	SE	740	0	740	0	740	0
DK2	SE	1700	0	0	735	0	732
FI	EE	365	365	0	365	0	350
FI	SE	1740	1410	191	0	175	0
NO1	NO2	1700	2500	0	2813	0	2811
NO1	NO3	-200	200	18	0	17	0
NO1	NO5	650	700	0	500	0	501
NO1	SE	600	95	1581	0	1581	0
NO2	NO5	250	700	0	150	0	151
NO3	NO4	0	900	0	486	0	485
NO3	SE	600	900	340	0	342	0
NO4	SE	800	700	514	0	516	0

Figure 4-31 and Figure 4-32 compare the new area prices to the area prices in the simplified model, but with the original Nord Pool Spot capacities. We can see that prices in NO1, NO2, NO3, and NO5 increase while the price in NO5 decreases. Using the optimal nodal price flow or the optimal zonal price flow as the basis for setting the capacities, leads to only small differences. This is shown in Table 4-11 as well. Table 4-11 also shows that the area prices that result when using the optimal nodal and zonal power flows to set transfer capacities are more similar to the optimal nodal and zonal prices than the prices found with the Nord Pool Spot capacities.

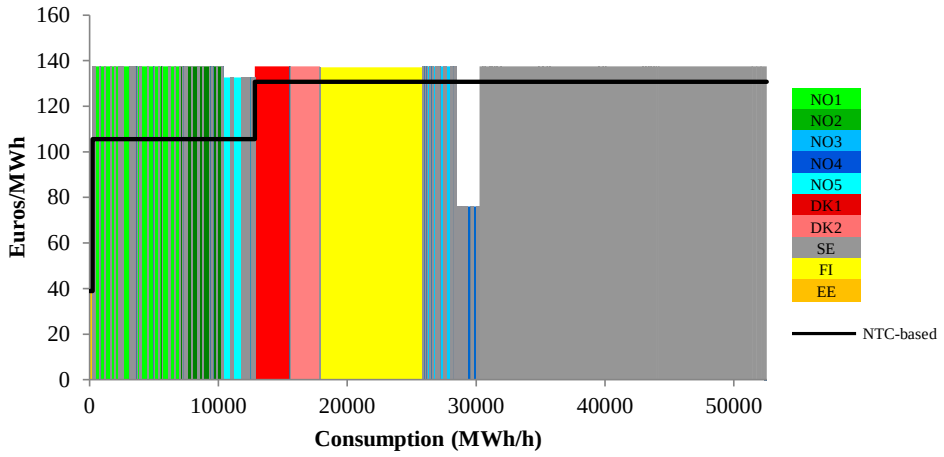

Figure 4-31 Simplified zonal prices with interzonal capacities from nodal flows

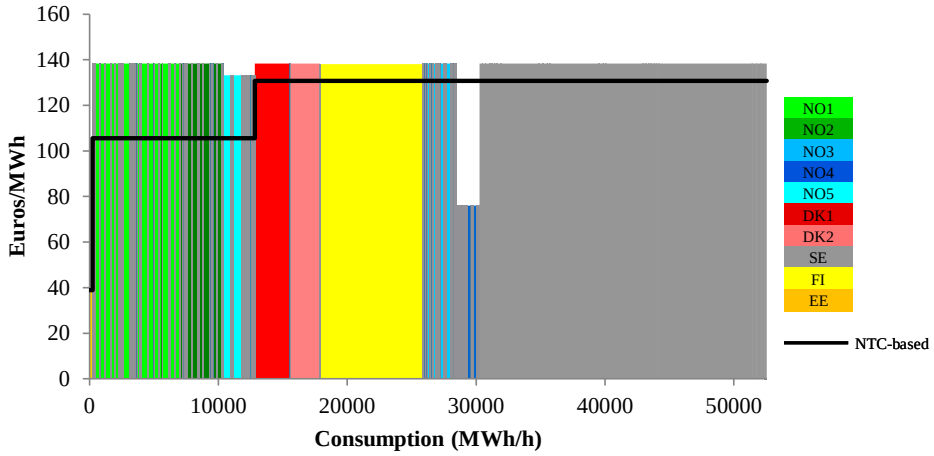

Figure 4-32 Simplified zonal prices with interzonal capacities from optimal zonal flows

Table 4-11 Prices with different aggregate transfer capacities, 15/12-2010, hour 19

Bidding area	Actual NPS	Simplified zonal			Optimal zonal	Optimal nodal (average)
		Actual NPS capacities	Cap. from nodal flow	Cap. from opt. zonal flow		
NO1	104,56	105,63	137,50	138,34	140,42	139,25
NO2	104,56	105,63	137,50	138,34	140,26	139,23
NO3	130,50	130,70	137,50	138,34	140,94	139,59
NO4	130,50	130,70	76,00	75,98	88,17	80,74
NO5	104,56	105,63	132,63	133,17	140,26	135,65
DK1	130,50	130,70	137,50	138,34	124,77	139,23
DK2	130,50	130,70	137,50	138,34	120,61	139,23
SE	130,50	130,70	137,50	138,34	140,59	138,51
FI	130,50	130,70	137,09	138,08	138,08	137,09
EE	38,95	38,95	38,95	38,90	36,10	38,95

In Table 4-12 we show the changes in surpluses and allocation of surpluses. The surpluses are not comparable since the infeasibilities are different, and we note that even if we use the flows from the optimal nodal and zonal price models to set capacities, the resulting flows still contain infeasibilities.

Table 4-12 Unconstrained surplus and surplus differences (1000 Euros) with different aggregate transfer limits

	Un-constrained	Simplified zonal			Nodal
		Actual NPS capacities	Cap. from nodal flow	Cap. from opt. zonal flow	
Producers	6799,5	38,0	560,1	600,6	624,8
Consumers	99249,1	-111,7	-678,0	-716,2	-761,4
Grid	0,0	68,6	103,2	99,3	120,9
Total	106048,7	-5,1	-14,7	-16,3	-15,6
Infeasibilities	2 ind. lines 1 cut	2 ind. lines 1 cut	1 ind. line 2 cuts	1 ind. line 2 cuts	None

(Bergen 1 and Bergen 2 are overloaded in all solutions.)

Looking more closely at the solutions, Table 4-13 and Table 4-14 show that the cut constraints, except for the Bergen cuts, are much closer to feasibility when using the optimal flows to set capacities. It is not surprising that the feasibility of the Bergen cuts is not improved when using the flow-based capacities, since these cut constraints have been excluded when computing the flows that we use to set the capacities.

Table 4-13 Overloaded lines under various model settings

Model settings		Line	Capacity	Overload	Overload %
Unconstrained		Torneham-Sildvik	166,2	18,7	11,3
		EE-FI	365	68,8	18,8
Simplified zonal model	Actual NPS capacities	Torneham-Sildvik	166,2	24,1	14,5
		Ranes-Aura	96	1,8	1,9
	Flow-based cap. from nodal model	Torneham-Sildvik	166,2	28,2	17,0
	Flow-based cap. from opt. zonal model	Torneham-Sildvik	166,2	28,7	17,3

Table 4-14 Overloaded cuts under various model settings

Model settings		Cut	Capacity	Overload	Overload %
Unconstrained		Nordland	1000	255,3	25,5
		Bergen 1	670	136,8	20,4
		Bergen 2	670	156,4	23,3
Simplified zonal model	Actual NPS capacities	Nordland	1000	274,2	27,4
		Bergen 1	670	146,8	21,9
		Bergen 2	670	163,3	24,4
	Flow-based cap. from nodal model	Nordland	1000	8,3	0,8
		Fardal overskudd 1	750	15	2,0
		Bergen 1	670	130,2	19,4
		Bergen 2	670	151,9	22,7
	Flow-based cap. from opt. zonal model	Nordland	1000	6,4	0,6
		Fardal overskudd 1	750	16,1	2,1
		Bergen 1	670	129,8	19,4
		Bergen 2	670	151,7	22,6

4.6.2 The number of price areas

In this section we discuss the effect of changing the number of price areas. We take the zones per 15/10-2010 as a starting point, and we discuss the effect of increasing the number of price areas in the simplified zonal pricing model. When we introduce new price areas, the total surplus will tend to decrease because of the more restricted model formulation, but the extra restrictions can also improve the feasibility of the resulting load flow.

Since we know that the optimal nodal prices result in a feasible load flow, it is natural to consider the level of the nodal prices when determining the price areas for the simplified zonal model[16]. Figure 4-33 shows nodal prices and load flow, as well as the assignment of nodes to price areas that was used on the date 15/12-2010. Of the NPS price areas it is only NO4, and to some extent NO5, where there is substantial variation in nodal price levels within the price area. In Sweden the node Tornehamn plays a special role, since it is disconnected from the rest of the Swedish network, and since its nodal price is much lower than the other Swedish nodes. These observations suggest some obvious alterations to the NPS zonal configuration, and we will now discuss them in more detail. The cases that we will discuss are briefly described in Table 4-15.

[16] It is however not necessarily so that the nodes with most similar prices should belong to the same zone. This is discussed by Bjørndal and Jörnsten (2001).

Table 4-15 Overview of the cases

Case	Capacities	Zonal configuration
I	Actual NPS capacities, with NTC values for new interconnections.	Actual NPS configuration on December 15, 2010.
II		Same as I, but with four price areas in Sweden.
III	Based on aggregate net flow over interconnections from nodal approach (see also Section 4.6.2).	Same as I.
IV		Same as III, but with Tornehamn transferred from SE to NO4.
V		Same as IV, but we create a new price area NO6 from some of the nodes in NO4. The two new price areas are separated by the line Nordreisa-Kvænangsbotn.
VI		Same as V, but we create a new price area NO7 in the northern part of NO5. The new price area is separated from the remaining nodes in NO5 by the Fardal overskudd 1 cut, i.e., by the lines Modalen-Evanger and Fardal-Aurland1.
VII		Same as VI, but NO6 is divided in two price areas separated by the line Lakselv-Adamselv.
VIII		Same as IV, but each node in the original NO4 is a separate price area.

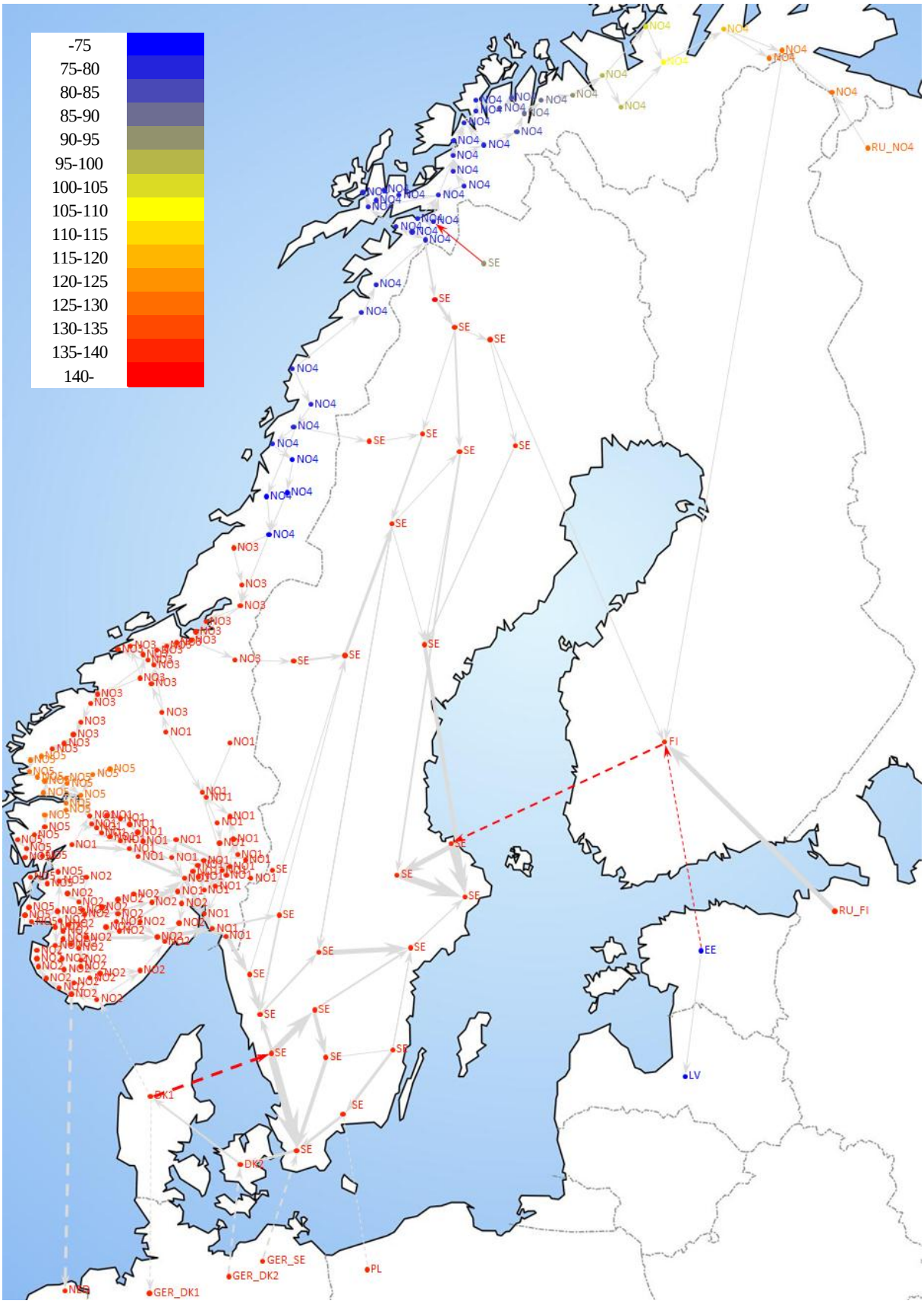

Figure 4-33 Nodal prices and load flow, red lines indicate binding line constraints

Our starting point is the actual price area configuration, shown as Case I in Table 4-15. As discussed previously, and shown in Table 4-16, this configuration gives a congestion cost (compared to the unconstrained case) of 5100 Euros, i.e., much lower than the cost of the nodal approach. However, the simplified approach gives a load flow that is not feasible, since two individual lines and one cut is overloaded.

Case II is the same as Case I, except that Sweden has been split into four price areas, as implemented by Nord Pool Spot from November 1, 2011. Splitting Sweden into several price areas makes it necessary to set capacities on a number of interconnections that were not present in the model from before. Also, it is not obvious that the capacities on the existing interconnections should be the same after the change. In Case II we have used the same capacities for existing interconnections, and we have set the capacities of new interconnections by using NTC values as of February 10, 2012[17]. We see from Table 4-16 that the change reduces the congestion cost somewhat, but that it does not alleviate the problem of all infeasible load flows. Interestingly, as can be seen from Figure 4-34 and Table 4-17, the splitting of Sweden has the opposite effect of what one might expect, i.e., that the prices become uniform over almost the whole Nord Pool area, with the exception of Estonia. Table 4-16 shows that there are still lines and cuts with infeasible flows given the solution from the simplified model. Increasing the number of price areas, introduce more constraints into the problem, which in itself should lead to increases in congestion cost. However, in practice more capacity can be given to the transfer capacities that are actually modeled, and this brings the congestion cost down. In this case the net effect is a reduction in congestion cost.

Table 4-16 Congestion costs (1000 Euros) and infeasibilities for various cases with the simplified zonal approach

		Uncon-strained surplus	Simpl. zonal with NPS/NTC cap.		Simplified zonal with flow-based capacities from nodal approach						Nodal
			I	II	III	IV	V	VI	VII	VIII	
Producers		6799,5	38,0	64,7	560,1	607,3	616,0	604,1	621,3	617,4	624,8
Consumers		99249,1	-111,7	-99,1	-678,0	-738,9	-748,9	-736,8	-759,6	-770,4	-761,4
Grid		0,0	68,6	31,1	103,2	116,4	117,6	117,2	122,9	137,5	120,9
Total		106048,7	-5,1	-3,3	-14,7	-15,2	-15,3	-15,4	-15,4	-15,6	-15,6
Infeasibilities		2 lines 1 cut	2 lines 1 cut	1 line 1 cut	1 line 2 cuts	0 lines 3 cuts	0 lines 3 cuts	0 lines 2 cuts	0 lines 2 cuts	0 lines 1 cut	None
Line overload (%)	Ranes-Aura	-	1,9	-	-	-	-	-	-	-	-
	Sildvik-Torneh.	11,3	14,5	12,1	16,9	-	-	-	-	-	-
	FI-EE	18,8	-	-	-	-	-	-	-	-	-
Cut overload (%)	Fardal oversk. 1	-	-	-	2,0	2,0	2,0	-	-	-	-
	Nordland	25,5	27,4	26,0	0,8	3,2	2,5	3,2	2,7	0,7	-
	Hasle eksport	-	-	-	-	0,2	0,1	0,2	0,1	-	-

[17] We have taken into account the fact that Fenno-Skan 2 did not exist in December 2010, hence the capacity on the interconnection between Finland and SE3 has been set to 550 MW, i.e., the capacity of Fenno-Skan 1.

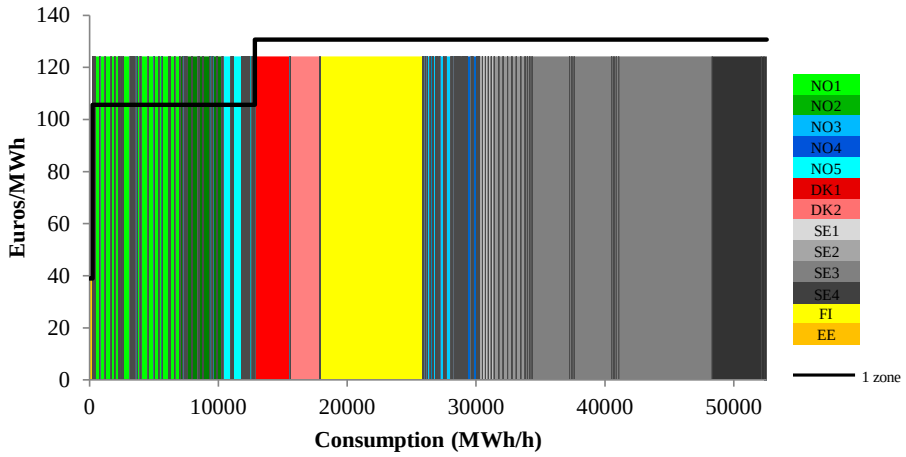

Figure 4-34 Simplified zonal prices with 4 zones in Sweden (Case II)

Table 4-17 Area prices for cases I-VIII

	Simpl. zonal prices with NPS/NTC cap.		Simplified zonal prices with flow-based capacities from nodal approach						Nodal prices	
	I	II	III	IV	V	VI	VII	VIII	Min	Max
NO1	105,63	124,21	137,50	139,34	139,34	139,34	139,34	139,34	139,21	139,40
NO2	105,63	124,21	137,50	139,34	139,34	139,34	139,34	139,33	139,23	139,24
NO3	130,70	124,21	137,50	139,34	139,34	139,34	139,34	139,34	139,45	139,91
NO4	130,70	124,21	76,00	76,31	76,12	76,12	76,12	75,10 - 89,21	74,77	93,65
NO6					107,76	107,76	97,00	92,45 - 105,39	92,45	105,39
NO8							122,25	119,63 - 126,58	119,63	126,58
NO5	105,63	124,21	132,63	132,63	132,63	139,23	139,23	139,23	139,23	139,24
NO7						125,22	125,22	125,22	125,22	125,22
DK1	130,70	124,21	137,50	139,34	139,34	139,34	139,34	139,33	139,23	139,23
DK2	130,70	124,21	137,50	139,34	139,34	139,34	139,34	139,34	139,23	139,23
SE1	130,70	124,21	137,50	139,34	139,34	139,34	139,34	139,34	138,03	140,83
SE2		124,21							138,76	139,41
SE3		124,21							139,17	139,28
SE4		124,21							139,21	139,23
FI	130,70	124,21	137,09	137,09	137,09	137,09	137,09	137,09	137,09	137,09
EE	38,95	38,95	38,95	38,95	38,95	38,95	38,95	38,95	38,95	38,95

As shown in Figure 4-33, NO4 and NO5 are the only price areas where the nodal prices differ substantially within the area, and this observation suggests that further splitting of NO4 and NO5 may be necessary in order to remove the flow infeasibilities. However, since we do not know how the system operators would set the interconnection capacities in a system with a different price area configuration, we shall not use the NPS/NTC capacities in the following discussion. Instead, we shall set the capacities of each interconnection based on aggregate net load flow from the nodal approach. Cases III-VIII are all based on this way of setting the capacities between the price areas.

Case III is based on the actual Nord Pool Spot price areas for December 2010, and will serve as the starting point for the discussion in the rest of this section. Comparing the area prices for Case III to the average nodal prices for the bidding areas in Table 4-11 (Section 4.6.1), we notice that they are quite similar. As seen from Table 4-16, however, the resulting flow in case III is still infeasible. The flow from Tornehamn to Sildvik is 16,9 % above the capacity limit. Note that the area price in Sweden is 137,5 Euros/MWh, while the area price in NO4 is 76 Euros/MWh. Hence the power flows from a high-price area to a low-price area, contrary to what one would expect. The explanation for this phenomenon is that Tornehamn is not connected to the rest of the Swedish network, hence it is not physically possible to trade power at the Swedish price in this node. The simplified zonal model does not "know" that the connection between Tornehamn and the rest of Sweden does not exist, and hence sets a common price for the entire price area. An obvious remedy in order to improve the quality of the solution from the simplified model is to assign Tornehamn to the price area NO4 instead of Sweden, as it is done in Case IV. We see from Table 4-17 that the price in Sweden goes up from 137,50 Euros/MWh to 139,34 Euros/MWh, and that the price in NO4 goes up from 76,00 Euros/MWh to 76,31 Euros/MWh. Since there is a uniform price in Sweden and Norway, except NO4 and NO5, the change also has effect for other price areas. Table 4-16 shows that the congestion cost goes up from 14,7 to 15,2. All the line capacity constraints are now satisfied, but there are still three cut constraints that are violated.

The two most violated cut constraints, as indicated by the shadow prices in Table 4-18, are the Nordland cut and the Fardal (overskudd 1) cut. The Nordland cut is illustrated by the green lines in Figure 4-35. The area price in NO4 in Case IV is 76,31 Euros/MWh, while the area price in NO3 and SE is 139,34 Euros/MWh. From the nodal prices in Figure 4-35 we see that there is a potential for a high-price area consisting of the northernmost nodes in NO4. If we can increase the price in Finnmark we can counteract the power flow southwards to NO3 and Sweden, over the Nordland cut. In Case V we create a price area, NO6, in Finnmark, delimited by the Nordreisa-Kvænangsbotn line. Table 4-17 shows an area price in NO6 of 107,76 Euros/MWh, while the area price in the "new" NO4 is 76,12 Euros/MWh. There is a slight reduction in the overload over the Nordland cut, from 3,2 % to 2,5 %.

Table 4-18 Shadow prices for cut capacity constraints with nodal pricing

Cut name	Capacity	From	To	Share of flow included	Shadow price
Hasle eksport	1600	Hasle	Borgvik	1	*0,08*
		Halden	Skogssäter	1	
Nordland	1000	Ofoten	Ritsem	1	*65,26*
		Nedre Røssåga	Ajaure	1	
		Tunnsjødal	Verdal	1	
		Tunnsjødal	Namsos	1	
		Sildvik	Tornehamn	1	
Fardal overskudd 1	750	Modalen	Evanger	1	*14,02*
		Fardal	Aurland1	1	

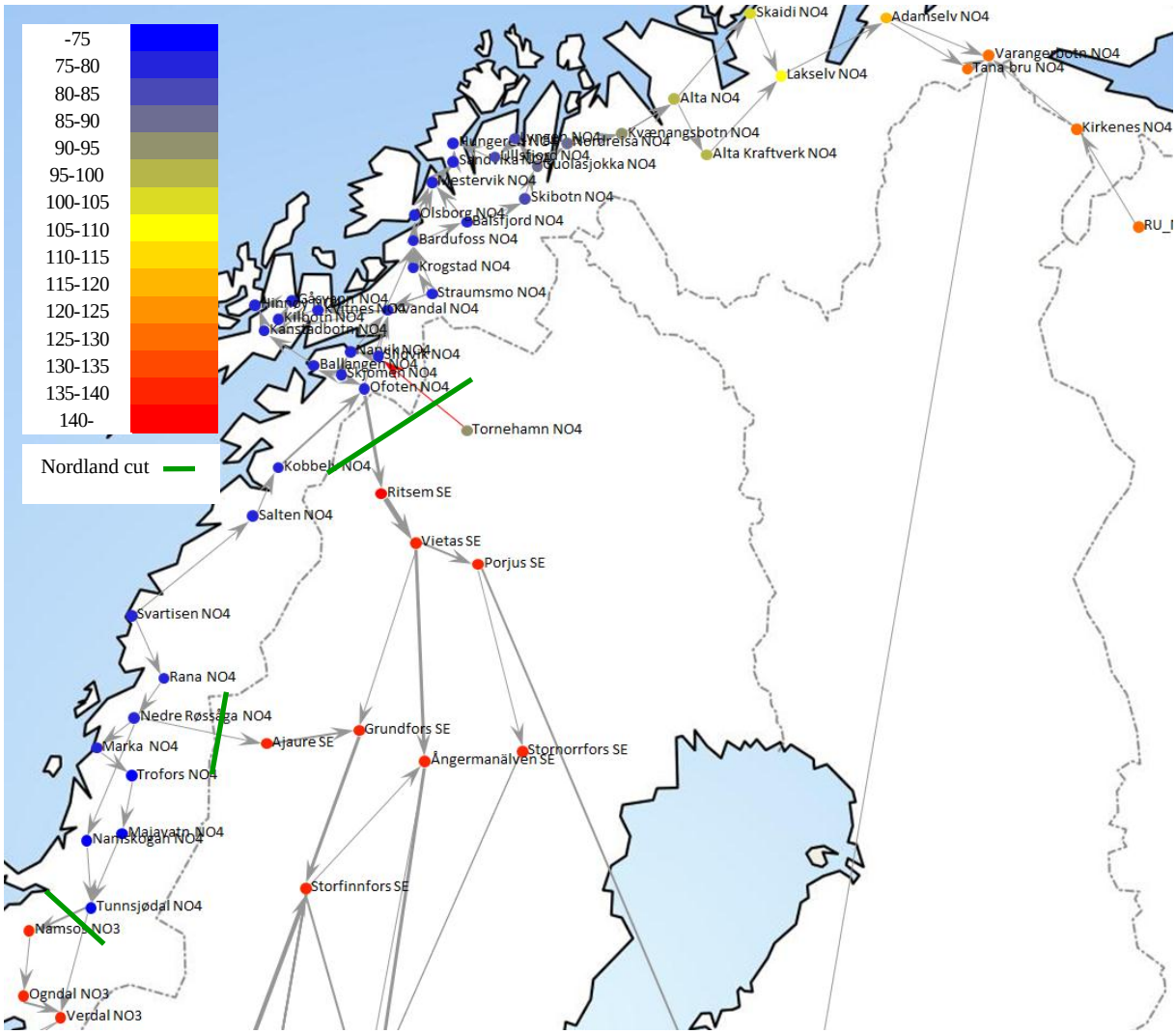

Figure 4-35 Nodal prices and load flow for NO4, binding line constraints are indicated by red lines

Figure 4-36 shows a similar picture for the NO5 price area. The level of the nodal prices indicate that the price level should be lower behind the Fardal cut, as illustrated by the green lines in the figure. In order to avoid excessive flow over this cut we can create a separate price area, NO7, for the nodes behind it (Case VI). We see that the price for NO7 becomes 125,22 Euros/MWh, while the remaining nodes in NO5 has a much higher price of 139,23 Euros/MWh. Table 4-16 also shows that the Fardal cut is no longer violated.

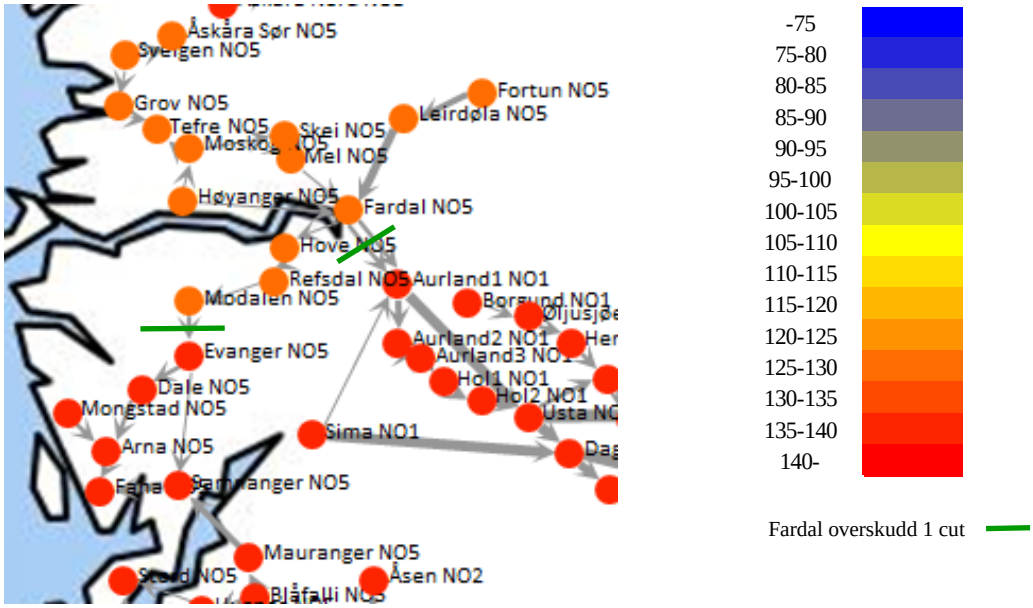

Figure 4-36 Nodal prices and load flow for NO5

Since the Nordland cut is slightly violated in all the cases up to now, we attempt to improve the situation by splitting NO6 into two price areas, separated by the Lakselv-Adamselv line. The price in the new area NO8 becomes 122,25 Euros/MWh, while the remaining nodes in NO6 has a price of 97,00 Euros/MWh. However, the Nordland cut is still violated by a few percentages. Table 4-17 and Figure 4-37 show that the resulting area prices match the nodal prices quite closely. We find the largest differences between nodal and simplified zonal prices in NO4, NO6, and NO8. In order to get rid of the infeasibilities in the simplified zonal approach we attempt to move the prices in these three areas even closer to the nodal prices. One way of doing this is to give each of the nodes in these areas their own price. I.e., we allow for nodal prices (in a simplified model) in NO4, NO6 and NO8, while we keep the area configuration for the rest of the network. We see from Table 4-16 that the congestion cost for Case VIII is approximately equal to the congestion cost for the nodal approach, and that the overload over the Nordland cut is now reduced to 0,7 %.

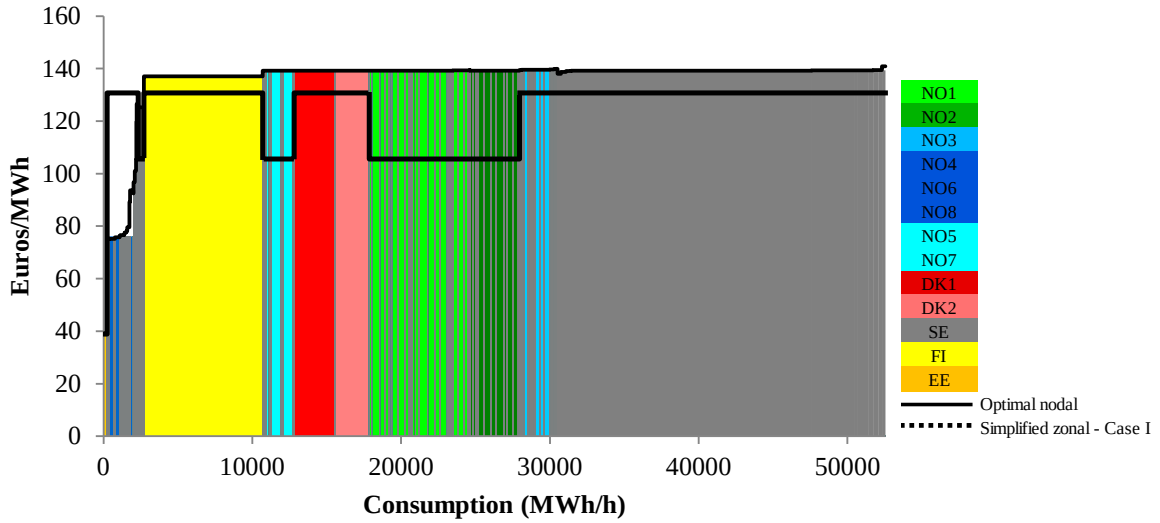

Figure 4-37 Area prices and consumption for Case VII

4.6.3 Security constraints

In the following we consider a different approach to the security constraints. Instead of the cut constraints we reduce the capacities of the individual lines to a fraction of the nominal thermal capacities, like in Neuhoff et al. Figure 4-38 – Figure 4-45 show the price changes (weighted by consumed quantities on the first axis) and the utilization of the cut constraints that follows from the computed prices and quantities. Only the cuts on the left hand side of Figure 4-39, Figure 4-41, Figure 4-43, and Figure 4-45 at utilization above 100 % are violated. In the price diagrams in Figure 4-38, Figure 4-40, Figure 4-42, and Figure 4-44 we compare nodal prices with the reduced individual line constraints to nodal prices with thermal and cut constraints (solid line) and simplified zonal prices (dotted line).

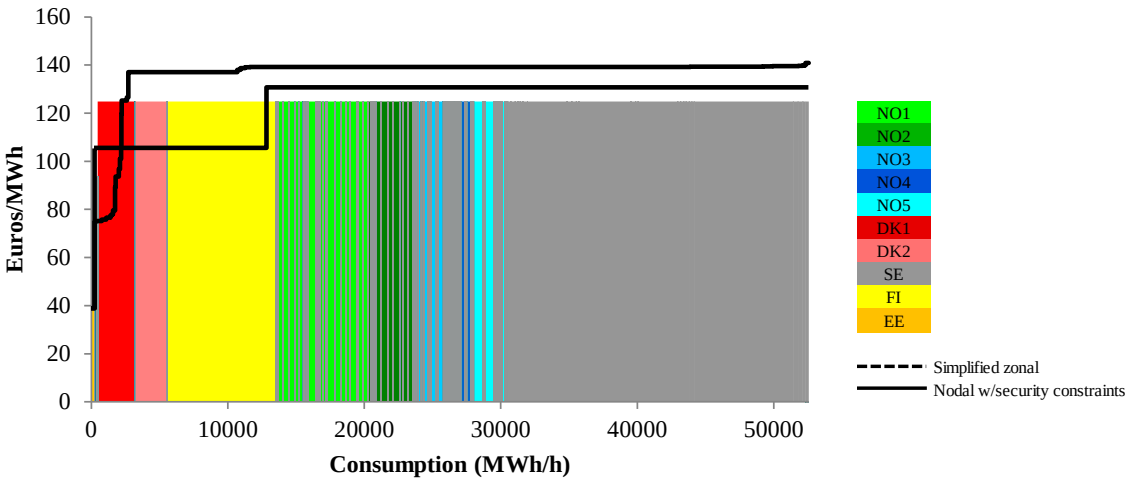

Figure 4-38 Nodal prices with line capacities set to 100 % of nominal capacities

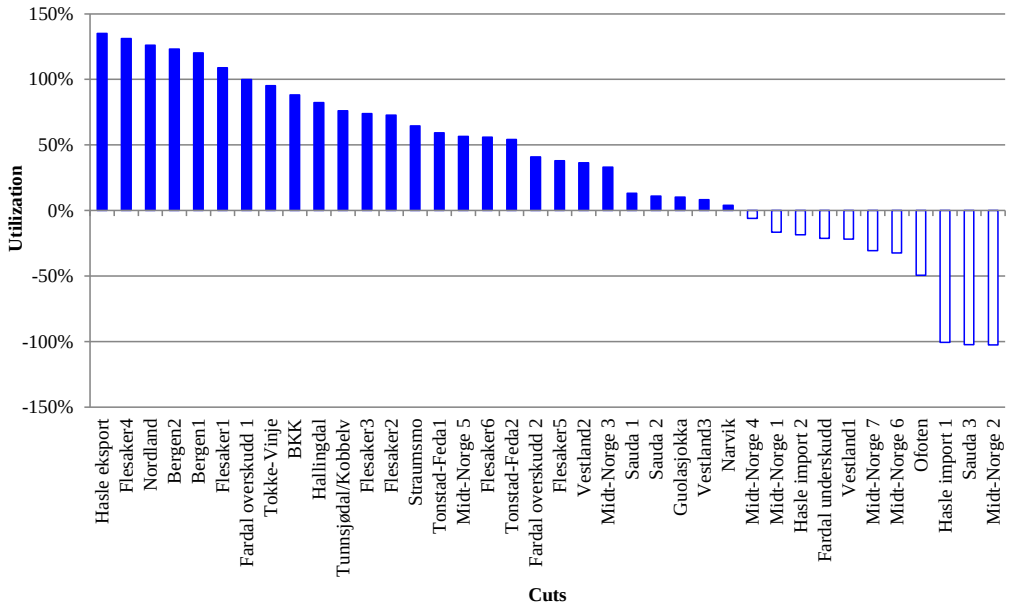

Figure 4-39 Security cut capacity utilization with line capacities set to 100 % of nominal capacities

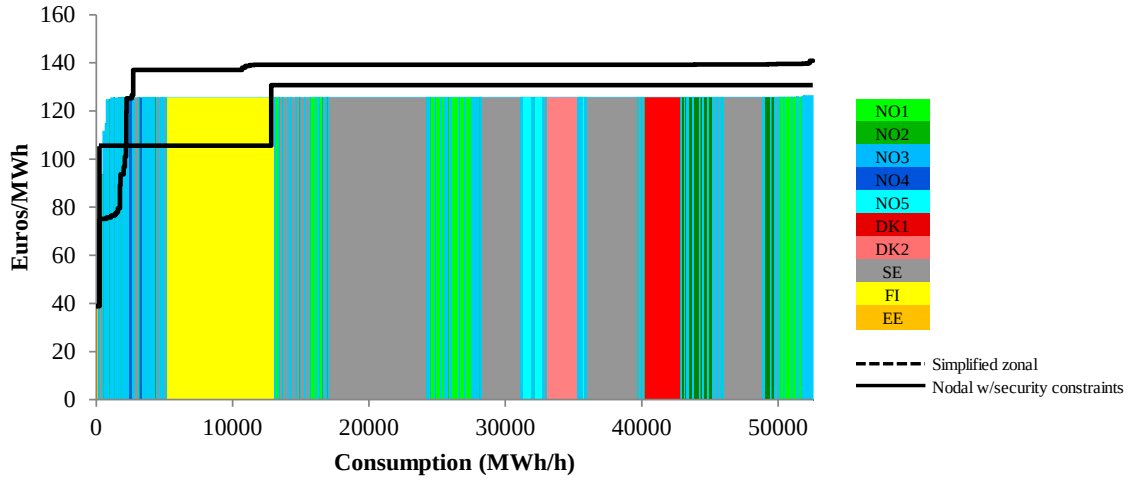

Figure 4-40 Nodal prices with line capacities set to 90 % of nominal capacities

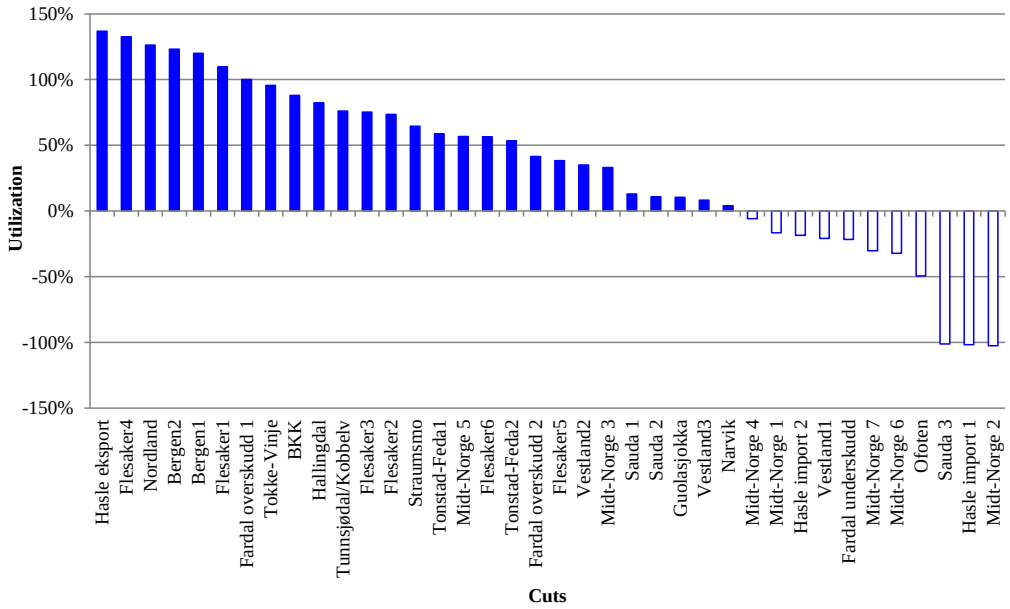

Figure 4-41 Security cut capacity utilization with line capacities set to 90 % of nominal capacities

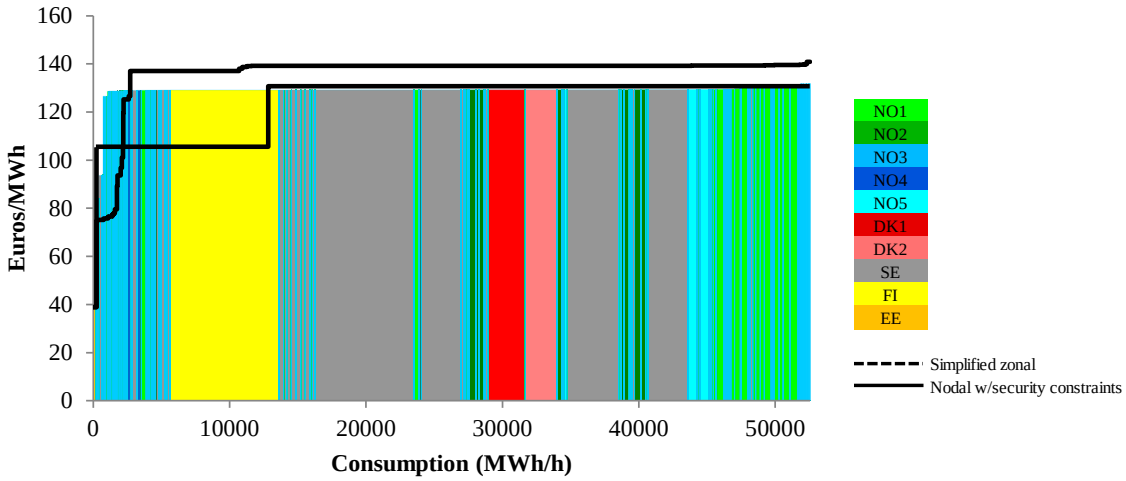

Figure 4-42 Nodal prices with line capacities set to 80 % of nominal capacities

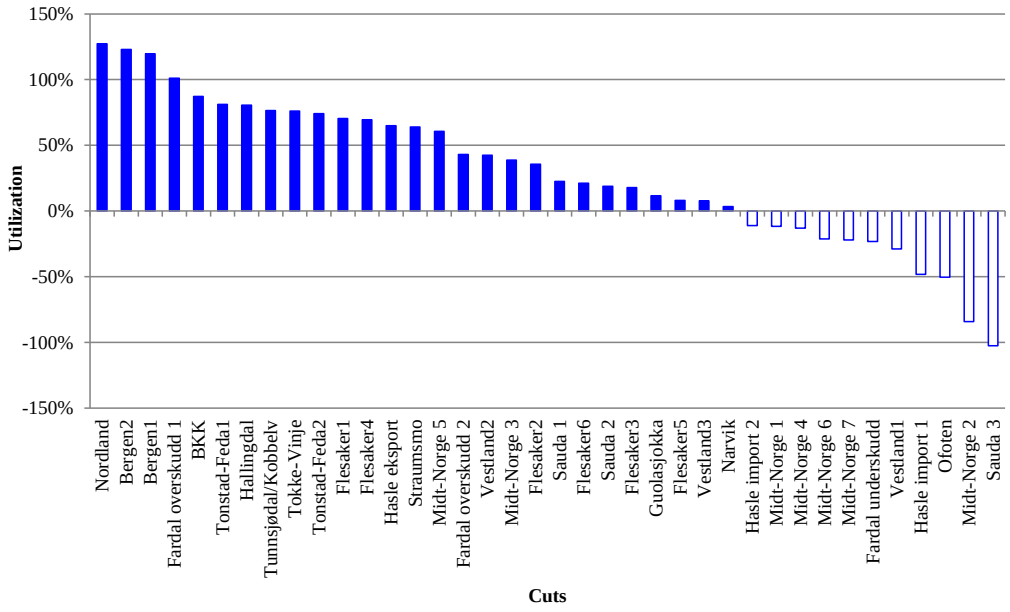

Figure 4-43 Security cut capacity utilization with line capacities set to 80 % of nominal capacities

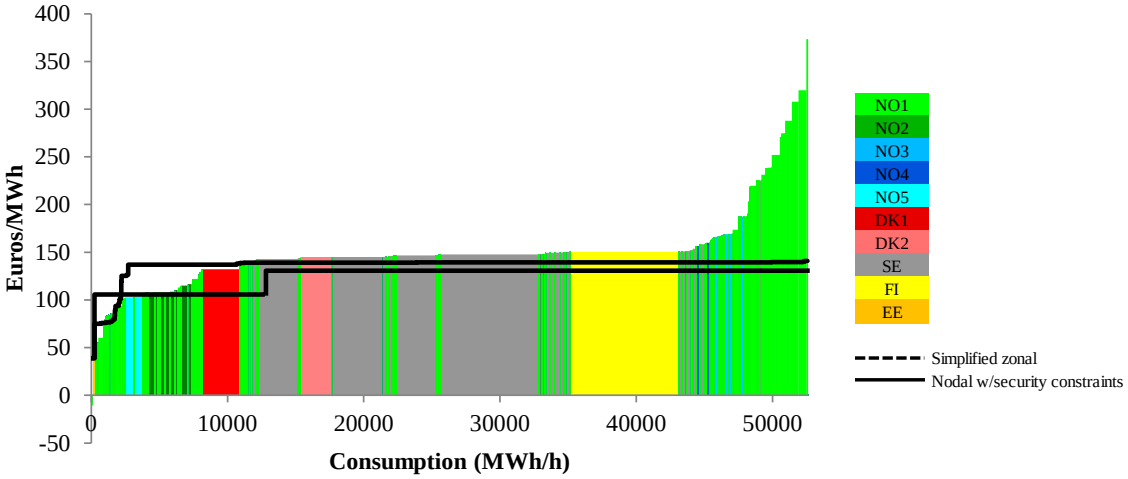

Figure 4-44 Nodal prices with line capacities set to 70 % of nominal capacities

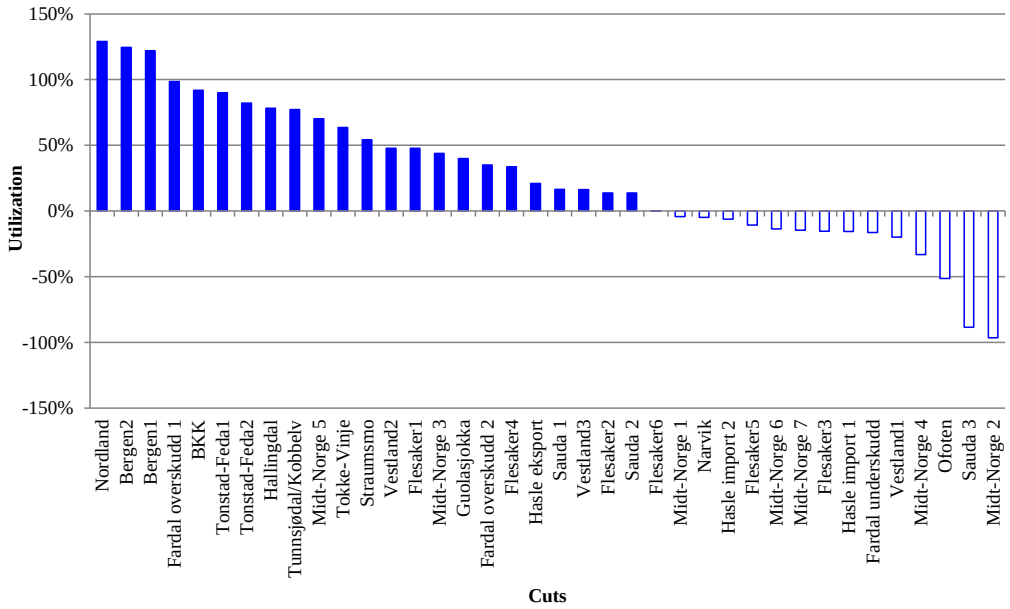

Figure 4-45 Security cut capacity utilization with line capacities set to 70 % of nominal capacities

When restricting the capacities more, the nodal prices increase and the price differences increase. On the other hand, the number of overloaded cuts decreases (except between 100 % and 90 %), and when the capacity is set to only 70 % of the nominal capacity, only 3 cut constraints are overloaded, i.e. the infeasible Bergen cuts and the Nordland cut. We can also see from the price figures that the prices in NO1 are the most affected when capacity decreases.

Table 4-19 shows the changes in surplus and infeasibilities. When restricting capacities, surplus is transferred from consumers to producers and the grid. When capacity is lowered to 70 % of the nominal values, we see that the grid revenues increase a lot, and that the total social surplus is also negatively affected. Note however again that the surpluses cannot be directly compared as the solutions differ when it comes to infeasibilities.

Table 4-19 Unconstrained surplus and surplus differences (1000 Euros) with different security constraints

	Un-constrained	Simplified zonal	Nodal with red. line capacities				Nodal w/sec. cut constraints
			100 %	90 %	80 %	70 %	
Producers	6799,5	38,0	85,8	108,1	274,8	949,9	624,8
Consumers	99249,1	-111,7	-126,0	-169,9	-355,3	-1498,9	-761,4
Grid	0,0	68,6	36,5	57,8	72,9	516,3	120,9
Total	106048,7	-5,1	-3,6	-4,0	-7,7	-32,6	-15,6
Infeasibilities	2 ind. lines 1 cut	2 ind. lines 1 cut	4 cuts	5 cuts	2 cuts	1 cut	None

(Bergen 1 and Bergen 2 are overloaded in all solutions.)

4.6.4 Demand elasticity

In this section we study the changes in prices when we allow for some elasticity of demand in the inelastic parts of the demand curves. As seen in Figure 3-5 the calibrated load curves are almost totally inelastic at high prices. In the present case, for most areas except NO4 and SE, this inelastic segment includes the Nord Pool Spot price. For each of the areas then, except NO4 and SE, we introduce a more elastic demand by tilting the inelastic segments of the demand curve around the "Nord Pool Spot" price point (i.e. the prices found in the simplified zonal price solution). This is illustrated in Figure 4-46 for NO1. The price elasticity of demand measures the change in quantity demanded as a result of a price change:

$$e = -\frac{\frac{\partial Q}{Q}}{\frac{\partial P}{P}} = -\frac{\partial Q \cdot P}{Q \cdot \partial P}$$

We use an approximation of the formula, using price and quantity increments from the given "Nord Pool" price point, to construct new demand curves with varying elasticities. We set the price reduction equal to the difference between the "Nord Pool Spot" price and the lowest price point of the original inelastic part. Then we increase the quantity such that the resulting elasticity is equal to the predefined level. The other sections of the load curve are shifted to the right according to the quantity increment. Figure 4-46 illustrates the new calibrated demand curves for NO1 with segments of various elasticities along with the actual Nord Pool Spot demand curve (blue curve) and our original calibrated demand curve with an inelastic segment (yellow curve). We can see that the new elastic demand curves "rotate" around the Nord Pool Spot price of 105.

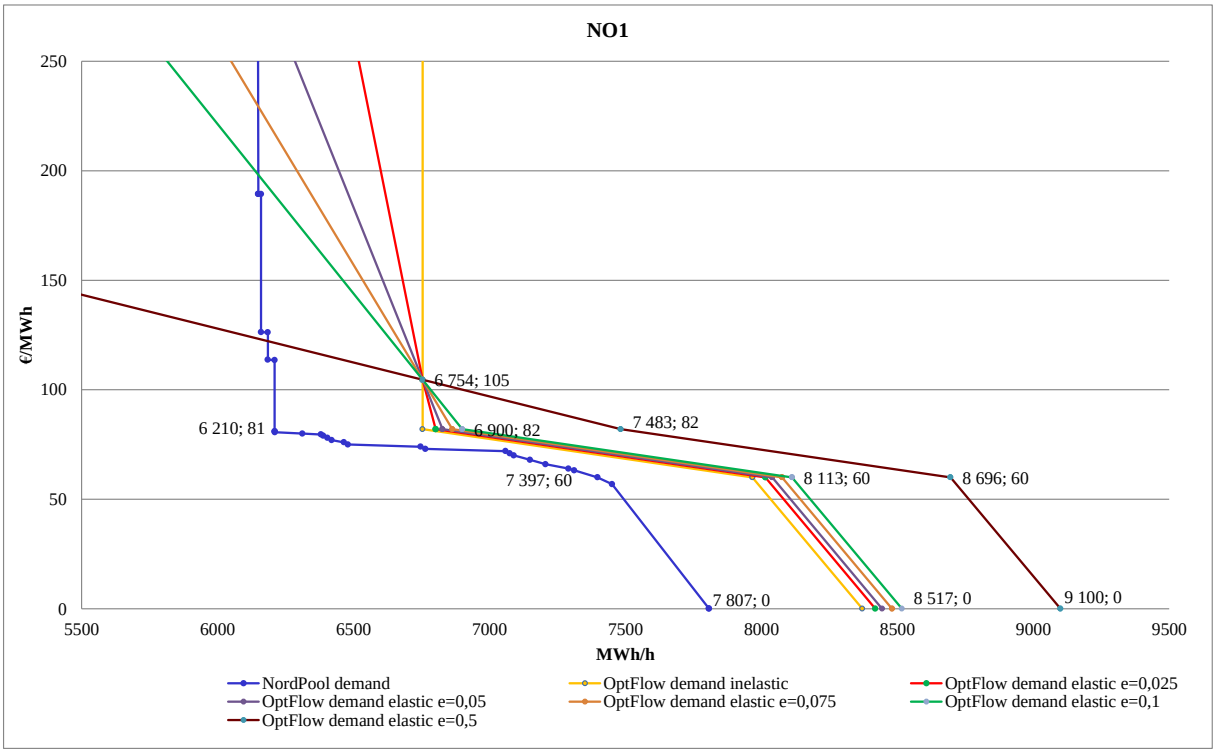

Figure 4-46 Comparison of demand curves, with and without the elastic segment, 15/12-2010, hour 19

The graphs in Figure 4-47 – Figure 4-51 show the consumption and production weighted nodal prices for different elasticities. We compare the new nodal prices with the original nodal prices (solid line) and the original simplified zonal prices (dotted line). We see that the nodal prices decrease with increasing elasticity. Moreover, the price variation decreases. In the Table 4-20 we show the mean and standard deviation values of the nodal prices with different demand elasticities. From columns 2 and 3 we see that both the mean and the standard deviation decrease with growing elasticity. In columns 4 and 5 we show the volume weighted mean and standard deviation, with 50 percent weight on production and consumption each, and they show the same effect.

Table 4-20 Nodal prices descriptive statistics for different elasticities of the demand curve segment, 15/12-2010, hour 19

			Weighted	
Demand elasticity	**Mean**	**SD**	**Mean**	**SD**
0,025	123,0	22,7	131,2	14,9
0,05	120,0	21,2	127,5	14,0
0,075	118,5	20,3	124,0	13,4
0,1	116,9	19,5	123,0	12,9

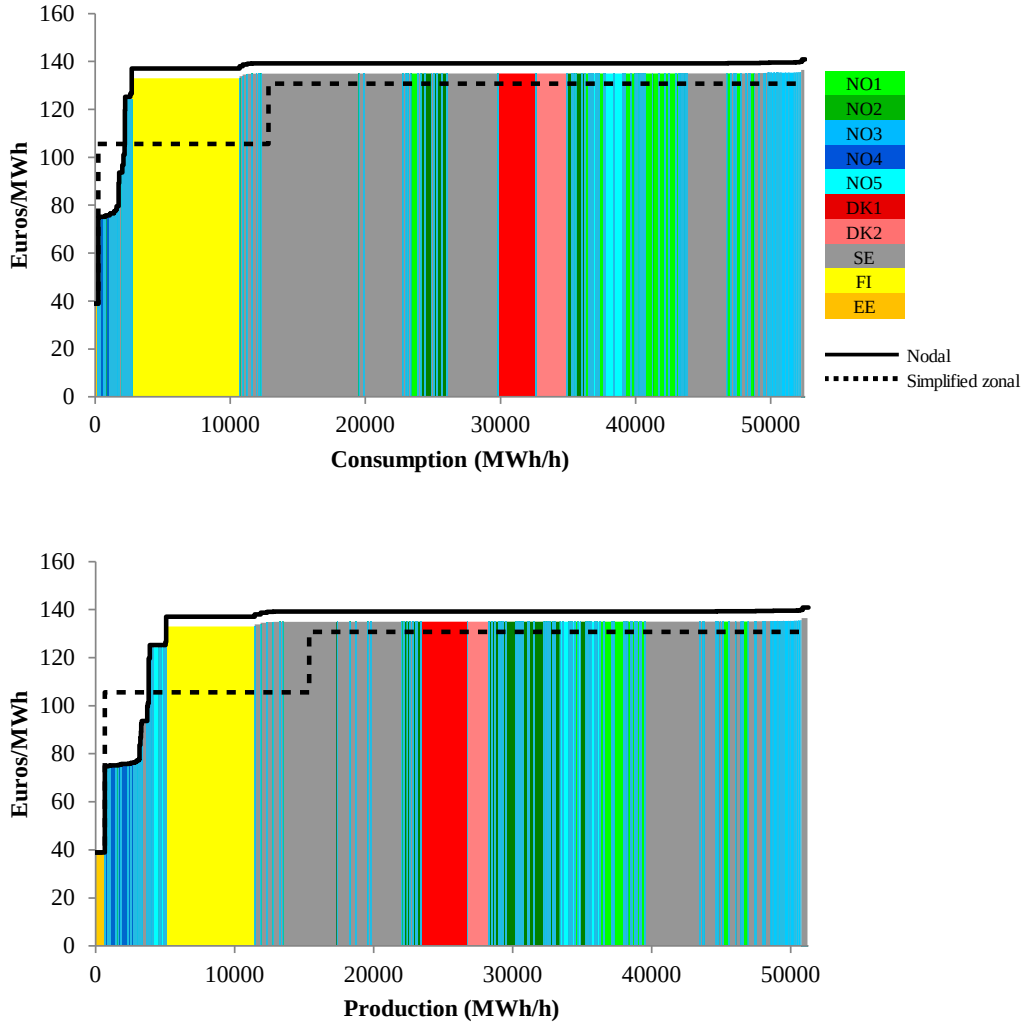

Figure 4-47 Nodal prices with more elastic demand curves (e = 0,025), 15/12-2010, hour 19

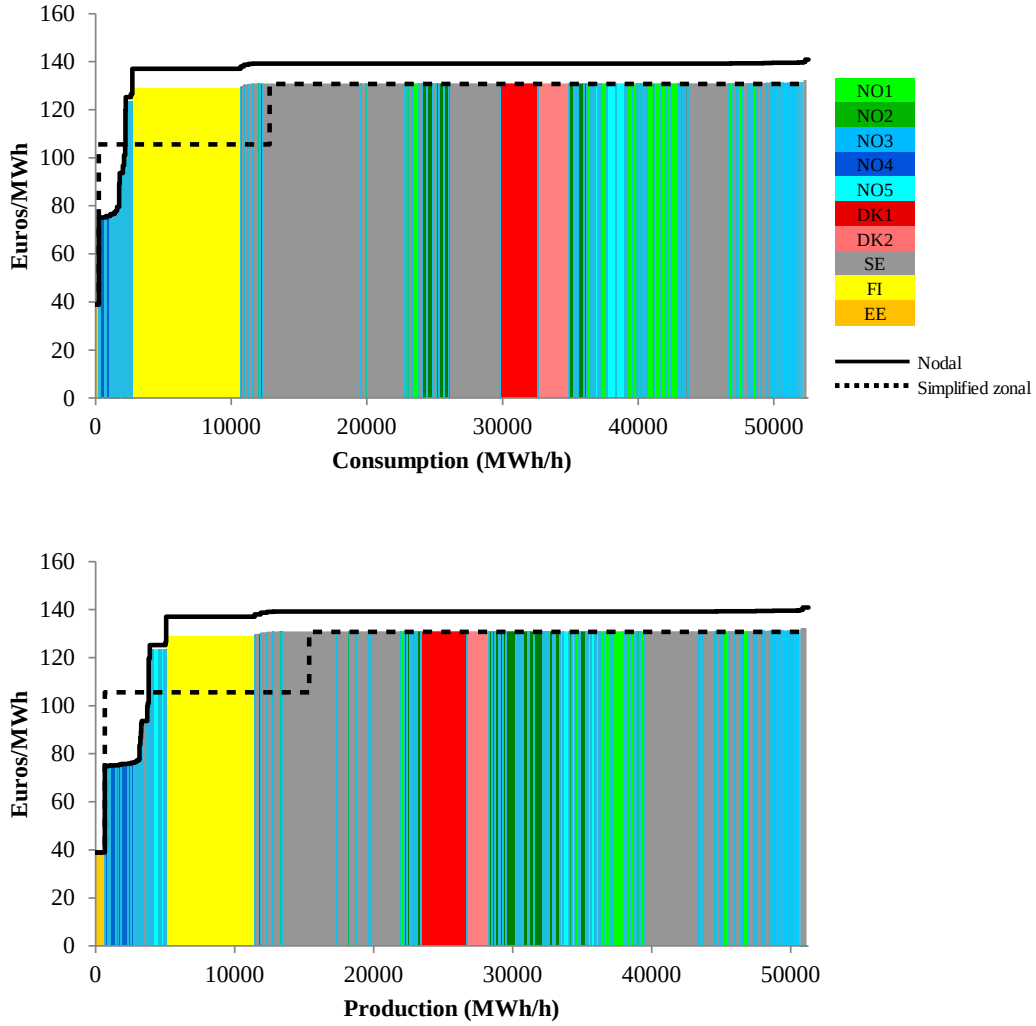

Figure 4-48 Nodal prices with more elastic demand curves (e = 0,05), 15/12-2010, hour 19

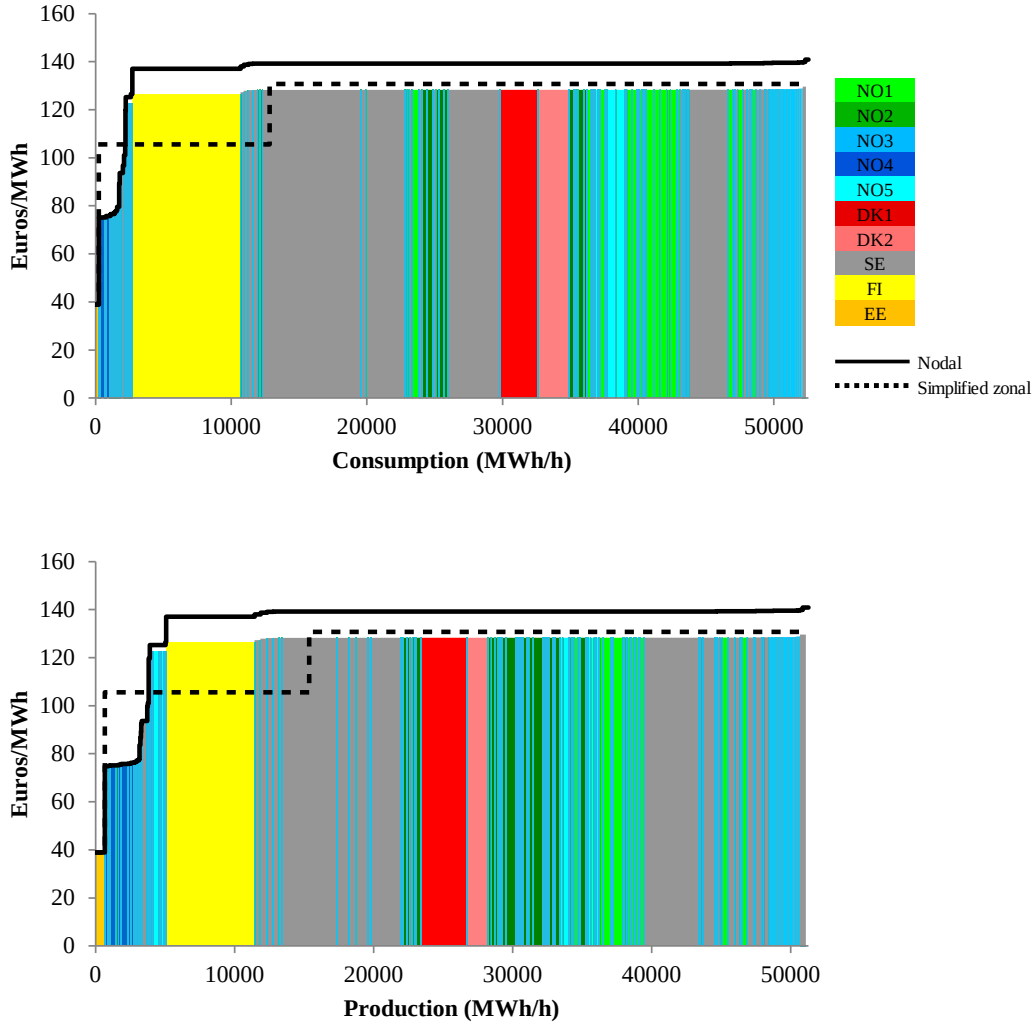

Figure 4-49 Nodal prices with more elastic demand curves (e = 0,075), 15/12-2010, hour 19

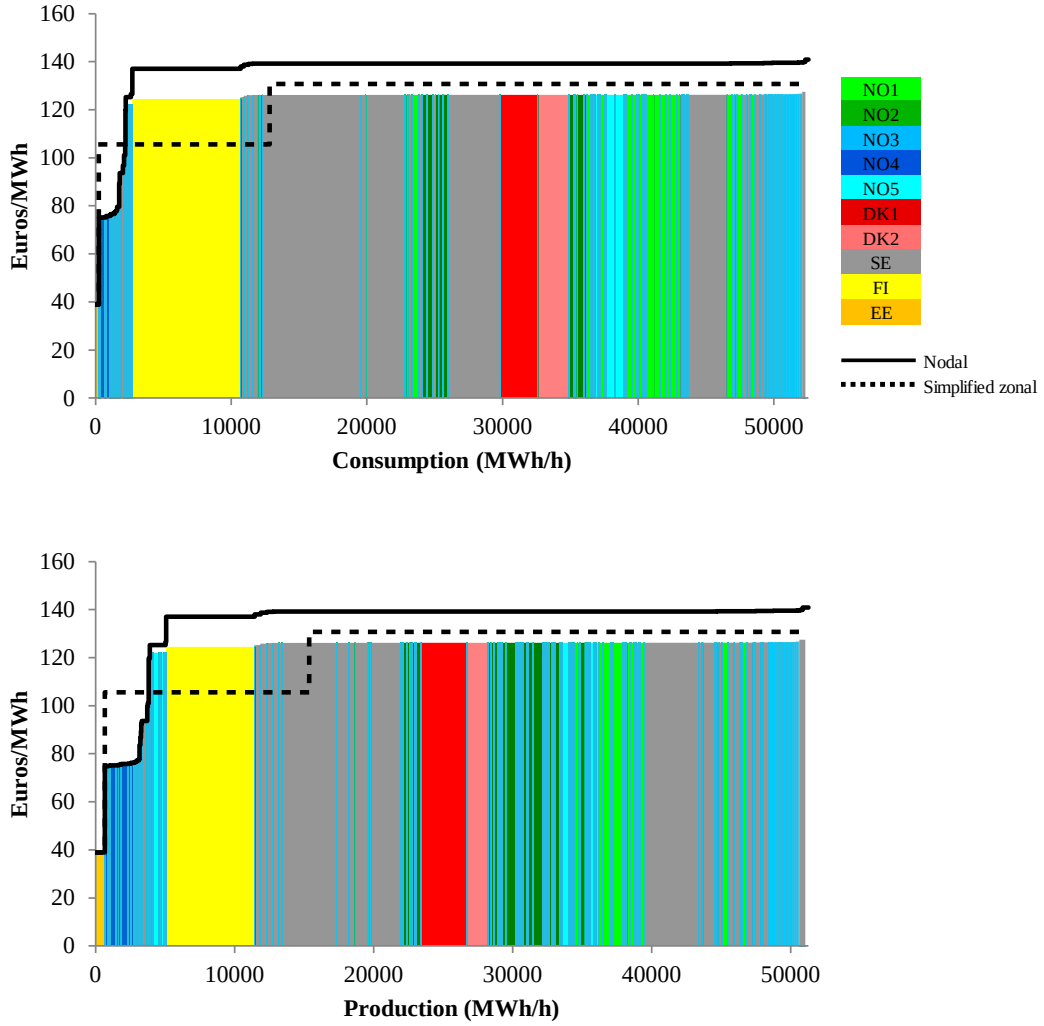

Figure 4-50 Nodal prices with more elastic demand curves (e = 0,1), 15/12-2010, hour 19

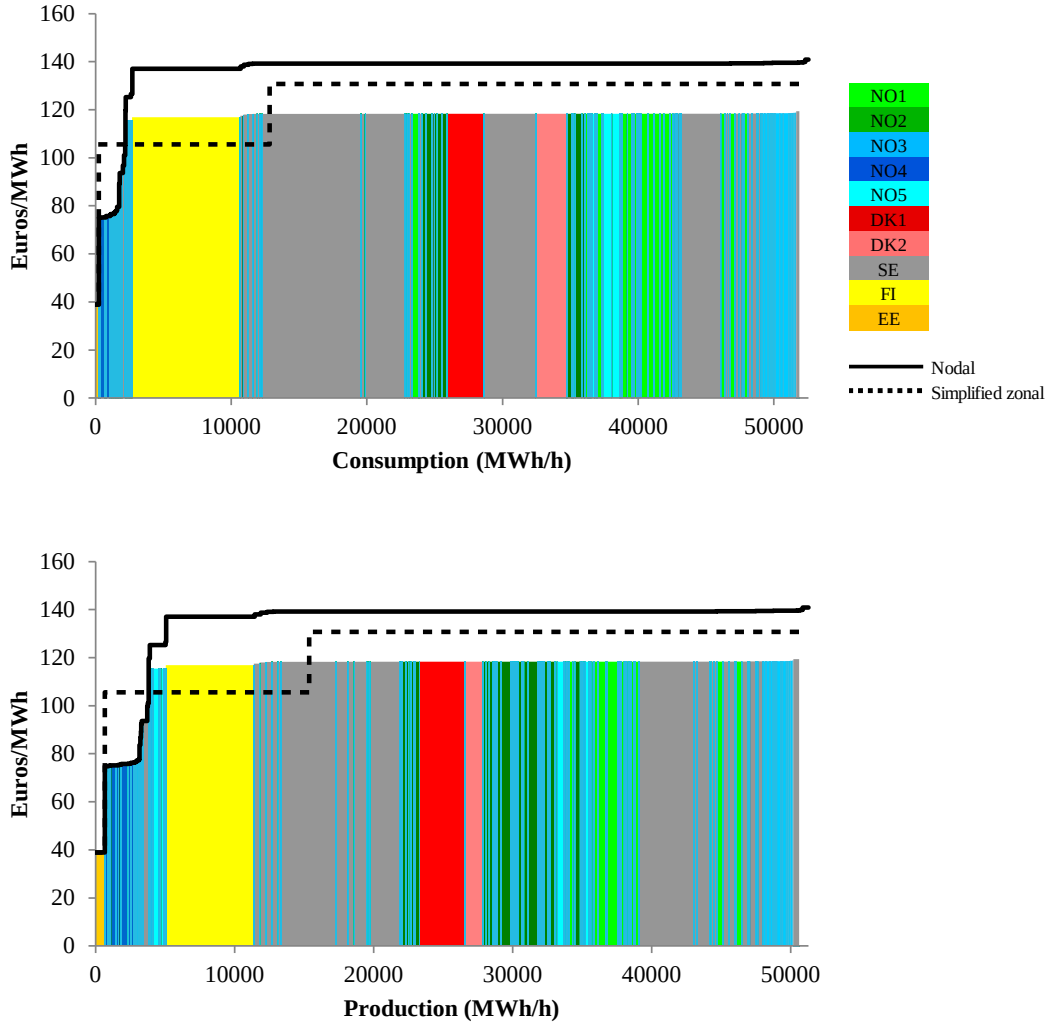

Figure 4-51 Nodal prices with more elastic demand curves (e = 0,5), 15/12-2010, hour 19

In Table 4-21 we show the surpluses for the different elasticities. We have one subtable for each elasticity since all the solutions, not only the nodal price solution, change when the elasticities change. By construction (tilting the demand curves in the "Nord Pool Spot" price point) the simplified zonal solution is almost the same for all cases, except the very last. We note that by increasing the elasticity, the allocation of surplus changes. Compared to the unconstrained cases the transfer from consumers to producers and the grid is smaller, particularly for the producers. The difference in total social surplus between the unconstrained solution and the nodal price solution shows the cost of the bottlenecks in the system. From Table 4-21, we can see that also the minimum congestion cost is somewhat reduced if demand becomes more elastic.

Table 4-21 Surpluses and surplus differences (1000 Euros) for various demand elasticities, 15/12-2010, hour 19

	Unconstrained	Simplified zonal	Nodal with demand elasticity e=0,025
Producers	6739,7	105,1	478,4
Consumers	93058,4	-178,3	-604,8
Grid	0,0	67,9	111,7
Total	99798,1	-5,4	-14,7
Infeasibilities	2 lines 1 cut	2 lines 1 cut	None

	Unconstrained	Simplified zonal	Nodal with demand elasticity e=0,05
Producers	6730,4	101,7	293,8
Consumers	86796,0	-176,7	-410,6
Grid	0,0	69,0	103,0
Total	93526,4	-6,0	-13,8
Infeasibilities	2 lines 3 cuts	2 lines 1 cut	None

	Unconstrained	Simplified zonal	Nodal with demand elasticity e=0,075
Producers	6729,1	101,4	164,5
Consumers	81683,5	-176,9	-275,1
Grid	0,0	69,2	97,3
Total	88412,6	-6,4	-13,2
Infeasibilities	2 lines 3 cuts	2 lines 1 cut	None

	Unconstrained	Simplified zonal	Nodal with demand elasticity e=0,1
Producers	6727,8	101,4	64,1
Consumers	78936,6	-177,4	-170,0
Grid	0,0	69,3	93,0
Total	85664,4	-6,8	-12,9
Infeasibilities	2 lines 3 cuts	2 lines 1 cut	None

	Unconstrained	Simplified zonal	Nodal with demand elasticity e=0,5
Producers	6433,3	-27,0	-27,0
Consumers	72639,4	-63,6	-56,4
Grid	0,0	79,7	72,8
Total	79072,7	-11,0	-10,7
Infeasibilities	2 lines 1 cut	2 lines 1 cut	None

5. Results for 07-10-2010 hour 11

5.1 Calibration of bid curves

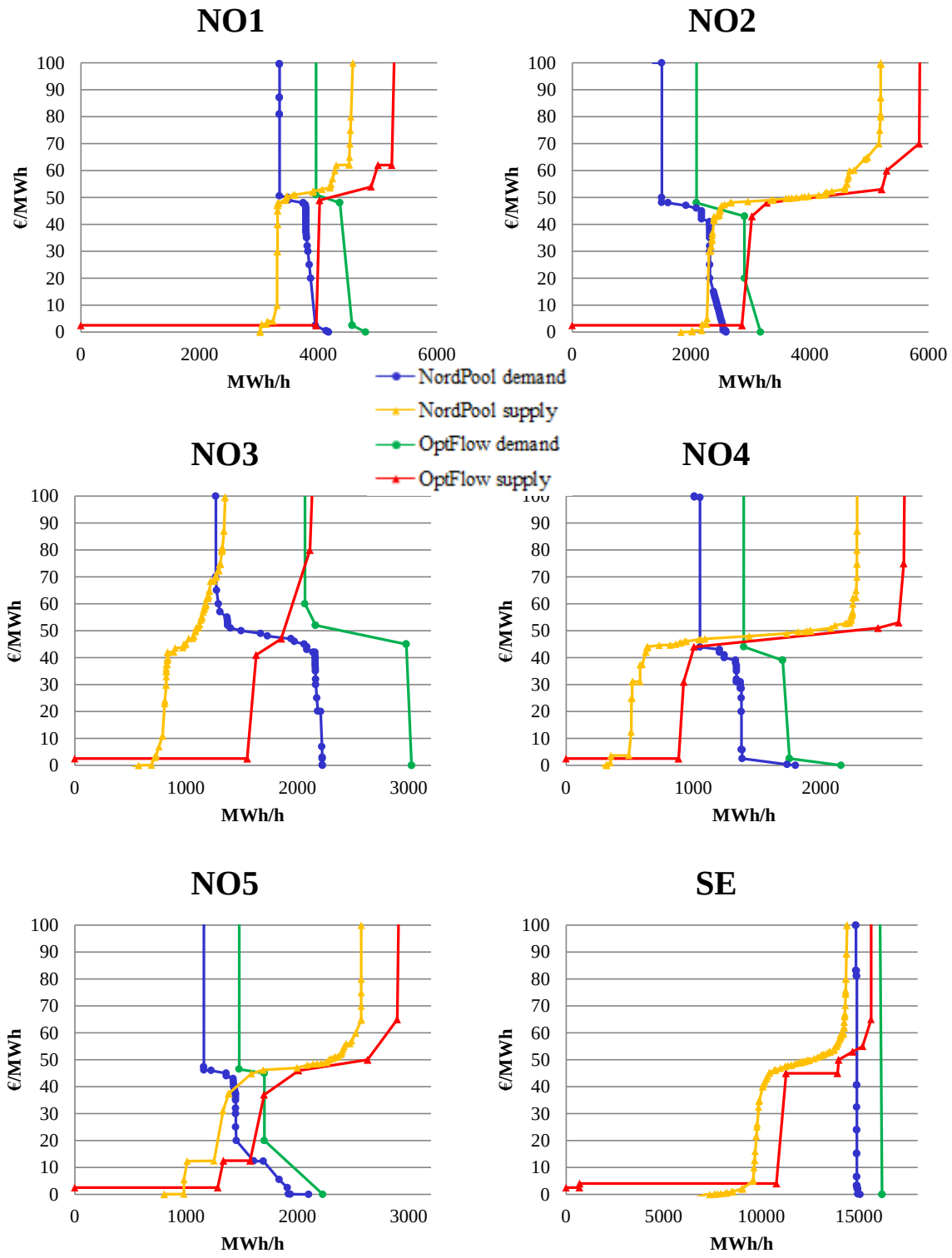

Figure 5-1 Nord Pool Spot bid curves and aggregate OptFlow bid curves for Norway and Sweden, 7/10-2010, hour 11

Figure 5-1 compares the constructed disaggregated bid curves to the actual Nord Pool bid curves, by aggregating the disaggregated curves of the OptFlow model for the different price areas. We have constructed the supply curves so that the aggregated nodal supply curves resemble the actual Nord Pool Spot curves, and so that the thermal capacities that we know is producing in this specific hour have marginal costs that allow them to do so. The information on the nodal supply curves are however so limited that we can only say that the case is inspired by 7-10-2010 hour 11. Figure 5-1 shows that in aggregate the nodal supply curves fit rather well. For this specific hour we have chosen supply and demand curves for the Swedish nodes such that the volumes in the OptFlow model are higher than the Nord Pool Spot volumes. The curves thus reflect the fact that Nord Pool Spot is not a mandatory pool, and that some of the trade is not going through Nord Pool Spot.

The remaining Elspot price areas are modeled as single nodes in the disaggregated OptFlow model, and we have used the actual Nord Pool bid curves for hour 11 on 7/10-2010 as shown in Figure 5-2.

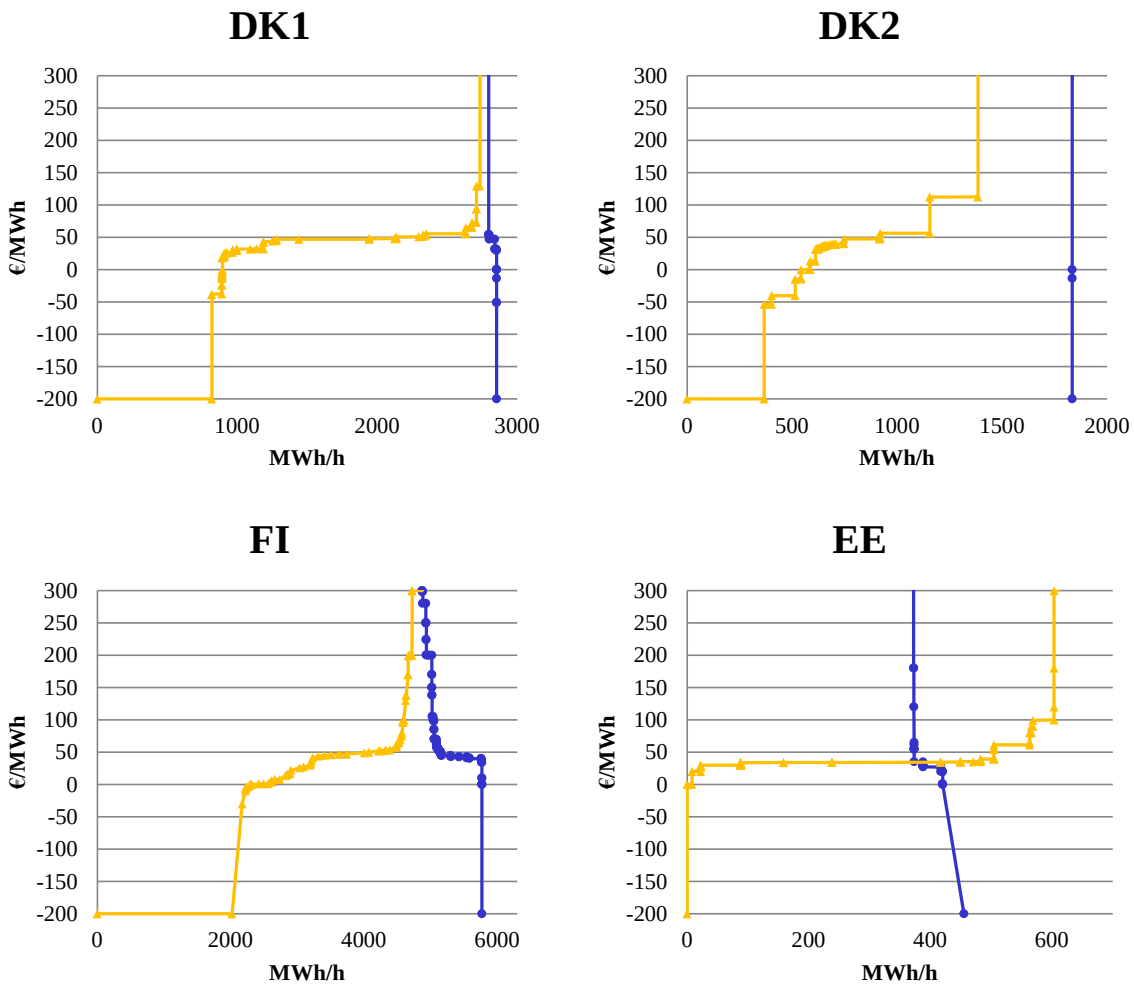

Figure 5-2 OptFlow bid curves = Nord Pool Spot for other Elspot areas, 7/10-2010, hour 11

Table 5-1 – Table 5-4 compare the actual Nord Pool Spot prices and quantities of hour 11 of 7/10-2010 to prices and quantities obtained from the OptFlow model. Columns (I) show the actual values from the Nord Pool Spot market clearing. The corresponding OptFlow values shown in columns (II)

and (III) are computed using the two different bid curve scenarios described earlier: For the values in columns (II), the actual Nord Pool Spot bid curves for this hour are used, whereas the numbers in columns (III) result from computing the "Nord Pool Spot market clearing" using our calibrated disaggregate bid curves. For these OptFlow computations we have used the actual Nord Pool capacities for (aggregate) interzonal connections. Intrazonal capacity constraints, constraints related to Kirchhoff's second law, as well as security constraints, have all been relaxed. Thus, these aggregated OptFlow prices are calculated the same way as the Elspot prices.

Table 5-1 shows that the Elspot prices (I) and the area prices calculated by the OptFlow model with Nord Pool Spot bid curves (II) match exactly, and that there are only very small differences between the Elspot prices (I) and the OptFlow simplified zonal prices based on the disaggregated OptFlow bid curves (III). Production and consumption numbers in Table 5-2 and Table 5-3 are higher for model III than for model II, since model III is to reflect all volumes. The exchange quantities in Table 5-4 are similar for the three model variants. The differences between I and II are due to imports and exports (see also the corresponding explanation for the case in Chapter 4), while the differences between II and III are due to the calibration of the disaggregated bid curves. For the latter, the biggest differences are for NO1 and NO2.

Even though the numbers do not match exactly, we use the calibrated disaggregate bid curves to evaluate the effects of different congestion management methods. As for the previous case, the following analyses use model III for comparisons with the simplified zonal price solution. This is to isolate the effects of the different congestion management methods from differences that are due to the lack of disaggregated data. In the following sections, we compare prices, quantities and surpluses for the different congestion management methods.

Table 5-1 Comparison of prices for three model variants, 7/10-2010, hour 11

Bidding area	(I) NPS actual area prices	(II) OptFlow prices with NPS bid curves	(III) OptFlow prices with calibrated bid curves
NO1	50,04	50,04	50,25
NO2	50,04	50,04	50,25
NO3	52,28	52,28	52,40
NO4	50,32	50,32	50,35
NO5	50,04	50,04	50,25
DK1	56,48	56,48	56,48
DK2	56,48	56,48	56,48
SE	52,28	52,28	52,40
FI	52,28	52,28	52,40
EE	52,28	52,28	52,40

Table 5-2 Comparison of production quantities for three model variants, 7/10-2010, hour 11

Bidding area	(I) NPS production	(II) OptFlow production with NPS bid curves	(III) OptFlow production with calibrated bid curves
NO1	3 461,9	3461,9	4239,2
NO2	3 796,9	3796,8	4151,1
NO3	1 120,7	1120,6	1897,0
NO4	2 001,9	1973,9	2318,0
NO5	2 287,2	2287,2	2635,2
DK1	2 634,8	2634,8	2634,8
DK2	1 150,2	1150,2	1150,2
SE	13 296,5	13296,6	14536,3
FI	5 575,3	4275,3	4285,3
EE	504,8	504,8	504,8

Table 5-3 Comparison of load quantities for three model variants, 7/10-2010, hour 11

Bidding area	(I) NPS load	(II) OptFlow load with NPS bid curves	(III) OptFlow load with calibrated bid curves
NO1	3 483,3	3483,3	4059,4
NO2	2 208,7	1508,7	2093,0
NO3	1 374,5	1374,5	2158,4
NO4	1 051,9	1051,9	1396,0
NO5	1 159,0	1159,0	1477,1
DK1	3 196,2	2796,2	2796,2
DK2	2 384,8	1834,8	1834,8
SE	15 226,8	14883,8	16127,1
FI	5 123,9	5123,9	5122,4
EE	621,1	373,5	373,5

Table 5-4 Comparison of exchange quantities for three model variants, 7/10-2010, hour 11

Bidding area	(I) NPS net exchange	(II) OptFlow net exchange with NPS bid curves	(III) OptFlow net exchange with calibrated bid curves
NO1	-21,4	-21,4	179,8
NO2	1 588,2	2288,1	2058,1
NO3	-253,8	-254,0	-261,3
NO4	950,0	922,0	922,0
NO5	1 128,2	1128,2	1158,2
DK1	-561,4	-161,4	-161,4
DK2	-1 234,6	-684,6	-684,6
SE	-1 930,3	-1587,2	-1590,8
FI	451,4	-848,5	-837,1
EE	-116,3	131,3	131,3

5.2 Prices

Table 5-5 compares four sets of prices for hour 11 on 7/10-2010. Actual Nord Pool Spot prices are given in the first price column (corresponding to (I) / (II) in Table 5-1), while the second and third columns show, respectively, the simplified and optimal zonal prices calculated by the OptFlow model. The simplified zonal prices correspond to (III) in Table 5-1, while optimal zonal prices take into account the specific location of all bids on the nodes and all constraints of the disaggregated power system. The three rightmost columns show descriptive statistics for the optimal nodal prices within each price zone.

Table 5-5 Prices 7/10-2010, hour 11

Bidding area	Actual NPS	Zonal prices		Optimal nodal prices		
		Simplified	Optimal	Average	Min	Max
NO1	50,04	50,25	51,81	51,12	50,95	51,81
NO2	50,04	50,25	51,06	51,02	51,01	51,04
NO3	52,28	52,40	52,56	52,60	52,09	52,84
NO4	50,32	50,35	55,22	50,97	50,61	52,65
NO5	50,04	50,25	51,04	48,23	47,45	51,04
DK1	56,48	56,48	51,65	53,24	53,24	53,24
DK2	56,48	56,48	56,35	53,24	53,24	53,24
SE	52,28	52,40	53,28	53,17	51,17	53,30
FI	52,28	52,40	53,02	53,02	53,02	53,02
EE	52,28	52,40	39,40	53,02	53,02	53,02

We see that when moving from simplified zonal prices (= area prices) to optimal nodal prices, there are rather small changes in prices. The price changes are somewhat larger for optimal zonal prices, the largest change being for Estonia.

Figure 5-3 and Figure 5-4 show the optimal nodal prices for consumption and production respectively, where prices are sorted from the lowest to the highest, and column widths represent volumes. The simplified zonal prices are shown in a similar way.[18] We notice that the lowest and highest prices are reduced, and that in the middle part of the figures, the nodal prices are very similar to the simplified zonal prices.

[18] Since the simplified zonal prices are also sorted from lowest to highest, the curves cannot be compared directly for each MW, as a specific point on the first axis may represent MWs at different locations.

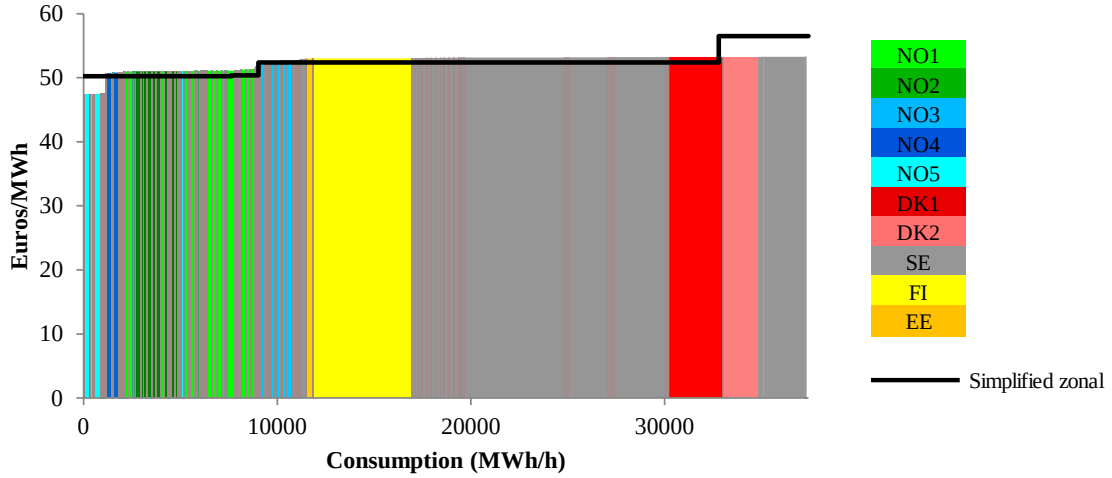

Figure 5-3 Nodal prices and load quantities, 7/10-2010, hour 11

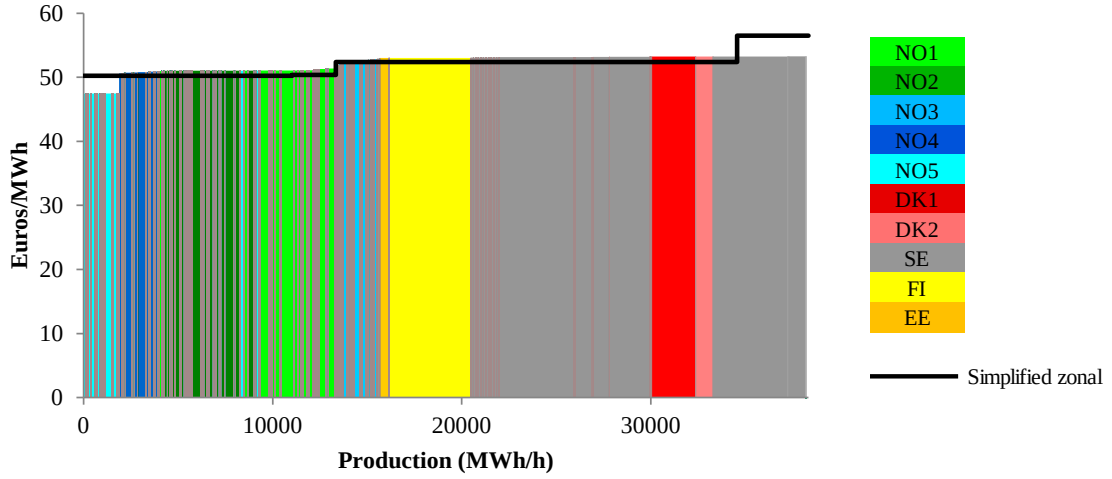

Figure 5-4 Nodal prices and production quantities, 7/10-2010, hour 11

Figure 5-5 and Figure 5-6 further illustrate the geographical variation in the optimal nodal prices. The color scale show different price intervals and the nodes are weighted by load and generation volumes. The node sizes show the concentration of load and production, although this also depends on the level of detail available on the power system in different parts of the Nordic power system (DK1, DK2, FI and EE being represented by single nodes).

The figures also show that for the present hour there are exports from the Nord Pool area to most of the adjacent areas, Russia being the exception from which there is a relatively large import to FI.

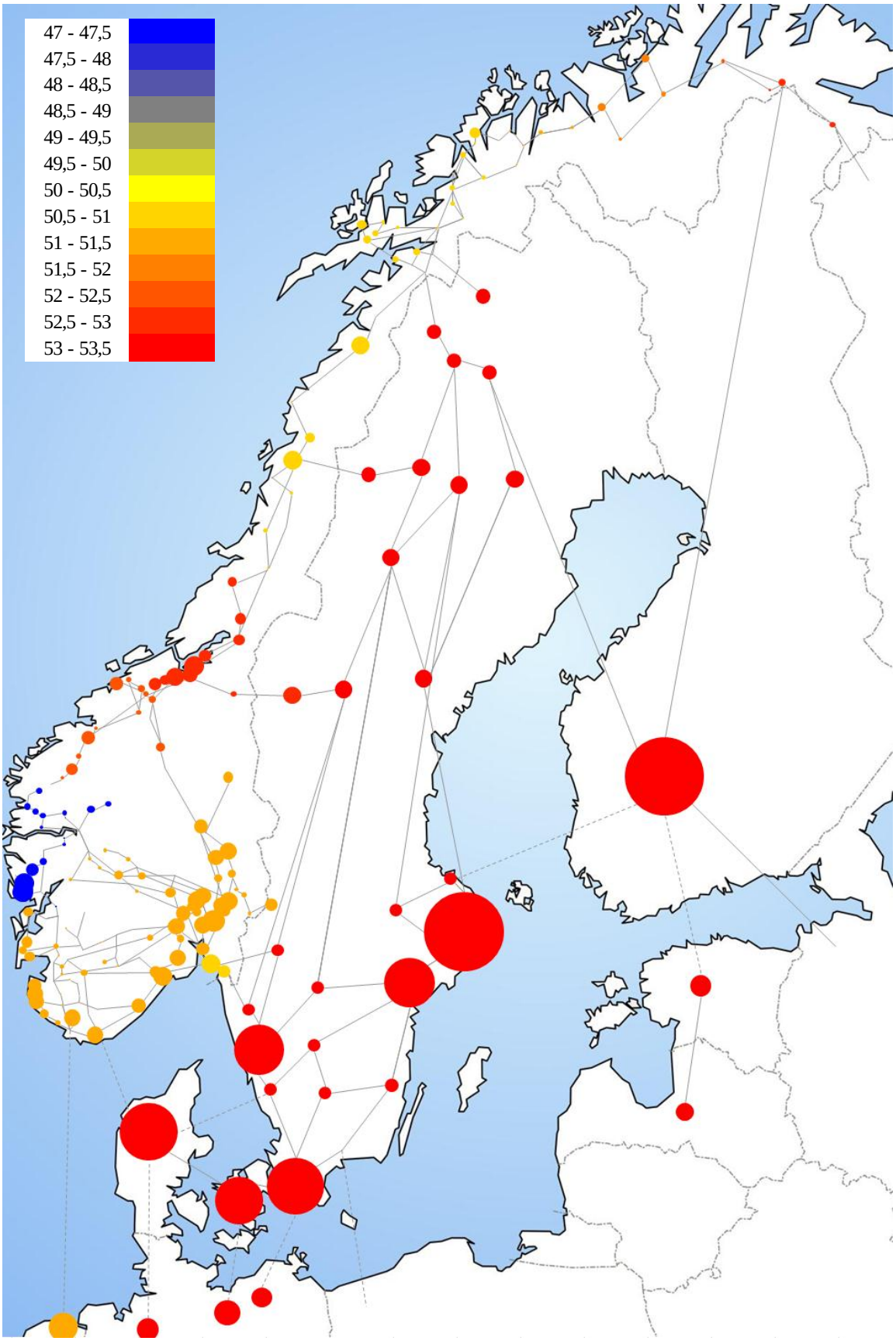

Figure 5-5 Nodal prices weighted by consumption, 7/10-2010, hour 11

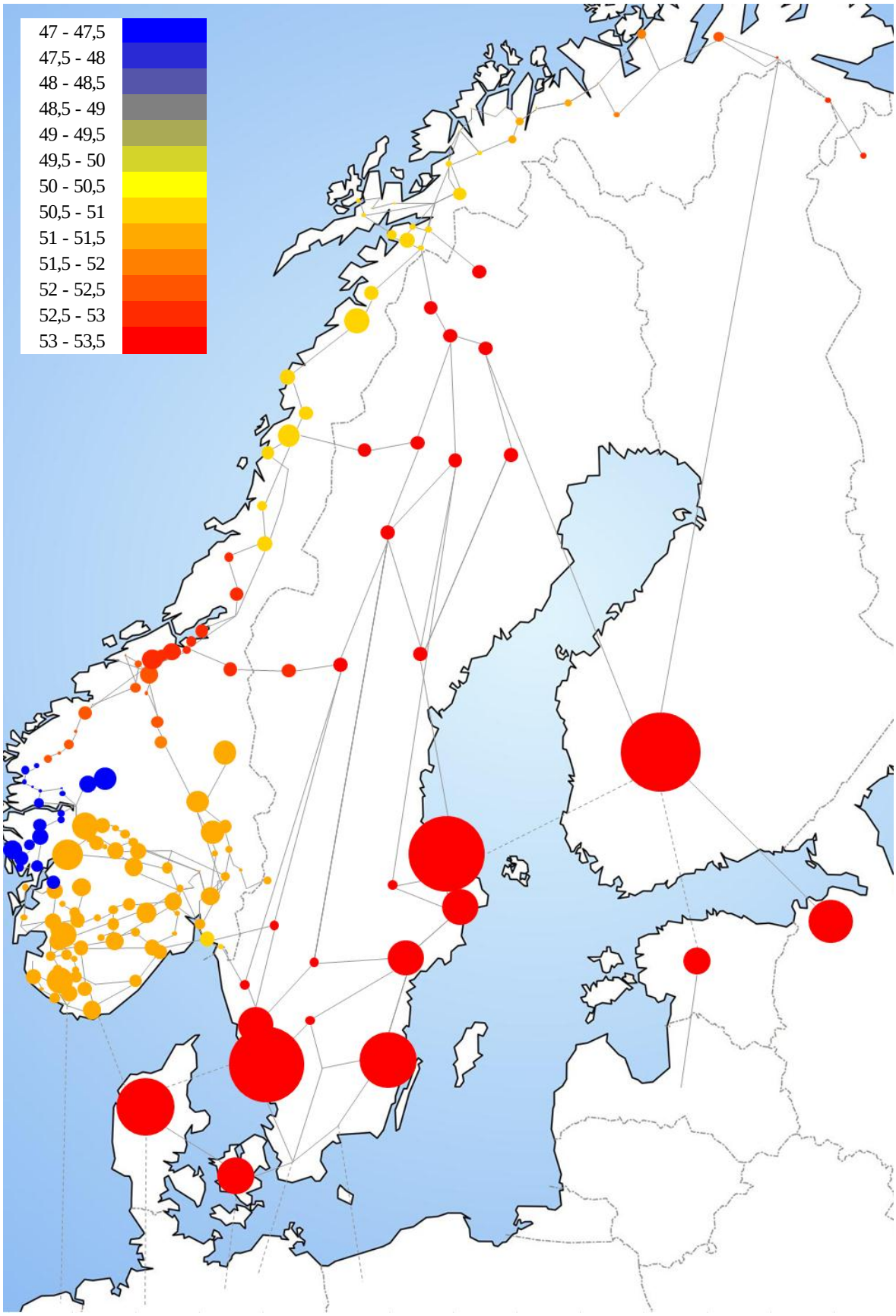

Figure 5-6 Nodal prices weighted by production, 7/10-2010, hour 11

Figure 5-7 and Figure 5-8 compare simplified and optimal zonal prices. The figures are similar to Figure 5-3 and Figure 5-4 for optimal nodal prices, except that we have sorted simplified zonal prices from the lowest to the highest, and shown the corresponding optimal zonal price in the same sequence. Thus it is easier to compare the changes that result in the zonal prices from taking into account all constraints and the specific location of bids to nodes (optimal zonal prices) instead of only a subset of the constraints or some indirect representation of the constraints (simplified zonal prices). As Table 5-5 shows already, Figure 5-7 and Figure 5-8 show that some zonal prices increase while others decrease.

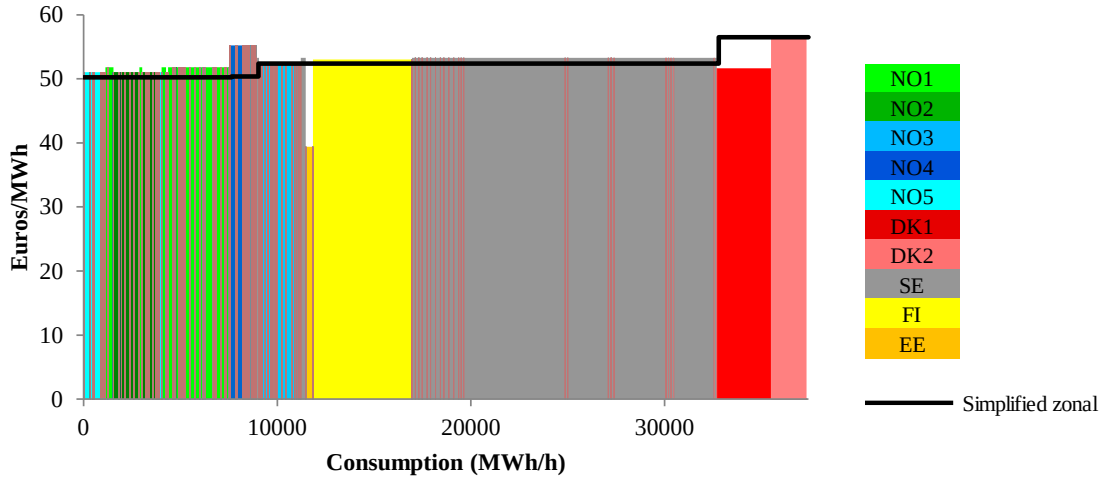

Figure 5-7 Optimal zonal prices and load quantities, 7/10-2010, hour 11

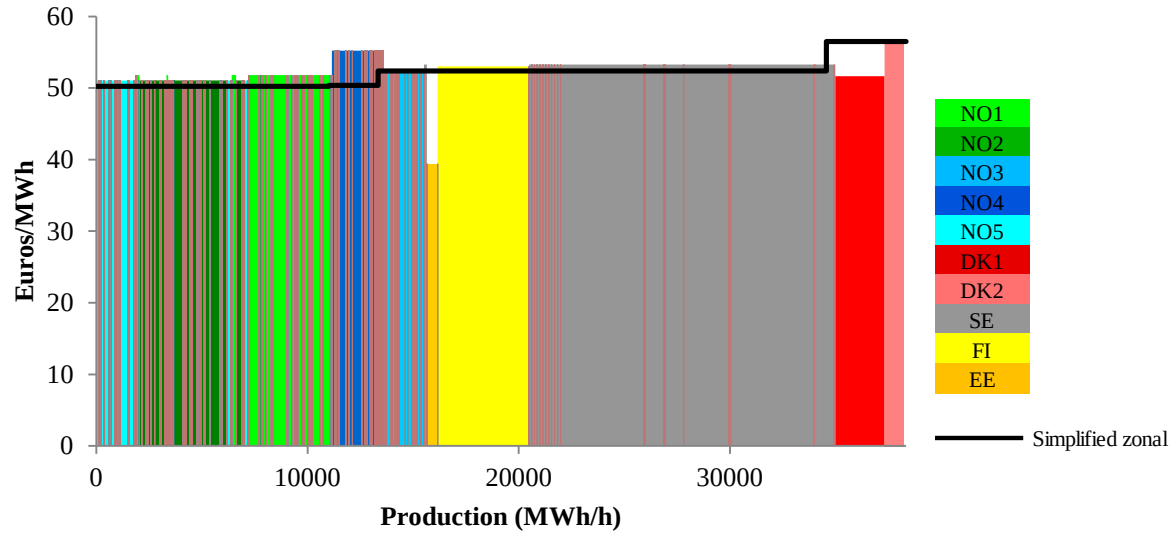

Figure 5-8 Optimal zonal prices and production quantities, 7/10-2010, hour 11

5.3 Power flows and bottlenecks

Figure 5-9 shows the power flow of the nodal price solution. The links are weighted by the flow sizes, HVDC links are shown by dotted lines, and the binding thermal capacity constraints are shown in red colors. We notice that there are three links that are operated on their thermal capacity limits, and their capacities and the shadow prices on the constraints are shown in Table 5-6. The shadow prices show the value of increasing the corresponding thermal capacity limits, i.e. the increase in social surplus. For the present case, the shadow prices on the thermal constraints are not very high.

Table 5-6 Shadow prices for binding capacity constraints with nodal pricing, 7/10-2010, hour 11

From	To	Max	Shadow price
Kristiansand	DK1	1000	2,22
Malmö	DK2	1300	0,03
FI	Forsmark	550	0,14

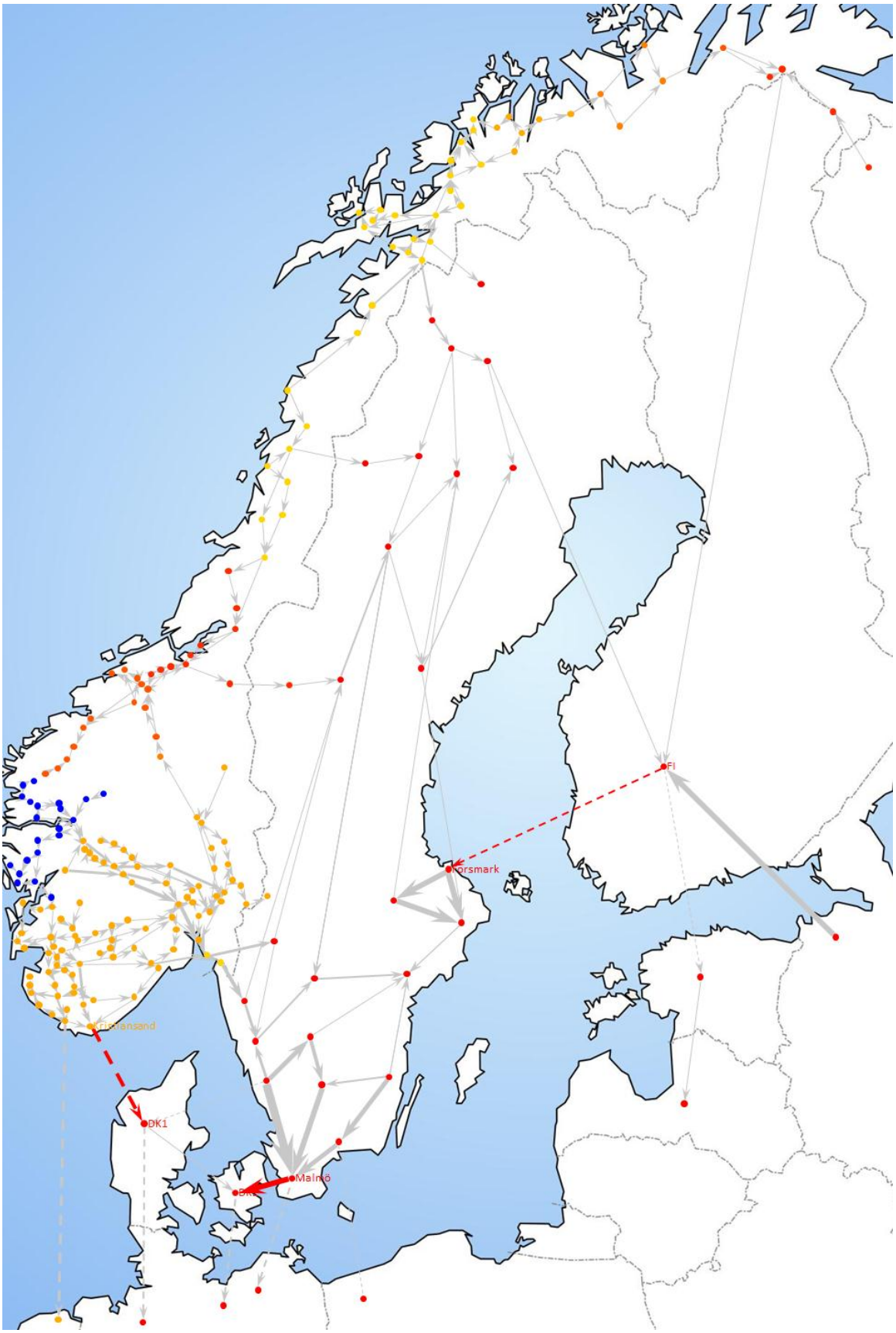

Figure 5-9 Line flows and thermal bottlenecks for optimal nodal price solution, 7/10-2010, hour 11

The histograms in Figure 5-10 – Figure 5-12 describe the utilization of the lines' thermal capacity limits under the three pricing methodologies. For nodal pricing, optimal, and simplified zonal pricing, respectively, the figures show the number of lines operating within different intervals of capacity utilization. We distinguish between inter-zonal lines (red color) and intra-zonal lines (blue color). Regardless of congestion management method, most of the lines are operated well below their thermal capacity limits, and for the present case we notice from Figure 5-12 that even the simplified zonal approach results in feasible power flows over all individual lines, i.e. no thermal constraints are violated.[19]

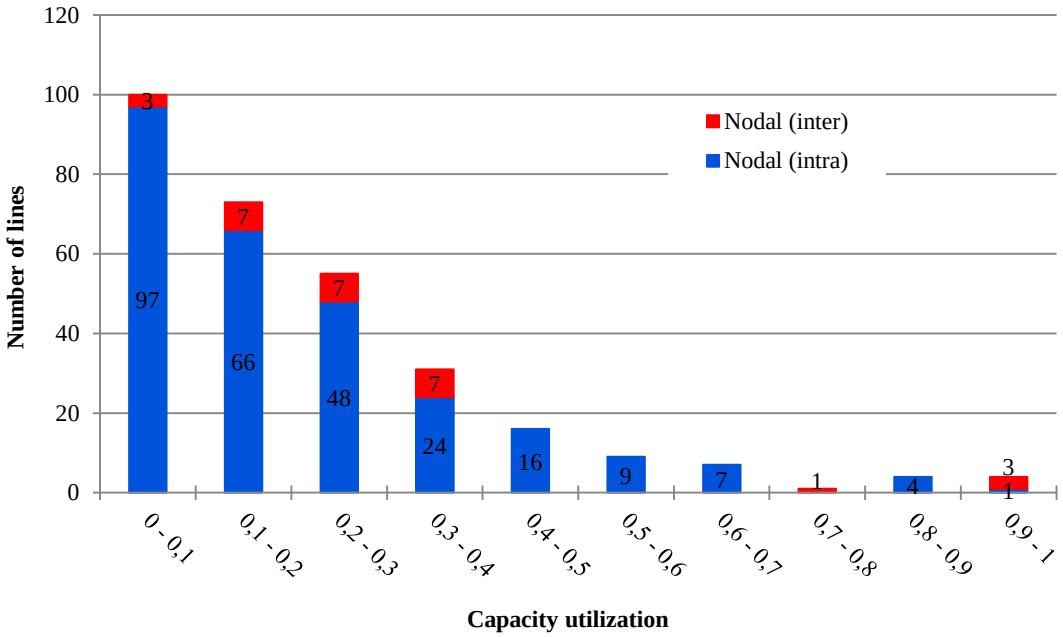

Figure 5-10 Line capacity utilization with nodal pricing, 7/10-2010, hour 11

[19] The procedure for calculating power flows from a given set of nodal prices and quantities are described in previous chapters.

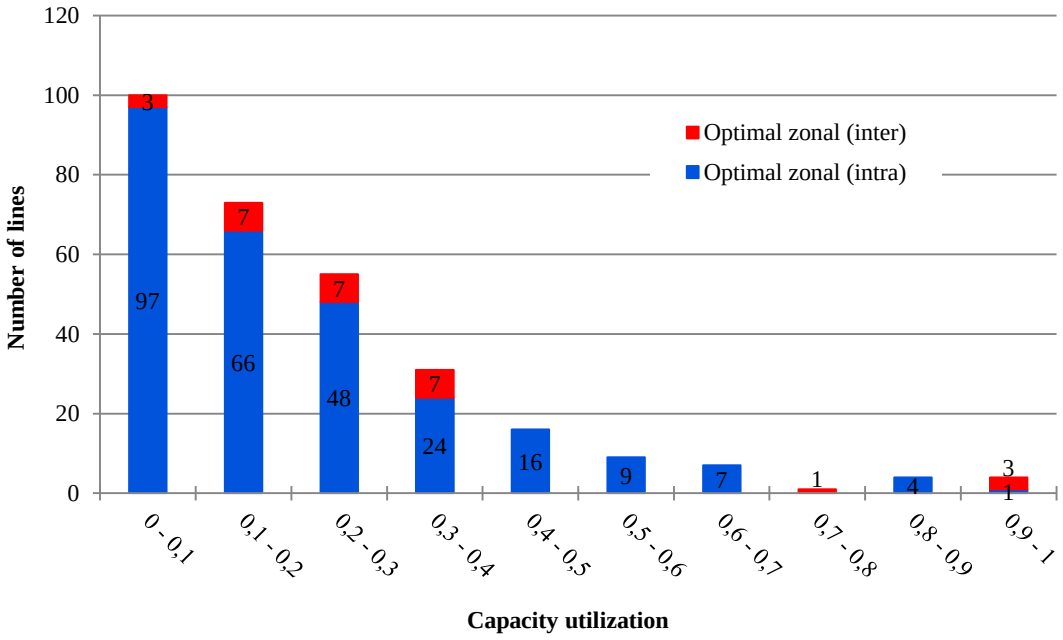

Figure 5-11 Line capacity utilization with optimal zonal pricing, 7/10-2010, hour 11

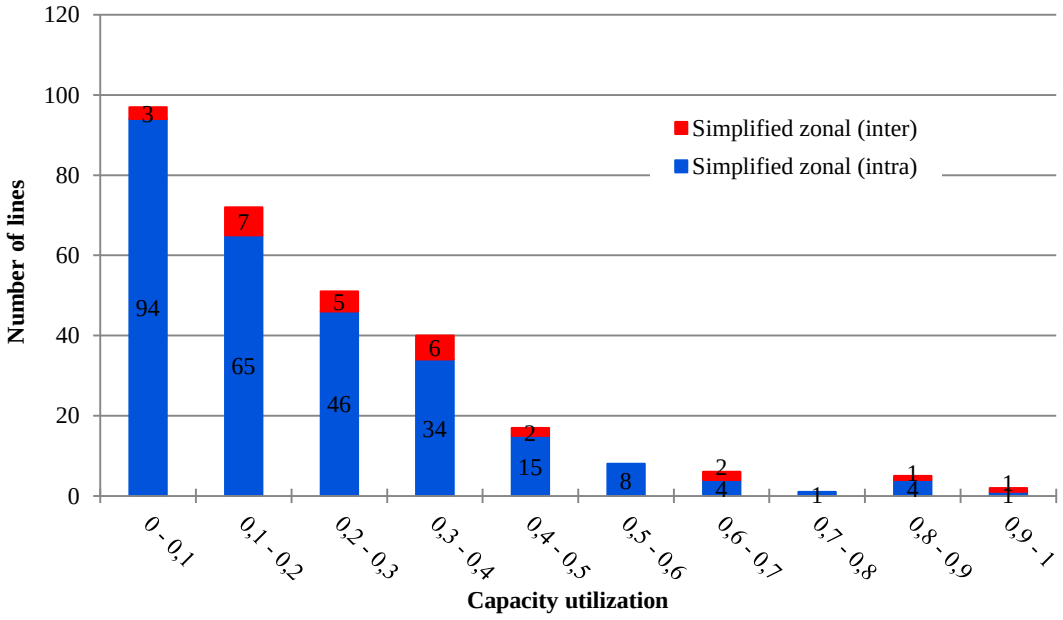

Figure 5-12 Line capacity utilization with simplified zonal pricing, 7/10-2010, hour 11

Figure 5-13 – Figure 5-15 show the utilization of the cut constraints for the different pricing methods. Looking more closely at the nodal price solution, there are three cut constraints that are operated on their capacity limit. The shadow prices for these three, Hasle eksport, Nordland, and Fardal overskudd 2, are given in Table 5-7.

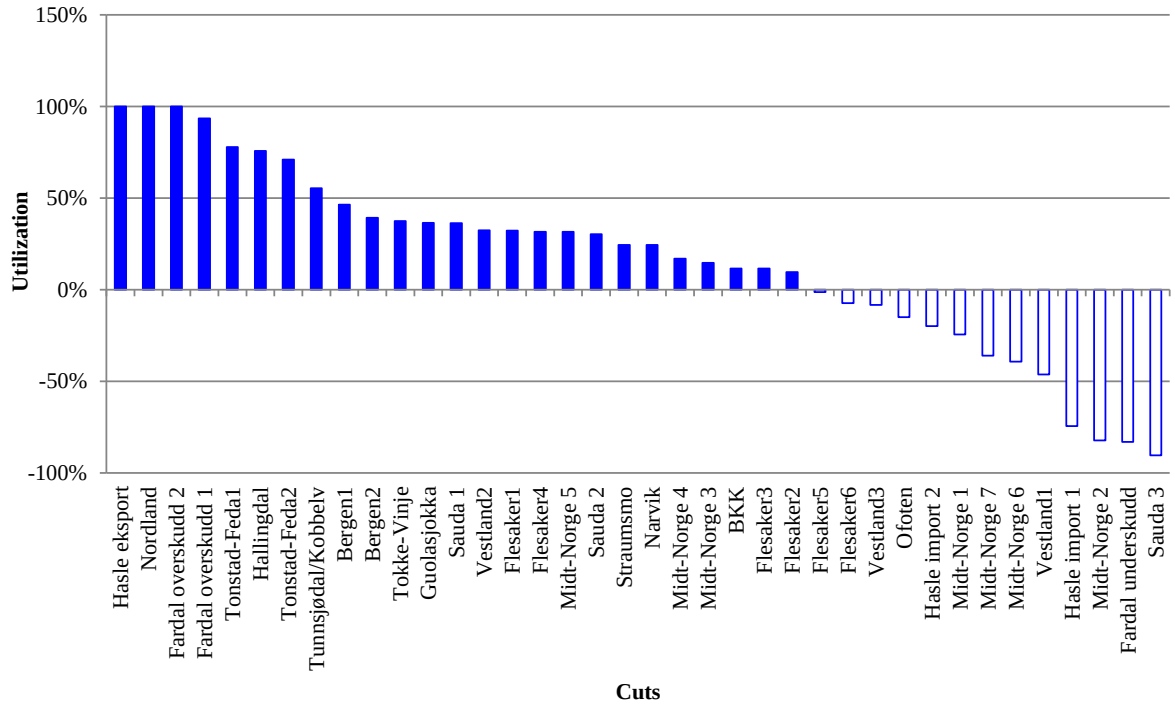

Figure 5-13 Cut capacity utilization with nodal pricing, 7/10-2010, hour 11

Table 5-7 Shadow prices for cut capacity constraints with nodal pricing, 7/10-2010, hour 11

Cut name	Capacity	From	To	Share of flow included	Shadow price
Hasle eksport	1600	Hasle	Borgvik	1	*2,39*
		Halden	Skogssäter	1	
Nordland	1000	Ofoten	Ritsem	1	*2,22*
		Nedre Røssåga	Ajaure	1	
		Tunnsjødal	Verdal	1	
		Tunnsjødal	Namsos	1	
		Sildvik	Tornehamn	1	
Fardal overskudd 2	750	Mauranger	Blåfalli	1	*3,59*
		Fardal	Aurland1	1	

While all the cut constraints are fulfilled in the optimal nodal and optimal zonal price solutions, we can see from Figure 5-15 that two of the cut constraints are violated in the simplified zonal solution. These are the Fardal overskudd 1 and Fardal overskudd 2 cuts. It is interesting to notice that the first of these two are not operated on its capacity limit neither in the optimal nodal solution nor in the optimal zonal solution.

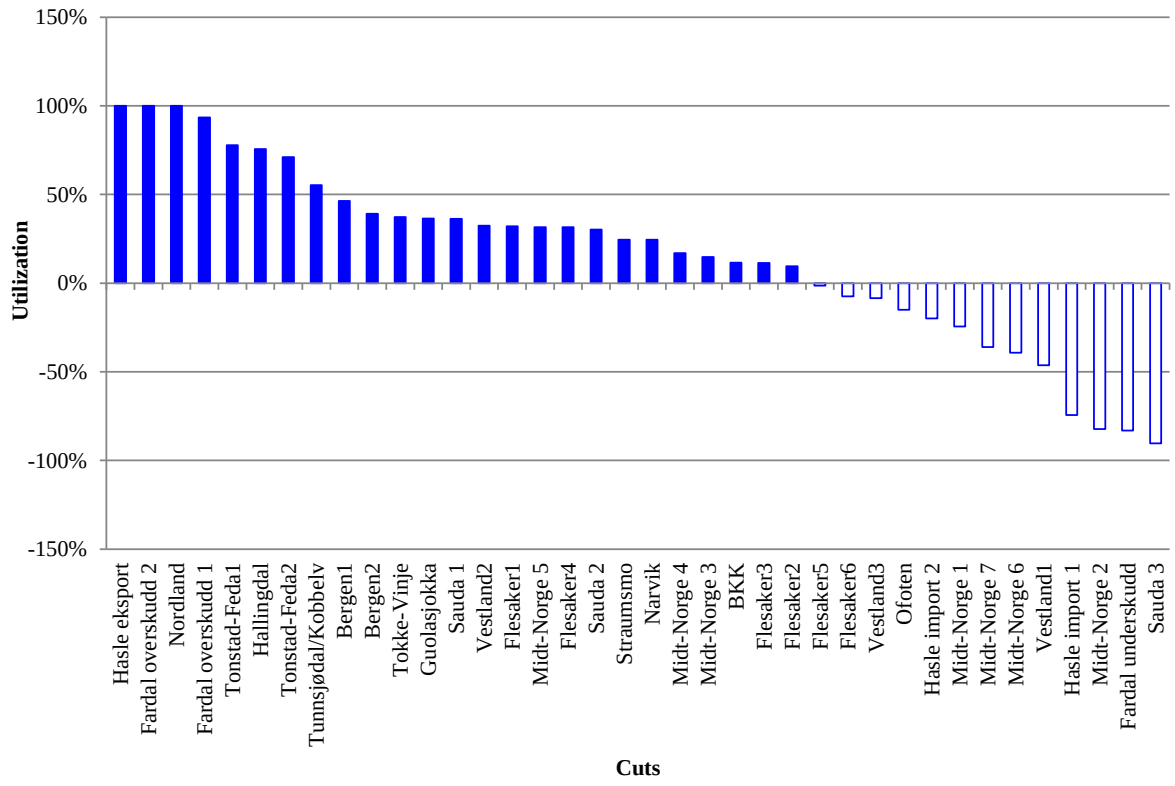

Figure 5-14 Cut capacity utilization with optimal zonal pricing, 7/10-2010, hour 11

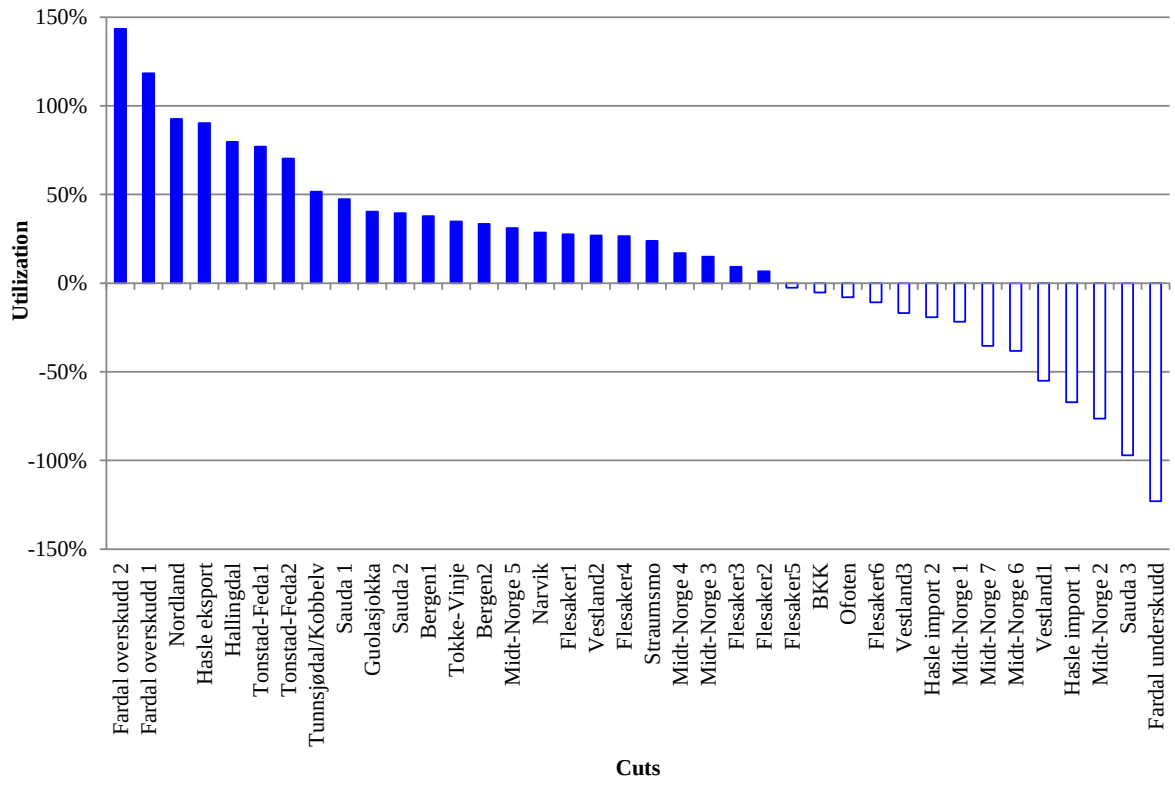

Figure 5-15 Cut capacity utilization with simplified zonal pricing, 7/10-2010, hour 11

5.4 Load and generation quantities

In Figure 5-16 we show the differences in load for each node, i.e. the difference between the quantities consumed in the simplified zonal solution and the quantities consumed in the optimal nodal and the optimal zonal solutions. We notice that the differences are very small between the optimal nodal and optimal zonal quantities. Compared to the case in chapter 4, the differences between the simplified zonal solution and the other two solutions are somewhat larger. The prices are lower for this case, and the elasticities are higher, and this explains the larger differences in consumed quantities even if the price differences are smaller.

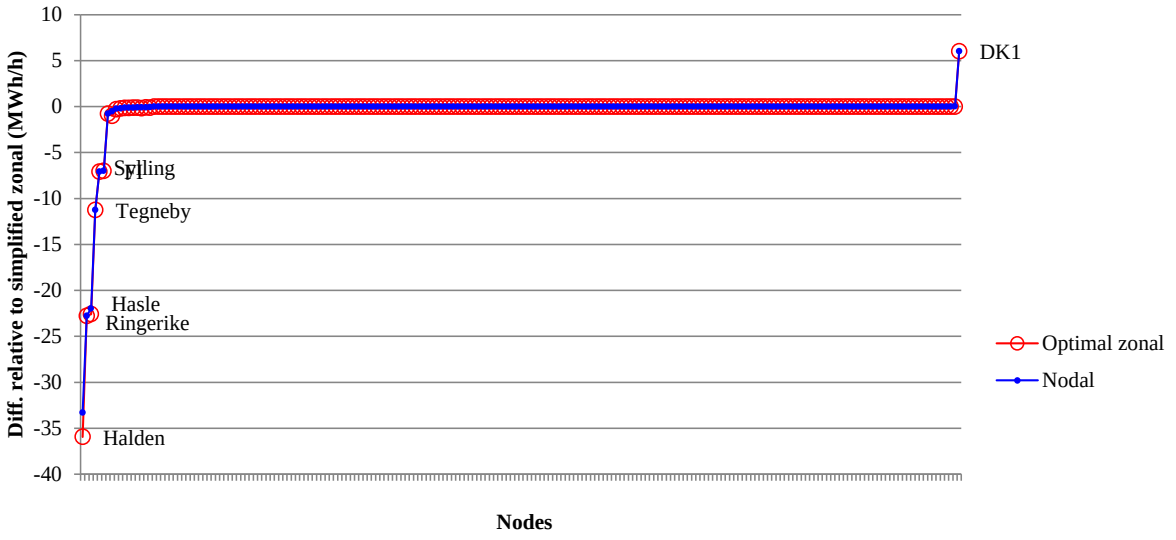

Figure 5-16 Differences in load between simplified zonal and the other two pricing approaches, 7/10-2010, hour 11

Figure 5-17 shows the same differences for generation quantities. Also for this case the quantity differences between the simplified zonal solution and the other two solutions are larger for generation than for consumption. The optimal nodal and optimal zonal quantities are very similar.

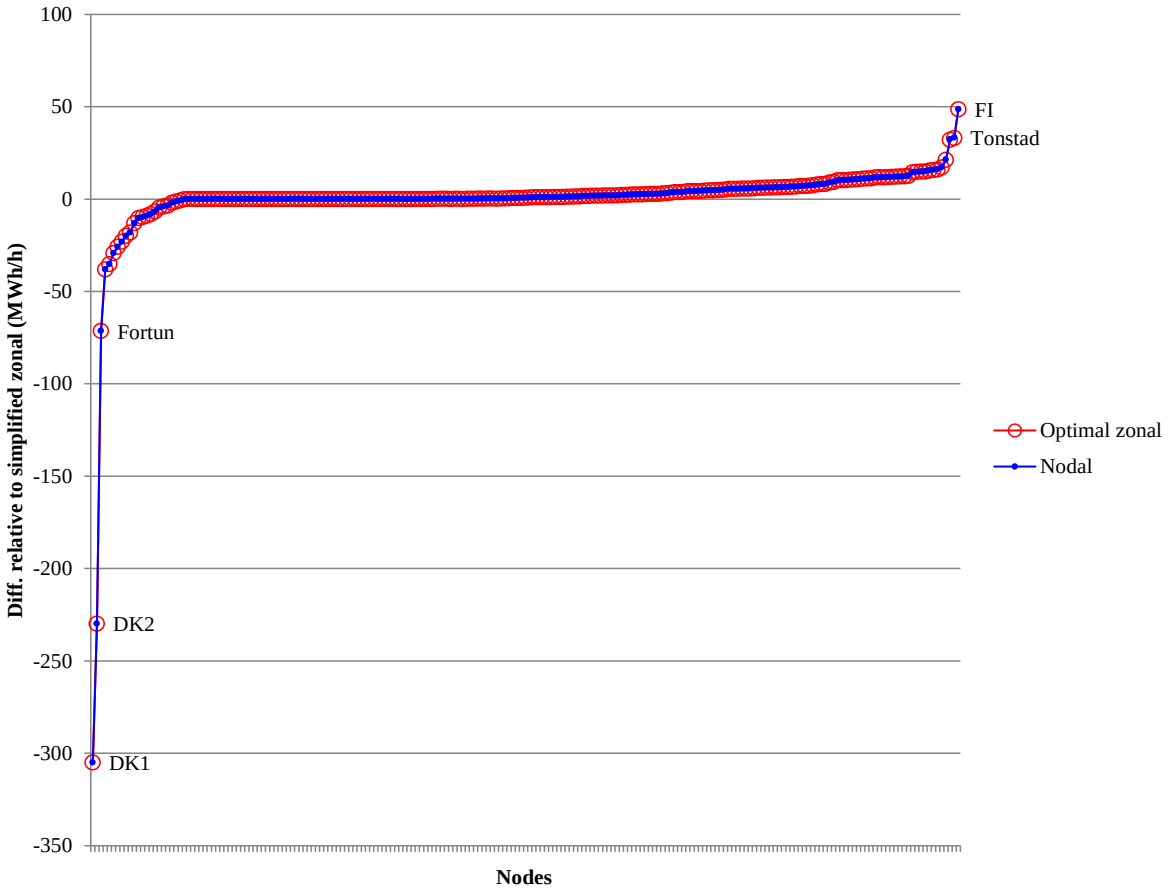

Figure 5-17 Differences in generation between simplified zonal and the other two pricing approaches, 7/10-2010, hour 11

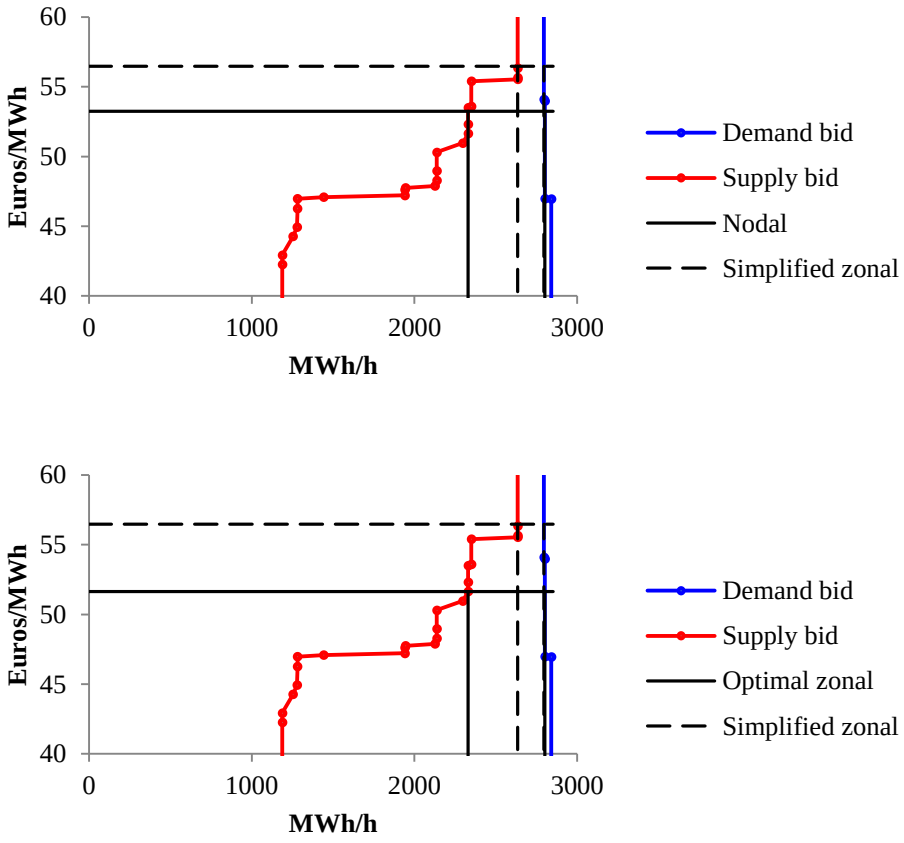

Figure 5-18 Differences in generation, DK1, 7/10-2010, hour 11

In Figure 5-18 we show the bid curves for DK1, the node where the optimal nodal / optimal zonal generation differs most from the generation at the simplified zonal price. We see that there is a horizontal part of the supply function at about 55 Euros/MWh. This bid is included at the simplified zonal price, but not at the optimal nodal or zonal price.

5.5 Surpluses

In Table 5-8 we show the changes in surplus compared to the unconstrained market solution. For the present case, we see that moving from simplified zonal prices to optimal zonal or nodal prices leads to a small increase in total surplus, and at the same time the infeasibilities are gone. The optimal nodal and optimal zonal solutions have opposite effects on producers, consumers and grid revenue. We notice that the optimal zonal prices lead to negative grid revenues. Since the simplified zonal solution also here implies some infeasibility, the total surpluses are not comparable. Relieving the infeasibilities in the simplified zonal solution will incur higher costs than those reflected in Table 5-8, since counter trading is needed in order to relieve the constraints.

Table 5-8 Unconstrained surplus and surplus differences (1000 Euros), 7/10-2010, hour 11

	Un-constrained	Simplified zonal	Optimal zonal	Nodal
Producers	2364,2	21,1	42,9	28,8
Consumers	75841,2	-39,3	-49,9	-41,4
Grid	0,0	15,1	5,5	11,1
Total	78205,4	-3,1	-1,5	-1,5
Infeasibilities	4 lines 6 cuts	0 lines 2 cuts	None	None

6. Results for 1-8-2010 hour 6

6.1 Calibration of bid curves

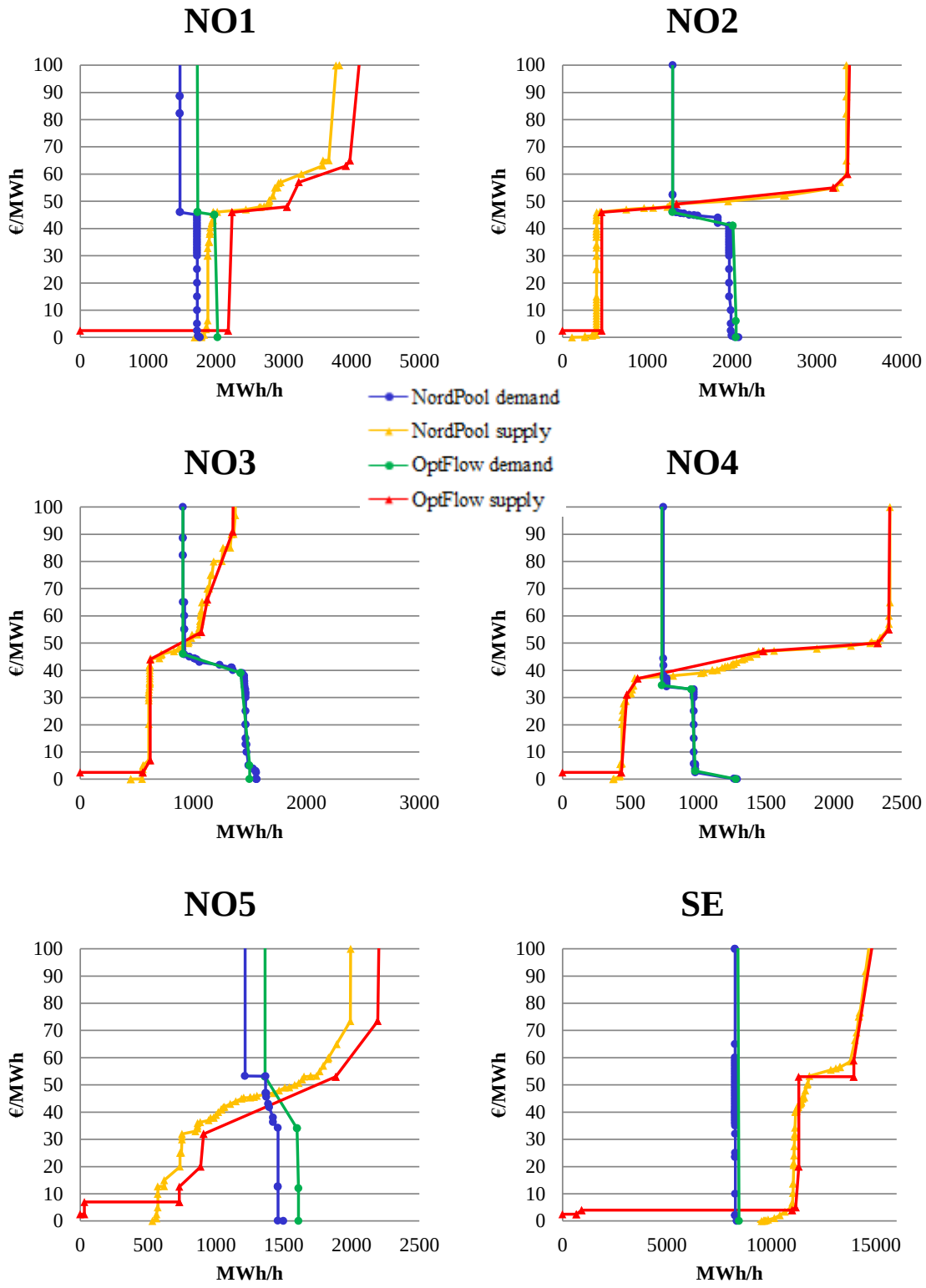

Figure 6-1 Nord Pool Spot bid curves and aggregate OptFlow bid curves for Norway and Sweden, 1/8-2010, hour 6

Figure 6-1compares the constructed disaggregated bid curves to the actual Nord Pool bid curves, by aggregating the disaggregated curves of the OptFlow model for the different price areas. Also for this case the figure shows that in aggregate the nodal bid curves fit rather well with the Nord Pool bid curves. For this case the volume differences between the Nord Pool curves and the constructed disaggregate bid curves seem smaller than for the previous cases. The supply and demand curves for the Elspot price areas that are modeled as single nodes in the disaggregated OptFlow model, and where we have used the actual Nord Pool bid curves for hour 6 on 1/8-2010 are shown in Figure 6-2.

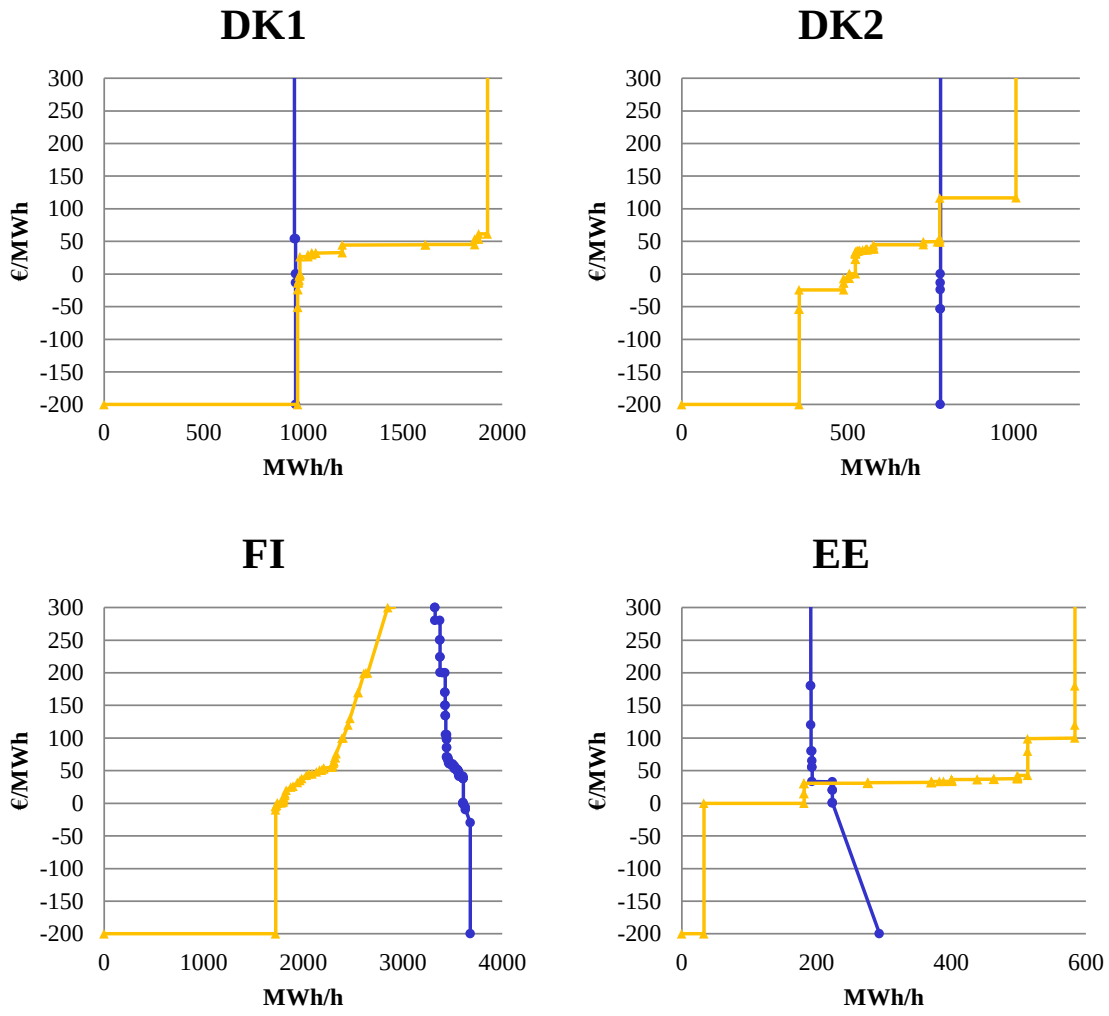

Figure 6-2 OptFlow bid curves = Nord Pool Spot for other Elspot areas, 1/8-2010, hour 6

As in previous chapters, Table 6-1 – Table 6-4 compare the actual Nord Pool Spot prices and quantities of hour 6 of 1/8-2010 to prices and quantities obtained from the two variants of simplified zonal solutions from the OptFlow model. Table 6-1 shows that the Elspot prices (I) and the area prices calculated by the OptFlow model with Nord Pool Spot bid curves (II) match almost exactly, and that there is a small difference between the Elspot prices (I) and the OptFlow simplified zonal prices based on the disaggregated OptFlow bid curves (III). Except for Estonia, all area prices are equal and very low for this case.

For the production, consumption and exchange numbers in Table 6-2 – Table 6-4 the differences between I and II are due to imports and exports, while the differences between II and III are due to the calibration of the bid curves, so as to include all production and load. For the exchange quantities the differences between II and III are quite small.

Based on this, we conclude that the calibrated data set is a reasonable starting point for analyzing the effects of different congestion management methods in an hourly market similar to hour 6 on 1/8-2010 in the following sections.

Table 6-1 Comparison of prices for three model variants, 1/8-2010, hour 6

Bidding area	(I) NPS actual area prices	(II) OptFlow prices with NPS bid curves	(III) OptFlow prices with calibrated bid curves
NO1	7,29	7,31	7,00
NO2	7,29	7,31	7,00
NO3	7,29	7,31	7,00
NO4	7,29	7,31	7,00
NO5	7,29	7,31	7,00
DK1	7,29	7,31	7,00
DK2	7,29	7,31	7,00
SE	7,29	7,31	7,00
FI	7,29	7,31	7,00
EE	30,63	30,63	30,63

Table 6-2 Comparison of production quantities for three model variants, 1/8-2010, hour 6

Bidding area	(I) NPS production	(II) OptFlow production with NPS bid curves	(III) OptFlow production with calibrated bid curves
NO1	1881	1881	2188
NO2	1095	400	461
NO3	607	607	619
NO4	438	438	440
NO5	572	572	715
DK1	1384	984	984
DK2	780	524	524
SE	11565	11015	11186
FI	3172	1808	1807
EE	207	207	207

Table 6-3 Comparison of load quantities for three model variants, 1/8-2010, hour 6

Bidding area	(I) NPS load	(II) OptFlow load with NPS bid curves	(III) OptFlow load with calibrated bid curves
NO1	1725	1725	2019
NO2	1987	1987	2045
NO3	1482	1482	1494
NO4	968	968	975
NO5	1458	1458	1609
DK1	963	963	963
DK2	780	780	780
SE	8272	8272	8446
FI	3609	3609	3609
EE	459	224	224

Table 6-4 Comparison of exchange quantities for three model variants, 1/8-2010

Bidding area	(I) NPS net exchange	(II) OptFlow net exchange with NPS bid curves	(III) OptFlow net exchange with calibrated bid curves
NO1	156	156	169
NO2	-891	-1586	-1583
NO3	-875	-875	-874
NO4	-529	-529	-534
NO5	-886	-886	-894
DK1	422	22	22
DK2	0	-256	-256
SE	3293	2743	2740
FI	-437	-1801	-1802
EE	-252	-17	-17

6.2 Prices

Table 6-5 compares the four sets of prices for hour 6 on 1/8-2010. The actual Nord Pool Spot prices are given in the first price column (corresponding to (I) in Table 6-1), while the second and third columns show, respectively, the simplified and optimal zonal prices calculated by the OptFlow model. The simplified zonal prices correspond to (III) in Table 6-1, while optimal zonal prices take into account the specific location of all bids on the nodes and all constraints of the disaggregated power system. The three rightmost columns show descriptive statistics for the optimal nodal prices within each price zone.

We see that when moving from the simplified zonal prices to optimal zonal or nodal prices, prices change a lot. In the simplified zonal price solution all prices except Estonia are equal. Moving to nodal prices or optimal zonal prices introduces much more variation.

Table 6-5 Prices 1/8-2010, hour 6

Bidding area	Actual NPS	Zonal prices		Optimal nodal prices		
		Simplified	Optimal	Average	Min	Max
NO1	7,29	7,00	7,16	34,54	32,14	35,21
NO2	7,29	7,00	2,50	34,81	34,75	34,87
NO3	7,29	7,00	2,50	27,52	2,50	52,74
NO4	7,29	7,00	6,63	28,14	26,97	29,94
NO5	7,29	7,00	12,60	34,75	34,70	34,79
DK1	7,29	7,00	0,00	10,53	10,53	10,53
DK2	7,29	7,00	0,40	10,53	10,53	10,53
SE	7,29	7,00	6,75	19,54	4,00	36,63
FI	7,29	7,00	6,39	26,82	26,82	26,82
EE	30,63	30,63	0,10	26,82	26,82	26,82

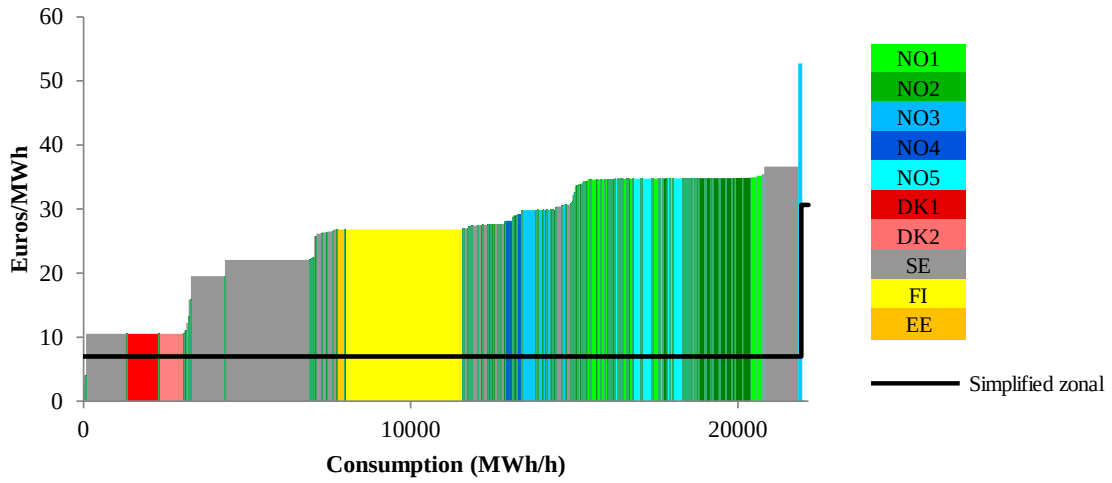

Figure 6-3 Nodal prices and load quantities, 1/8-2010, hour 6

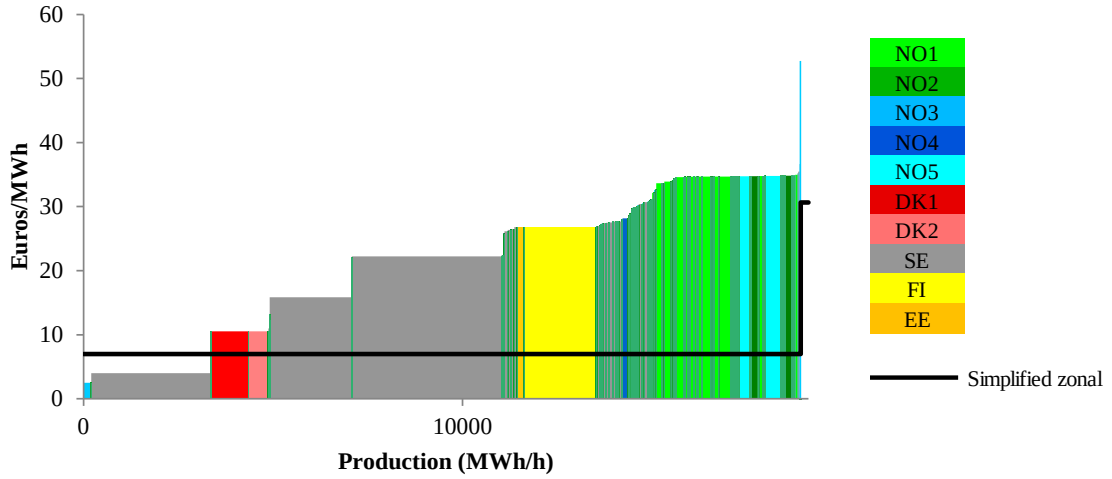

Figure 6-4 Nodal prices and production quantities, 1/8-2010, hour 6

Figure 6-3 and Figure 6-4 show the optimal nodal prices for consumption and production respectively, where prices are sorted from the lowest to the highest, and column widths represent volumes. The nodal prices are compared to the sorted simplified zonal prices, and we notice that for this hourly case, the nodal prices are for the most part higher than the simplified zonal prices, and in many nodes considerably higher. The reason for this is that the nodal prices include shadow prices for all transmission constraints, whereas the simplified zonal prices do not (we will come back to this in the next section).

Figure 6-5 and Figure 6-6 illustrate the geographical variation in the optimal nodal prices. The lowest prices are in the southern part of the Nord Pool area and the highest prices are in southern and mid Norway and on the west coast of Sweden. The figures also show that for the present hour there are imports to the Nord Pool area from most of the adjacent areas (Figure 6-3), except Lithuania (Figure 6-4).

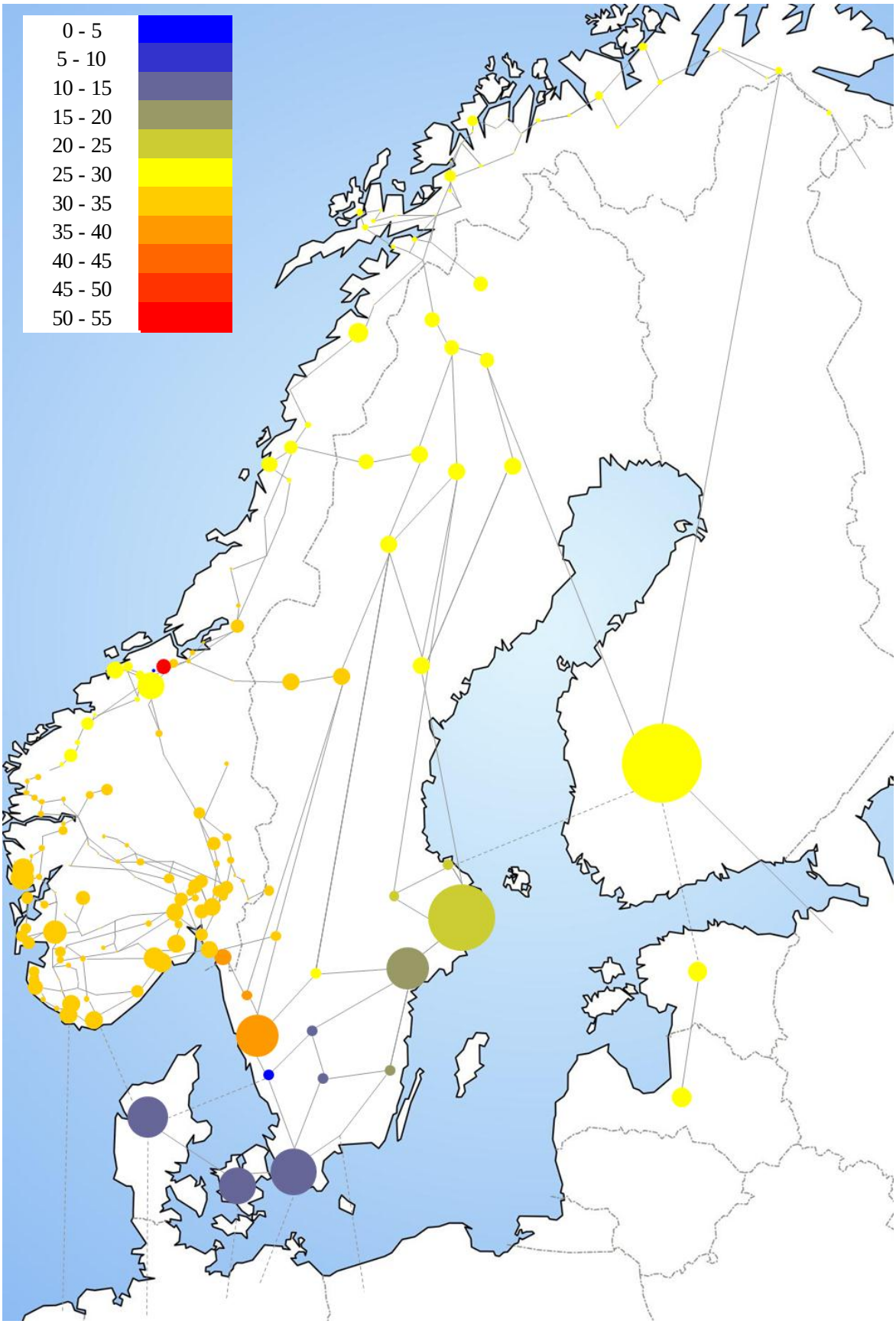

Figure 6-5 Nodal prices weighted by consumption, 1/8-2010, hour 6

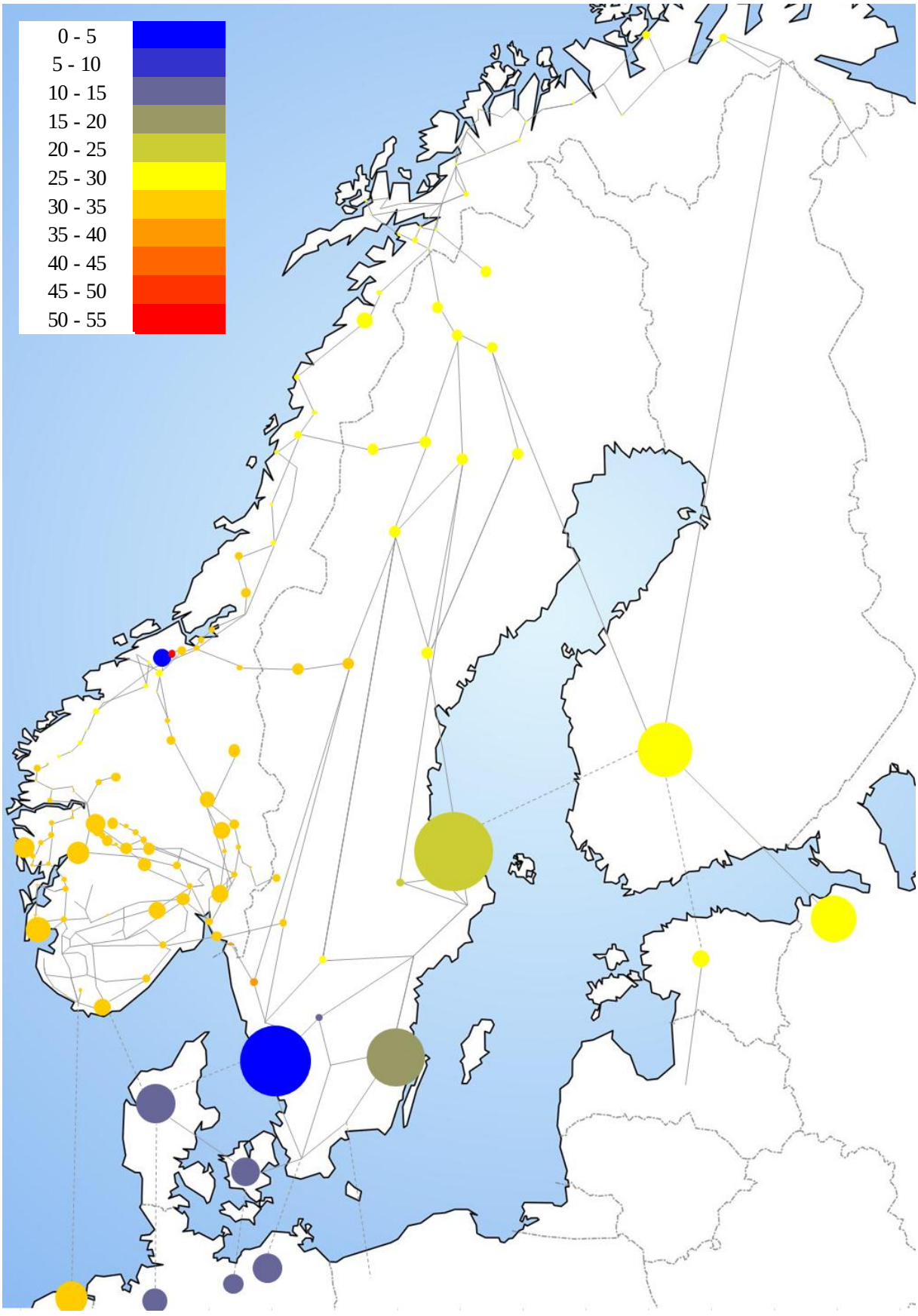

Figure 6-6 Nodal prices weighted by production, 1/8-2010, hour 6

In Figure 6-7 and Figure 6-8 we compare the simplified and optimal zonal prices. Like Table 6-5 the figures show that some zonal prices increase while others decrease.

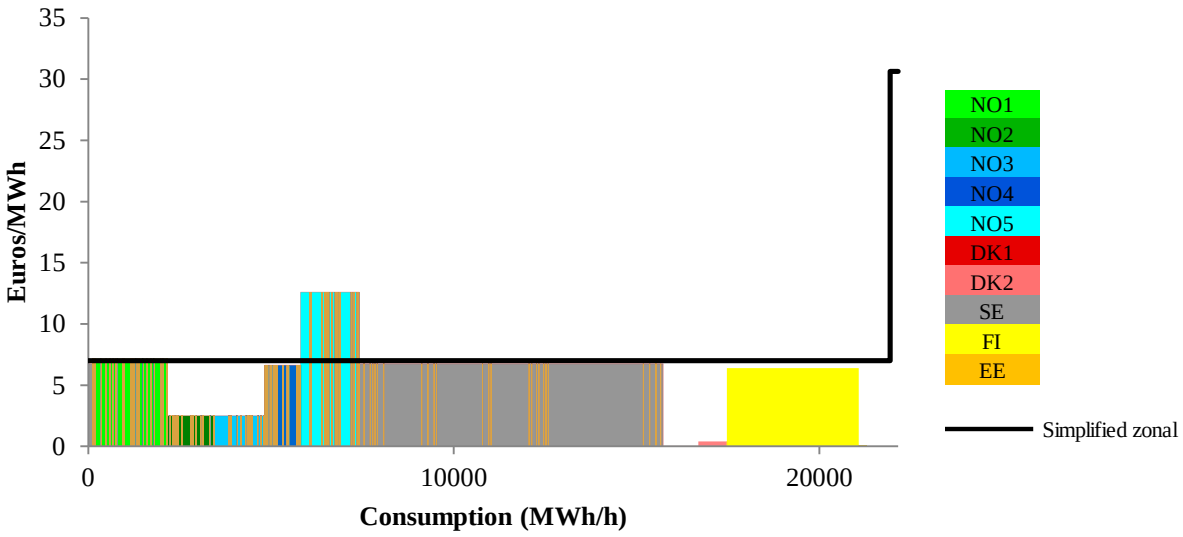

Figure 6-7 Optimal zonal prices and load quantities, 1/8-2010, hour 6

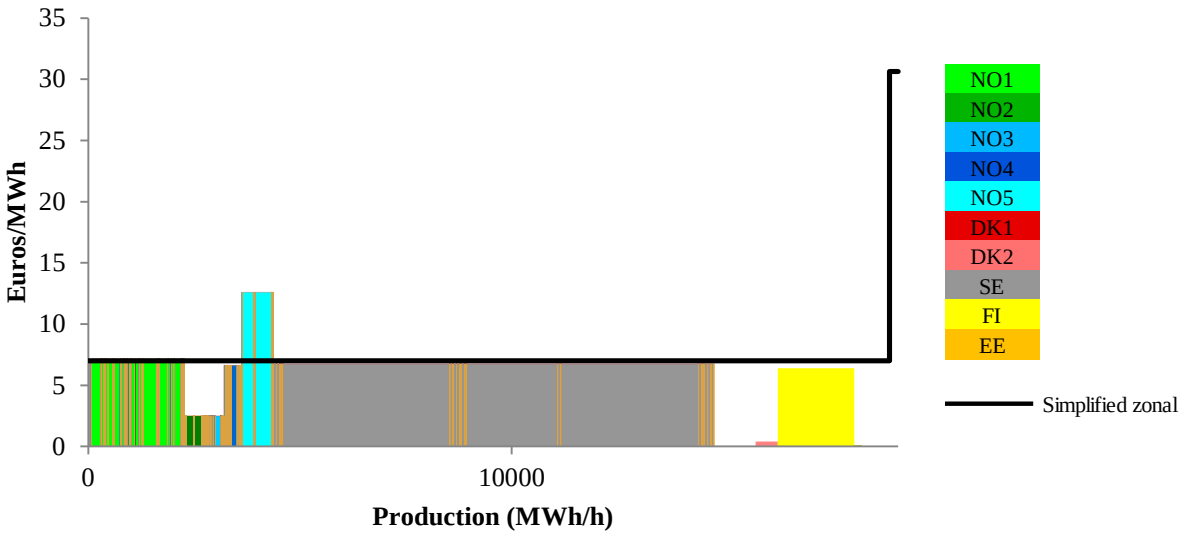

Figure 6-8 Optimal zonal prices and production quantities, 1/8-2010, hour 6

Some of the zonal prices change a lot, and one of them is Estonia, where the price is reduced from 30,63 Euros/MWh to 0,10 Euros/MWh. To explain how this can happen we show the bid curves and prices in Estonia in Figure 6-9. We see that the simplified zonal price is at a horizontal part of the supply curve, and even a small quantity change can change the price dramatically since the supply curve is a step-wise curve and the price difference between the two steps in this case is very large. For the optimal zonal prices we choose the lowest price when the supply curve has vertical segments (see also appendix A5).

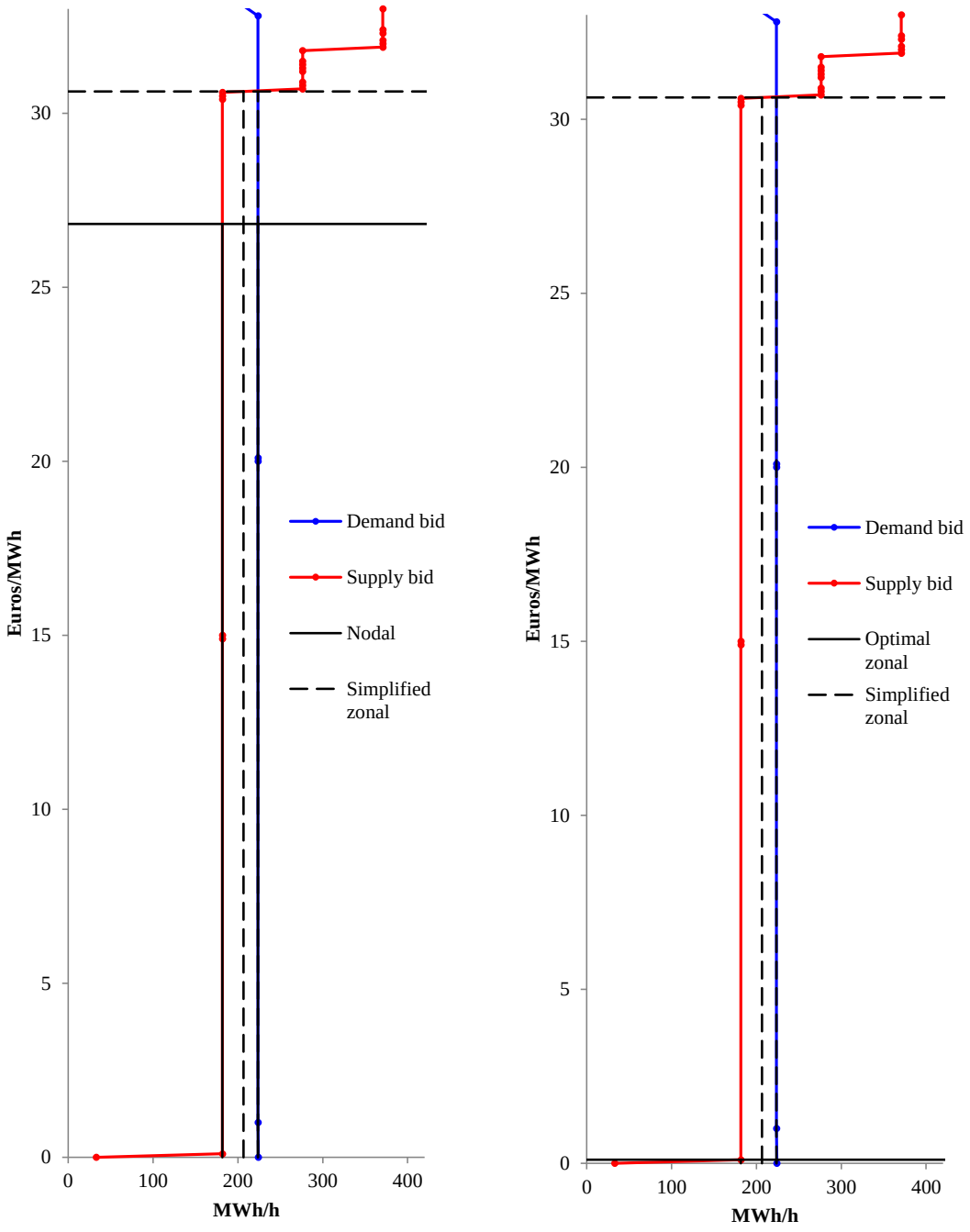

Figure 6-9 Nodal prices and load quantities, 1/8-2010, hour 6

6.3 Power flows and bottlenecks

Figure 6-10 shows the power flow of the nodal price solution. The links are weighted by the flow sizes, HVDC links are shown by dotted lines, and the binding thermal capacity constraints are shown in red colors. We notice that there are six links that are operated on their thermal capacity limits, and their capacities and the shadow prices on the constraints are shown in Table 6-6.

Figure 6-10 Line flows and thermal bottlenecks for optimal nodal price solution, 1/8-2010, hour 6

The shadow prices show the value of increasing the corresponding thermal capacity limits, i.e. the increase in social surplus. For the present case, there are three links with relatively high shadow prices, and two of them are intrazonal links, i.e. Ranes – Trollheim and Ringhals – Göteborg. These links are not easily represented in the simplified zonal model.

Table 6-6 Shadow prices for binding capacity constraints with nodal pricing, 1/8-2010, hour 6

From	To	Max	Shadow price
DK1	Kristiansand	1000	24,30
Ranes	Aura	96,02	7,73
Ranes	Trollheim	96,02	56,27
Ringhals	Göteborg	2099,45	37,80
Ringhals	DK1	680	6,53
Forsmark	FI	550	4,59

The histograms in Figure 6-11 – Figure 6-13 describe the utilization of the lines' thermal capacity limits. The figures show the number of lines operating within different intervals of capacity utilization. We distinguish between inter-zonal lines (red color) and intra-zonal lines (blue color). Also for the present case, most of the lines are operated well below their thermal capacity limits. However, from Figure 6-13 we notice that the simplified zonal approach results in considerable overload on the two intrazonal links mentioned above, Ranes – Trollheim and Ringhals – Göteborg.

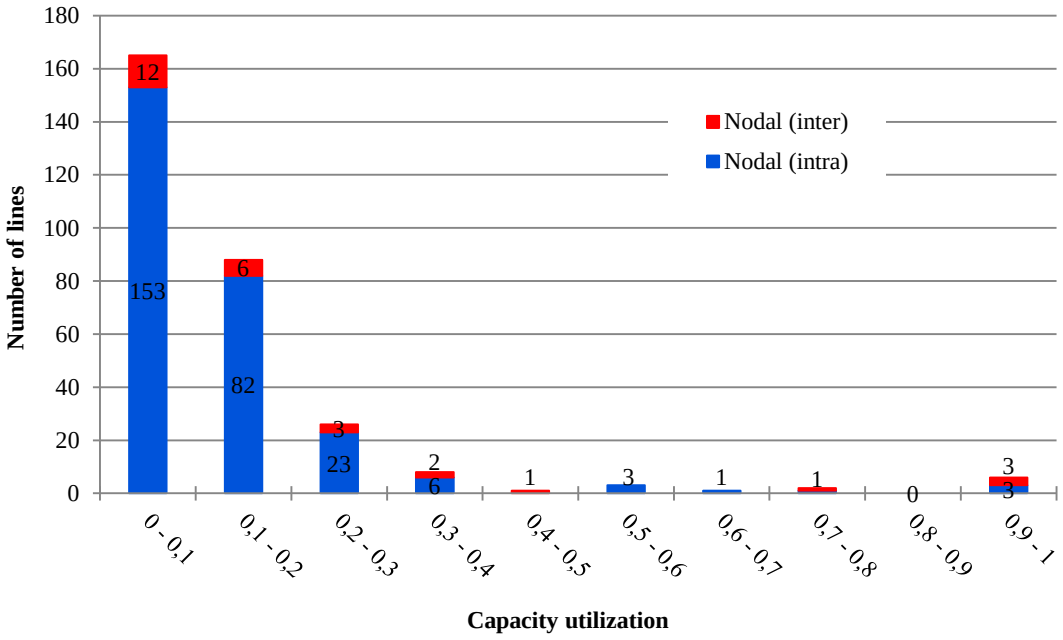

Figure 6-11 Line capacity utilization with nodal pricing, 1/8-2010, hour 6

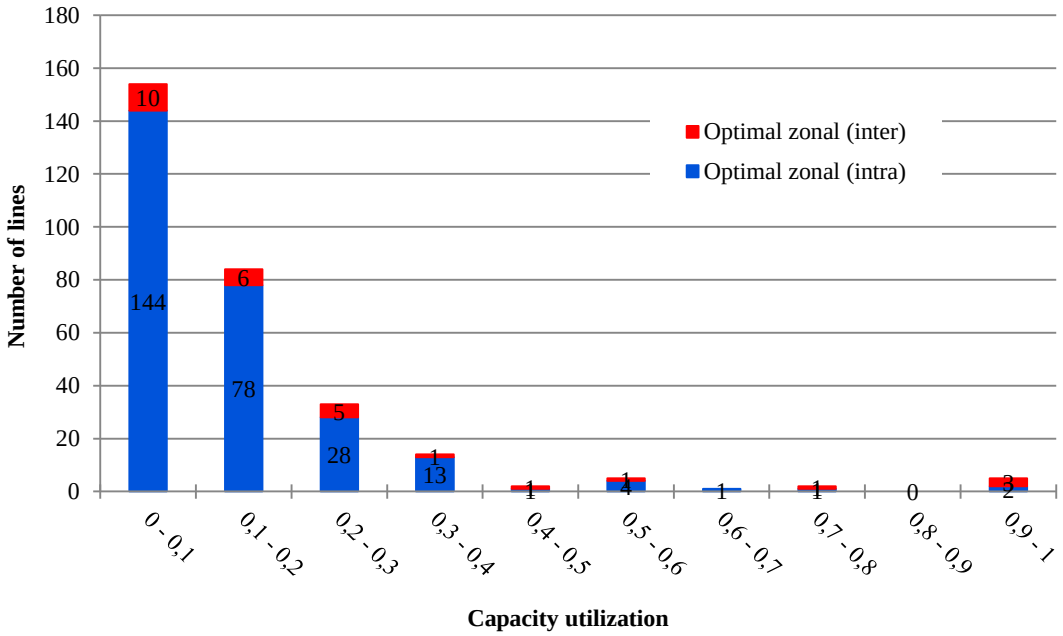

Figure 6-12 Line capacity utilization with optimal zonal pricing, 1/8-2010, hour 6

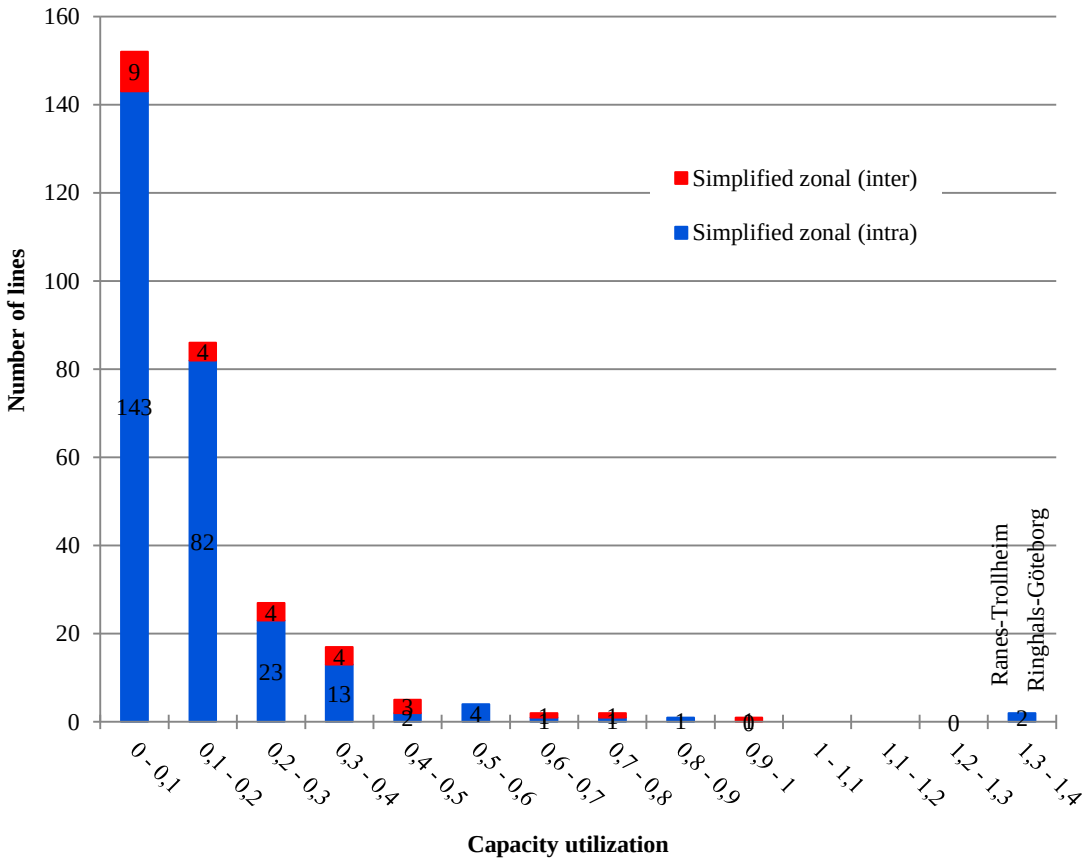

Figure 6-13 Line capacity utilization with simplified zonal pricing, 1/8-2010, hour 6

Figure 6-14 – Figure 6-16 show the utilization of the cut constraints. In the nodal price solution, there is one cut constraint that is operated on its capacity limit. The shadow price for this, Midt-Norge 2, is given in Table 6-7. The shadow price is close to 0.

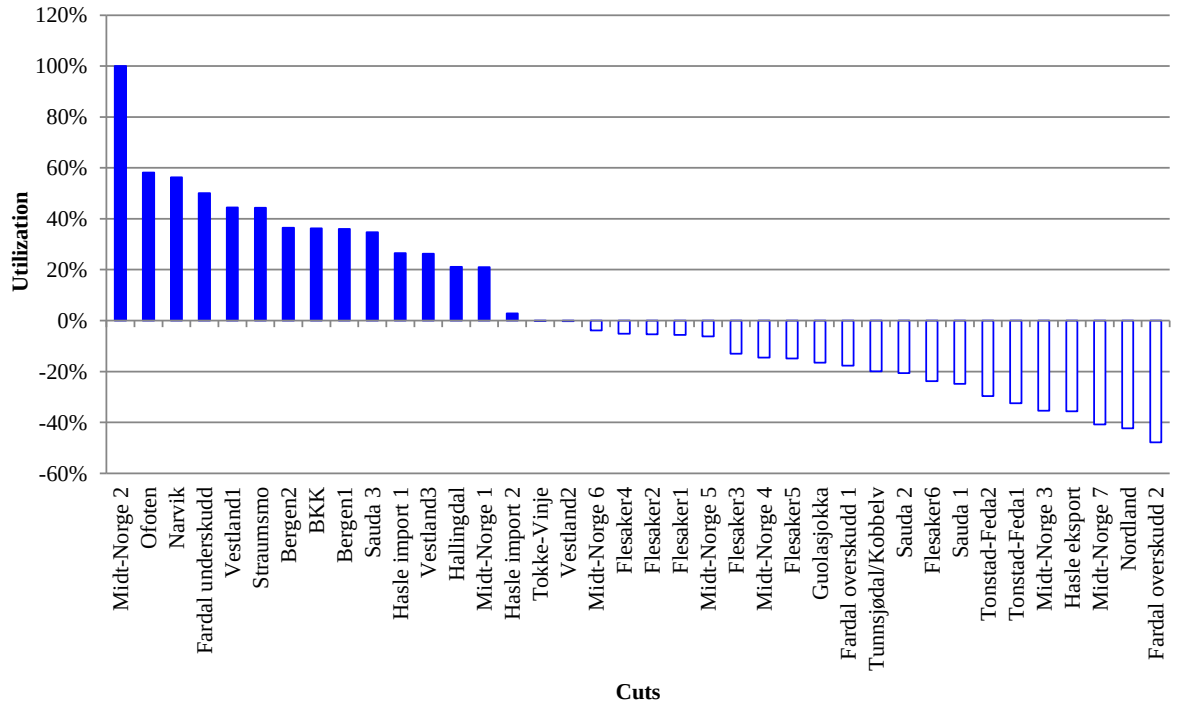

Figure 6-14 Cut capacity utilization with nodal pricing, 1/8-2010, hour 6

Table 6-7 Shadow prices for cut capacity constraints with nodal pricing, 1/8-2010, hour 6

Cut name	Capacity	From	To	Share of flow included	Shadow price
Midt-Norge 2	415	Nea	Klæbu	1	0,00
		Ajaure	Nedre Røssåga	1	

While all the cut constraints are fulfilled in the optimal nodal and optimal zonal price solutions, we notice from Figure 6-16 that the Midt-Norge 2 cut is not satisfied in the simplified zonal solution.

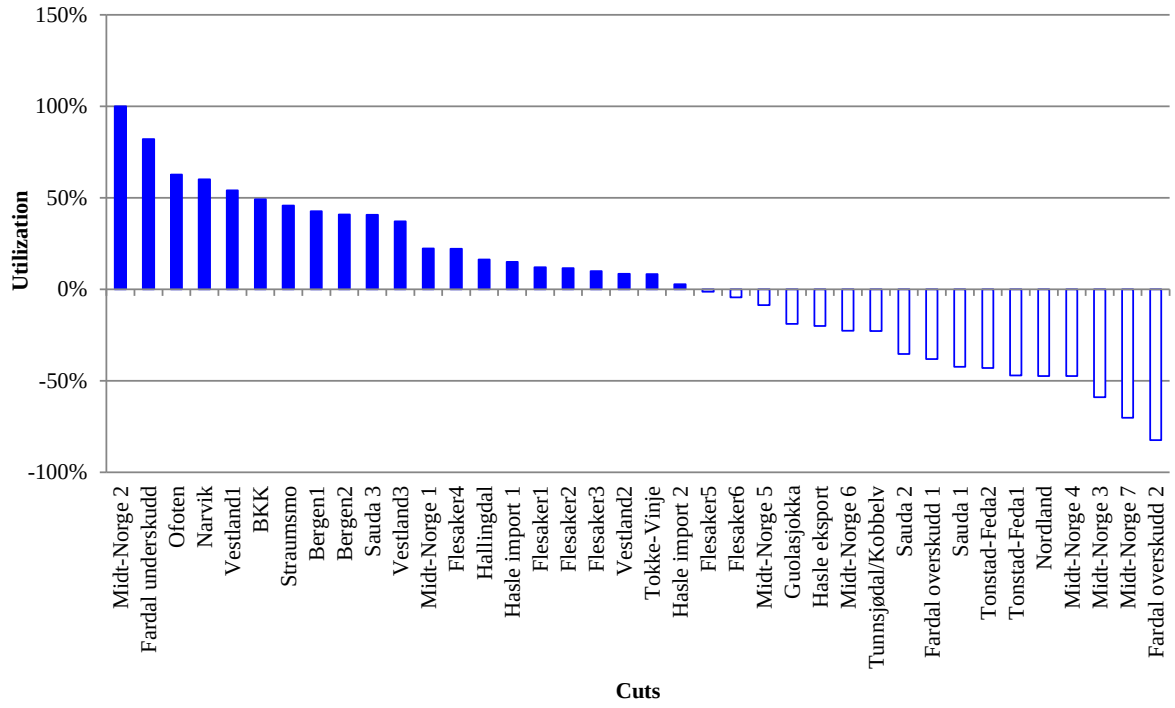

Figure 6-15 Cut capacity utilization with optimal zonal pricing, 1/8-2010, hour 6

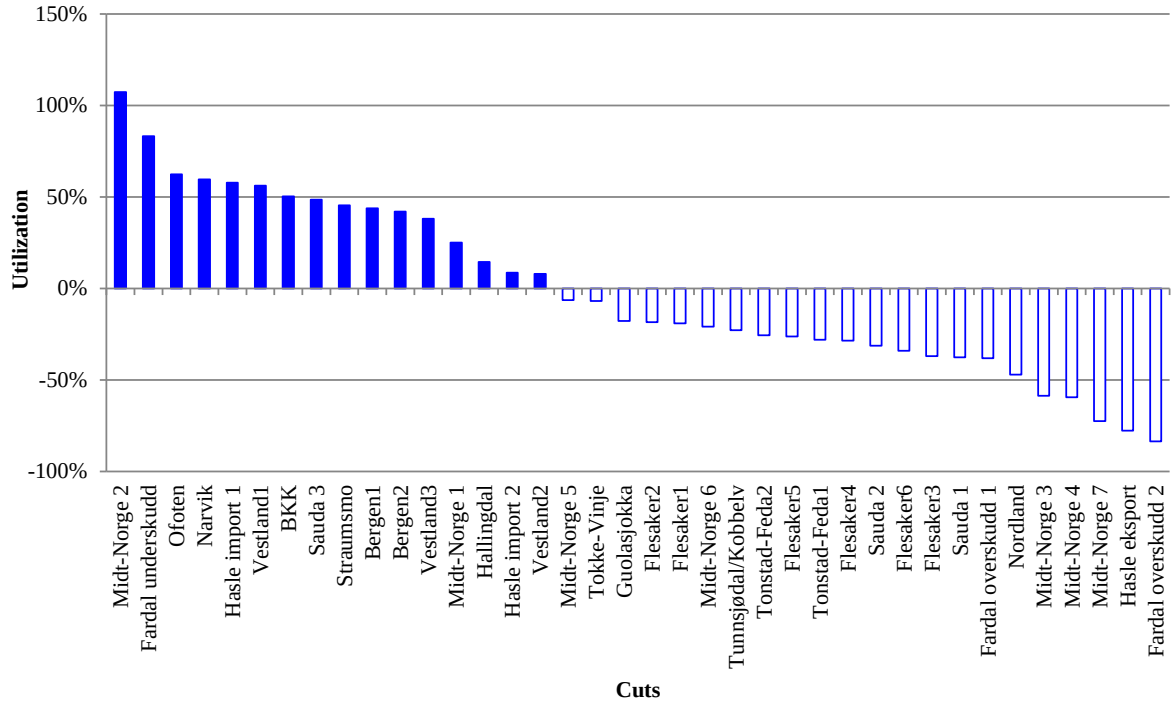

Figure 6-16 Cut capacity utilization with simplified zonal pricing, 1/8-2010, hour 6

6.4 Load and generation quantities

Figure 6-17 shows the differences between the quantities consumed in the simplified zonal solution and the quantities consumed in the optimal nodal and the optimal zonal solutions. In this case some of the differences are large, especially between the optimal zonal solution and the other solutions.

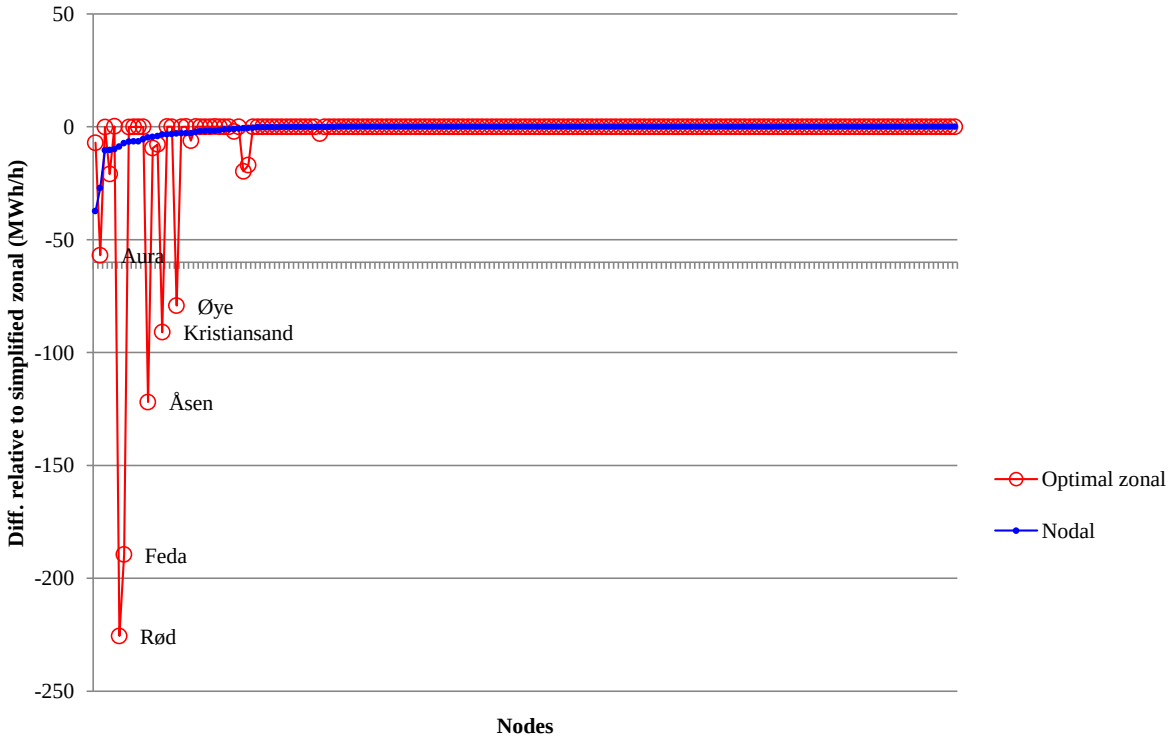

Figure 6-17 Differences in load between simplified zonal and the other two pricing approaches, 1/8-2010, hour 6

In Figure 6-18 we show the bid curves for Rød, one of the nodes where the optimal zonal load differs most from the load at the simplified zonal price / optimal nodal price. From the upper part of the figure we see that both the simplified zonal price and the optimal nodal price, even if they are quite different, are on the almost vertical part of the demand curve on the right hand side of the figure. Thus, the quantities in the simplified zonal and optimal nodal solutions are quite similar. The optimal zonal price is on the vertical part of the demand curve, so we would expect the corresponding load quantity to be close to the load quantities from the other two models. However, we see that the load is curtailed, as described in Appendix A.5, hence the marginal benefit of increased consumption in this node is in fact lower than the optimal zonal price.

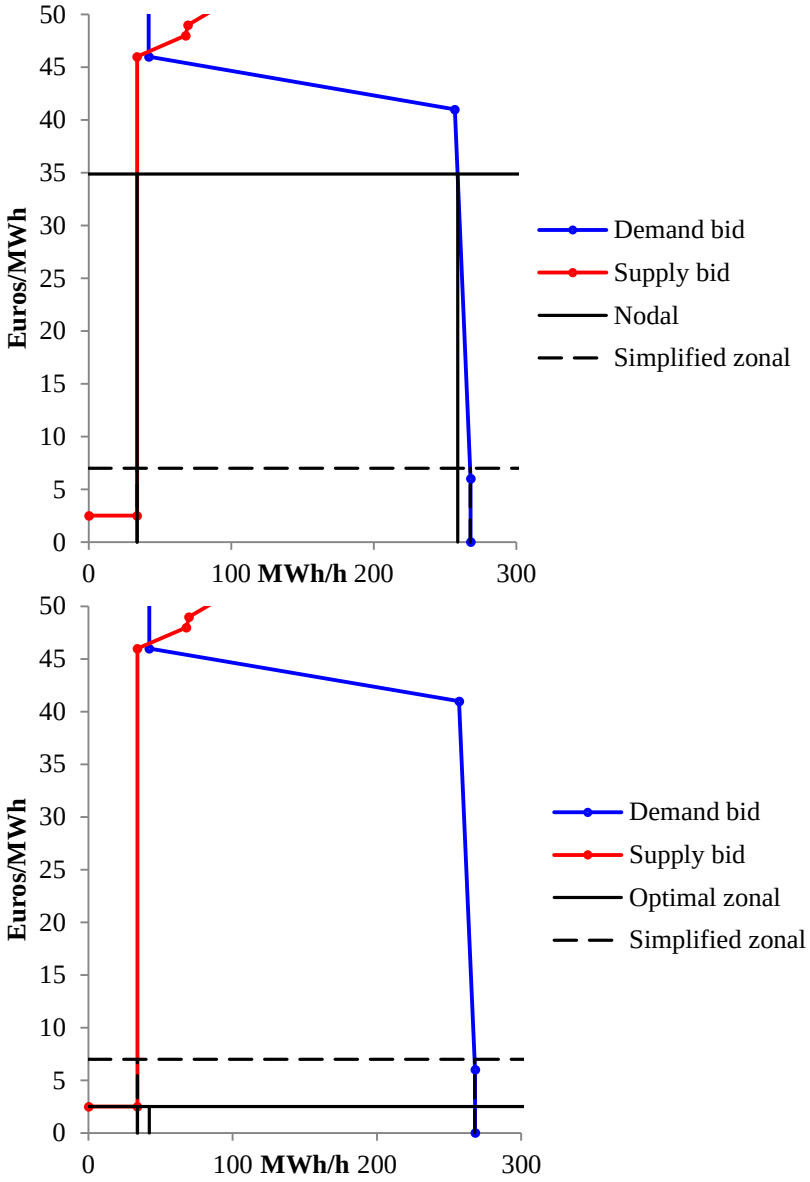

Figure 6-18 Differences in generation, Rød

Figure 6-19 shows the quantity differences for generation. In this case, generation quantities are quite similar, except for Ringhals, Ranes, and to some extent Mongstad.

In Figure 6-20 we show the bid curves for Ringhals. We notice that the supply bid is at a constant marginal cost up to the capacity limit that is close to 4000 MW. The simplified zonal price is well over the marginal cost, and the generation is at the capacity limit. The nodal price is equal to the marginal cost, and the producer will be indifferent to which quantity is produced. However, due to the thermal constraints on the links connecting Ringhals to Göteborg and DK1, the optimal nodal solution reduces the quantity produced in Ringhals compared to the simplified zonal solution. Since we allow prices to be strictly greater than marginal cost, even if the production is not on the capacity limit in the optimal zonal solution (cf. appendix A5), and the optimal zonal solution takes into account all constraints, the optimal zonal solution is also at a quantity lower than the generation in the simplified zonal solution.

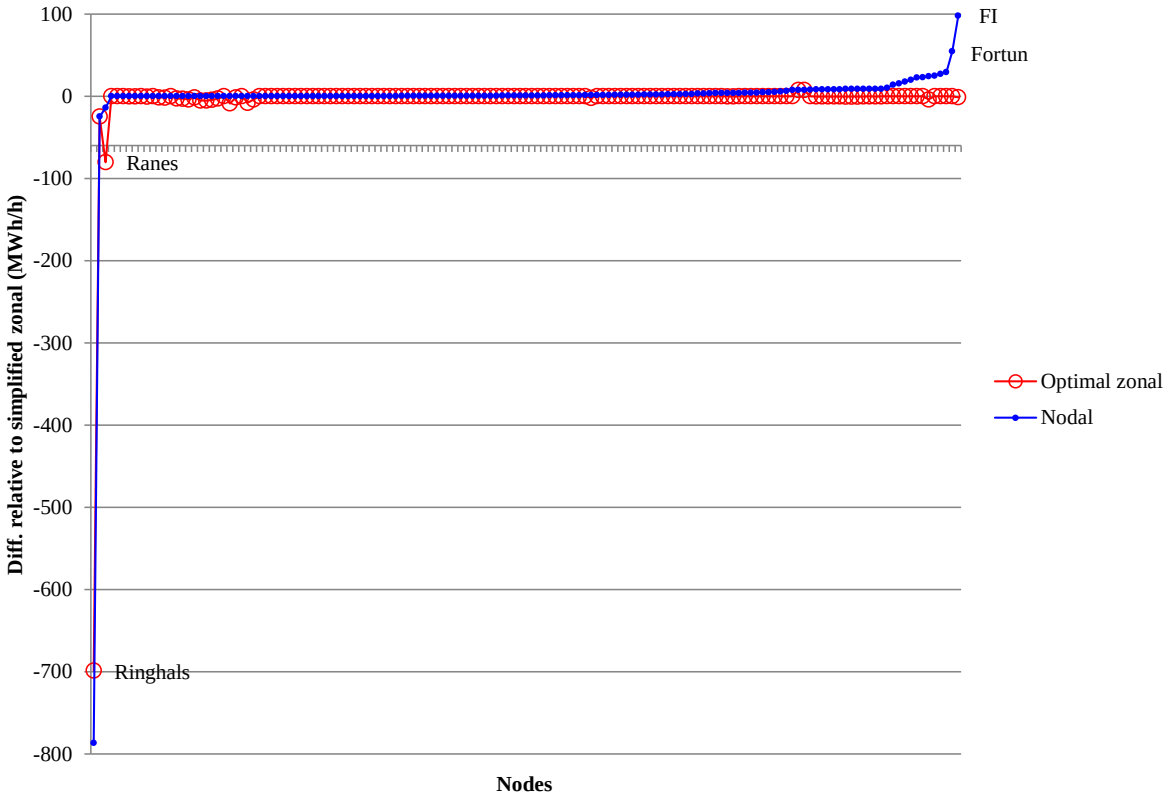

Figure 6-19 Differences in generation between simplified zonal and the other two pricing approaches, 1/8-2010, hour 6

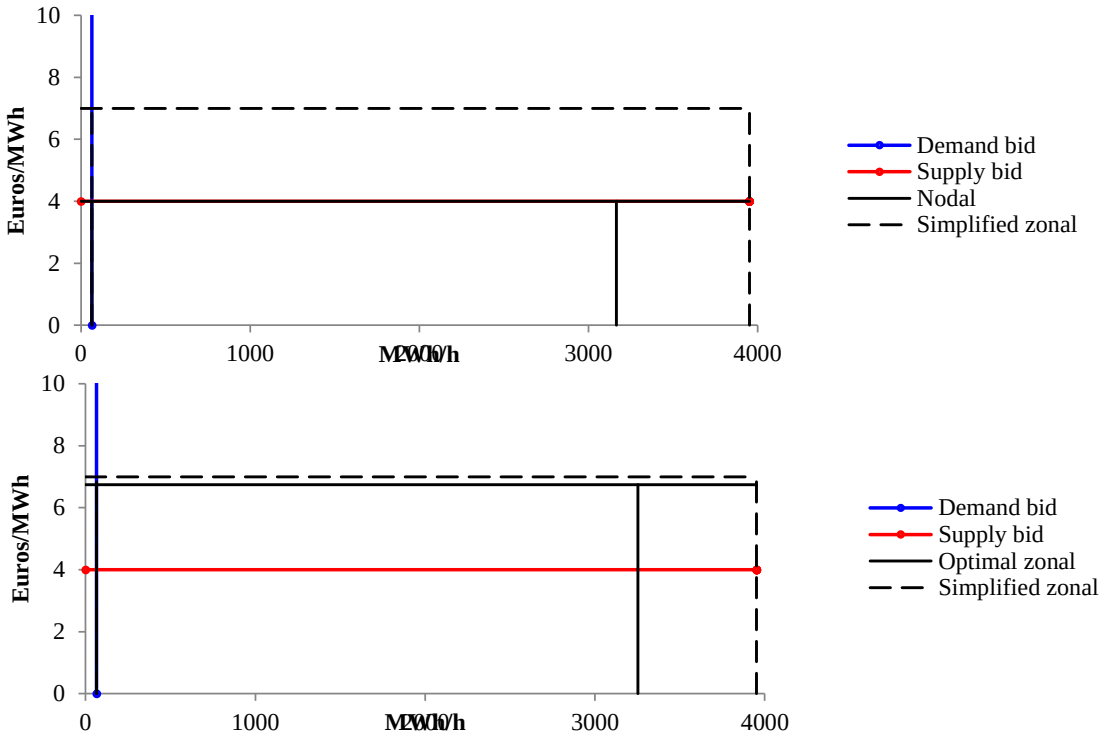

Figure 6-20 Differences in generation, Ringhals

6.5 Surpluses

Table 6-8 shows the changes in surplus compared to the unconstrained market solution. For the present case, we see that moving from simplified zonal prices to optimal zonal or nodal prices leads to a reduction in consumer surplus, and an increase in grid revenue, especially for the nodal price solution. The change in producer surplus is ambiguous, in the nodal pricing case we see a rather large increase, while the optimal zonal solution leads to a reduction in producer surplus compared to the simplified zonal solution. Note again that the surpluses are not comparable since the simplified zonal solution is not feasible.

Table 6-8 Unconstrained surplus and surplus differences (1000 Euros), 1/8-2010, hour 6

	Un-constrained	Simplified zonal	Optimal zonal	Nodal
Producers	1382,6	-6,5	-37,3	293,1
Consumers	39286,0	-0,1	4,3	-424,8
Grid	0,0	6,0	1,4	116,8
Total	40668,6	-0,6	-31,5	-15,0
Infeasibilities	2 lines 1 cut	2 lines 1 cut	None	None

7. Results for 6-1-2010 hour 10

7.1 Calibration of bid curves

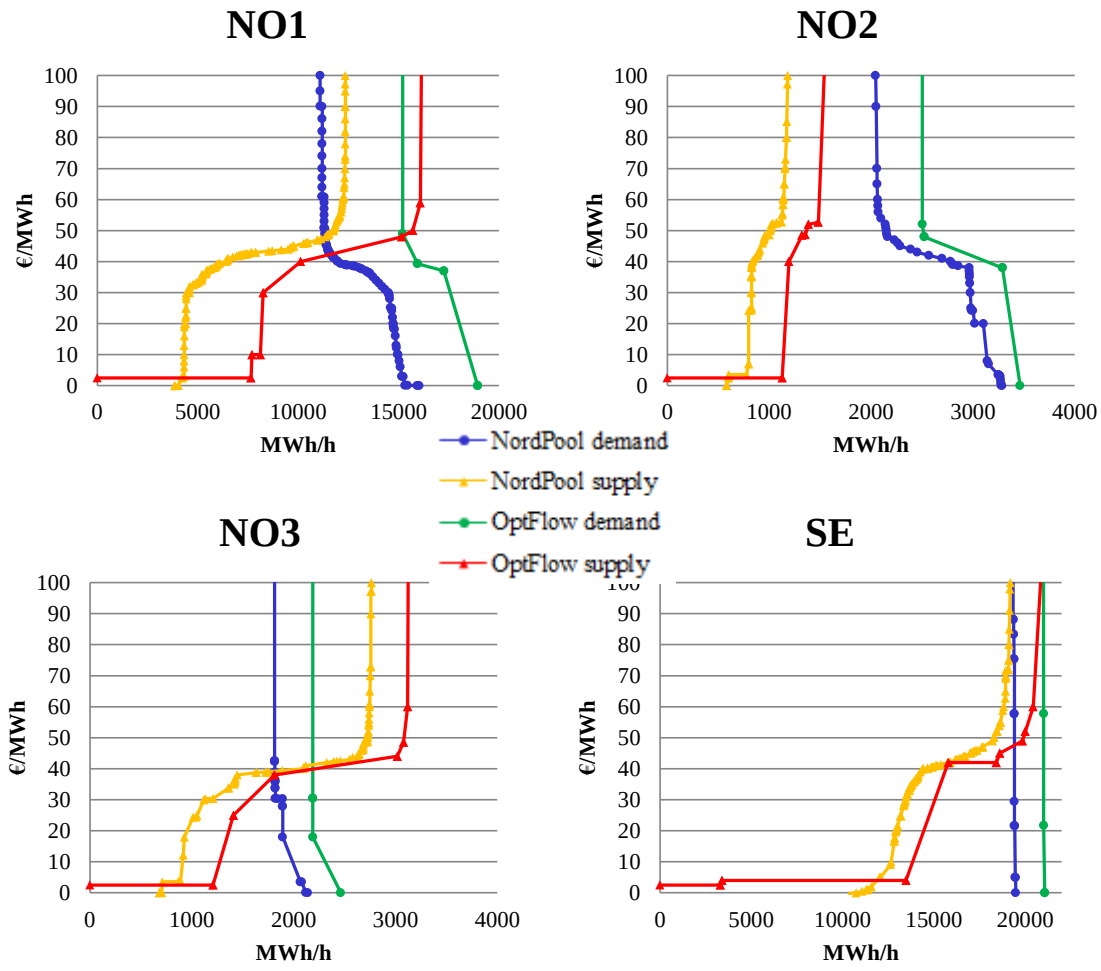

Figure 7-1 Nord Pool Spot bid curves and aggregate OptFlow bid curves for Norway and Sweden, 6/1-2010, hour 10

Figure 7-1 compares the constructed disaggregated bid curves to the actual Nord Pool bid curves, by aggregating the disaggregated curves of the OptFlow model for the different price areas. For this case, there are only three bidding areas in Norway. The figure shows that in aggregate the nodal supply and demand curves fit rather well with the Nord Pool bid curves. The volume differences between the Nord Pool curves and the constructed disaggregate bid curves are due to the need for all production and consumption being represented in order to evaluate the effect of different congestion management methods on the disaggregated power system. The supply and demand curves for the Elspot price areas that are modeled as single nodes in the disaggregated OptFlow model, and where we have used the actual Nord Pool bid curves for hour 6 on 1/8-2010 are shown in Figure 7-2.

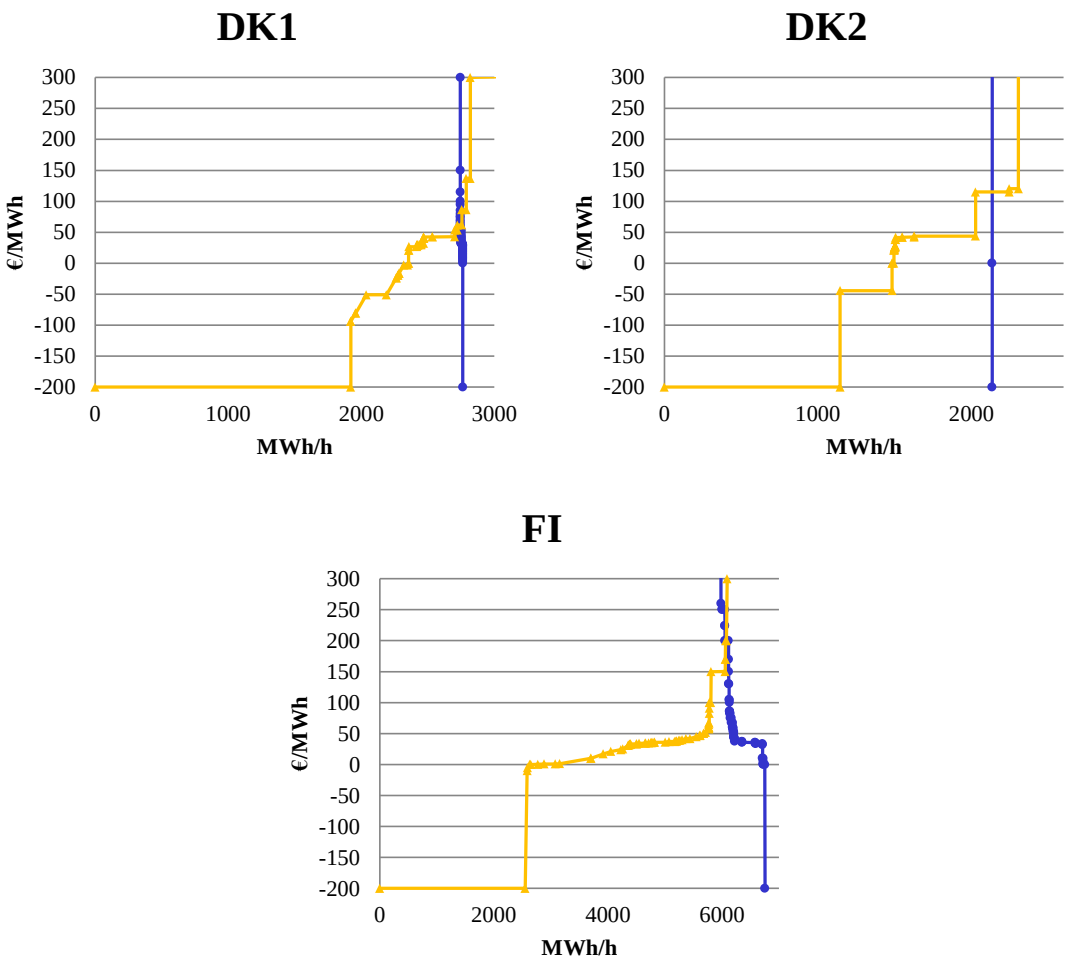

Figure 7-2 OptFlow bid curves = Nord Pool Spot for other Elspot areas, 6/1-2010, hour 10

Table 7-1 shows that the prices in model variants I, II, and III are identical except for a very small difference between II and III for NO1. Table 7-2 – Table 7-4 show the same pattern for the quantity differences as in previous cases, except that the production and load differences between II and III in NO1 are rather large. The differences between I and II are as before due to imports and exports. The differences between production and consumption in II and III are due to the production and load that is not traded at Nord Pool Spot. The exchange quantities are however very similar in II and III. We use III as the starting point for analyzing the effects of different congestion management methods in the following sections.

Table 7-1 Comparison of prices for three model variants, 6/1-2010, hour 10

Bidding area	(I) NPS actual area prices	(II) OptFlow prices with NPS bid curves	(III) OptFlow prices with calibrated bid curves
NO1	47,54	47,54	47,95
NO2	48,45	48,45	48,45
NO3	48,20	48,20	48,20
DK1	42,65	42,65	42,65
DK2	48,20	48,20	48,14
SE	48,20	48,20	48,14
FI	48,20	48,20	48,14

Table 7-2 Comparison of production quantities for three model variants, 6/1-2010, hour 10

Bidding area	(I) NPS production	(II) OptFlow production with NPS bid curves	(III) OptFlow production with calibrated bid curves
NO1	11185	11185	15118
NO2	959	959	1321
NO3	2712	2689	3074
DK1	3621	2597	2597
DK2	2576	2026	2026
SE	17983	17983	19587
FI	7017	5641	5640

Table 7-3 Comparison of load quantities for three model variants, 6/1-2010, hour 10

Bidding area	(I) NPS load	(II) OptFlow load with NPS bid curves	(III) OptFlow load with calibrated bid curves
NO1	11585	11349	15282
NO2	2159	2159	2521
NO3	1813	1813	2188
DK1	2751	2751	2751
DK2	2135	2135	2135
SE	19404	19404	21015
FI	6207	6207	6207

Table 7-4 Comparison of exchange quantities for three model variants, 6/1-2010, hour 10

Bidding area	(I) NPS net exchange	(II) OptFlow net exchange with NPS bid curves	(III) OptFlow net exchange with calibrated bid curves
NO1	-400	-164	-164
NO2	-1200	-1200	-1200
NO3	899	876	886
DK1	870	-154	-154
DK2	442	-109	-109
SE	-1421	-1421	-1428
FI	810	-566	-567

7.2 Prices

This case is similar to the one in chapter 4, since the Bergen 1 and Bergen 2 cuts are infeasible in the nodal price solution. As in the previous case, we choose to relax these cut constraints in the following analyses.

Table 7-5 compares the four sets of prices for hour 10 on 6/1-2010. Actual Nord Pool Spot prices are given in the first price column (corresponding to (I) / (II) in Table 7-1), while the second and third columns show, respectively, the simplified and optimal zonal prices calculated by the OptFlow model. The simplified zonal prices correspond to (III) in Table 7-1, while optimal zonal prices take into account the specific location of all bids on the nodes and all constraints of the disaggregated power system. The three rightmost columns show descriptive statistics for the optimal nodal prices within each price zone.

When moving from simplified zonal prices to optimal nodal prices, there are some significant prices changes, especially for the Norwegian areas. The nodal prices for an area with several nodes vary typically around the simplified zonal price. Comparing the prices under simplified and optimal zonal prices, we notice that the price changes considerably for DK2, but also for NO3 and SE.

Table 7-5 Prices 6/1-2010, hour 10

Bidding area	Actual NPS	Zonal prices		Optimal nodal prices		
		Simplified	Optimal	Average	Min	Max
NO1	47,54	47,95	47,22	49,95	41,02	62,92
NO2	48,45	48,45	48,02	49,38	33,88	53,25
NO3	48,20	48,14	66,08	49,93	49,21	50,50
DK1	42,65	42,65	42,74	47,56	47,56	47,56
DK2	48,20	48,14	120,14	48,09	48,09	48,09
SE	48,20	48,14	56,31	48,99	45,09	54,45
FI	48,20	48,14	49,39	49,09	49,09	49,09

Figure 7-3 and Figure 7-4 show the optimal nodal prices for consumption and production respectively, where prices are sorted from lowest to highest, and column widths represent volumes. The nodal prices are compared to the simplified zonal prices. We notice that on average the nodal prices are a little higher than the simplified zonal prices. The variation in the optimal nodal prices is not very large, but larger than for the simplified zonal prices. The highest prices, but also some of the lowest, are in NO1.

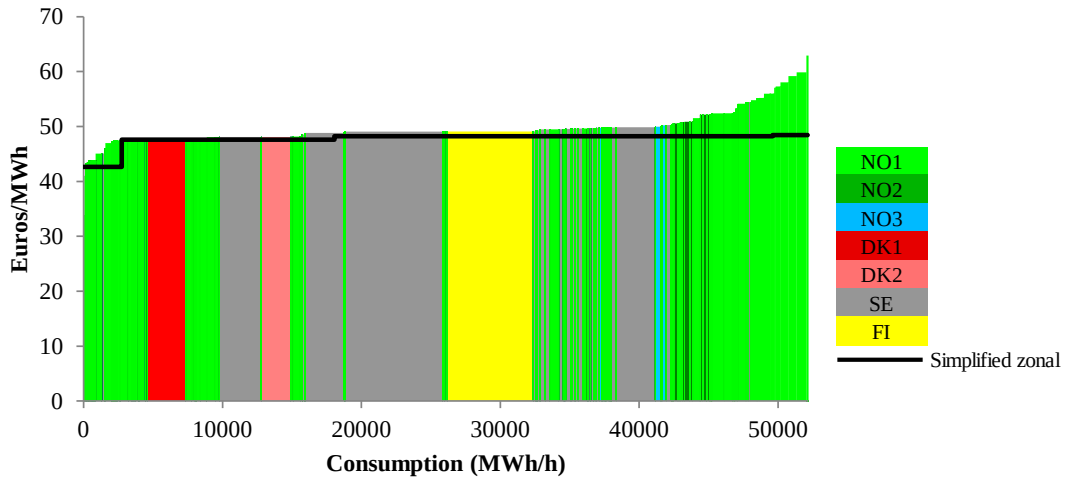

Figure 7-3 Nodal prices and load quantities, 6/1-2010, hour 10

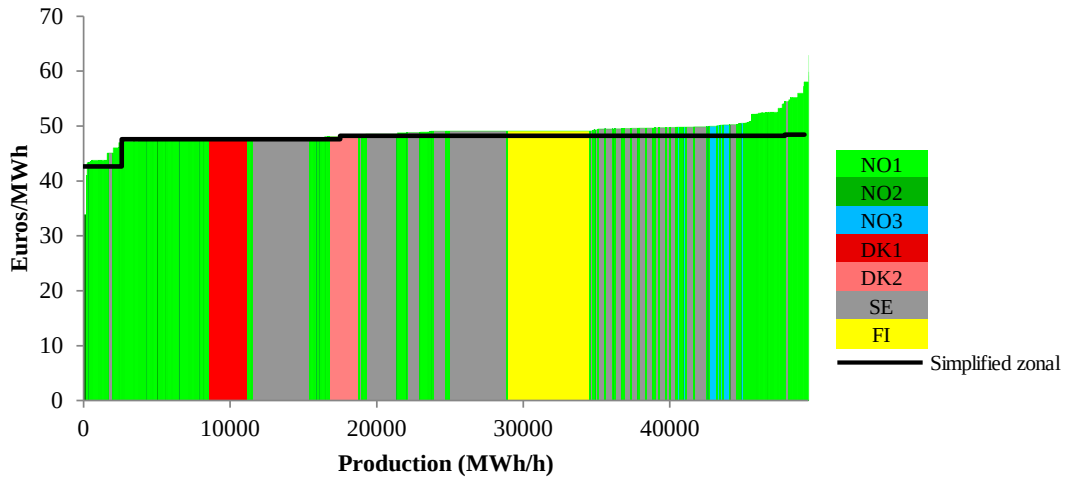

Figure 7-4 Nodal prices and production quantities, 6/1-2010, hour 10

Figure 7-5 and Figure 7-6 illustrate the geographical variation in the optimal nodal prices. They also show that the Nord Pool area is in a net import situation in the present case.

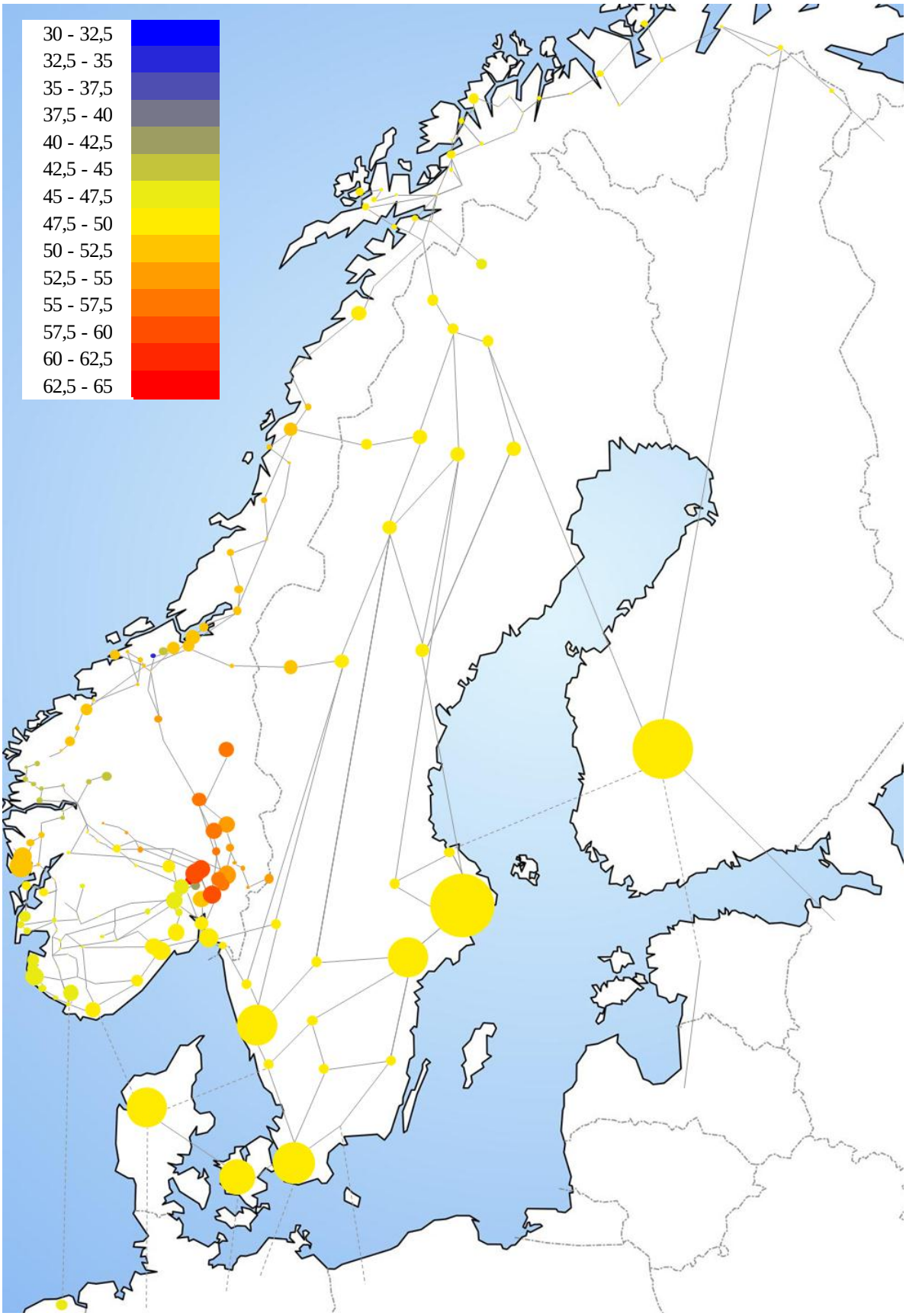

Figure 7-5 Nodal prices weighted by consumption, 6/1-2010, hour 10

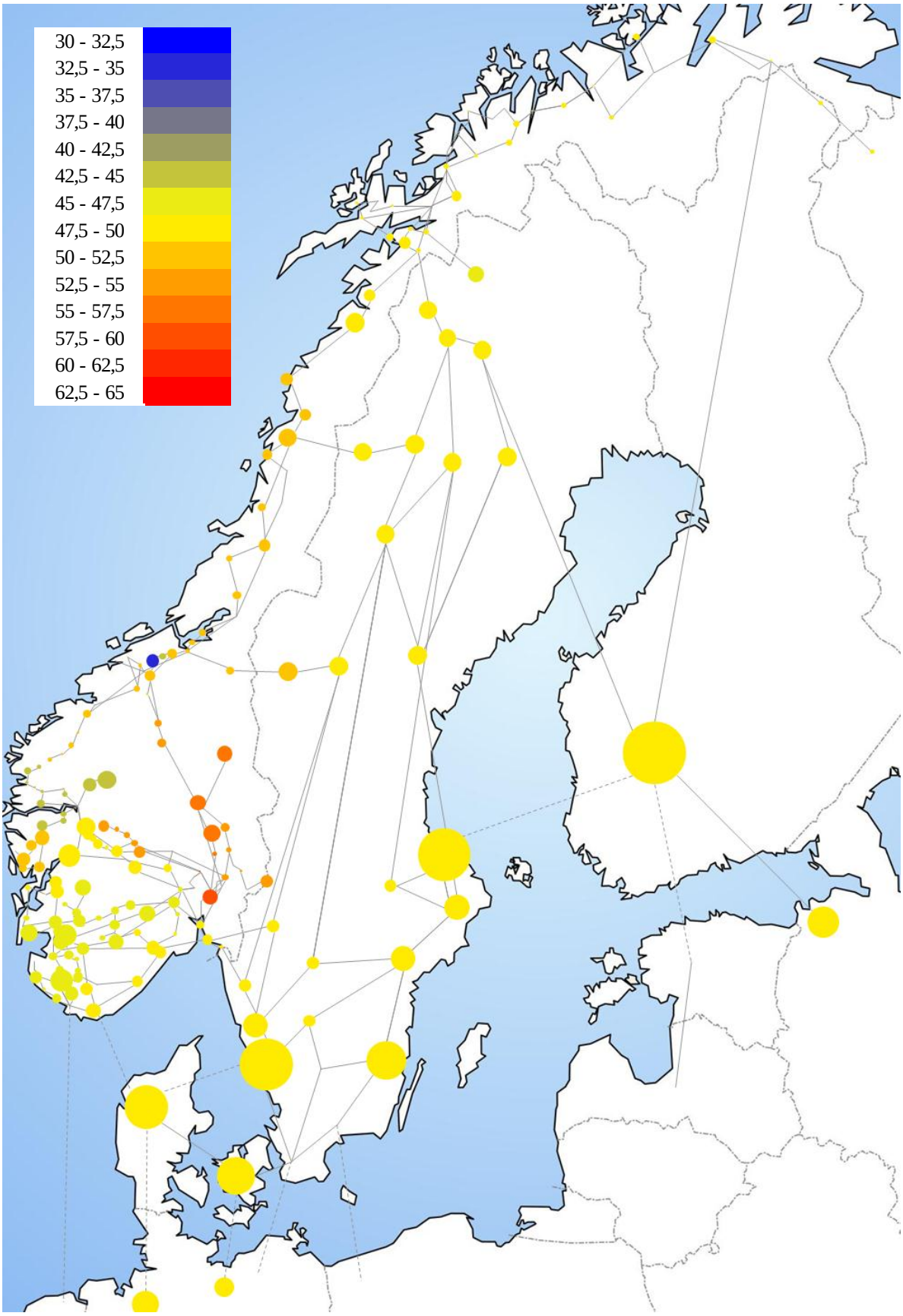

Figure 7-6 Nodal prices weighted by production, 6/1-2010, hour 10

Figure 7-7 and Figure 7-8 compare the simplified and optimal zonal prices. They show that on average the optimal zonal prices are higher than the simplified zonal prices, and that the increase is largest in DK2.

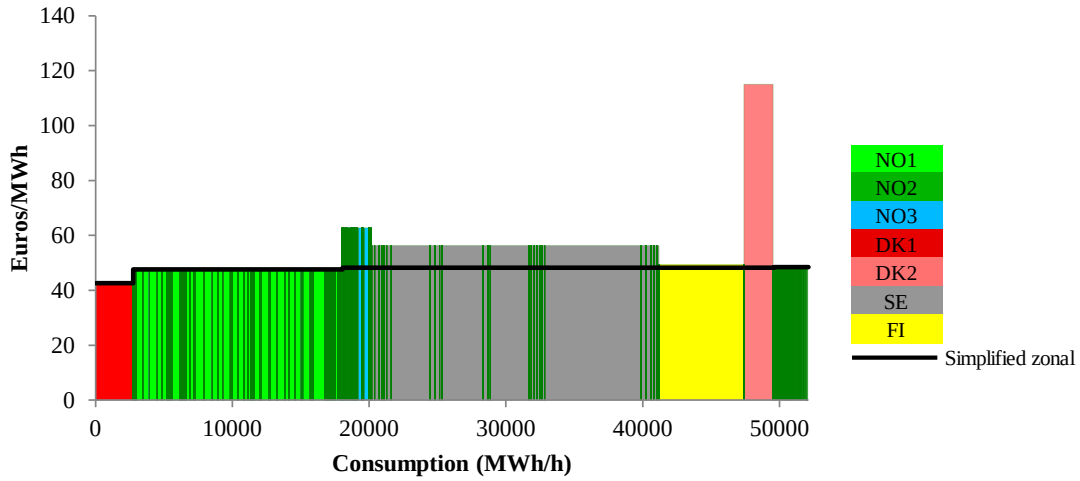

Figure 7-7 Optimal zonal prices and load quantities, 6/1-2010, hour 10

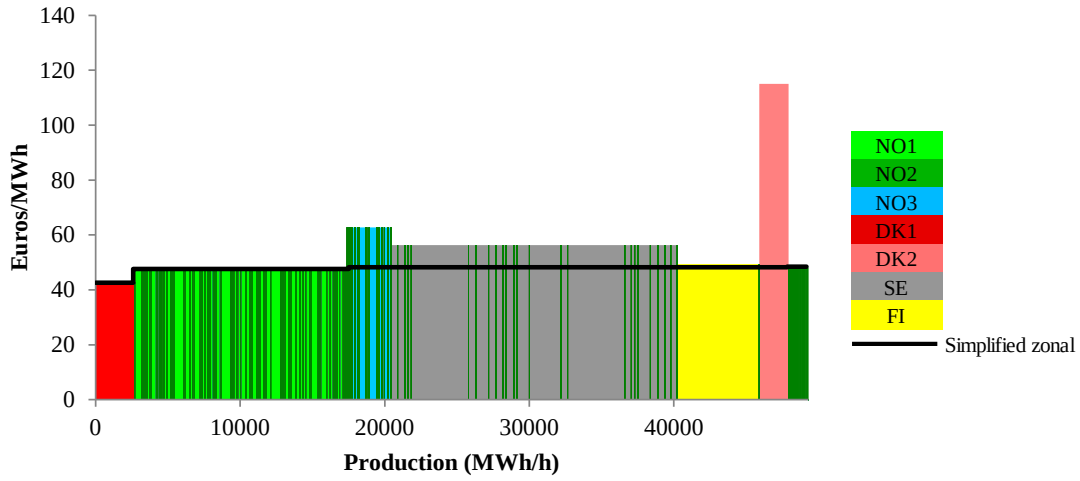

Figure 7-8 Optimal zonal prices and production quantities, 6/1-2010, hour 10

7.3 Power flows and bottlenecks

Figure 7-9 shows the power flow of the nodal price solution. The links are weighted by the flow sizes, HVDC links are shown by dotted lines, and the binding thermal capacity constraints are shown in red colors. We notice that there are seven links that are operated on their thermal capacity limits. The capacities and the shadow prices on these constraints are shown in Table 7-6. For the present case, the shadow prices are highest on the intrazonal links Hamang-Bærum and Ranes-Aura.

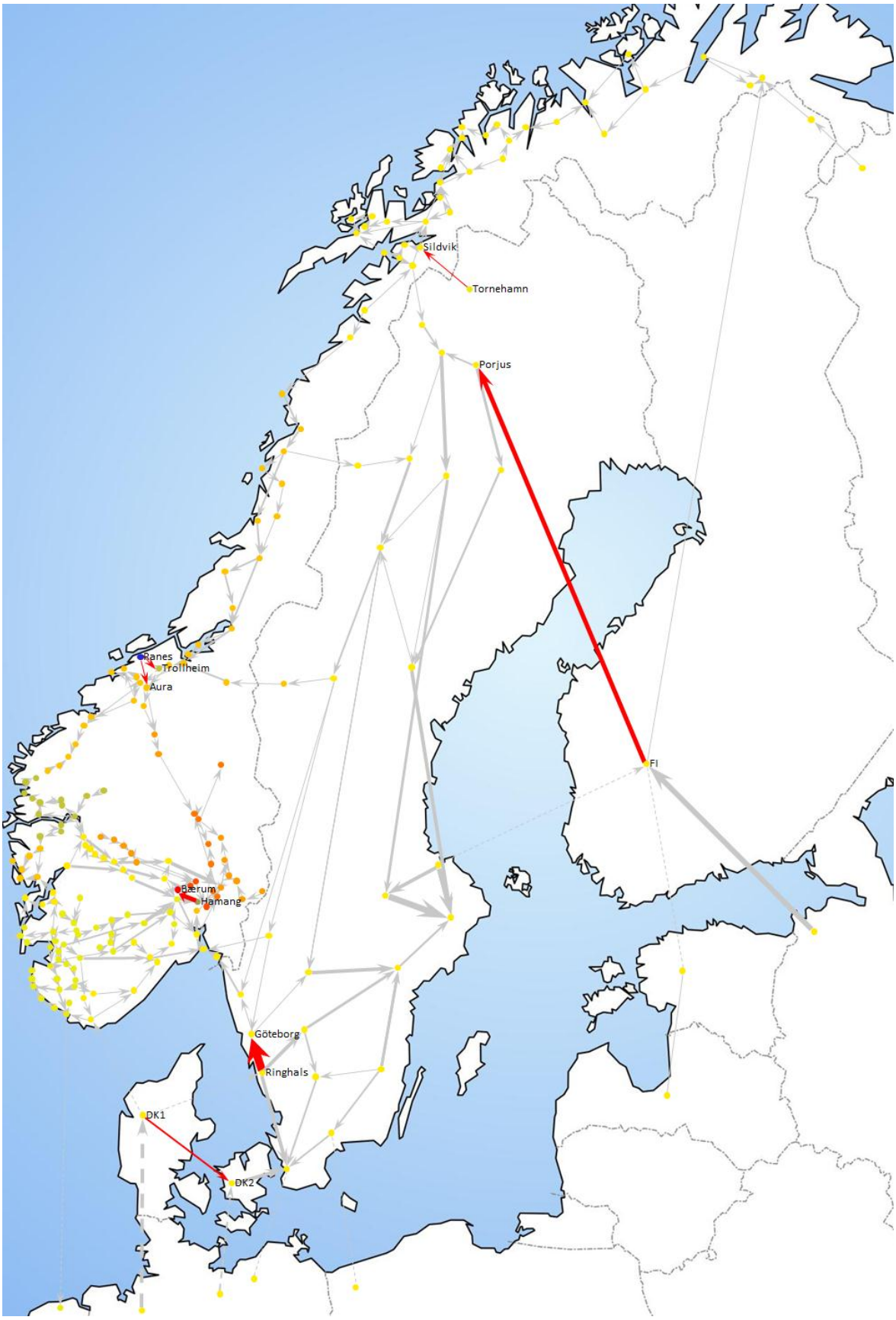

Figure 7-9 Line flows and thermal bottlenecks for optimal nodal price solution, 6/1-2010, hour 10

Table 7-6 Shadow prices for binding capacity constraints with nodal pricing, 6/1-2010, hour 10

From	To	Max	Shadow price
Hamang	Bærum	1258,51	24,08
Ranes	Aura	96,02	25,24
Ranes	Trollheim	96,02	7,41
Tornehamn	Sildvik	166,21	4,71
Ringhals	Göteborg	2099,45	2,72
FI	Porjus	1500,00	0,51
DK1	DK2	590,00	0,53

The histograms in Figure 7-10 – Figure 7-12 describe the utilization of the lines' thermal capacity. We notice for the present case that in the optimal nodal and optimal zonal price solutions 8 links are utilized between 90 and 100 %, and of these are 5 intrazonal links. From Figure 7-12 we notice that the simplified zonal approach results in 4 overloaded lines, 3 of them being intrazonal links.

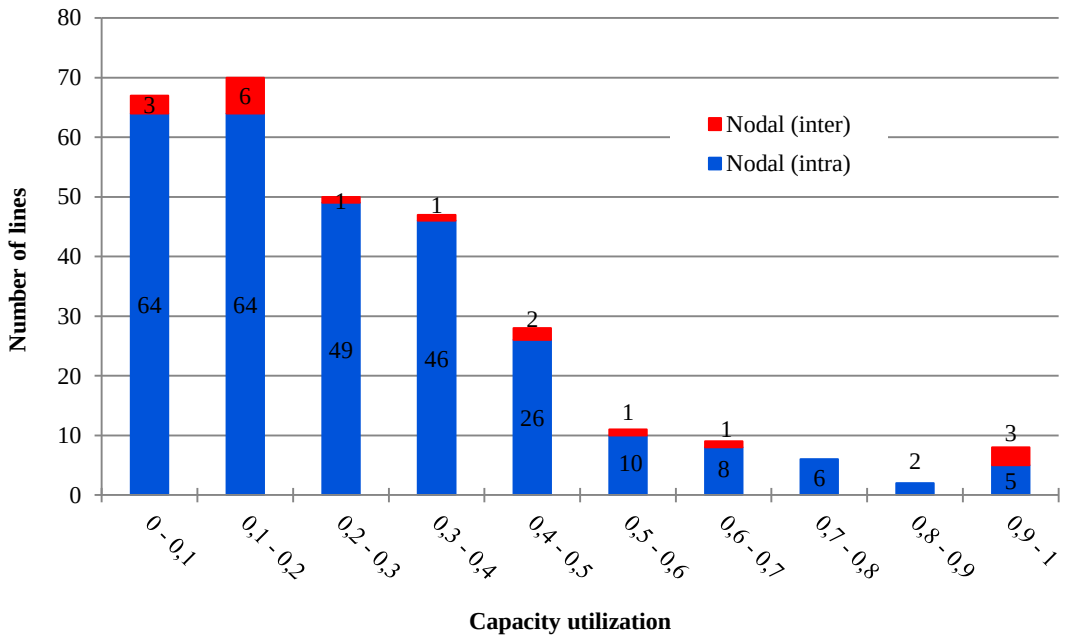

Figure 7-10 Line capacity utilization with nodal pricing, 6/1-2010, hour 10

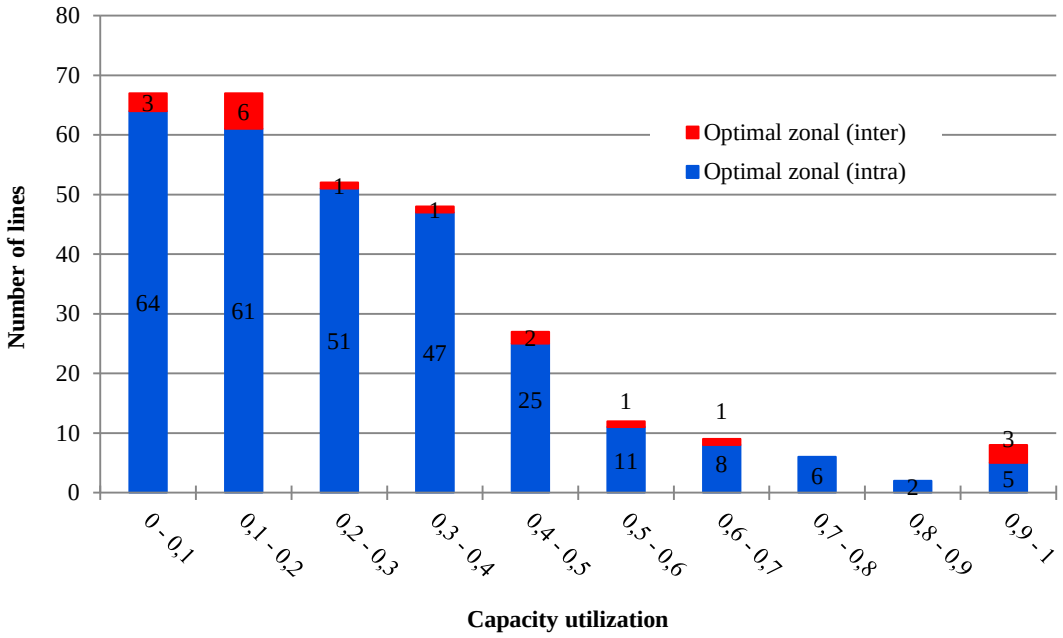

Figure 7-11 Line capacity utilization with optimal zonal pricing, 6/1-2010, hour 10

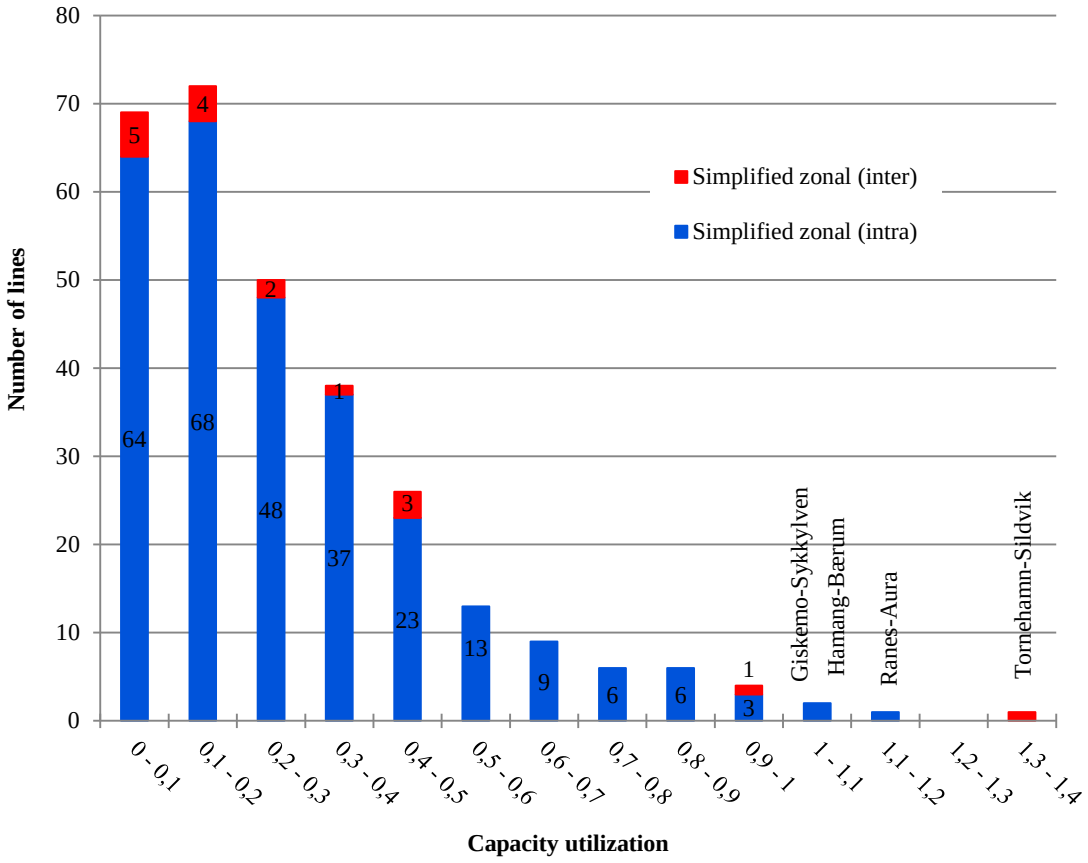

Figure 7-12 Line capacity utilization with simplified zonal pricing, 6/1-2010, hour 10

Figure 7-13 – Figure 7-15 show the utilization of the cut constraints, including the relaxed Bergen cuts. The figures show that Bergen 1 and Bergen 2 are infeasible in all the three solutions. Looking more closely at the nodal price solution, there are two more cut constraints that are operated on their capacity limits. The shadow prices for these two, Fardal overskudd 1 and BKK, are given in Table 7-7.

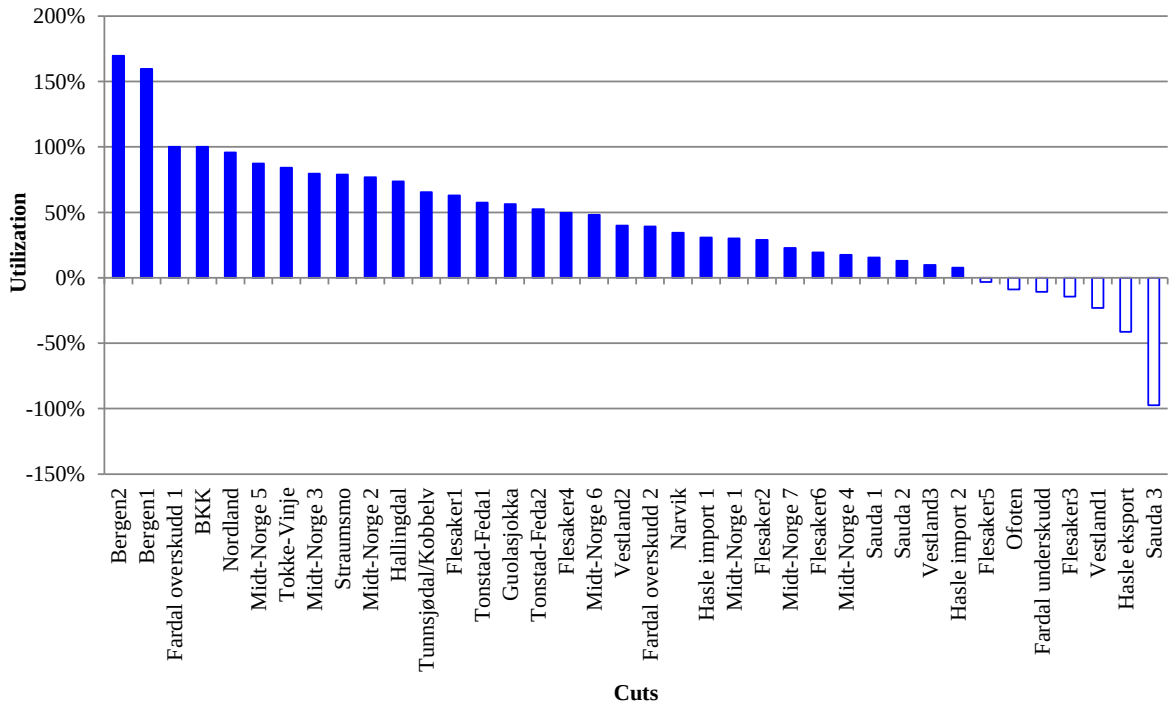

Figure 7-13 Cut capacity utilization with nodal pricing, 6/1-2010, hour 10

Table 7-7 Shadow prices for cut capacity constraints with nodal pricing, 6/1-2010, hour 10

Cut name	Capacity	From	To	Share of flow included	Shadow price
Fardal overskudd 1	750	Modalen	Evanger	1	*5,01*
		Fardal	Aurland1	1	
BKK	670	Modalen	Evanger	1	*4,28*
		Mauranger	Samnanger	1	

In the optimal nodal and optimal zonal price solutions all cut constraints except the infeasible Bergen cuts are fulfilled. We see from Figure 7-15 that in the simplified zonal solution the Fardal overskudd 1 and the BKK cuts are overloaded as well. I.e. in addition to 4 thermal constraints, 2 cut constraints (plus Bergen 1 and Bergen 2) are violated in the simplified zonal solution.

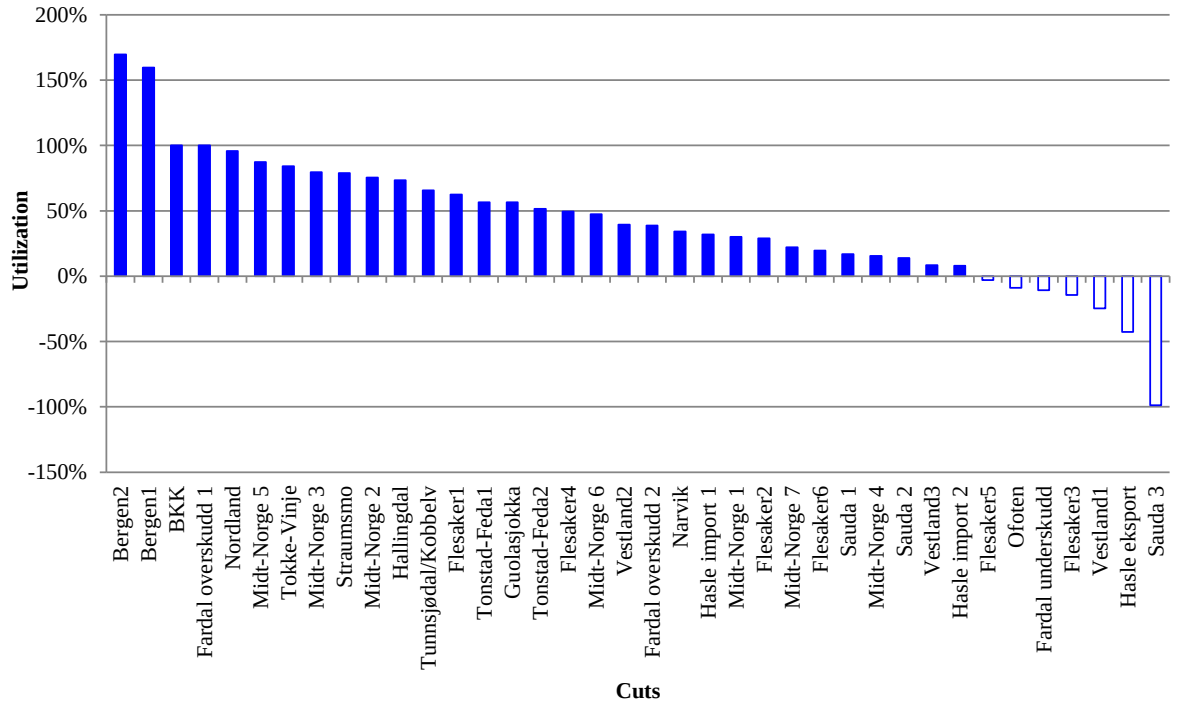

Figure 7-14 Cut capacity utilization with optimal zonal pricing, 6/1-2010, hour 10

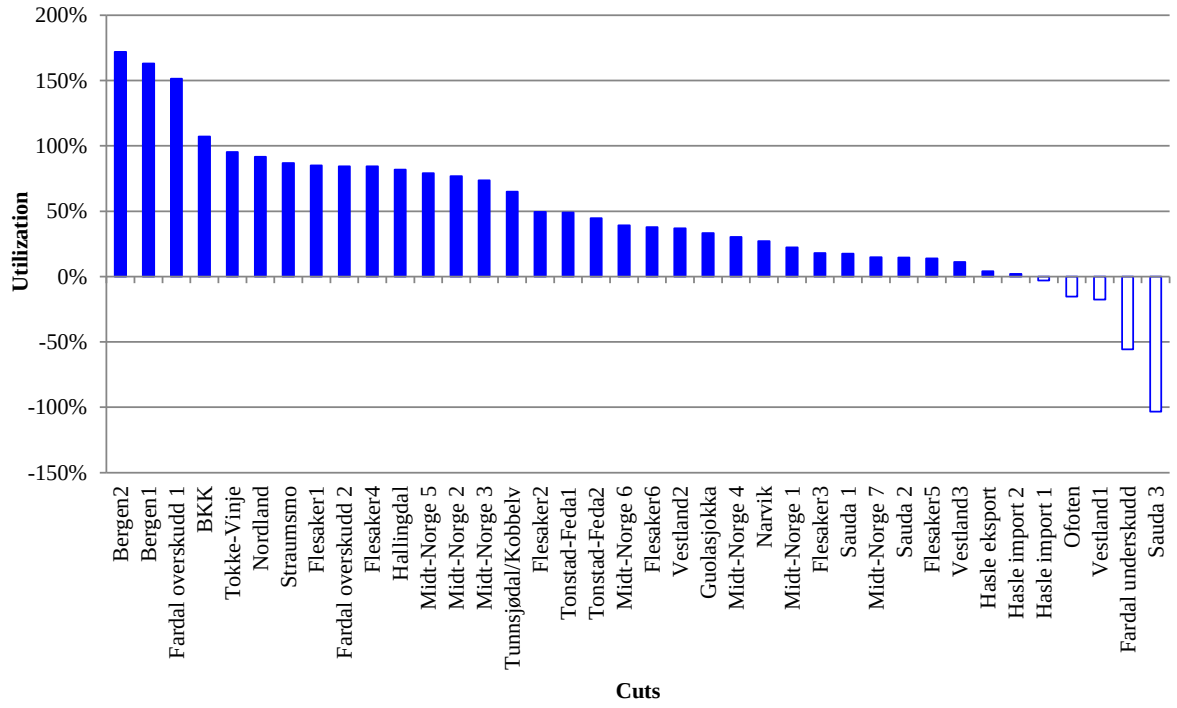

Figure 7-15 Cut capacity utilization with simplified zonal pricing, 6/1-2010, hour 10

7.4 Load and generation quantities

Figure 7-16 shows the differences in load for each node between the quantities consumed in the simplified zonal solution and the quantities consumed in the optimal nodal and the optimal zonal solutions. The differences are mostly small, with some exceptions located in the right hand side of the figure.

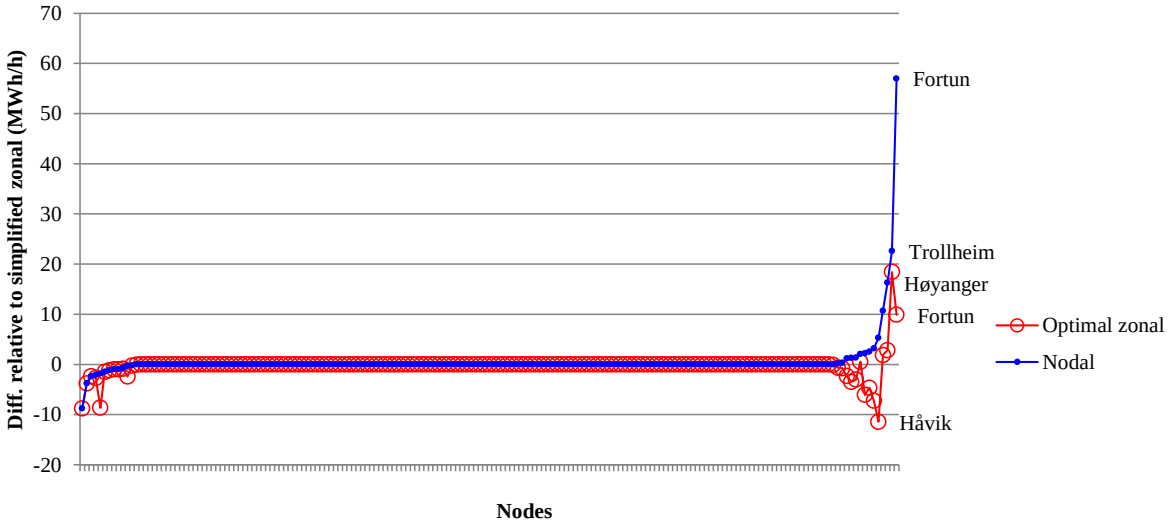

Figure 7-16 Differences in load between simplified zonal and the other two pricing approaches, 6/1-2010, hour 10

Figure 7-17 shows the same differences for the generation quantities. The quantity differences are larger for generation than for consumption, especially between the simplified zonal solution and the other two solutions. Optimal nodal and optimal zonal quantities are here quite similar.

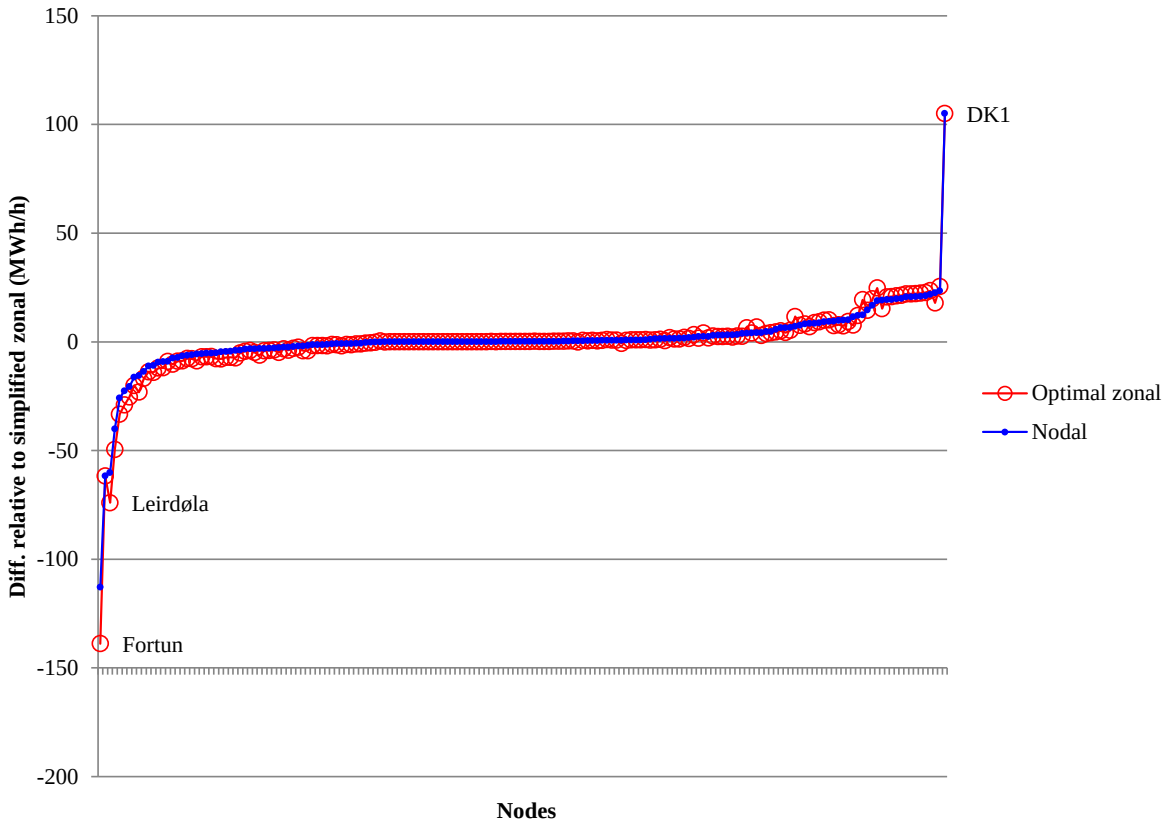

Figure 7-17 Differences in generation between simplified zonal and the other two pricing approaches, 6/1-2010, hour 10

In Figure 7-18 we show the bid curves for Fortun. For Fortun both consumption and generation quantities vary a lot between the simplified zonal solution and the other solutions. The nodal price is lower than the simplified zonal price, thus consumption increases and production decreases. The optimal zonal price is at the same level as the simplified zonal price, the demand is approximately the same while the generation is reduced, taking advantage of the fact that we allow the price to be strictly greater than the marginal cost in the optimal zonal price solution.

Figure 7-19 shows the bid for DK1. This is the node with the largest generation difference between the simplified zonal solution and the other two solutions. The optimal nodal and optimal zonal solutions are equal. From the figure we see that the large quantity difference is due to the step wise supply function.

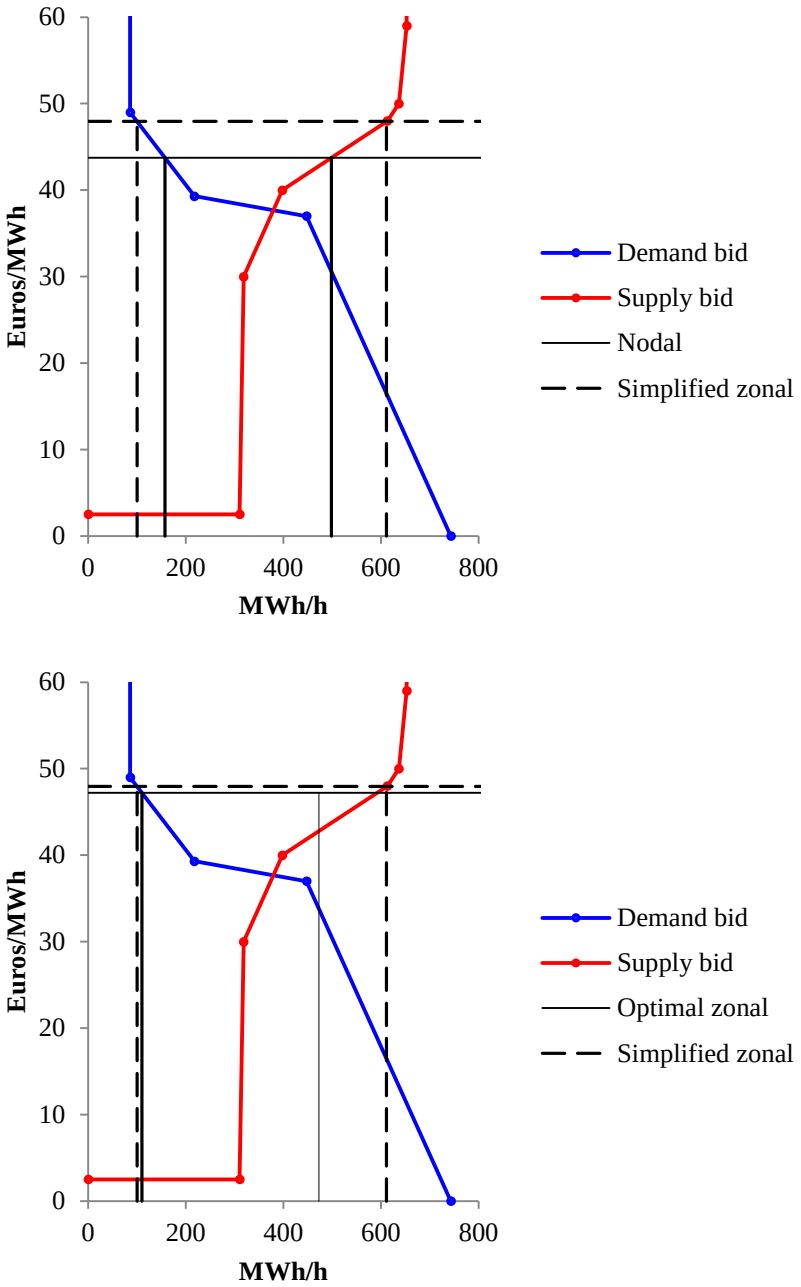

Figure 7-18 Differences in generation and consumption, Fortun, 6/1-2010, hour 10

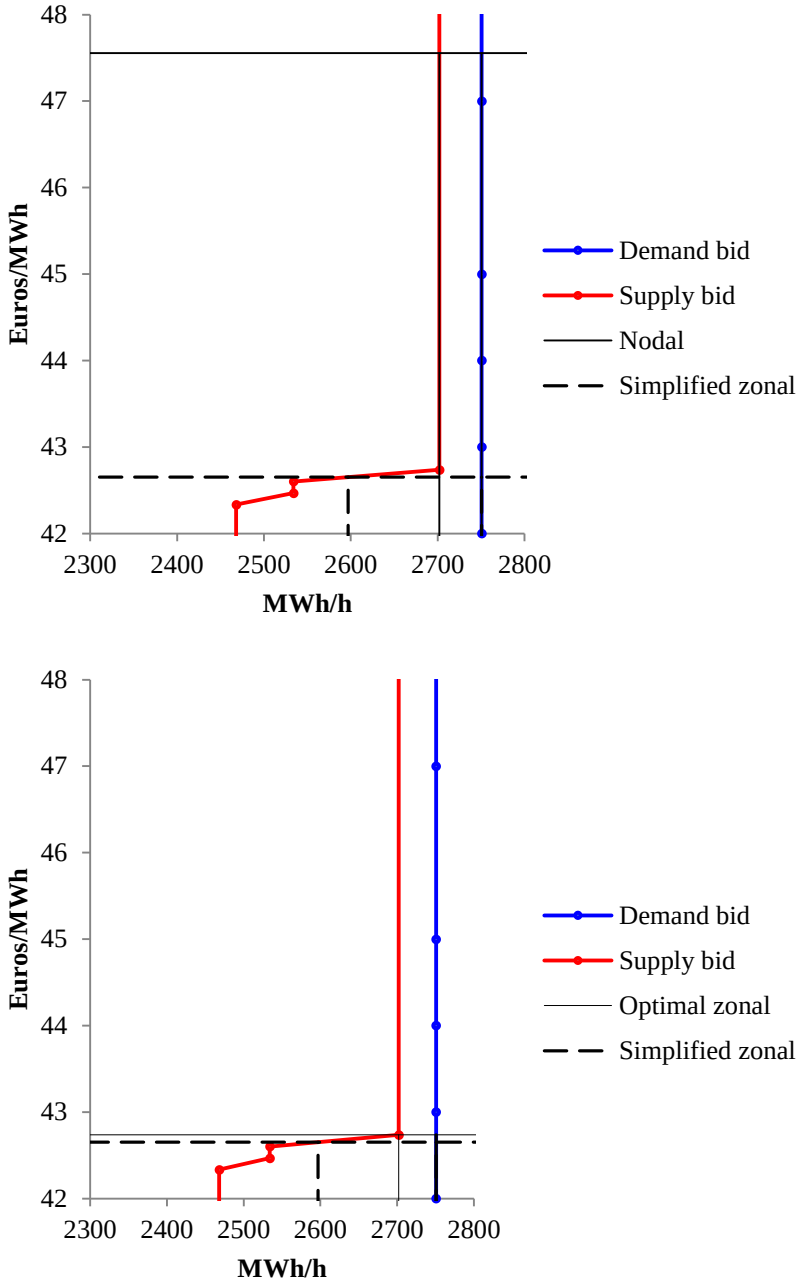

Figure 7-19 Differences in generation, DK1, 6/1-2010, hour 10

7.5 Surpluses

In Table 7-8 we show the changes in surplus compared to the unconstrained market solution. In this case, we see that moving from simplified zonal prices to optimal zonal or nodal prices leads to an increase in consumer surplus, producer surplus and grid revenue. In this case the total social surplus is and an increase in producer surplus and grid revenue, especially for the optimal zonal solution.

Table 7-8 Unconstrained surplus and surplus differences (1000 Euros), 6/1-2010, hour 10

	Unconstrained	Simplified zonal	Optimal zonal	Nodal
Producers	3510,4	-11,8	387,2	43,1
Consumers	101332,0	6,2	-354,2	-92,4
Grid	0,0	5,1	-35,3	47,4
Total	104842,4	-0,6	-2,3	-1,8
Infeasibilities	7 lines 2 cuts	5 lines 2 cuts	None	None

(Bergen 1 and Bergen 2 are overloaded in all solutions.)

8. Conclusions and recommendations

We have simulated the effect that different congestion management methods have on the market outcomes for a few specific hours with given bid curves, i.e. we assume that bids do not change even if the congestion management method does. The bid curves are related to specific hours during 2009-2010. The results that we report are for 4 calibrated bid scenarios for 2010 with varying prices, load and import and export levels. We have calibrated hourly supply and demand curves based on Nord Pool Spot sales and purchase bids, Statnett data on nodal production and exchange, information on generation technologies and capacities, information on the location of energy-intensive industries, and imports and exports with adjacent power markets given at Nord Pool Spot's web page.

The calibrated nodal bid curves match relatively well with the aggregated Nord Pool Spot bid curves. However, the disaggregation depends on a many assumptions, and may not reflect the actual nodal bid curves lying behind the actual Nord Pool Spot bid curves. Thus, the simulation performed must be evaluated not with respect to the actual power flows in the specific hours that we have considered, but with the calibrated nodal bid curves as the starting point.

The findings of the analyses indicate that in many cases the price changes with nodal pricing are not dramatic and the price variation is related to small volumes of production and consumption. When intrazonal constraints are badly represented by the aggregated transfer capacities in the simplified zonal model, the nodal prices tend to become higher on average than the simplified zonal prices. We have also found instances where the nodal prices are lower than the simplified zonal prices, and where the price variation is smaller. This may be the result of badly (too tight) set aggregate transfer capacities. In these cases surpluses may be higher and infeasibilities removed when introducing nodal prices. In some cases the simplified zonal prices lead to the "wrong constraints" being violated compared to the nodal price solution, i.e. even if a constraint is not binding in the optimal nodal price solution, it may be overloaded in the simplified zonal price solution. Moreover, it is very visible if the security constraints cannot be fulfilled. The result is very high prices and curtailment of load if the security requirements are not possible to accommodate. This happened in two of the cases analyzed for the Bergen 1 and Bergen 2 cuts. In order to resolve this problem, we have relaxed the cut constraints.

For one of the cases we have performed a sensitivity analysis, where we consider the effects on prices and flows from changing the aggregate transfer capacities. We have investigated what happens if we increase the number of bidding areas in various ways. We have tested another heuristic for implementing the N-1 criterion, i.e. using a fraction of the thermal capacity constraints instead of the cut constraints that Statnett uses. Finally we have looked at how prices, quantities and surpluses change when the demand elasticity changes. All of these choices have a profound effect on the market outcomes that are computed. The number of bidding area is important for how well the simplified zonal price model works. How to split the market into more areas is case dependent, so if one wants to have fixed bidding areas, this may be of little help. Different implementations of security constraints lead to different price structures. Increasing the responsiveness of the demand reduces the problems of congestion and leads to increases in surplus, especially for consumers, by shifting the burden of bottlenecks from consumers to producers.

For further analyses of a nodal pricing model, we recommend establishing better data sets. In the present project, we have had only data for individual hours, and we have had to collect information

from many different sources, the data not being established for this purpose and thus not really fitting together. We recommend establishing data sets for longer periods, for instance a whole week or a whole month. Then it would also be possible to take into account intertemporal considerations, like block bids, ramping constraints and water values.

A topic for future research is to model counter trading. One has to take into account the cost of real time adjustment compared to day ahead scheduling. In general, we would like to find ways to compare solutions that are infeasible to those that are not.

References

Baldursson, Fridrik Mar, Olvar Bergland and Cathrine Hagem (2011), Konsekvensene av at man trenger lenger tid på en ny overføringsforbindelse til Bergensområdet (BKK-området), Rapport fra Sjøkabelutredningen, Utvalg III, til Olje og energidepartementet.

Bjørndal, M. (2000), *Topics on electricity transmission pricing*. A dissertation submitted for the degree of dr.oecon. Norwegian School of Economics and Business Administration, Bergen, Norway.

Bjørndal, Mette and Kurt Jörnsten (2001), "Zonal Pricing in a Deregulated Electricity Market," *The Energy Journal*, 22, 51-73.

Bye, Torstein, Mette Bjørndal, Gerard Doorman, Gerd Kjølle, and Cristian Riis (2010), "Flere og riktigere priser – Et mer effektivt kraftsystem", Rapport fra Ekpertutvalget om driften av kraftsystemet, nedsatt av OED.

Chao, H.-P., Peck, S. (1996), A market mechanism for electric power transmission. *Journal of Regulatory Economics*, 10, 25-59.

Christie, R.D., Wangensteen, I., Wollenberg, B.F. (2000), Transmission management in the deregulated environment. *Proceedings of the IEEE*, Vol.88, No.2, 170-195.

Delarue, E., Bekaert, D., Belmans, R., D'haeseleer, W. (2007), Development of a comprehensive electricity generation simulation model using a mixed integer programming approach. *World Academy of Science, Engineering and Technology*, 28, 99-104.

Harvey, S., Hogan, W. and Pope, S. (1996), Transmission capacity reservations and transmission congestion contracts. Putham, Hayes & Bartlett.

Hogan, W.W. (1992), Contract networks for electric power transmission. *Journal of Regulatory Economics*, 4, 211-242.

Hogan, W.W., Read, E.G, Ring, B.J. (1996), Using mathematical programming for electricity spot pricing. *International Transactions in Operational Research*, Vol.3, No.3/4, 209-221.

Hogan,W.W. (1997), A market power model with strategic interaction in electricity networks. *The Energy Journal*, Vol.18, No.4, 107-141.

Neuhoff, Karsten, Rodney Boyd, Thilo Grau, Julian Barquin, Francisco Echavarren, Janusz Bialek, Chris Dent, Christian von Hirschhausen, Benjamin Hobbs, Friedrich Kunz, Hannes Weight, Christian Nabe, Georgios Papaefthymiou, and Christoph Weber (2011), "Renewable Electric Energy Integration: Quantifying the Value of Design of Markets for International Transmission Capacity, Climate Policy Initiative, Berlin.

Nord Pool Spot (2011), Installed generation capacity larger than 100 MW per station or per unit in Sweden (02.03.2011) http://www.nordpoolspot.com/Global/Download%20Center/TSO/Generation-capacity_%20Sweden_larger-than-100MW_20110302.pdf

Nord Pool Spot (2012), Maximum NTC capacities, http://nordpoolspot.com/Global/Download%20Center/TSO/Max_NTC_20111010_valid-from-15-Dec.pdf.

Overbye, T.J., Cheng, X., Sun, Y. (2004), A comparison of the AC and DC power flow models for LMP calculations. *Proceedings of the 37th Hawaii International Conference on System Sciences*.

Pepermans, Guido and Willems, Bert (2003), Regulating Transmission in a Spatial Oligopoly: A Numerical Illustration for Belgium. Energy, Transport and Environment Working Paper No. 2003-14. Available at SSRN: http://ssrn.com/abstract=528483 or doi:10.2139/ssrn.528483.

Schweppe, F.C., Caramanis, M.C., Tabors, R.D., Bohn, R.E. (1988), Spot Pricing of Electricity. Boston: Kluwer Academic Publishers.

SINTEF (2012), Description of the Samlast model, http://www.sintef.no/home/SINTEF-Energy-Research/Project-work/Samlast/.

Statnett (2010), Kraftsystemutredning for Sentralnettet 2010 – 2025.

Stott, B., Jardim, J., Alsaç, O. (2009), DC power flow revised. *IEEE Transactions on Power Systems*, Vol.24, No.3, 1290-1300.

Sun, J., Tesfatsion, L. (2010), DC optimal power flow formulation and solution using QuadProgJ. *Working paper No. 06014, Department of Economics, Iowa State University*, Ames, IA.

Van Hertem, D., Verboomen, J., Purchala, K., Belmans, R., Kling, W.L. (2006), Usefulness of DC power flow for active power flow analysis with flow controlling devices. *The 8th IEE International Conference on AC and DC Power Transmission*, 28-31 March, 58-62.

Varaiya, P., Wu, F.F. (1999), Coordinated multilateral trades for electric power networks: theory and implementation. *Electrical Power and Energy Systems*, 21, 75-102.

Wu, Felix, Pravin Varaiya, Pablo Spiller, and Shmuel Oren (1996), "Folk Theorems on Transmission Access: Proofs and Counterexamples," *Journal of Regulatory Economics*, 10, 5-23.

Appendices

A.1 Power flow approximations

AC power flow model

We consider a three-phase power network operating in sinusoidal steady-state. Let *I* be the vector of complex currents, *V* the vector of complex voltages and $Y = [Y_{ik}]$ the admittance matrix. In an AC model the admittance matrix is constructed of complex impedances of the transmission lines. The *impedance* of the line is Z_{ik} and given by

$$Z_{ik} = R_{ik} + jX_{ik} = Z_{ki}$$

where R_{ik} is the *resistance* and X_{ik} is the *reactance* and $j = \sqrt{-1}$. The admittance of the line between two nodes is the inverse of its impedance. Admittance is composed of real and imaginary parts as following

$$Y_{\substack{ik \\ i \neq k}} = G_{ik} + jB_{ik}$$

where G_{ik} is the *conductance* and B_{ik} the *susceptance* of the line *ik*. Conductance and susceptance are functions of resistance and reactance as below.

$$G_{ik} = \frac{R_{ik}}{R_{ik}^2 + X_{ik}^2}$$

$$B_{ik} = -\frac{X_{ik}}{R_{ik}^2 + X_{ik}^2}$$

The power flow can be divided into *real* and *reactive* power. Real power is the power that is useful, i.e., provides energy and is the commodity traded in the market. At the same time reactive power is usually considered as an ancillary service that has to be provided by the system operator (SO), stored and returned to the circuit as electric and magnetic fields, and its costs are divided among all users of the system. While reactive power is important for maintaining voltage stability in the network, its economic effects can be considered unimportant in the short run. If P_i and Q_i are the *real* and *reactive* power then the apparent power is given by

$$S_i = P_i + jQ_i \qquad (1\text{-}1)$$

From Kirchhoff's laws, the real and reactive power equations can be written as (see Chao, Peck (1996), Bjørndal (2000))

$$P_{ik} = G_{ik}V_i^2 - G_{ik}V_iV_k\cos(\theta_i - \theta_k) + B_{ik}V_iV_k\sin(\theta_i - \theta_k) \qquad (1\text{-}2)$$

$$Q_{ik} = G_{ik}V_i^2 + G_{ik}V_iV_k \sin(\theta_i - \theta_k) - B_{ik}V_iV_k \cos(\theta_i - \theta_k) \qquad (1\text{-}3)$$

where real and reactive power are functions of phase angles θ_i and voltages magnitudes V_i given in *rms* (root-mean-square) values. Terms involving conductance *G* represent series branch losses. For a rigorous derivation of the above equations from Ohm's law, see Sun and Tesfatsion (2010).

DC approximations and assumptions

The DC power flow problem simplifies the AC power flow by making it linear under certain assumptions. A large number of applications like Hogan (1992), Varaiya & Wu (1999), Hogan et al. (1996), Chao & Peck (1996), Hogan (1997), Christie et al (2000), Overbye et al. (2004), Van Hertem et al. (2006), and Delarue et al. (2007), follow the development of a DC power flow in Schweppe et al. (1988). This can be called a $B-P$ or a pseudo DC, or a DC model.

The assumptions applied in the DC model are 1) only real power balance is considered; 2) the resistance of a line is negligible compared to the line's reactance and is thus set to 0, then the conductance becomes zero as well, i.e. lossless model; 3) voltage magnitudes are equal to 1 in a per-unit system; 4) voltage angle differences across any line are small so that the cosine of the difference is equal to 1 and the sine to its argument (flat voltage profile). Applying these assumptions one at a time we can derive the DC power flow approximation from equations (1-2) and (1-3). Given assumption 1) it follows that only equation (1-2) is considered. From assumption 2) in a lossless model $G_{ik} = 0$ and $B_{ik} = -1/X$, where *X* is reactance for line *i-k*, thus active power transported over a transmission line between node k and l is

$$P_{ik} = \frac{|V_i||V_k|}{X_{ik}} \sin(\theta_{ik}). \qquad (1\text{-}4)$$

Assumption 3) implies $V_i = V_k = 1 p.u.$, and therefore

$$P_{ik} = \frac{\sin(\theta_{ik})}{X_{ik}}. \qquad (1\text{-}5)$$

Finally, by assumption 4) $|\theta_{ik}| \to 0$ then $\sin(\theta_{ik}) = \theta_{ik}$ and our power flow equation is transformed into

$$P_{ik} = \frac{\theta_{kl}}{X_{ik}} = B_{ik} \cdot \theta_{kl}, \qquad (1\text{-}6)$$

where B_{ik} is line susceptance. This is also called the classical DC power flow model (see Stott et al (2009)).

A.2 Mathematical description of OptFlow models

The models and the optimal prices

The optimal nodal pricing model is defined by (2-1)-(2-6) below. The optimal zonal pricing model has the same objective function and constraints as the optimal nodal model, and in addition the prices are restricted by (2-7)-(2-9). The simplified model is defined by (2-1), (2-2) and (2-10).

The nodal prices in the optimal nodal model are given by the shadow prices of constraint (2-2). In the optimal zonal pricing model, the price in zone $z \in Z$ is given by the optimal value of the variable p_z. The zonal prices in the simplified model are given by the shadow prices of constraint (2-2). In the simplified model we have removed the line capacity constraints between any two nodes that are located in the same zone. This fact, and the fact that the simplified model does not take into account Kirchhoff's 2nd law as stated in (2-3) and (2-4), or the security cut constraints as stated in (2-6), makes the nodal prices uniform within any price zone.

List of symbols

N	Set of nodes.
L	Set of lines.
L^{DC}	Set of HVDC lines.
H_{ij}	"Admittance" of the line between the nodes *i* and *j*. This number is calculated using the formula $(V_{ij})^2 \Big/ \sqrt{X_{ij}^2 + R_{ij}^2}$, i.e., using the voltage level, reactance and resistance of the line.
CAP_{ij}	Thermal capacity limit of the line from *i* to *j*. This number is calculated using the formula $\sqrt{3} V_{ij} I_{ij}^{MAX}$, i.e., using the voltage level and the maximal current of the line.
q_i^s	Generation quantity (MWh/h) in node *i.*
q_i^d	Load quantity (MWh/h) in node *i.*
$p_i^s(\bullet)$	Function that represents the supply bid curve in node *i.* See Appendix A.4.
$p_i^d(\bullet)$	Function that represents the demand bid curve in node *i.* See Appendix A.4.
f_{ij}	Load flow from node *i* to node *j*.
θ_i	Phase angle variable for node *i*.
$CUTS$	Set of security cuts.
$CCAP_k$	Upper limit for the flow over a cut $k \in CUTS$.
α_{ij}^k	A constant between 0 and 1 that represents the share of the flow over line *(i,j)* that is included in the cut constraint $k \in CUTS$.
β_i^k	A constant that represents the share of the generation in node *i* that is deducted from the upper limit of the cut constraint $k \in CUTS$.
γ_i^k	A constant that represents the share of the load in node *i* that is deducted from the upper limit of the cut constraint $k \in CUTS$.
Z	Set of price areas (zones) in the simplified/optimal zonal pricing models.
N^z	Subset of nodes that are included in the price area $z \in Z$.

p_i Variable that represents the price in node *i*. This variable is only used in the optimal zonal pricing model.

p_z Variable that represents the price in zone *z*. This variable is only used in the optimal zonal pricing model.

CAP_{xz} Upper limit on the flow from zone $x \in Z$ to zone $z \in Z$ in the simplified model.

Objective function

$$\underset{q^d, q^s, f, \theta}{\text{Maximize}} \sum_{i \in N} \left[\int_0^{q_i^d} p_i^d(q) dq - \int_0^{q_i^s} p_i^s(q) dq \right] \tag{2-1}$$

Load flow constraints

$$q_i^s - q_i^d = \sum_{j:(i,j) \in L} f_{ij} - \sum_{j:(j,i) \in L} f_{ji} \qquad i \in N \tag{2-2}$$

$$f_{ij} = H_{ij}(\theta_i - \theta_j) \qquad (i,j) \in L \setminus L^{DC} \tag{2-3}$$

$$\theta_1 = 0 \tag{2-4}$$

$$-CAP_{ji} \le f_{ij} \le CAP_{ij} \qquad (i,j) \in L \tag{2-5}$$

Security cut constraints

$$\sum_{(i,j) \in L} \alpha_{ij}^k f_{ij} + \sum_{i \in N} \beta_i^k q_i^s + \sum_{i \in N} \gamma_i^k q_i^d \le CCAP_k \qquad k \in CUTS \tag{2-6}$$

Price constraints in the optimal zonal pricing model

$$p_i = p_z \qquad i \in N^z, z \in Z \tag{2-7}$$

$$p_i \le p_i^d\left(q_i^d\right) \qquad i \in N \tag{2-8}$$

$$p_i \ge p_i^s\left(q_i^s\right) \qquad i \in N \tag{2-9}$$

Flow capacity constraints in the simplified model

$$-CAP_{zx} \le \sum_{\substack{(i,j) \in L \\ i \in N^x \\ j \in N^z}} f_{ij} - \sum_{\substack{(i,j) \in L \\ j \in N^x \\ i \in N^z}} f_{ij} \le CAP_{xz} \qquad x, z \in Z \tag{10}$$

A.3 Cut constraints

A cut *k* is defined by a set of transmission lines for which the total flow must not exceed the number $CCAP_k$, i.e., the inequality constraint (2-6) must be satisfied. The relationship between the transmission line (i,j) and the cut *k* is given by the parameter α_{ij}^k. If $\alpha_{ij}^k = 1$, the power flow from *i* to

j is included in the cut k, whereas $\alpha_{ij}^{k} = 0$ means that the flow is not included. Note that α_{ij}^{k} may also take on a value between 0 and 1, meaning that some, but not all, of the flow from i to j is included in the cut constraint. Cut capacities are sometimes adjusted based on observed production quantities in the nodes (PFK). For the production node i and the cut k this adjustment is modeled using the constant β_{i}^{k}. Similarly, the capacity of a cut can be adjusted based on consumption in one or more nodes (BFK). For the consumption node i and the cut k this adjustment is modeled using the constant γ_{i}^{k}.

Table A-1 Capacity limits of cut constraints at 10°C. From Statnett (2010)

Cut (*k*)	***CCAP*$_k$**
Hasle import 1	2150
Hasle import 2	840
Hasle eksport	1600
Flesaker1	3000
Flesaker2	3100
Flesaker3	1170
Flesaker4	1170
Flesaker5	695
Flesaker6	695
Hallingdal	2800
Tokke-Vinje	710
Tonstad-Feda1	855
Tonstad-Feda2	1005
Sauda 1	1000
Sauda 2	1200
Sauda 3	950
Midt-Norge 1	415
Midt-Norge 2	415
Midt-Norge 3	1350
Midt-Norge 4	700
Midt-Norge 5	855
Midt-Norge 6	925
Midt-Norge 7	925
Tunnsjødal/Kobbelv	1200
Nordland	1000
Ofoten	375
Narvik	315
Straumsmo	395
Guolasjokka	135
Fardal overskudd 1	750
Fardal overskudd 2	750
Fardal underskudd	750
Vestland1	950
Vestland2	940
Vestland3	1600
BKK	670
Bergen1	670
Bergen2	670

Table A-2 Description of cut constraints from Statnett (2010)

Cut (*k*)	**From (*i*)**	**To (*j*)**	α_{ij}^{k}
Hasle import 1	Borgvik	Hasle	1
Hasle import 1	Skogssäter	Halden	1
Hasle import 2	Hasle	Tegneby	0,42

Cut (*k*)	**From (*i*)**	**To (*j*)**	α_{ij}^{k}
Hasle eksport	Hasle	Borgvik	1
Hasle eksport	Halden	Skogssäter	1
Flesaker1	Rjukan	Sylling	1
Flesaker1	Rød	Hasle	1
Flesaker1	Flesaker	Sylling	1
Flesaker1	Flesaker	Tegneby	1
Flesaker2	Rjukan	Sylling	1
Flesaker2	Rød	Hasle	1
Flesaker2	Flesaker	Sylling	1
Flesaker2	Flesaker	Tegneby	1
Flesaker3	Sylling	Tegneby	0,25
Flesaker3	Rød	Hasle	1
Flesaker4	Rjukan	Sylling	0,45
Flesaker4	Rød	Hasle	1
Flesaker5	Flesaker	Sylling	0,45
Flesaker5	Flesaker	Tegneby	1
Flesaker6	Flesaker	Tegneby	0,8
Flesaker6	Flesaker	Sylling	1
Hallingdal	Usta	Ådal	1
Hallingdal	Dagali	Ringerike	1
Hallingdal	Nore	Sylling	1
Tokke-Vinje	Vemork	Flesaker	0,35
Tokke-Vinje	Tokke	Flesaker	1
Tonstad-Feda1	Tonstad	Feda	0,6
Tonstad-Feda1	Tonstad	Feda	1
Tonstad-Feda2	Tonstad	Feda	0,6
Tonstad-Feda2	Tonstad	Feda	1
Sauda 1	Sauda	Nesflaten	0,85
Sauda 1	Sauda	Hylen	1
Sauda 2	Sauda	Nesflaten	0,85
Sauda 2	Sauda	Hylen	1
Sauda 3	Liastøl	Hylen	0,85
Sauda 3	Songa	Kjela	1
Midt-Norge 1	Rana	Nedre Røssåga	0,35
Midt-Norge 1	Ajaure	Nedre Røssåga	1
Midt-Norge 2	Nea	Klæbu	1
Midt-Norge 2	Ajaure	Nedre Røssåga	1
Midt-Norge 3	Nea	Klæbu	0,5
Midt-Norge 3	Tunnsjødal	Verdal	1
Midt-Norge 3	Tunnsjødal	Namsos	1
Midt-Norge 4	Nea	Klæbu	0,5
Midt-Norge 4	Vågåmo	Aura	1
Midt-Norge 5	Tunnsjødal	Namsos	0,7
Midt-Norge 5	Tunnsjødal	Verdal	1
Midt-Norge 6	Klæbu	Viklandet	0,85
Midt-Norge 6	Klæbu	Orkdal	1
Midt-Norge 7	Klæbu	Viklandet	0,85
Midt-Norge 7	Orkdal	Trollheim	1
Tunnsjødal/Kobbelv	Tunnsjødal	Verdal	1
Tunnsjødal/Kobbelv	Tunnsjødal	Namsos	1
Tunnsjødal/Kobbelv	Nedre Røssåga	Ajaure	1
Tunnsjødal/Kobbelv	Kobbelv	Ofoten	1
Nordland	Ofoten	Ritsem	1
Nordland	Nedre Røssåga	Ajaure	1
Nordland	Tunnsjødal	Verdal	1
Nordland	Tunnsjødal	Namsos	1
Nordland	Sildvik	Tornehamn	1
Ofoten	Ofoten	Kvandal	0,8
Ofoten	Ofoten	Skjomen	1
Narvik	Ofoten	Kvandal	0,65

Cut (*k*)	**From (*i*)**	**To (*j*)**	α_{ij}^{k}
Narvik	Skjomen	Narvik	1
Straumsmo	Kvandal	Bardufoss	1
Straumsmo	Straumsmo	Bardufoss	1
Straumsmo	Straumsmo	Krogstad	1
Guolasjokka	Skibotn	Balsfjord	1
Guolasjokka	Guolasjokka	Lyngen	1
Fardal overskudd 1	Modalen	Evanger	1
Fardal overskudd 1	Fardal	Aurland1	1
Fardal overskudd 2	Mauranger	Blåfalli	1
Fardal overskudd 2	Fardal	Aurland1	1
Fardal underskudd	Mauranger	Samnanger	1
Fardal underskudd	Aurland1	Fardal	1
Vestland1	Modalen	Evanger	0,7
Vestland1	Hylen	Sauda	1
Vestland2	Modalen	Evanger	0,3
Vestland2	Nesflaten	Sauda	1
Vestland3	Nesflaten	Sauda	1
Vestland3	Modalen	Evanger	1
Vestland3	Hylen	Sauda	1
BKK	Modalen	Evanger	1
BKK	Mauranger	Samnanger	1
Bergen1	Samnanger	Fana	1
Bergen1	Evanger	Dale	1
Bergen2	Samnanger	Fana	1
Bergen2	Dale	Arna	1

Table A-3 Cut capacity adjustment based on nodal quantities. From Statnett (2010)

Cut (*k*)	Node (*i*)	β_i^k	γ_i^k
Flesaker2	Kvilldal	-1	
Flesaker2	Tokke	-1	
Flesaker3	Tonstad	-0,35	
Flesaker3	Kvilldal	-0,3	
Flesaker3	Vinje	-0,3	
Flesaker3	Tokke	-0,3	
Flesaker3	Sima	-0,1	
Flesaker3	Aurland1	-0,1	
Flesaker4	Kvilldal	-0,4	
Flesaker5	Tokke	-0,3	
Flesaker5	Vinje	-0,3	
Flesaker5	Kvilldal	-0,2	
Flesaker5	Tonstad	-0,2	
Flesaker6	Tokke	-0,3	
Flesaker6	Vinje	-0,3	
Flesaker6	Kvilldal	-0,15	
Flesaker6	Tonstad	-0,15	
Midt-Norge 2	Aura		-0,15
Midt-Norge 3	Aura		-0,6
Midt-Norge 4	Aura		-0,6
Midt-Norge 6	Aura		-0,4
Midt-Norge 7	Aura		-0,6
Tunnsjødal/Kobbelv	Kobbelv	-1	
Tunnsjødal/Kobbelv	Svartisen	-0,5	

A.4 Formulation of bid curves

The bid curves are piece-wise linear, and they can have horizontal as well as vertical segments. The integrals below the demand bid curve and the supply bid curve, for each node, are calculated as a sum of a number of rectangles and triangles, as illustrated by Figure A-2 and Figure A-2 below.

In each node the supply bid curve consists of R segments. Each segment r has a production capacity of $\bar{q}_r^s$. Hence, the production q_r^s for segment r must satisfy the constraint

$$0 \le q_r^s \le \bar{q}_r^s \tag{4-1}$$

Each segment has, in addition to its capacity, two non-negative parameters: c_r and e_r. The parameter c_r gives the slope of the segment, and e_r is used to allow for a vertical jump in front of segment r, as illustrated in the example in Figure A-1.

In the example shown in Figure A-1, the total production quantity is given by the sum $q_1^s + q_2^s + q_3^s$. The production in the first two segments are at the respective capacity limits, whereas production in the third segment is strictly below the capacity limit. The area under the supply bid curve to the left of the total production quantity is given by the expression

$$C\left(q_1^s, q_2^s, \ldots, q_R^s\right) = \sum_{r=1}^{R} q_r^s \sum_{r'=1}^{r} e_{r'} + 0.5 \sum_{r=1}^{R} c_r \left(q_r^s\right)^2 + \sum_{r=2}^{R} q_r^s \sum_{r'=1}^{r-1} c_{r'} \bar{q}_{r'}^s . \tag{4-2}$$

The red part of (4-2) gives the area of the red rectangles in Figure A-1. The green part of the expression corresponds to the green triangles, and the blue part of the expression gives the area of the blue rectangles.

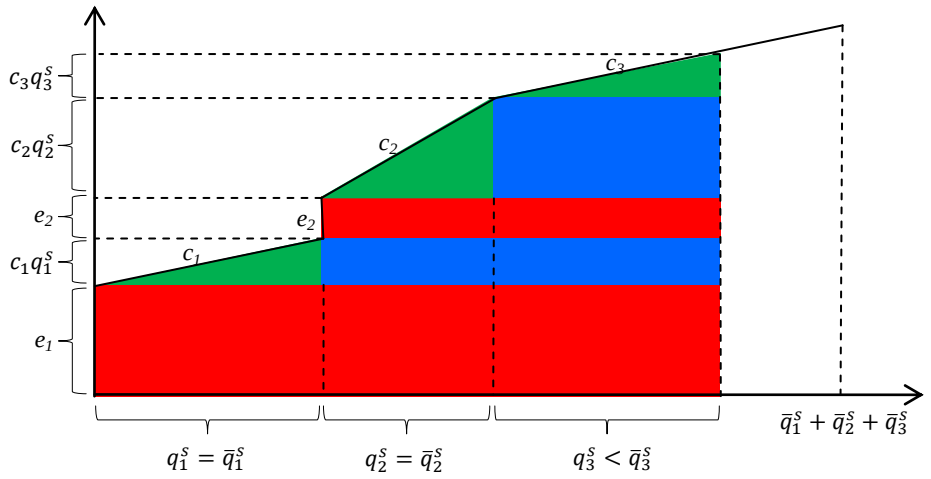

Figure A-1 Supply bid curve with 3 segments

Likewise, in each node the demand bid curve consists of T segments. Each segment t has a maximal demand of $\bar{q}_t^d$. Hence, the demand q_t^d in segment t must satisfy the constraint

$$0 \le q_t^d \le \bar{q}_t^s \,. \qquad (4\text{-}3)$$

Each segment has, in addition to its capacity, two non-negative parameters: b_t and a_t. The parameter b_t gives the (negative) slope of the segment, and a_t is used to allow for a vertical drop/jump in front of segment t, as illustrated in the example in Figure A-2. Note that a_1 indicates the intersection of the demand curve with the vertical axis, while a_t for $t > 1$ indicate vertical drops in the demand curve.

In the example shown in Figure A-2, the total consumption quantity is given by $q_1^d + q_2^d + q_3^d$. The consumption in the first two segments are at the respective upper limits, whereas consumption in the third segment is strictly below the upper limit. The area under the demand bid curve to the left of the total consumption quantity is given by the expression

$$B\left(q_1^d, q_2^d, \ldots, q_T^d\right) = a_1 \sum_{t=1}^{T} q_t^d - \sum_{t=2}^{T} a_t \sum_{t'=t}^{T} q_{t'}^d - 0.5 \sum_{t=1}^{T} b_t \left(q_t^s\right)^2 - \sum_{t=2}^{T} q_t^s \sum_{t'=1}^{t-1} b_{t'} \bar{q}_{t'}^d \,. \qquad (4\text{-}4)$$

The first part of (4-4) gives the area of the rectangle containing the solid grey and the hatched areas in Figure A-2. In order to get the area under the demand curve, we must deduct the areas of the colored triangles and rectangles. The red part of (4-4) gives the area of the red hatched rectangle in the figure, while the green part of (4-4) gives the area of the green hatched triangles. Finally, the blue part of (4-4) gives the area of the blue hatched rectangles in the figure.

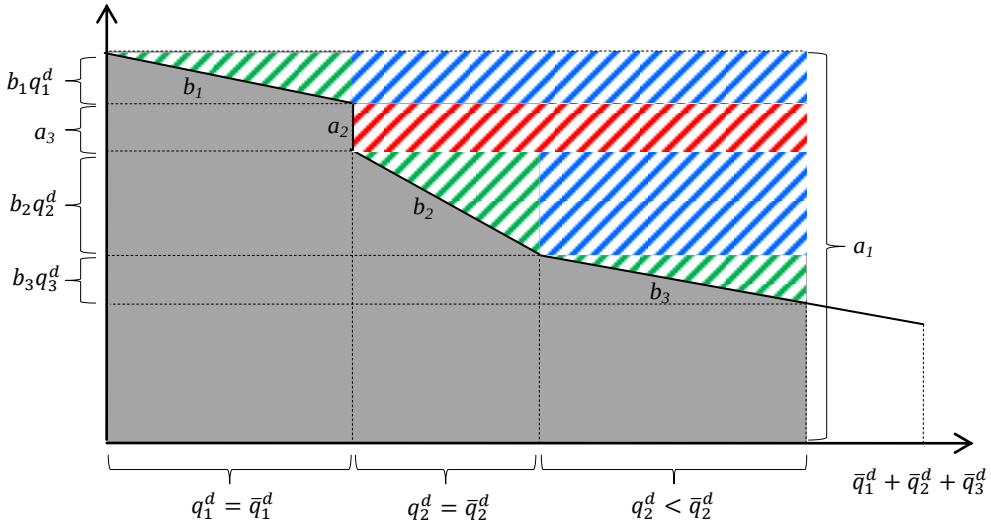

Figure A-2 Demand bid curve with 3 segments

Note that, in the case of the nodal pricing model and the simplified model, the fact that the supply bid curves are non-decreasing implies that we will always have

$$q_r^s > 0 \Rightarrow q_{r'}^s = \bar{q}_{r'}^s \qquad \forall r' < r \tag{4-5}$$

i.e., lower bid curve segments will be "filled up" before the higher segments are used. Similarly, for the demand bid curves we will have

$$q_t^d > 0 \Rightarrow q_{t'}^d = \bar{q}_{t'}^d \qquad \forall t' < t\,. \tag{4-6}$$

For the optimal zonal model, where the nodal prices are modeled explicitly via (2-7)-(2-9), the properties (4-5) and (4-6) must be modeled explicitly. This requires the use of binary variables and extra constraints in the optimal zonal model.

A.5 Some characteristics of the optimal zonal solutions

The optimal zonal pricing model differs from the optimal nodal pricing model and the simplified model in that the prices are modeled explicitly via (2-7)-(2-9). Since the prices are not "true" shadow prices some peculiarities may arise, and we will describe these peculiarities.

Vertical bid curve segments

Figure A-3 illustrates the situation in a node where both the supply bid curve and the demand bid curve have vertical segments. Such a situation can lead to non-uniqueness with respect to the price. This will happen, e.g., if the node is alone in its zone. Any solution with a price between *p*' and *p* will satisfy constraints (2-7) and (2-8). All the possible values will give the same social surplus, but will differ with respect to the distribution of the surplus between producers, consumers and the grid. We

handle such non-uniqueness by choosing the lowest one of the equivalent prices, i.e., *p'* in the example.

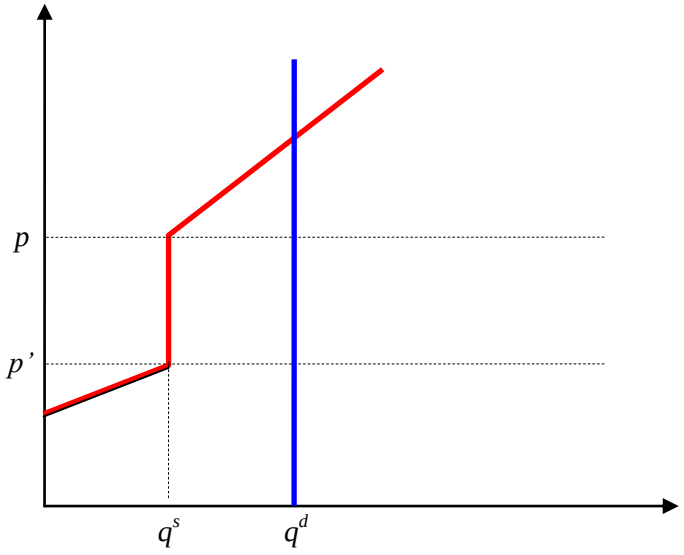

Figure A-3 Non-unique price

Insufficient price signals

Optimal zonal prices are not true marginal costs, since they are not based on shadow prices of model constraints. The resulting prices may not give correct incentives for individual generators or consumers. A typical example is illustrated in Figure A-4. The optimal zonal price is p^*, with the corresponding optimal generation quantity q^*. The marginal cost of increasing production at the quantity q^* is given by $MC(q^*)$. Since $p^* > MC(q^*)$, it would be profitable to increase production in this node. The generator(s) would prefer to increase their production until the price is equal to the marginal cost, i.e., they would prefer the quantity *q'*.

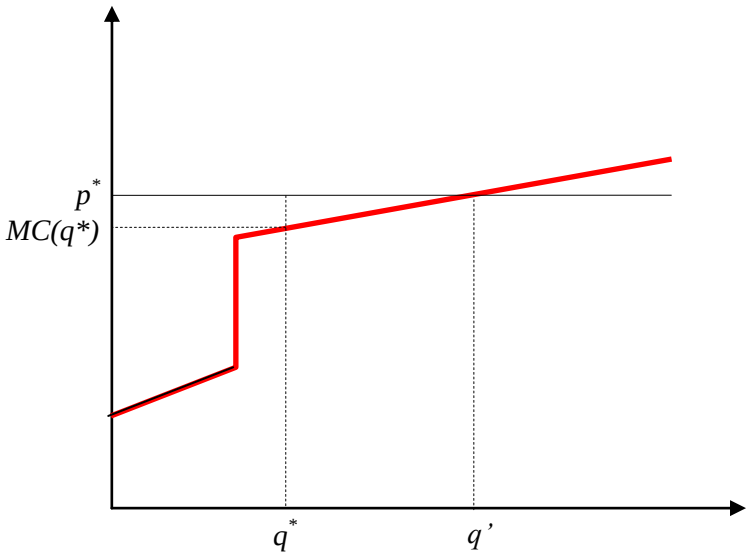

Figure A-4 Insufficient price signal for generation

The fact that the producers have incentive to deviate from the optimal quantities makes it necessary for the system operator to restrict the production quantity. Hence, it is not sufficient to specify the area prices; the system operator also has to specify the individual production quantities. With multiple producers in each node, it is not obvious how the necessary "curtailment" should be allocated among the producers.

In the Nordic day-ahead electricity market zonal pricing or market splitting is used for relieving congestion between a predetermined set of price areas. This congestion management method represents an aggregation of individual connection points into price areas, and flows in the actual electricity network are only partially represented in the market clearing. Because of several strained situations in the power system during 2009 and 2010, changes in the congestion management method are under consideration by the Norwegian regulator NVE. We discuss three different congestion management methods – nodal pricing, and optimal and simplified zonal pricing. Four hourly cases from 2010 are used to illustrate the effects of different congestion management methods on prices, surpluses and network utilization.

SNF
Et selskap i NHH-miljøet

SAMFUNNS- OG NÆRINGSLIVSFORSKNING AS

Institute for Research in Economics and Business Administration

Helleveien 30
NO-5045 Bergen
Norway
Phone: (+47) 55 95 95 00
E-mail: snf@snf.no
Internet: http://www.snf.no/

Trykk: Allkopi Bergen